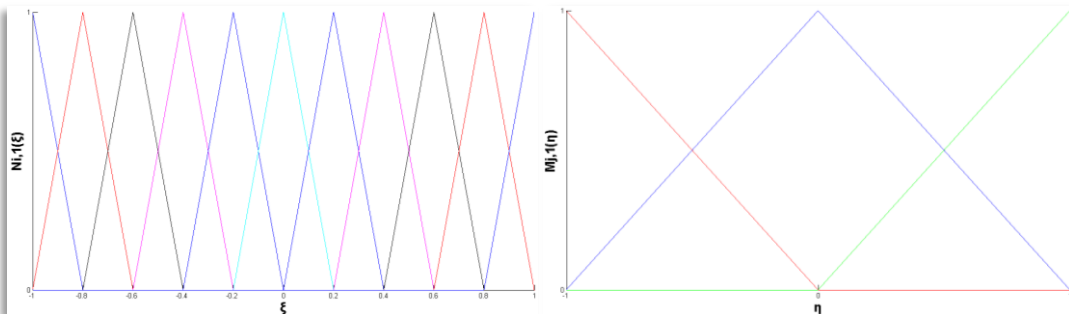
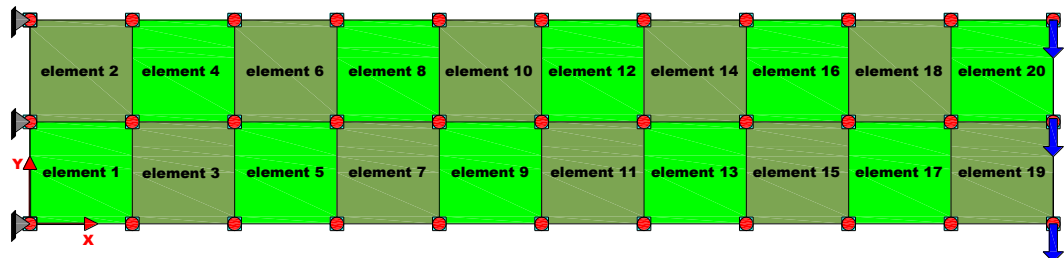




ΕΘΝΙΚΟ ΜΕΤΣΟΒΙΟ ΠΟΛΥΤΕΧΝΕΙΟ
ΤΜΗΜΑ ΠΟΛΙΤΙΚΩΝ ΜΗΧΑΝΙΚΩΝ
ΤΟΜΕΑΣ ΔΟΜΟΣΤΑΤΙΚΗΣ
ΕΡΓΑΣΤΗΡΙΟ ΣΤΑΤΙΚΗΣ & ΑΝΤΙΣΕΙΣΜΙΚΩΝ ΕΡΕΥΝΩΝ
ΑΚΑΔΗΜΑΪΚΟ ΕΤΟΣ 2010-2011
ΔΠΜΣ “ΔΟΜΟΣΤΑΤΙΚΟΣ ΣΧΕΔΙΑΣΜΟΣ & ΑΝΑΛΥΣΗ ΚΑΤΑΣΚΕΥΩΝ”

ΙΣΟΓΕΩΜΕΤΡΙΚΗ ΑΝΑΛΥΣΗ ΜΕ B-SPLINES & NURBS

ΜΕΤΑΠΤΥΧΙΑΚΗ ΕΡΓΑΣΙΑ
ΚΑΡΑΚΙΤΣΙΟΣ ΠΑΝΑΓΙΩΤΗΣ
ΥΠΟΤΡΟΦΟΣ
ΙΔΡΥΜΑΤΟΣ ΠΑΙΔΕΙΑΣ & ΕΥΡΩΠΑΪΚΟΥ ΠΟΛΙΤΙΣΜΟΥ



ΕΠΙΒΛΕΠΩΝ ΚΑΘΗΓΗΤΗΣ: ΠΑΠΑΔΡΑΚΑΚΗΣ ΜΑΝΟΛΗΣ

ΑΘΗΝΑ, ΟΚΤΩΒΡΙΟΣ 2011

Isogeometric Analysis

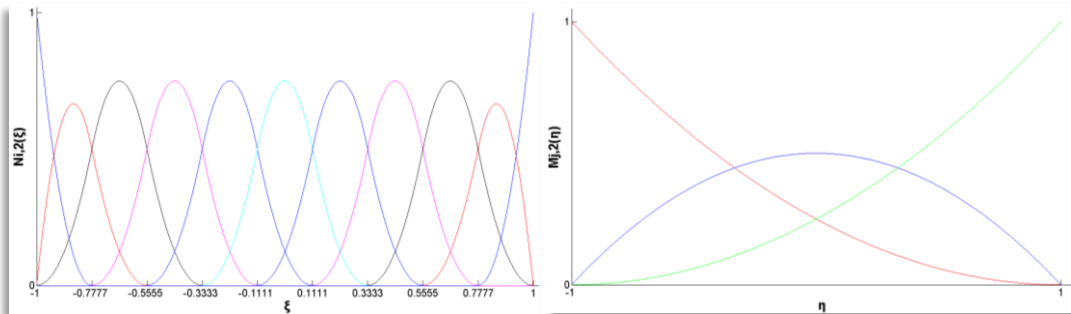
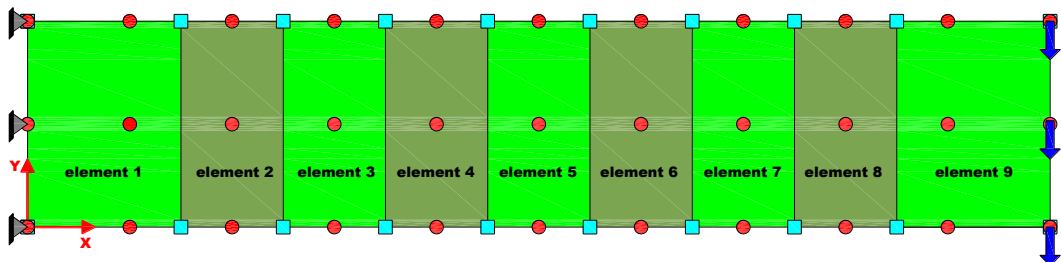


NATIONAL TECHNICAL UNIVERSITY OF ATHENS
SCHOOL OF CIVIL ENGINEERING
DEPARTMENT OF STRUCTURAL ENGINEERING
STATIC & ASEISMIC RESEARCH LABORATORY
ACADEMIC YEAR 2010-2011

MSc in ANALYSIS & DESIGN of EARTHQUAKE RESISTANCE STRUCTURE

ISOGEOMETRIC ANALYSIS WITH B-SPLINES & NURBS

THESIS
KARAKITSIOS PANAGIOTIS
SCHOLAR OF
FOUNDATION FOR EDUCATION AND EUROPEAN CULTURE



SUPERVISOR PROFESSOR:
PAPADRAKAKIS MANOLIS

ATHENS, OCTOBER 2011

Isogeometric Analysis

ΣΥΝΟΨΗ

Πρωταρχικός σκοπός της μεταπτυχιακής μου εργασίας είναι να παρουσιάσω και να προτείνω τη μέθοδο της Ισογεωμετρικής Ανάλυσης (IsoGeometric Analysis, IGA), η οποία αναπτύχθηκε πρόσφατα προκειμένου να καλύψει το τεράστιο κενό μεταξύ της Ανάλυσης με Πεπερασμένα Στοιχεία (Finite Element Analysis, FEA) και των σχεδιαστικών προγραμμάτων CAD (Computer-Aided Design) και να συνδέσει τα δύο αυτά επιστημονικά πεδία. Χάριν αυτής είμαστε σε θέση να ενισχύσουμε τη μεθοδολογία της κλασικής Ανάλυσης με Πεπερασμένα Στοιχεία με τις δυνατότητες του CAD. Στις μέρες μας, είναι πολύ σημαντικό να μπορούμε να μετατρέπουμε δεδομένα του CAD σε αντίστοιχα που μπορεί να χρησιμοποιήσει η IGA, προκειμένου εύκολα και αποδοτικά να είμαστε σε θέση αναλύουμε νέα σχέδια (φορείς) κατά την ανάπτυξή τους, γεγονός δύσκολο καθώς η κάθε κατηγορία προγραμμάτων προσεγγίζει με διαφορετικό υπολογιστικό τρόπο τη γεωμετρία. Η προτεινόμενη μέθοδος χρησιμοποιεί ως συναρτήσεις βάσης τις NURBS, δηλαδή τη πιο διαδεδομένη βάση που χρησιμοποιείται από πλειάδα προγραμμάτων CAD. Αυτό μας επιτρέπει να σχεδιάζουμε, ελέγχουμε και αναπροσαρμόζουμε τα προσομοιώματα των αναλύσεων μας με μία κίνηση χρησιμοποιώντας ένα κοινό σύνολο δεδομένων.

Η συγκεκριμένη μεταπτυχιακή περιλαμβάνει δύο κύριες ενότητες. Η πρώτη ενότητα πραγματεύεται το θεωρητικό υπόβαθρο της μεθόδου και η δεύτερη διάφορες εφαρμογές μέσω των οποίων καταλήγω σε χρήσιμα συμπεράσματα. Ειδικότερα, στην πρώτη ενότητα περιγράφω λεπτομερώς τη μεθοδολογία και δίνω ιδιαίτερη έμφαση σε βασικούς όρους, όπως ομάδα ισογεωμετρικών στοιχείων (patch), ισογεωμετρικό στοιχείο (isogeometric element), σημείο ελέγχου (control point), control polygon, convex hull, συναρτήσεις B-SPLine (Basis Smooth Polynomial Line), αναδρομικός τύπος Cox-de Boor, πολυωνυμικός βαθμός των B-SPLine, NURBS (Non Uniform Rational B-SPLines), B-SPLine καμπύλη, B-SPLine επιφάνεια, B-SPLine στερεό, κόμβος (knot), διάνυσμα κόμβων (knot vector), χώρος δεικτών (index space), παραμετρικός χώρος (parameter space), φυσικός χώρος (physical space). Τέλος, θα περιγράψω πως μπορούμε να βελτιώσουμε ένα δίκτυο ισογεωμετρικών στοιχείων. Στη δεύτερη ενότητα, παραθέτω με κάθε λεπτομέρεια τις πιο βασικές από τις εφαρμογές (γραμμική στατική ανάλυση) που έχω πραγματοποιήσει με τη μέθοδο αυτή. Κάθε πρόβλημα επιλύεται και με πεπερασμένα στοιχεία. Μέσω της σύγκρισης των αποτελεσμάτων της IGA με τα αντίστοιχα της FEA, καθώς επίσης και με τα ήδη υπάρχοντα στη διεθνή βιβλιογραφία και τις αναλυτικές λύσεις, έχω εμπεδώσει τη συγκεκριμένη μέθοδο, αποδείξει την αποδοτικότητά της (ακόμη και σε φορείς με πολύπλοκη γεωμετρία) και συνειδητοποιήσει ότι πρόκειται για μία πανίσχυρη επέκταση της κλασικής FEA. Προς την κατεύθυνση αυτή έχουν συμβάλει καθοριστικά και οι παραμετρικές διερευνήσεις, οι οποίες με βοήθησαν να μετρήσω τον αντίκτυπο σημαντικών χαρακτηριστικών, όπως των σημείων ελέγχου, των κόμβων και της τάξης των συναρτήσεων B-SPLine.

ABSTRACT

My thesis' primary goal is to introduce IsoGeometric Analysis (IGA). The development of this method was motivated by the existing gap between the worlds of Finite Element Analysis (FEA) and Computer-Aided Design (CAD), so its initial purpose is to unify the fields of FEA and CAD. IGA is a recently developed computational approach that give us the opportunity to integrate Finite Element Analysis into conventional NURBS-based CAD design tools. Currently, it is necessary to convert data between CAD and FEA packages to analyze new designs during development, a difficult task since the computational geometric approach for each is different. This method employs complex NURBS geometry (the basis of most CAD packages) in the FEA application directly. This allows models to designed, tested and adjusted in one go, using a common data set. I have selected NURBS as the initial basis, because it's the most widely used computational geometry technology in engineering design. That's why I will introduce them with an initial focus on geometric design and the particular features that make this technology unique.

In order to present this method with optimum way, my thesis includes two parts. Part 1 introduces the theory behind Isogeometric Analysis. I will analyze the way it works and I will explain in details IGA's keywords, such as patch, isogeometric element, control point, control polygon, convex hull, B-SPLine functions (Basis Smooth Polynomial Line functions), Cox-de Boor recursion formula, polynomial order of B-SPLines, NURBS (Non Uniform Rational Basis SPLines), B-SPLine curve, B-SPLine surface, B-SPLine solid, knot, knot vector, index space, parameter space, physical space. Lastly, I will describe how refinement in IGA is carried out. In Part 2, I will present again in details applications of this method. For every problem (static linear analysis), I have executed parameter investigation in order to research the affection of control points, knots and B-SPLines' polynomial order on the results. I have solved the same problems with classic Finite Element Method. Comparing the results, I will come into very interesting and fundamental deductions. With these applications I have arrived at the conclusion that IGA is simply an expansion and powerful generalization of traditional FEA.

The proposed modeling method uses NURBS as shape functions. The performance of the proposed modeling is demonstrated by comparing the numerical predictions with existing experimental results in the literature, analytic solutions and Finite Element Analysis' corresponding results. The results show that the proposed IGA predicts accurately the static linear elastic behavior of structures with complex geometry achieving numerical robustness and computational efficiency.

Ευχαριστίες

Θα ήθελα να ευχαριστήσω ιδιαίτερα τον Καθηγητή του Εργαστηρίου Στατικής & Αντισεισμικών Ερευνών και Διευθυντή του τομέα Δομοστατικής της Σχολής Πολιτικών Μηχανικών του Εθνικού Μετσόβιου Πολυτεχνείου και επιβλέποντα της μεταπτυχιακής μου εργασίας, κ. Παπαδρακάκη Μανόλη, για την καθοδήγησή του, την πίστη στις δυνατότητές μου, το γεγονός ότι αποτελεί υπόδειγμα τόσο επιστήμονα όσο και ανθρώπου για μένα σε μία εποχή έλλειψης υγιών προτύπων αλλά κυρίως επειδή η ενασχόληση με το επιστημονικό του πεδίο έδωσε νόημα στις σπουδές μου και αποτέλεσε κίνητρο για τη συνέχισή τους.

Θα ήθελα να ευχαριστήσω ιδιαίτερα τον Πρόεδρο του Ιδρύματος Παιδείας και Ευρωπαϊκού Πολιτισμού, κ. Ν. Τρίχα, για την εμπιστοσύνη που έδειξε στο πρόσωπό μου καθώς το Ίδρυμα του με επέλεξε ως υπότροφο και με στήριξη οικονομικά κατά τη διάρκεια των μεταπτυχιακών μου σπουδών στο Διατμηματικό Πρόγραμμα «Δομοστατικός Σχεδιασμός και Ανάλυση Κατασκευών». Η οικονομική ενίσχυση ήταν καθοριστική για την απρόσκοπτη επιτυχημένη μου πορεία, ειδικά δε στην πρωτοφανή περίοδο οικονομικής κρίσης που βιώνει η χώρα μας.

Τέλος, νιώθω την ανάγκη να ευχαριστήσω βαθύτατα τον αδερφό μου Καρακίτσιο Αλέξανδρο για την ηθική στήριξη και συμπαράσταση καθ' όλη τη διάρκεια των σπουδών μου.

Thanks to

I would like to thank especially the Professor of Static & Aseismic Research Laboratory and Director of Department of Structural Engineering (National Technical University of Athens) and supervisor of my thesis, Mr Papadrakakis Manolis, for being a role model for me and for believing in my potential.

I would like to thank especially the Director of Foundation for Education and European Culture, Mr N. Trichas, for his financial support, which was essential in order to finish successfully my postgraduate studies in MSc “Analysis & Design of Earthquake Resistant Structures”.

Last but not least, I want to thank my brother Karakitsios Alexandros for his support.

CONTENTS

1 The Theory behind the Isogeometric Analysis.....	11
1.1 B-SPLINE	13
1.1.1 Knot Vector	14
1.1.2 Basis Functions.....	15
• De Boor's algorithm.....	15
• Example 1 (De Boor's algorithm)	16
• Important Features.....	23
• Continuity	24
1.1.3 B-SPLINE Geometry.....	26
• B-SPLINE Curve	26
• Example 2 (B-SPLINE Curve)	28
• B-SPLINE Surface	29
• Example 3 (B-SPLINE Surface)	30
• B-SPLINE Solid	34
1.1.4 Refinement.....	35
• Knot Insertion.....	35
• Example 4 (Knot Insertion)	36
• Order Elevation	38
• Example 5 (Order Elevation).....	38
1.2 NURBS	41
1.2.1 NURBS Basis Functions.....	41
1.2.2 Derivatives of NURBS Basis Functions	44
1.3 Multiple Patches	45
1.4 NURBS Mesh Generation.....	47
1.4.1 Basis Features' Selection.....	47
1.4.2 Polynomial Orders' Selection	48
1.4.3 Knot Vectors' Selection	48
1.4.4 Control Points' Selection.....	48
1.5 Comparison between IGA and FEA Code Architecture	49
1.5.1 Code Architecture	49
1.5.2 Similarities and Differences	52
2 Applications	54
2.1 Introduction (2D Problem)	59
2.2 Control Points/ Nodes: 33 & Shape Functions: Linear	60
2.2.1 Isogeometric Analysis	60
• Axis ξ	62
• Axis η	69
• Combinations Axes ξ, η (ΞH).....	71
• Control Net	72
• Index Space	73
• Parameter Space	74
• Physical Space	75
• Elasticity Matrix [E]	77
• Deformation Matrix [B]..	77
• Local Stiffness Matrix [k°].....	80
• Total Stiffness Matrix [K]	86
• Control Points' External Forces {P}	87
• Control Points' Displacements {U}	87
• Stress Field at Gauss Points	89

2.2.2 Finite Element Analysis	92
• 2D 4-sided 4-noded Finite Element	95
• Shape Functions	95
• Elasticity Matrix [E]	96
• Deformation Matrix [B]	96
• Local Stiffness Matrix [k^e]	97
• Control Net	99
• Parameter Space	100
• Physical Space	100
• Total Stiffness Matrix [K]	101
• Nodes' External Forces {P}	101
• Nodes' Displacements {U}	101
• Stress Field at Gauss Points	104
2.2.3 Comparison	109
• Shape Functions	110
• Control/ Node Net	111
• Parameter Space	111
• Physical Space	112
• Total Stiffness Matrix [K]	113
• Control Points'/ Nodes' Displacements {U}	114
• Stress Field at Gauss Points	116
2.3 Control Points/ Nodes: 33 & Shape Functions: Quadratic	117
2.3.1 Isogeometric Analysis	117
• Axis ξ	119
• Axis η	128
• Combinations Axes ξ, η (ExH)	132
• Control Net	133
• Index Space	134
• Parameter Space	135
• Physical Space	136
• Elasticity Matrix [E]	138
• Deformation Matrix [B]	138
• Local Stiffness Matrix [k^e]	141
• Total Stiffness Matrix [K]	147
• Control Points' External Forces {P}	148
• Control Points' Displacements {U}	148
• Stress Field at Gauss Points	150
2.3.2 Finite Element Analysis	154
• Isoparametric 2D 4-sided 9-noded (Lagrange) Finite Element	155
• Shape Functions	155
• Elasticity Matrix [E]	156
• Deformation Matrix [B]	156
• Local Stiffness Matrix [k^e]	156
• Control Net	158
• Parameter Space	159
• Physical Space	159
• Total Stiffness Matrix [K]	160
• Nodes' External Forces {P}	160
• Nodes' Displacements {U}	160
• Stress Field at Gauss Points	163
2.3.3 Comparison	166
• Shape Functions	167
• Control/ Node Net	168
• Parameter Space	168
• Physical Space	169
• Total Stiffness Matrix [K]	170
• Control Points'/ Nodes' Displacements {U}	171
• Stress Field at Gauss Points	173
Literature	175

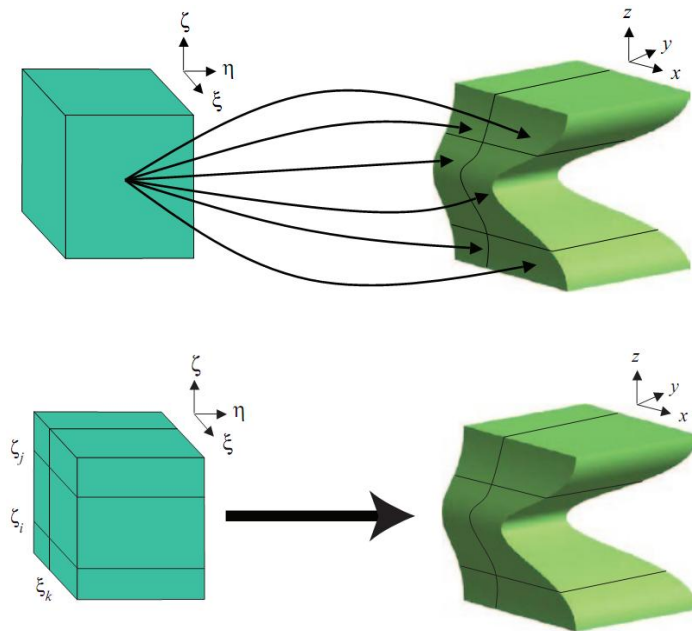


NATIONAL TECHNICAL UNIVERSITY OF ATHENS
SCHOOL OF CIVIL ENGINEERING
DEPARTMENT OF STRUCTURAL ENGINEERING
STATIC & ASEISMIC RESEARCH LABORATORY
ACADEMIC YEAR 2010-2011

MSc in ANALYSIS & DESIGN of EARTHQUAKE RESISTANCE STRUCTURE

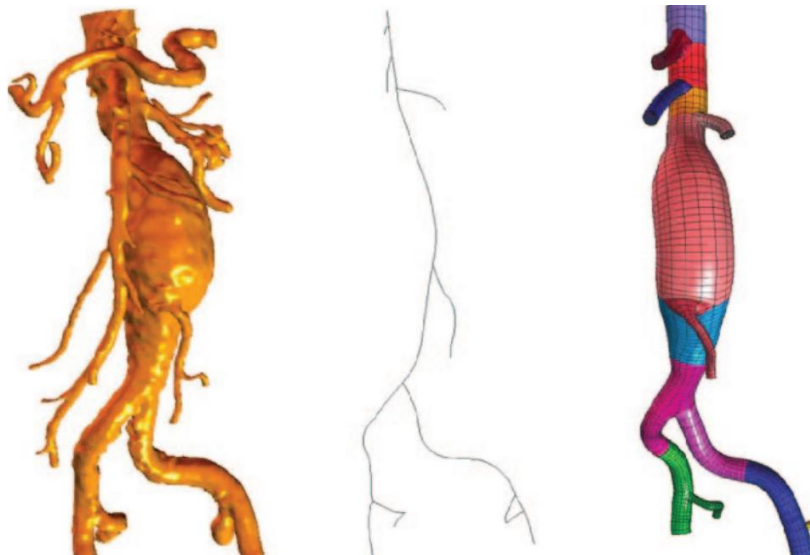
ISOGEOMETRIC ANALYSIS WITH B-SPLINES & NURBS

CHAPTER 1 The Theory behind the Isogeometric Analysis



CONTENTS

1.1 B-SPLine	13
1.1.1 Knot Vector	14
1.1.2 Basis Functions.....	15
• De Boor's algorithm	15
• Example 1 (De Boor's algorithm)	16
• Important Features.....	23
• Continuity.....	24
1.1.3 B-SPLine Geometry.....	26
• B-SPLine Curve	26
• Example 2 (B-SPLine Curve)	28
• B-SPLine Surface	29
• Example 3 (B-SPLine Surface)	30
• B-SPLine Solid.....	34
1.1.4 Refinement.....	35
• Knot Insertion	35
• Example 4 (Knot Insertion).....	36
• Order Elevation.....	38
• Example 5 (Order Elevation).....	38
1.2 NURBS	41
1.2.1 NURBS Basis Functions.....	41
1.2.2 Derivatives of NURBS Basis Functions	44
1.3 Multiple Patches	45
1.4 NURBS Mesh Generation.....	47
1.4.1 Basis Features' Selection.....	47
1.4.2 Polynomial Orders' Selection	48
1.4.3 Knot Vectors' Selection	48
1.4.4 Control Points' Selection.....	48
1.5 Comparison between IGA and FEA Code Architecture	49
1.5.1 Code Architecture	49
1.5.2 Similarities and Differences	52



1.

THE THEORY BEHIND THE ISOGEOMETRIC ANALYSIS

1.1 B-SPLine

IGA uses NURBS (Non-Uniform Rational Basis SPLines) as shape functions. With this mathematical model (commonly used in computer graphics), I can generate curves and surfaces and handle with great flexibility and precision both analytic and freeform shapes. NURBS are built from B-SPLines (Basis Smooth Polynomial Lines), which are described below.

In classical Finite Element Analysis (**FEA**), the parameter space ("reference/ parent element") is local to individual elements and is mapped into a single element in the physical space. Each finite element has its own mapping from the reference element.

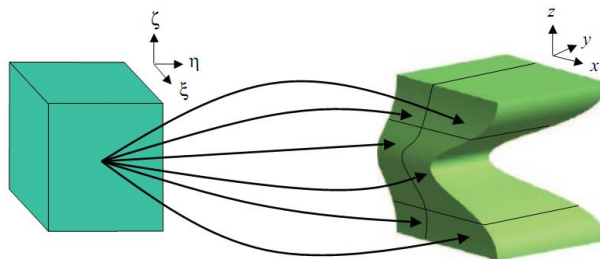


Figure 1.1. Parameter (1 element) and physical space (6 finite elements). (FEA)

In Isogeometric Analysis (**IGA**), the B-SPLine parameter space is local to the entire patch rather than element. The B-SPLine mapping (a single map) takes a patch of multiple elements in the parameter space into the physical space, but the mapping itself is global to the whole patch, rather than to elements. **Patches** play the role of subdomains within which element types and material models are assumed to be uniform. Many simple domains can be represented by a single patch. **Internal knots** partition the patch into elements.

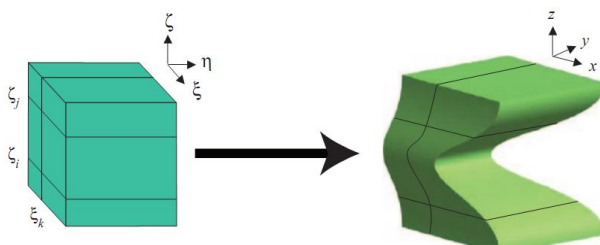


Figure 1.2. Parameter (6 elements) and physical space (6 isogeometric elements). (IGA)

1.1.1 Knot Vector

A **knot vector** in one dimension is a non-decreasing coordinates' set in the parameter space, written:

$$\Xi = \{\xi_1, \xi_2, \dots, \xi_{n+p+1}\} \quad (1.1)$$

where:

- $\xi_i \in \mathbb{R}$: **parametric coordinate** of i^{th} knot value.
- $i = 1, 2, \dots, n+p+1$: **knot index**. Knot values may be repeated, that is, more than one knot may take on the same value. This fact has important implications for the basis' properties.
- **p: basis functions' polynomial order**. Alternatively, I can use polynomial constant $K=p+1$.
- **n: number of basis functions/ control points**. I combine linearly basis functions in order to construct B-Spline curve.

Knots partition **parameter space** into **isogeometric elements**. Element boundaries in the physical space are simply the images of knot lines under the B-Spline mapping. Figure 1.2 shows a 3-D parameter space ($\Xi \times \Eta \times \Zeta$) and a patch. As far as this patch is concerned, there are 3 knots (2 spans) in the parametric axis ξ , 2 knots (1 span) in the parametric axis η and 4 knots (3 spans) in the parametric axis ζ . These knots partition the patch into $2 \cdot 1 \cdot 3 = 6$ isogeometric elements. Every face ξ, η, ζ has correspondingly 6, 7, 5 knot lines.

There are two different views as far as the distinction between "elements" and "patches" is concerned.

- According to Kagan et al., the patches themselves are referred to as elements. This is not unreasonable as the parameter space is local to patches and a finite element code must include a loop over the patches during assembly.
- Meanwhile, I choose the alternate Hughes' view that **patches** are subdomains comprised of many elements, namely the "knot spans", because it seems more appropriate as, in my work, numerical quadrature is carried out at the knot span level. Furthermore, in the case of B-SPLines, the functions are piecewise polynomials where the different "pieces" join along knot lines. In this way the functions are C^∞ within an element. Lastly, surprisingly complicated domains can be described by a single patch. Describing such domains as being comprised of one element seems inconsistent with the traditional notion of what an element is.

I use **uniform open knot vectors**, which are the standard in the CAD literature.

- **Uniform** knot vector means that the knots are equally spaced in the parameter space. If they are unequally spaced, the knot vector is non-uniform.
- A knot vector is said to be **open** if its first and last knot values appear $p+1$ times. In one dimension, basis functions formed from open knot vectors are interpolatory at

the ends of the parameter space interval $[\xi_1, \dots, \xi_{n+p+1}]$ and at the corners of patches in multiple dimensions, but they are not, in general, interpolatory at interior knots. This is a distinguishing feature between IGA's **knots** and FEA's **nodes**. A further consequence of open knot vectors in multiple dimensions is that the boundary of a B-SPLine object with d parametric dimensions is itself a B-SPLine object of dimension $d-1$. For example, each edge of a B-SPLine surface is itself a B-SPLine curve.

1.1.2 Basis functions

De Boor's algorithm

In the mathematical subfield of numerical analysis, **B-SPLine** is a SPLine function that has minimal support with respect to a given degree (p), smoothness and domain partition (knot vector). B-SPLines were investigated as early as the nineteenth century by Nikolai Lobachevsky from Kazan State University, Russia. A fundamental theorem states that every SPLine function of a given degree, smoothness and domain partition, can be uniquely represented as a linear combination of B-SPLines of that same degree and smoothness and over that same partition.

The term "B-SPLine" was coined by Isaac Jacob Schoenberg and is short for basis SPLine. B-SPLines can be evaluated in a numerically stable way by the de Boor algorithm. Simplified, potentially faster variants of the de Boor algorithm have been created but they suffer from comparatively lower stability.

With a knot vector and n control points in hand, the n B-SPLine basis functions are defined recursively starting with piecewise constants ($p=0$). Every B-SPLine function corresponds to a control point.

$$N_{i,0}(\xi) = \begin{cases} 1 & \text{if } \xi_i \leq \xi < \xi_{i+1} \\ 0 & \text{otherwise} \end{cases} \quad (1.2)$$

For $p=1,2,3,\dots$, they are defined by:

$$N_{i,p}(\xi) = \frac{\xi - \xi_i}{\xi_{i+p} - \xi_i} \cdot N_{i,p-1}(\xi) + \frac{\xi_{i+p+1} - \xi}{\xi_{i+p+1} - \xi_{i+1}} \cdot N_{i+1,p-1}(\xi) \quad (1.3)$$

where $i=1,\dots,n$.

This is referred to as the **Cox-de Boor recursion formula** (Cox 1971; de Boor 1972).

It is worth mentioning that according to Fisher, the B-SPLine basis is equal to:

$$N_{1,K}, \dots, N_{n,K}$$

where $N_{i,K}$ is constructed using the following recursive formula:

$$N_{i,l}(\xi) = \begin{cases} 1 & \text{if } \xi_i \leq \xi < \xi_{i+1} \\ 1 & \text{if } i=n \text{ and } \xi = \xi_{n+1} \\ 0 & \text{otherwise} \end{cases} \quad (1.4)$$

$$N_{i,k}(\xi) = \frac{\xi - \xi_i}{\xi_{i+k-1} - \xi_i} \cdot N_{i,k-1}(\xi) + \frac{\xi_{i+k} - \xi}{\xi_{i+k} - \xi_{i+1}} \cdot N_{i+1,k-1}(\xi) \quad (1.5)$$

where $i=1,\dots,n$ and $k=2,\dots,K$.

K is BSpline's polynomial order according to Fisher. Because the denominators in the second relation can be zero, the convention $0/0=0$ is used; in other words $0x(.)=0$ even if $(.)$ is undefined. When $i=n$, the second term is omitted. The connection between Fisher's K and Hughes' p is given by the following mathematical relation:

$$K = p + 1 \quad (1.6)$$

Example 1

In order to produce the 6 quadratic ($p=2$, $K=3$) B-Spline basis functions (its support is three knot spans) for $n=6$ control points, I have to calculate the $6+1=7$ corresponding linear B-Spline functions (its support is two knot spans) and the $6+2=8$ constant B-Spline functions (its support is one knot span). I work as follows using Fisher's K :

I calculate the open uniform knot vector Ξ , which has $n+p+1=6+2+1=9$ knot values. Its first (0) and last (4) knot values appear $p+1=2+1=3$ times (open knot vector). The remaining $9-2\cdot3=3$ knot values are 1, 2, 3 (equally spaced, uniform knot vector).

$$\Xi = \{0, 0, 0, 1, 2, 3, 4, 4, 4\}$$

I form below the $n+2=8$ constant B-SPLines.

$$N_{i,l}(\xi) = \begin{cases} 1 & \text{if } \xi_i \leq \xi < \xi_{i+1} \\ 1 & \text{if } i=n \text{ and } \xi = \xi_{n+1} \\ 0 & \text{otherwise} \end{cases}$$

 K=1

- $N_{1,1}(\xi)$:

$$N_{1,1} \quad \xi = \begin{cases} 1 & \text{if } \xi_1 \leq \xi < \xi_2 \Leftrightarrow 0 \leq \xi < 0 \Rightarrow \xi = 0 \\ 0 & \text{otherwise} \end{cases}$$

- $N_{2,1}(\xi)$:

$$N_{2,1} \quad \xi = \begin{cases} 1 & \text{if } \xi_2 \leq \xi < \xi_3 \Leftrightarrow 0 \leq \xi < 0 \Rightarrow \xi = 0 \\ 0 & \text{otherwise} \end{cases}$$

- $N_{3,1}(\xi)$:

$$N_{3,1} \quad \xi = \begin{cases} 1 & \text{if } \xi_3 \leq \xi < \xi_4 \Leftrightarrow 0 \leq \xi < 1 \\ 0 & \text{otherwise} \end{cases}$$

- $N_{4,1}(\xi)$:

$$N_{4,1} \quad \xi = \begin{cases} 1 & \text{if } \xi_4 \leq \xi < \xi_5 \Leftrightarrow 1 \leq \xi < 2 \\ 0 & \text{otherwise} \end{cases}$$

- $N_{5,1}(\xi)$:

$$N_{5,1} \quad \xi = \begin{cases} 1 & \text{if } \xi_5 \leq \xi < \xi_6 \Leftrightarrow 2 \leq \xi < 3 \\ 0 & \text{otherwise} \end{cases}$$

- $N_{6,1}(\xi)$:

$$N_{6,1} \quad \xi = \begin{cases} 1 & \text{if } \xi_6 \leq \xi < \xi_7 \Leftrightarrow 3 \leq \xi < 4 \\ 0 & \text{otherwise} \end{cases}$$

- $N_{7,1}(\xi)$:

$$N_{7,1} \quad \xi = \begin{cases} 1 & \text{if } \xi_7 \leq \xi < \xi_8 \Leftrightarrow 4 \leq \xi < 4 \Rightarrow \xi = 4 \\ 0 & \text{otherwise} \end{cases}$$

- $N_{8,1}(\xi)$:

$$N_{8,1} \quad \xi = \begin{cases} 1 & \text{if } \xi_8 \leq \xi < \xi_9 \Leftrightarrow 4 \leq \xi < 4 \Rightarrow \xi = 4 \\ 0 & \text{otherwise} \end{cases}$$

Then, I produce the $n+1=7$ linear B-Spline functions.

$$\begin{aligned} N_{i,k}(\xi) &= \frac{\xi - \xi_i}{\xi_{i+k-1} - \xi_i} \cdot N_{i,k-1}(\xi) + \frac{\xi_{i+k} - \xi}{\xi_{i+k} - \xi_{i+1}} \cdot N_{i+1,k-1}(\xi) \xrightarrow{k=2} \\ N_{i,2}(\xi) &= \frac{\xi - \xi_i}{\xi_{i+1} - \xi_i} \cdot N_{i,1}(\xi) + \frac{\xi_{i+2} - \xi}{\xi_{i+2} - \xi_{i+1}} \cdot N_{i+1,1}(\xi) \end{aligned}$$

Isogeometric Analysis

 K=2

- $N_{1,2}(\xi)$:

$$N_{1,2}(\xi) = \frac{\xi - \xi_1}{\xi_2 - \xi_1} \cdot N_{1,1}(\xi) + \frac{\xi_3 - \xi}{\xi_3 - \xi_2} \cdot N_{2,1}(\xi) = \frac{\xi - 0}{0 - 0} \cdot N_{1,1}(\xi) + \frac{0 - \xi}{0 - 0} \cdot N_{2,1}(\xi) \Rightarrow$$

$$N_{1,2}(\xi) = 0 \cdot N_{1,1}(\xi) + 0 \cdot N_{2,1}(\xi) \Rightarrow \boxed{N_{1,2}(\xi) = 0}$$

- $N_{2,2}(\xi)$:

$$N_{2,2}(\xi) = \frac{\xi - \xi_2}{\xi_3 - \xi_2} \cdot N_{2,1}(\xi) + \frac{\xi_4 - \xi}{\xi_4 - \xi_3} \cdot N_{3,1}(\xi) = \frac{\xi - 0}{0 - 0} \cdot N_{2,1}(\xi) + \frac{1 - \xi}{1 - 0} \cdot N_{3,1}(\xi) \Rightarrow$$

$$N_{2,2}(\xi) = 1 - \xi \cdot N_{3,1}(\xi) \Rightarrow$$

$$N_{2,2}(\xi) = \begin{cases} 1 - \xi \cdot 1 & \text{if } 0 \leq \xi < 1 \\ 1 - \xi \cdot 0 & \text{otherwise} \end{cases} \Rightarrow \boxed{N_{2,2}(\xi) = \begin{cases} -\xi + 1 & \text{if } 0 \leq \xi < 1 \\ 0 & \text{otherwise} \end{cases}}$$

- $N_{3,2}(\xi)$:

$$N_{3,2}(\xi) = \frac{\xi - \xi_3}{\xi_4 - \xi_3} \cdot N_{3,1}(\xi) + \frac{\xi_5 - \xi}{\xi_5 - \xi_4} \cdot N_{4,1}(\xi) = \frac{\xi - 0}{1 - 0} \cdot N_{3,1}(\xi) + \frac{2 - \xi}{2 - 1} \cdot N_{4,1}(\xi) \Rightarrow$$

$$N_{3,2}(\xi) = \xi \cdot N_{3,1}(\xi) + 2 - \xi \cdot N_{4,1}(\xi) \Rightarrow$$

$$N_{3,2}(\xi) = \begin{cases} \xi \cdot 1 + 2 - \xi \cdot 0 & \text{if } 0 \leq \xi < 1 \\ \xi \cdot 0 + 2 - \xi \cdot 1 & \text{if } 1 \leq \xi < 2 \\ 0 & \text{otherwise} \end{cases} \Rightarrow \boxed{N_{3,2}(\xi) = \begin{cases} \xi & \text{if } 0 \leq \xi < 1 \\ -\xi + 2 & \text{if } 1 \leq \xi < 2 \\ 0 & \text{otherwise} \end{cases}}$$

- $N_{4,2}(\xi)$:

$$N_{4,2}(\xi) = \frac{\xi - \xi_4}{\xi_5 - \xi_4} \cdot N_{4,1}(\xi) + \frac{\xi_6 - \xi}{\xi_6 - \xi_5} \cdot N_{5,1}(\xi) = \frac{\xi - 1}{2 - 1} \cdot N_{4,1}(\xi) + \frac{3 - \xi}{3 - 2} \cdot N_{5,1}(\xi) \Rightarrow$$

$$N_{4,2}(\xi) = \xi - 1 \cdot N_{4,1}(\xi) + 3 - \xi \cdot N_{5,1}(\xi) \Rightarrow$$

$$N_{4,2}(\xi) = \begin{cases} \xi - 1 \cdot 1 + 3 - \xi \cdot 0 & \text{if } 1 \leq \xi < 2 \\ \xi - 1 \cdot 0 + 3 - \xi \cdot 1 & \text{if } 2 \leq \xi < 3 \\ 0 & \text{otherwise} \end{cases} \Rightarrow \boxed{N_{4,2}(\xi) = \begin{cases} \xi - 1 & \text{if } 1 \leq \xi < 2 \\ 3 - \xi & \text{if } 2 \leq \xi < 3 \\ 0 & \text{otherwise} \end{cases}}$$

- $N_{5,2}(\xi)$:

$$\boxed{N_{5,2}(\xi) = \begin{cases} \xi - 2 & \text{if } 2 \leq \xi < 3 \\ -\xi + 4 & \text{if } 3 \leq \xi < 4 \\ 0 & \text{otherwise} \end{cases}}$$

- $N_{6,2}(\xi)$:

$$\boxed{N_{6,2}(\xi) = \begin{cases} \xi - 3 & \text{if } 3 \leq \xi < 4 \\ 0 & \text{otherwise} \end{cases}}$$

- $N_{7,2}(\xi)$:

$$\boxed{N_{7,2}(\xi) = 0}$$

 K=3

Then, I calculate the n=6 quadratic B-SPLines functions.

$$N_{i,k}(\xi) = \frac{\xi - \xi_i}{\xi_{i+k-1} - \xi_i} \cdot N_{i,k-1}(\xi) + \frac{\xi_{i+k} - \xi}{\xi_{i+k} - \xi_{i+1}} \cdot N_{i+1,k-1}(\xi) \xrightarrow{k=3}$$

$$N_{i,3}(\xi) = \frac{\xi - \xi_i}{\xi_{i+2} - \xi_i} \cdot N_{i,2}(\xi) + \frac{\xi_{i+3} - \xi}{\xi_{i+3} - \xi_{i+1}} \cdot N_{i+1,2}(\xi)$$

- $N_{1,3}(\xi)$:

$$N_{1,3}(\xi) = \frac{\xi - \xi_1}{\xi_3 - \xi_1} \cdot N_{1,2}(\xi) + \frac{\xi_4 - \xi}{\xi_4 - \xi_2} \cdot N_{2,2}(\xi) = \frac{\xi - 0}{0 - 0} \cdot N_{1,2}(\xi) + \frac{1 - \xi}{1 - 0} \cdot N_{2,2}(\xi) \Rightarrow$$

$$N_{1,3}(\xi) = 0 \cdot N_{1,2}(\xi) + 1 - \xi \cdot N_{2,2}(\xi) \Rightarrow$$

$$N_{1,3}(\xi) = \begin{cases} 1 - \xi & \text{if } 0 \leq \xi < 1 \\ 0 & \text{otherwise} \end{cases}$$

- $N_{2,3}(\xi)$:

$$N_{2,3}(\xi) = \frac{\xi - \xi_2}{\xi_4 - \xi_2} \cdot N_{2,2}(\xi) + \frac{\xi_5 - \xi}{\xi_5 - \xi_3} \cdot N_{3,2}(\xi) = \frac{\xi - 0}{1 - 0} \cdot N_{2,2}(\xi) + \frac{2 - \xi}{2 - 0} \cdot N_{3,2}(\xi) \Rightarrow$$

$$N_{2,3}(\xi) = \xi \cdot N_{2,2}(\xi) + \frac{2 - \xi}{2} \cdot N_{3,2}(\xi) \Rightarrow$$

$$N_{2,3}(\xi) = \begin{cases} \xi \cdot (1 - \xi) + \frac{2 - \xi}{2} \cdot \xi = -\frac{3\xi^2}{2} + 2\xi & \text{if } 0 \leq \xi < 1 \\ \xi \cdot 0 + \frac{2 - \xi}{2} \cdot (2 - \xi) = \frac{\xi^2}{2} - 2\xi + 2 & \text{if } 1 \leq \xi < 2 \\ \xi \cdot 0 + \frac{2 - \xi}{2} \cdot 0 = 0 & \text{otherwise} \end{cases}$$

- $N_{3,3}(\xi)$:

$$N_{3,3}(\xi) = \frac{\xi - \xi_3}{\xi_5 - \xi_3} \cdot N_{3,2}(\xi) + \frac{\xi_6 - \xi}{\xi_6 - \xi_4} \cdot N_{4,2}(\xi) = \frac{\xi - 0}{2 - 0} \cdot N_{3,2}(\xi) + \frac{3 - \xi}{3 - 1} \cdot N_{4,2}(\xi) \Rightarrow$$

$$N_{3,3}(\xi) = \frac{\xi}{2} \cdot N_{3,2}(\xi) + \frac{3 - \xi}{2} \cdot N_{4,2}(\xi) \Rightarrow$$

$$N_{3,3}(\xi) = \begin{cases} \frac{\xi}{2} \cdot \xi + \frac{3 - \xi}{2} \cdot 0 = \frac{\xi^2}{2} & \text{if } 0 \leq \xi < 1 \\ \frac{\xi}{2} \cdot 2 - \xi + \frac{3 - \xi}{2} \cdot \xi - 1 = -\xi^2 + 3\xi - \frac{3}{2} & \text{if } 1 \leq \xi < 2 \\ \frac{\xi}{2} \cdot 0 + \frac{3 - \xi}{2} \cdot 3 - \xi = \frac{\xi^2}{2} - 3\xi + \frac{9}{2} & \text{if } 2 \leq \xi < 3 \\ \frac{\xi}{2} \cdot 0 + \frac{3 - \xi}{2} \cdot 0 = 0 & \text{otherwise} \end{cases}$$

- Similarly, I produce $N_{4,3}(\xi)$, $N_{5,3}(\xi)$ and $N_{6,3}(\xi)$.

Isogeometric Analysis

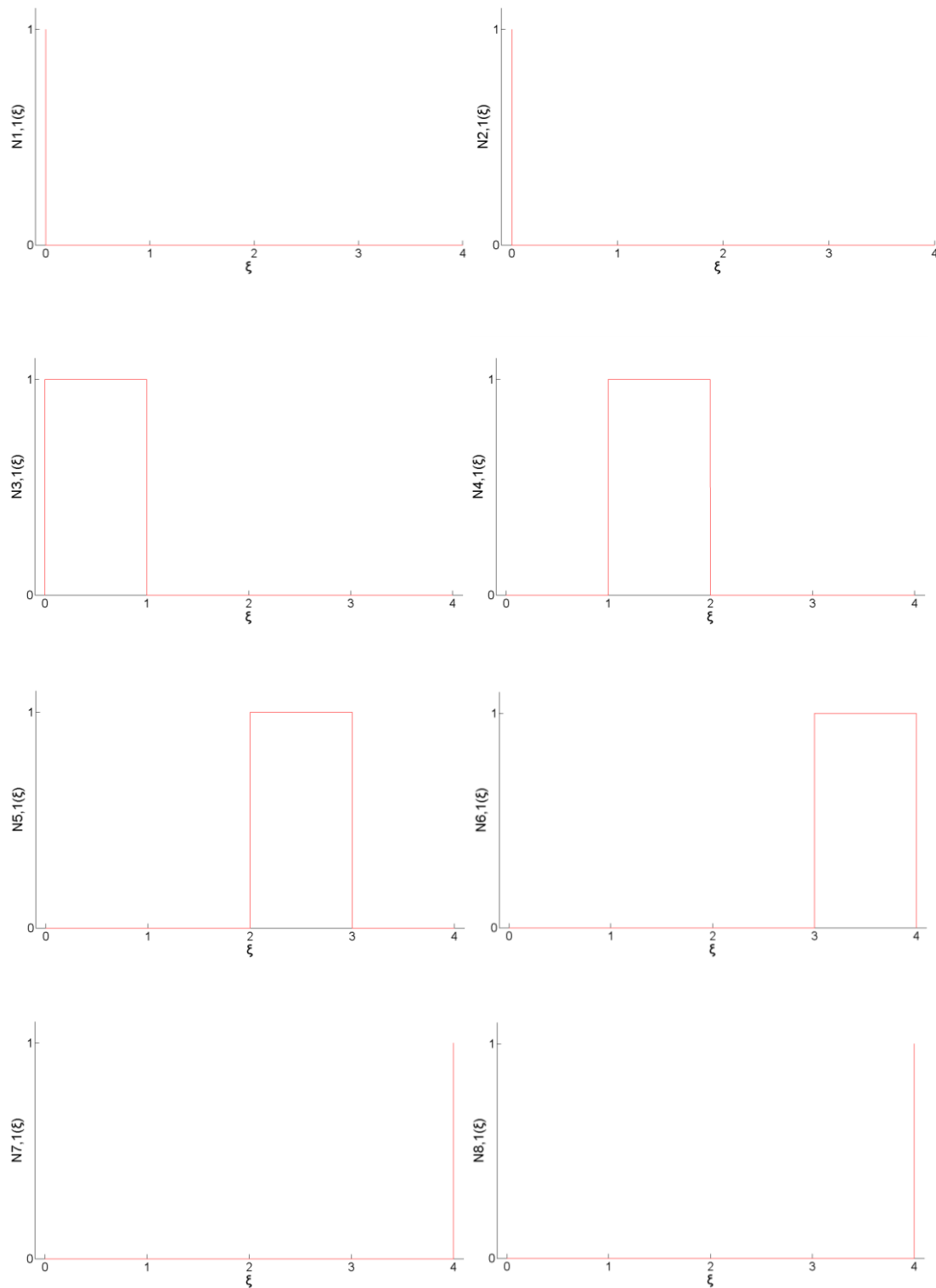


**Figure 1.3.a. Constant Basis SPLine functions for open, uniform knot vector
 $\Xi=\{0,0,0,1,2,3,4,4,4\}$.**

Isogeometric Analysis

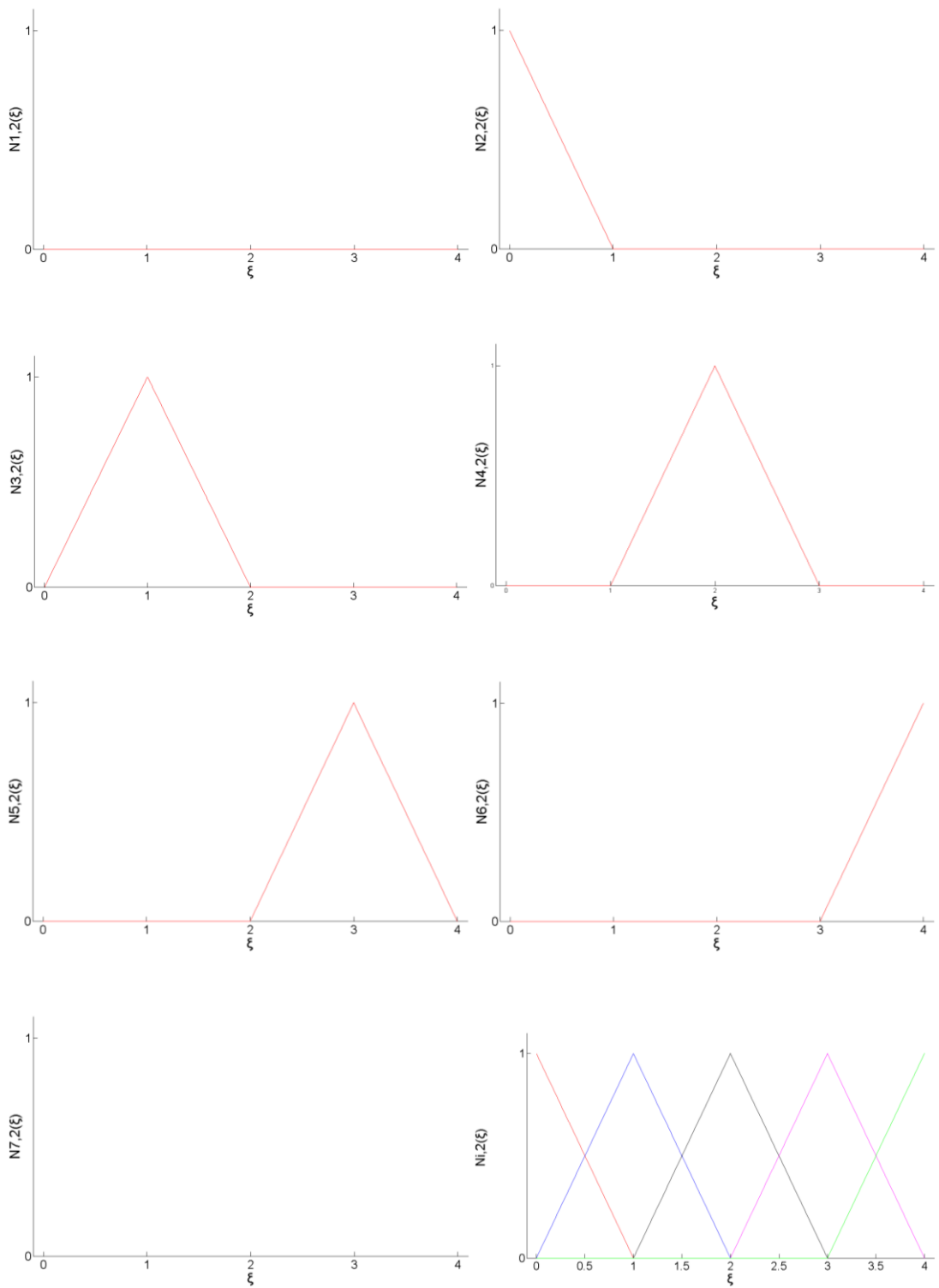


**Figure 1.3.b. Linear Basis SPLine functions for open, uniform knot vector
 $\Xi=\{0,0,0,1,2,3,4,4,4\}$.**

Isogeometric Analysis

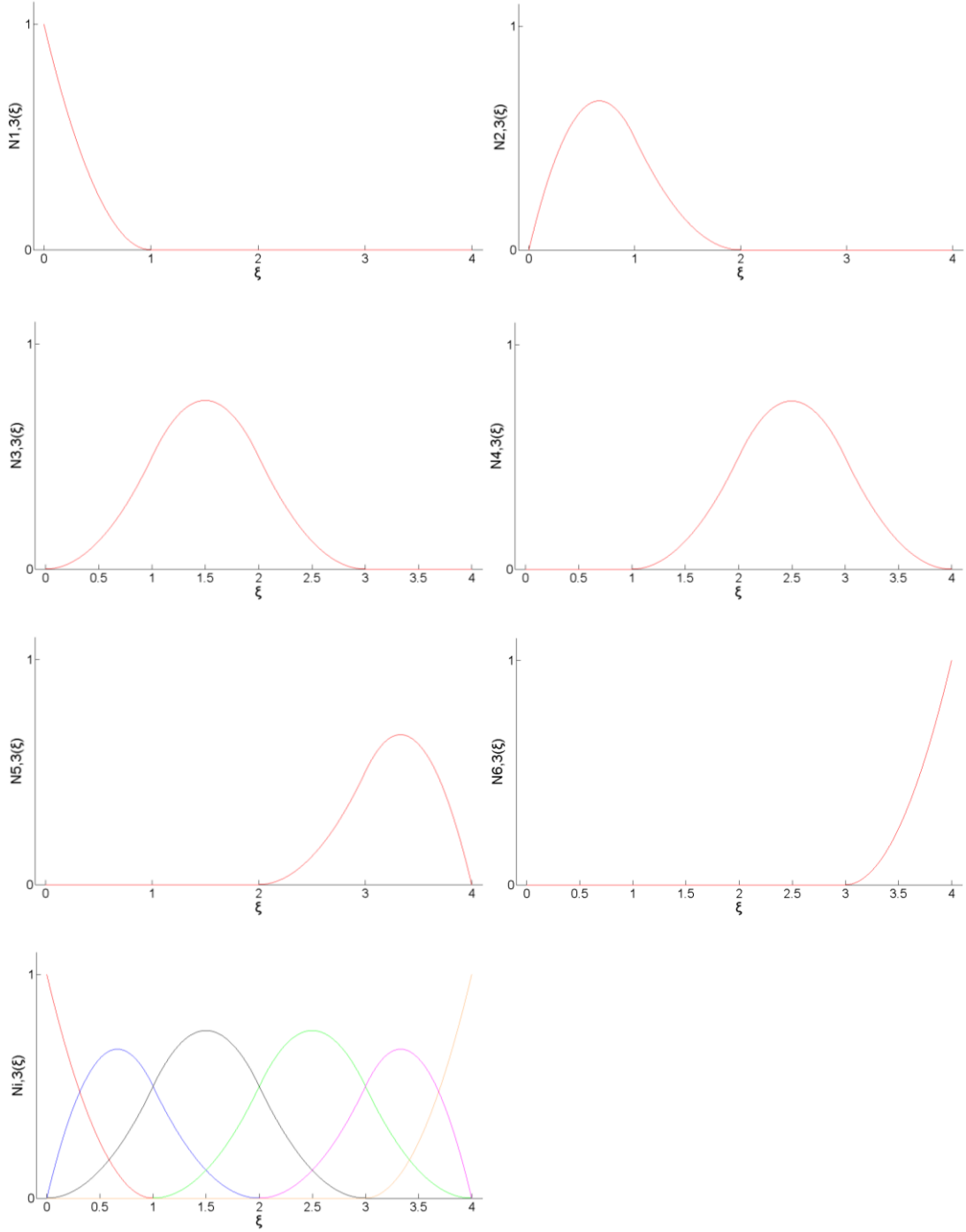


**Figure 1.3.c. Quadratic Basis SPLine functions for open, uniform knot vector
 $\Xi=\{0,0,0,1,2,3,4,4,4\}$.**

For constant and linear B-SPLine functions, we have the same result as for standard piecewise constant and linear finite element shape functions, respectively. Quadratic B-SPLine basis functions, however, differ from their FEA counterparts. They are each identical, but shifted relative to each other, whereas the shape of a quadratic finite element function depends on whether it corresponds to an internal node or an end node. This “homogeneous” pattern continues for the B-SPLines as we continue to higher-orders.

Important Features

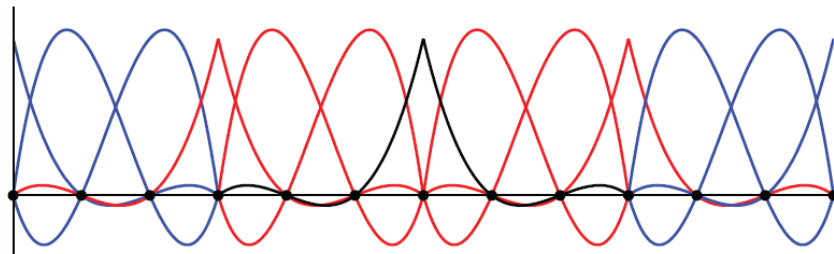
- ⊕ The basis constitutes a partition of unity, that is, for every ξ :

$$\sum_{i=1}^n N_{i,p}(\xi) = 1 \quad (1.7)$$

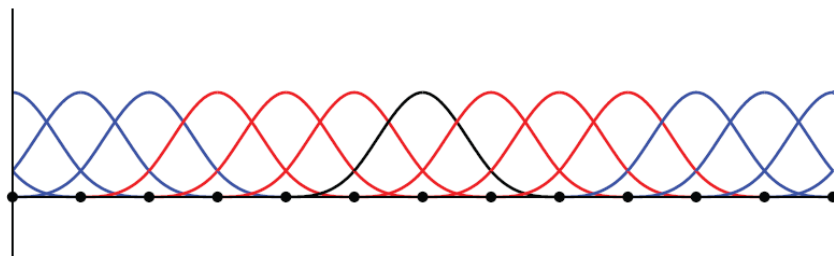
- ⊕ Each basis function is pointwise nonnegative over the entire domain, that is, for every ξ :

$$N_{i,p}(\xi) \geq 0 \quad (1.8)$$

- ⊕ One of the most distinctive features of isogeometric analysis, which has many extremely important implications for SPLines' use as a basis for analysis, is that each p^{th} order function has $p-1$ continuous derivatives across element boundaries (i.e. across knots).
- ⊕ The support of B-SPLine functions of order p is always $p+1$ knot spans. As a consequence, higher-order functions have support over much larger portions of the domain than do classical FEA functions. It is important to mention that this increasing support of the functions leads to increased skyline and not bandwidth in a numerical method.



(a) Standard cubic finite element basis functions with equally spaced nodes



(b) Cubic B-spline basis functions with equally spaced knots

Figure 1.4. Bandwidth comparison for FEA and B-SPLine functions.

The total number of functions that any given function shares support with (including itself) is $2p+1$ regardless of whether we are using an FEA basis or B-SPLines. We can observe that in Figure 1.4, which depicts cubic shape functions for both FEA and IGA. Regardless of whether I use the C^0 FEA cubics or the C^2 B-SPLine cubics, the bandwidth of the resulting matrices will be $2p+1=7$. In each case, the function in black has overlapping support with each of the six functions in red, as well as with itself.

Continuity

An essential B-SPLine's feature is that a B-SPLine of order p is interpolatory at the ends of the interval and at those interior knots which repeat themselves p times.

With the following non-uniform knot vector in hand,

$$\Xi = \{\xi_1, \xi_2, \xi_3, \xi_4, \xi_5, \xi_6, \xi_7, \xi_8, \xi_9, \xi_{10}, \xi_{11}\} = \{0, 0, 0, 1, 2, 3, 4, 4, 5, 5, 5\}$$

Figure 1.5 presents the corresponding 8 quadratic basis SPLine functions.

It is worth underlining that the use of a non-uniform knot vector allows us to obtain much richer behavior than is possible with a simple uniform one

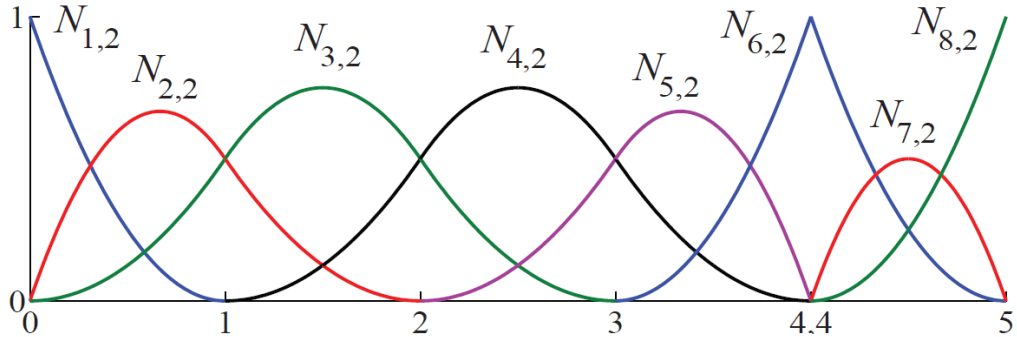


Figure 1.5. Quadratic basis functions for open, non-uniform knot vector

$$\Xi = \{0, 0, 0, 1, 2, 3, 4, 4, 5, 5, 5\}.$$

As far as Figure's 1.5 basis functions, they are interpolatory at the ends of the interval and also at $\xi=4$, the location of a twice repeated knot. At this repeated knot, only C^0 -continuity is attained. Elsewhere, the functions are C^1 -continuous.

In general, basis functions of order p have $p-m_i$ continuous derivatives across knot ξ_i , where m_i is knot values' ξ_i multiplicity in the knot vector. When the multiplicity of a knot value is exactly p , the basis is interpolatory at that knot. When the multiplicity is $p+1$, the basis becomes discontinuous and the patch boundary is formed.

This relationship between continuity and the multiplicity of the knots is even more apparent in Figure 1.6, in which we have a fourth order curve with differing levels of continuity at every element boundary.

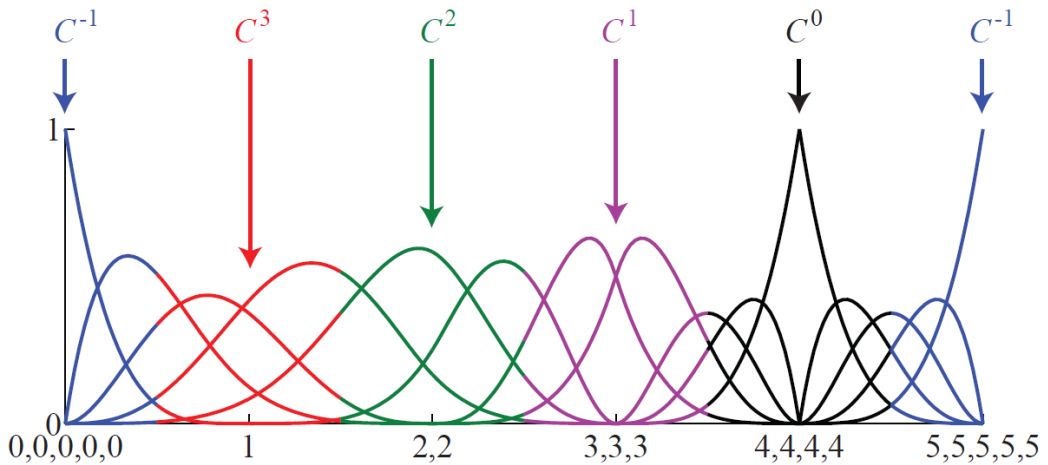


Figure 1.6. Quadratic ($p=4$) basis functions for an open, non-uniform knot vector
 $\Xi = \{0,0,0,0,0,1,2,2,3,3,3,4,4,4,4,5,5,5,5,5\}$.

At the first internal element boundary, $\xi=1$, the knot value appears only once in the knot vector and so we have the maximum level of continuity possible: $C^{p-1}=C^3$. At each subsequent internal knot value, the multiplicity is increased by one and so the number of continuous derivatives is decreased by one. Note, as before, that when a knot value is repeated p times, in this case at $\xi=4$, the C^0 basis is interpolatory. The basis is also interpolatory at the boundary of the domain, where the open knot vector demands that the first and last knot value be repeated $p+1$ times. The result is C^1 continuity, that is, the basis is fully discontinuous, naturally terminating the domain.

Observe that increasing the multiplicities of the knot values seems to have decreased the support of some of the functions. This is not a contradiction with the trend we observed previously as the support of each function $N_{i,p}$ still begins at knot ξ_i and ends at ξ_{i+p+1} . That is, the support of each function is still $p+1$ knot spans, but some of those knot spans have zero measure due to the repetition of knot values. Surprisingly, none of this has any effect on the bandwidth.

The continuity across an interior element boundary is a direct result of the polynomial order and the multiplicity of the corresponding knot value.

1.1.3 B-SPLine Geometry

B-SPLine Curve

In the computer science subfields of computer-aided design and computer graphics, the term B-SPLine frequently refers to a SPLine curve parameterized by SPLine functions that are expressed as linear combinations of B-splines (in the mathematical sense above). A B-SPLine is simply a generalization of a Bézier curve and it can avoid the Runge phenomenon without increasing the degree of the B-SPLine

B-SPLine curves in R^d are constructed by taking a linear combination of B-SPLine basis functions, just as in classical FEA. The vector-valued coefficients of the basis functions are referred to as **control points**. That is why the number of control points is equal to the number of basis functions. These are analogous to nodal coordinates in finite element analysis in that they are the coefficients of the basis functions, but the non-interpolatory nature of the basis does not lead to a concrete interpretation of the control point values.

Given n basis functions $N_{i,p}$ ($i=1,\dots,n$) and corresponding control points $B_i \in R^d$ ($i=1,\dots,n$), a piecewise-polynomial B-SPLine curve is given by:

$$C(\xi) = \sum_{i=1}^n N_{i,p}(\xi) \cdot B_i \quad (1.9)$$

Note that the index i in B_i serves to identify the control point and is not a reference to one of its d components. Piecewise linear interpolation of the control points gives the so-called **control polygon**.

B-SPLine curve has many important properties, that follow directly from the properties of their corresponding basis functions. I describe them as follows:

- B-SPLine curve of degree p has $p-1$ continuous derivatives in the absence of repeated knots or control points. In general, a curve will have at least as many continuous derivatives across an element boundary as its basis functions have across the corresponding knot value.
- B-SPLine curve inherits from its basis locality. Due to the compact support of the B-SPLine basis functions, moving a single control point can affect the geometry of no more than $p+1$ elements of the curve.
- B-SPLines obey a strong **convex hull** property. The non-negativity and partition of basis' unity properties, combined with functions' compact support, lead to the fact that a B-SPLine curve is completely contained within the convex hull defined by its control points. Convex hull of a curve of degree p is defined as the union of all of the convex hulls formed by $p+1$ successive control points.

Figure 1.7.a presents convex hulls for $p=1$ through $p=5$ for a given set of control points. Note, in particular, that the convex hull for a piecewise linear curve is just the control polygon itself. Figure 1.7.b shows the corresponding curves that we obtain by pairing these control points with the different bases. As the polynomial order increases, the curves become smoother and the effect of each individual control point is diminished.

We have 9 control points. Control Points 1 is the extreme left one. For a curve of degree p , in order to construct the convex hulls, I connect every control point with the p following control points. For Figure 1.7.a, I connect with linear lines the following control points:

$p=1$	$p=2$	\dots	$p=5$
C.P.1 → C.P.2	C.P.1 → C.P.2, C.P.3		C.P.1 → C.P.2, C.P.3, C.P.4, C.P.5, C.P.6
C.P.2 → C.P.3	C.P.2 → C.P.3, C.P.4		C.P.2 → C.P.3, C.P.4, C.P.5, C.P.6, C.P.7
...
C.P.7 → C.P.8	C.P.7 → C.P.8, C.P.9		C.P.7 → C.P.8, C.P.9
C.P.8 → C.P.9	C.P.8 → C.P.9		C.P.8 → C.P.9

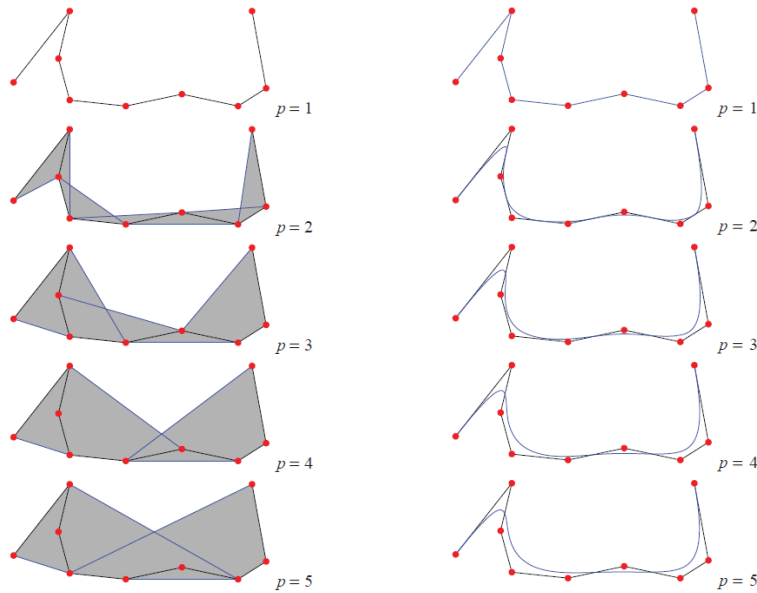


Figure 1.7. (a) Convex hulls for $p=1$ through $p=5$. (b) B-Spline curves for $p=1$ through $p=5$.

Example 2

Considering the following open non-uniform knot vector:

$$\Xi = \{0, 0, 0, 1, 2, 3, 4, 4, 5, 5, 5\}$$

the corresponding quadratic B-Spline functions are shown in Figure 1.7.

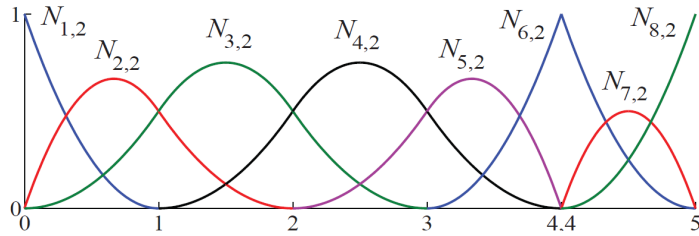


Figure 1.7. Quadratic basis functions for open, non-uniform knot vector
 $\Xi = \{0,0,0,1,2,3,4,4,5,5,5\}$.

The number of knot values is equal to:

$$n + p + 1 = 11$$

The basis functions are quadratic, so the polynomial order is equal to 2.

$$n + p + 1 = 11 \Rightarrow n + 2 + 1 = 11 \Rightarrow n = 8$$

The control points are eight, as we can see in Figure 1.8.a.

Figure 1.8.a presents the resulting quadratic B-Spline curve (blue curve), the 8 control points (red circles, ●) and the corresponding control polygon (gray piecewise polynomial line) (physical space). Figure 1.8.b depicts the 6 knots (red squares, ■), which partition BSpline curve into 5 isogeometric elements (1D knot spans) (mesh of isogeometric elements) (physical space).

We can observe that the curve is interpolatory at the first and last control points, as it is built from an open knot vector (general feature), and at the sixth control point due to the fact that the multiplicity of the knot $\xi=4$ is equal to the polynomial order. The curve is also tangent to the control polygon at the first, last and sixth control point. The curve is $C^{p-1}=C^1$ -continuous everywhere except at the location of the repeated knot, $\xi=4$, where it is $C^{p-2}=C^0$ -continuous. It is very important to mention for another time that it is the knots, mapped into the physical space, and not the control points that partition the curve into isogeometric elements and define the mesh of isogeometric elements.

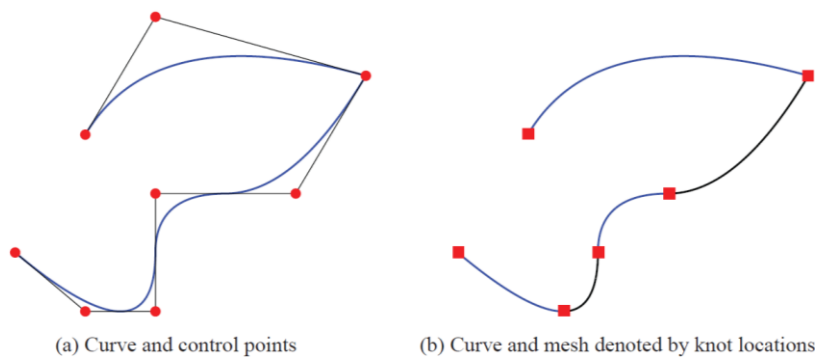


Figure 1.8. B-Spline, piecewise quadratic curve in R^2 .

B-SPLINE SURFACES

Given:

- a control net $\{B_{i,j}\}$ where $i=1,2,\dots,n$ and $j=1,2,\dots,m$,
- polynomial orders p and q and
- knot vectors $\Xi=\{\xi_1, \xi_2, \dots, \xi_{n+p+1}\}$ and $H=\{\eta_1, \eta_2, \dots, \eta_{m+q+1}\}$

a tensor product B-SPLINE surface is defined by:

$$S(\xi, \eta) = \sum_{i=1}^n \sum_{j=1}^m N_{i,p}(\xi) M_{j,q}(\eta) B_{i,j} \quad (1.10)$$

where $N_{i,p}(\xi)$, $M_{j,q}(\eta)$ are univariate B-SPLINE basis functions of order p and q , corresponding to knot vectors Ξ and H , respectively.

B-SPLINE surface has very interesting properties, which are the result of its tensor product nature.

- The basis is pointwise nonnegative and forms a partition of unity as

$$\forall \xi, \eta \in [\xi_1, \xi_{n+p+1}] \times [\eta_1, \eta_{m+q+1}] \quad (1.11)$$

I have that:

$$\sum_{i=1}^n \sum_{j=1}^m N_{i,p}(\xi) M_{j,q}(\eta) = \left(\sum_{i=1}^n N_{i,p}(\xi) \right) \cdot \left(\sum_{j=1}^m M_{j,q}(\eta) \right) = 1 \quad (1.12)$$

- The number of continuous partial derivatives in a given parametric direction may be determined from the associated one-dimensional knot vector and polynomial order.
- The surface again possesses the property of affine covariance and has a strong convex hull property.
- The local support of the basis functions also follows directly from the 1D functions that produce them. The support of a given bivariate function:

$$\tilde{N}_{i,j;p,q}(\xi) = N_{i,p}(\xi) M_{j,q}(\eta) \quad (1.13)$$

is exactly:

$$[\xi_i, \xi_{i+p+1}] \times [\eta_j, \eta_{j+q+1}].$$

Example 3

Let us consider a specific example:

- of a biquadratic ($p=q=2$) surface formed from
- $n=4$ (control points in parametric axis ξ) and
- $m=3$ (control points in parametric axis η).

Figure 1.9 gives us 2D control points' coordinates.

i	j	$\mathbf{B}_{i,j}$
1	1	(0, 0)
1	2	(-1, 0)
1	3	(-2, 0)
2	1	(0, 1)
2	2	(-1, 2)
2	3	(-2, 2)
3	1	(1, 1.5)
3	2	(1, 4)
3	3	(1, 5)
4	1	(3, 1.5)
4	2	(3, 4)
4	3	(3, 5)

**Figure 1.9. Control points
for the biquadratic B-SPLLine surface.**

For parametric axis ξ , I have that:

- $p=2$ and $n=4 \rightarrow n+p+1=4+2+1=7$ knot values, which produces knot vector $\Xi=\{-1,-1,-1,0,1,1,1\}$.

For parametric axis η , I have that:

- $q=2$ and $m=3 \rightarrow m+q+1=3+2+1=6$ knot values, which produces knot vector $H=\{-1,-1,-1,1,1,1\}$.

Figure 1.10 depicts the resulting control net and mesh of 2 isogeometric elements.

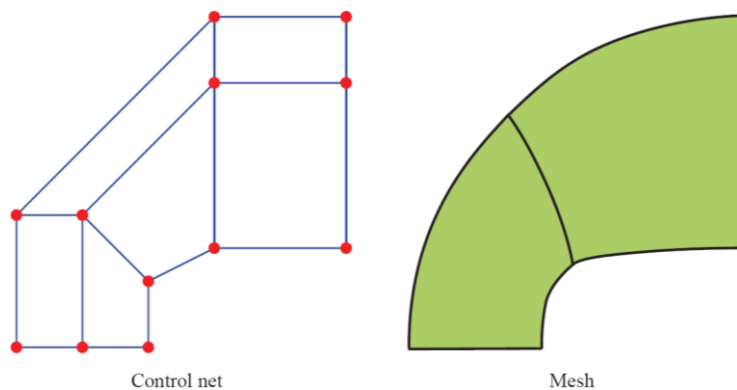


**Figure 1.10. The control net and mesh for the biquadratic B-SPLLine surface with
 $\Xi=\{-1,-1,-1,0,1,1,1\}$ and $H=\{-1,-1,-1,1,1,1\}$.**

The three ways of viewing a B-Spline are:

 Index Space

Figure 1.11.a shows the support of two biquadratic basis functions, which are $\tilde{N}_{1,1;2,2}(\xi, \eta)$ and $\tilde{N}_{3,2;2,2}(\xi, \eta)$ in index space. The support of $\tilde{N}_{1,1;2,2}(\xi, \eta) \quad [\xi_1, \xi_4] \times [\eta_1, \eta_4]$ is shown in red, while the support of $\tilde{N}_{3,2;2,2}(\xi, \eta) \quad [\xi_3, \xi_6] \times [\eta_2, \eta_5]$ is in blue. The region in which they overlap is purple.

By equally spacing each of the knots in the plot, I can see exactly which knot spans each of the functions are supported in, including where they overlap. Such a viewpoint is very useful when developing algorithms.

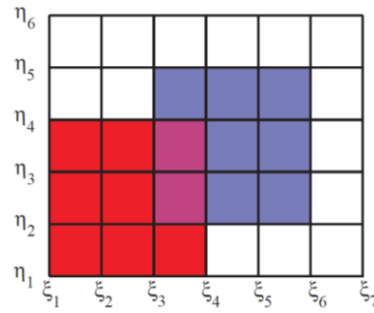


Figure 1.11.a. Index Space. The support of $\tilde{N}_{1,1;2,2}(\xi, \eta)$ & $\tilde{N}_{3,2;2,2}(\xi, \eta)$ and their overlapping.

Figure 1.12.a shows the two isogeometric elements in index space.



Figure 1.12.a. Index Space. The support of isogeometric element 1 & 2.

 Parameter space

Figure 1.11.b shows the support of two biquadratic basis functions, which are $\tilde{N}_{1,1;2,2}(\xi, \eta)$ and $\tilde{N}_{3,2;2,2}(\xi, \eta)$ in parameter space. The support of $\tilde{N}_{1,1;2,2}(\xi, \eta) \quad [\xi_1, \xi_4] \times [\eta_1, \eta_4]$ is shown in red, while the support of $\tilde{N}_{3,2;2,2}(\xi, \eta) \quad [\xi_3, \xi_6] \times [\eta_2, \eta_5]$ is in blue. The region in which they overlap is purple. I only have two nontrivial elements (elements with positive measure), and therefore only two elements in which calculations need to be performed during analysis. Function $\tilde{N}_{3,2;2,2}(\xi, \eta)$ has support in both of these elements, while $\tilde{N}_{1,1;2,2}(\xi, \eta)$ is only supported in the leftmost element.

Parameter space takes into account the actual knot values.

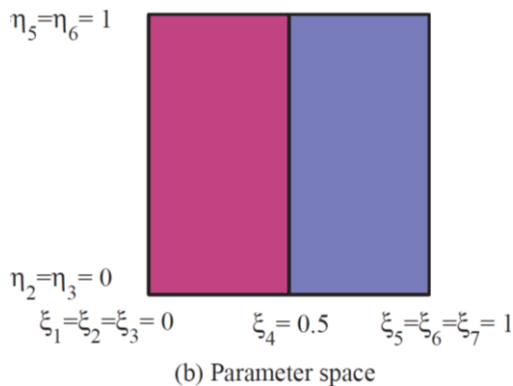


Figure 1.11.b. Parameter Space. $\tilde{N}_{3,2;2,2}(\xi, \eta)$ is supported in both elements, while $\tilde{N}_{1,1;2,2}(\xi, \eta)$ is only supported in one.

Figure 1.12.b shows the two isogeometric elements in parameter space. We can see knots as cyan knots.

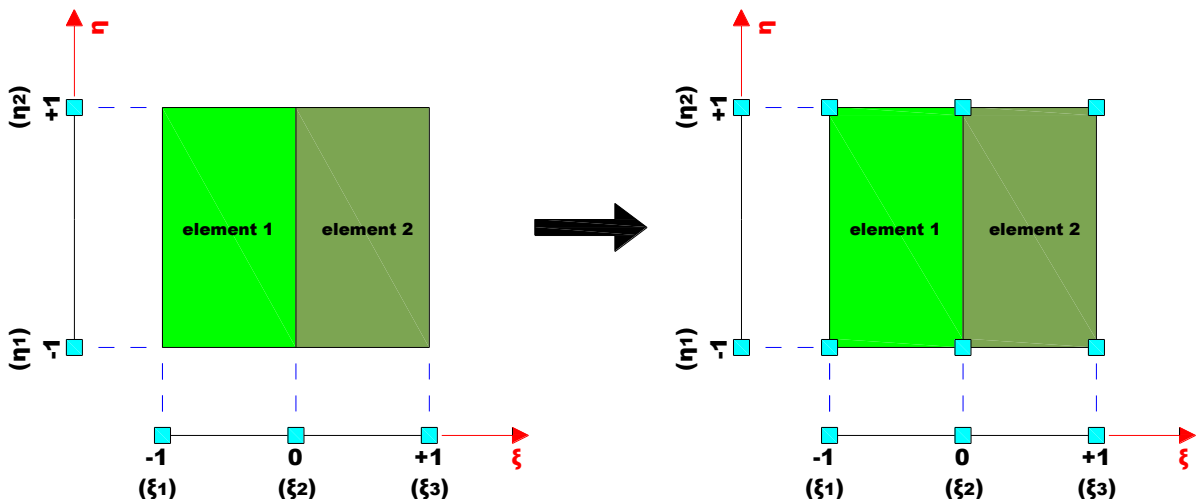


Figure 1.12.b. Parameter Space. Mesh of Isogeometric Elements.

 Physical space

Figure 1.11.c shows the support of two biquadratic basis functions, which are $\tilde{N}_{1,1;2,2}(\xi, \eta)$ and $\tilde{N}_{3,2;2,2}(\xi, \eta)$ in physical space. The support of $\tilde{N}_{1,1;2,2}(\xi, \eta) \quad [\xi_1, \xi_4] \times [\eta_1, \eta_4]$ is shown in red, while the support of $\tilde{N}_{3,2;2,2}(\xi, \eta) \quad [\xi_3, \xi_6] \times [\eta_2, \eta_5]$ is in blue. The region in which they overlap is purple. Function $\tilde{N}_{3,2;2,2}(\xi, \eta)$ has support in both of these elements, while $\tilde{N}_{1,1;2,2}(\xi, \eta)$ is only supported in the leftmost element. This figure makes it clear which portions of the actual domain are influenced by each of the basis functions.

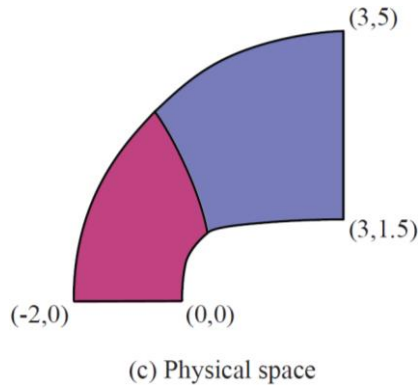


Figure 1.11.c. Physical Space. Again, $\tilde{N}_{3,2;2,2}(\xi, \eta)$ is supported in both elements, while $\tilde{N}_{1,1;2,2}(\xi, \eta)$ is only supported in one.

Figure 1.12.c shows the two isogeometric elements in physical space. Element 1 has purple color, while element 2 is blue.

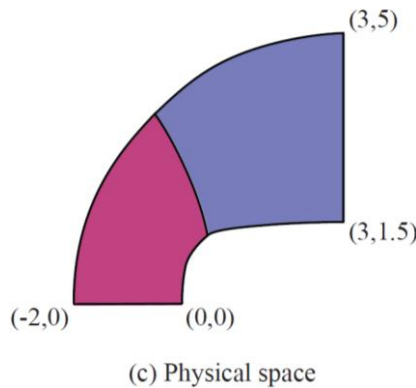


Figure 1.12.c. Physical Space. Mesh of Isogeometric Elements.

Figure 1.13 has plotted the actual functions themselves in the physical space. $\tilde{N}_{1,1;2,2}(\xi, \eta)$ takes on positive values on two of the edges and it is interpolatory in the corner. Alternatively, $\tilde{N}_{3,2;2,2}(\xi, \eta)$ is identically zero on all of the edges.

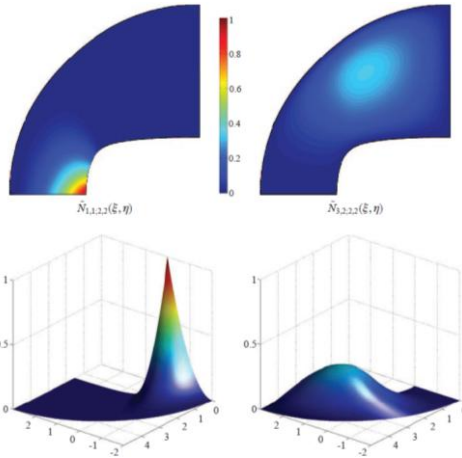


Figure 1.13. Biquadratic functions $\tilde{N}_{1,1;2,2}(\xi, \eta)$ and $\tilde{N}_{3,2;2,2}(\xi, \eta)$ plotted in the physical space, from two different angles.

B-SPLINE SOLIDS

Given:

- a control lattice $\{B_{i,j,k}\}$ where $i=1,2,\dots,n$, $j=1,2,\dots,m$ and $k=1,2,\dots,l$
- polynomial orders p , q and r
- knot vectors $\Xi = \{\xi_1, \xi_2, \dots, \xi_{n+p+1}\}$, $H = \{\eta_1, \eta_2, \dots, \eta_{m+q+1}\}$ and $Z = \{\zeta_1, \zeta_2, \dots, \zeta_{l+r+1}\}$

a tensor product B-SPLINE solid is defined by:

$$S(\xi, \eta, \zeta) = \sum_{i=1}^n \sum_{j=1}^m \sum_{k=1}^l N_{i,p}(\xi) M_{j,q}(\eta) L_{k,r}(\zeta) B_{i,j,k} \quad (1.14)$$

where $N_{i,p}(\xi)$, $M_{j,q}(\eta)$, $L_{k,r}(\zeta)$ are univariate B-SPLINE basis functions of order p , q and r , corresponding to knot vectors Ξ , H and Z , respectively.

The properties of a B-SPLINE solid like the one shown in Figure 1.14 are trivariate generalizations of those for B-SPLINE surfaces.



Figure 1.14. A simple B-SPLINE solid.

1.1.4 Refinement

One of the most interesting aspects of B-SPLines is the myriad of ways in which the basis may be enriched while leaving the underlying geometry and its parameterization intact. To fully recognize the many possibilities, it is important first to understand the subtle ways in which the basic mechanisms of B-Spline refinement differ from their finite element counterparts. These differences lead to more richness in the overall refinement space. In particular, not only do I have control over the element size and the order of the basis, but I can also control the continuity of the basis as well.

Below, I will analyze two different types of refinement, which are:

- Knot Insertion
- Order Elevation.

Knot insertion

The first mechanism by which one can enrich the basis is knot insertion. Knots may be inserted without changing a curve geometrically or parametrically. Given a knot vector $\Xi = \xi_1, \xi_2, \dots, \xi_{n+p+1}$, I introduce the notion of an extended knot vector $\bar{\Xi} = \bar{\xi}_1 = \xi_1, \bar{\xi}_2, \dots, \bar{\xi}_{n+m+p+1} = \xi_{n+p+1}$, such that $\Xi \subset \bar{\Xi}$. As before, the new $n+m$ basis functions are formed by (1.2) and (1.3), now by applying them to the new knot vector $\bar{\Xi}$. The new $n+m$ control points, $\bar{B} = \bar{B}_1, \bar{B}_2, \dots, \bar{B}_{n+m}^T$, are formed from linear combinations of the original control points, $B = B_1, B_2, \dots, B_n^T$, by

$$\bar{B} = T^p \cdot B \quad (1.15)$$

where

$$T_{ij}^0 = \begin{cases} 1 & \bar{\xi}_i \in [\xi_j, \xi_{j+1}) \\ 0 & \text{otherwise} \end{cases} \quad (1.16)$$

and

$$T_{ij}^{q+1} = \frac{\bar{\xi}_{i+q} - \xi_j}{\xi_{j+q} - \xi_j} \cdot T_{ij}^q + \frac{\xi_{j+q+1} - \bar{\xi}_{i+q}}{\xi_{j+q+1} - \xi_{j+1}} \cdot T_{ij+1}^q \quad \text{for } q = 0, 1, 2, \dots, p-1 \quad (1.17)$$

Knot values already present in the knot vector may be repeated in this way, thereby increasing their multiplicity, but the continuity of the basis will be reduced. However, continuity of the curve is preserved by choosing the control points as in the three previous equations.

Example 4

Figure 1.15 depicts an example of knot insertion for a simple, one-element, quadratic B-Spline curve.

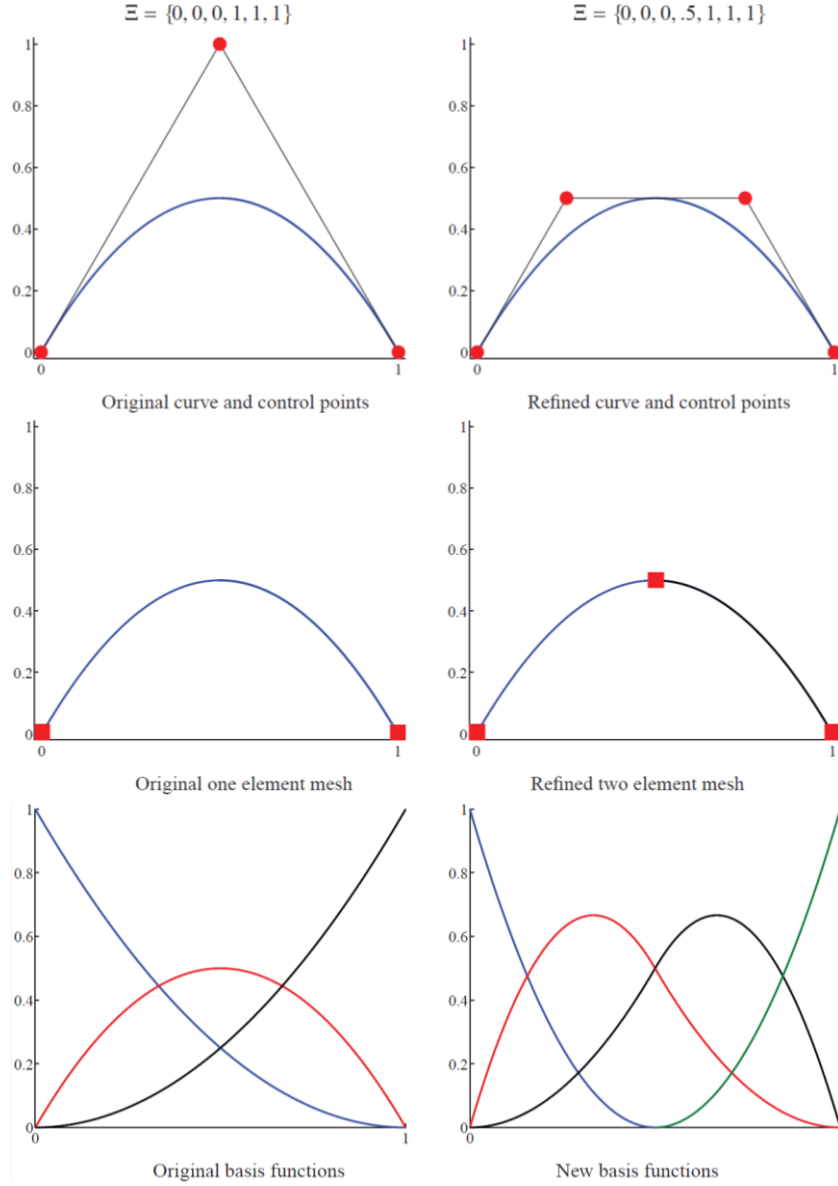


Figure 1.15. Knot insertion. Control points are denoted by ●. The knots, which define a mesh by partitioning the curve into elements, are denoted by ■.

The knot vector of the original curve is:

$$\Xi = 0,0,0,1,1,1$$

The control points, mesh and basis functions of the unrefined curve are shown on the left. A new knot is inserted at:

$$\bar{\xi} = 0.5$$

The new curve, shown on the right, is geometrically and parametrically, identical to the original curve, but:

- the control points are changed
- the mesh is partitioned and
- the basis is richer.

There is one more control point, one more element and one more basis function than in the unrefined case. This process may be repeated to enrich the solution space by adding more basis functions of the same order while leaving the curve unchanged. Figure 1.16 shows the more advanced case of a global refinement of the curve from Figure 1.15.

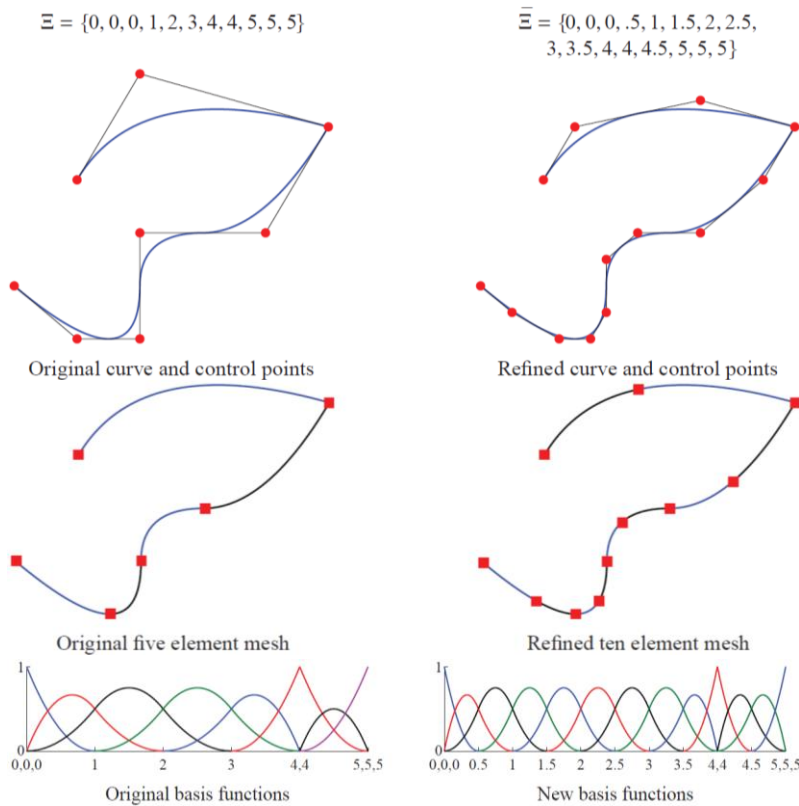


Figure 1.16. Knot insertion. Control points are denoted by •. The knots, which define a mesh by partitioning the curve into elements, are denoted by ■.

Insertion of new knot values clearly has similarities with the classical h-refinement strategy in finite element analysis as it splits existing elements into new ones. It differs, however,:

- in the number of new functions that are created, as well as
- in the basis' continuity across newly created element boundaries (C_{p-1} in this case).

To perfectly replicate h-refinement, one would need to insert each of the new knot values p times so that the functions will be C^0 across the new boundary. The alternative to insert new knot values – increasing the multiplicity of existing knot values to decrease the continuity of the basis without creating new element – does not have an analogue in FEA, as FEA meshes have C^0 element boundaries to begin with. In this way, knot insertion is very closely related, but not identical to h-refinement.

Order Elevation

Order elevation involves raising the polynomial order of the basis functions used to represent the geometry. The basis has $p-m_i$ continuous derivatives across element boundaries. Thus, if I increase basis' polynomial order p and I want to preserve the discontinuities in the various derivatives already existing in the original curve, m_i will be also increased. During order elevation, the multiplicity of each knot value is increased by one, but no new knot values are added. As with knot insertion, neither the geometry nor the parameterization are changed.

Example 5

Figure 1.17 depicts an example of order elevation for a simple, one-element, quadratic B-Spline curve.

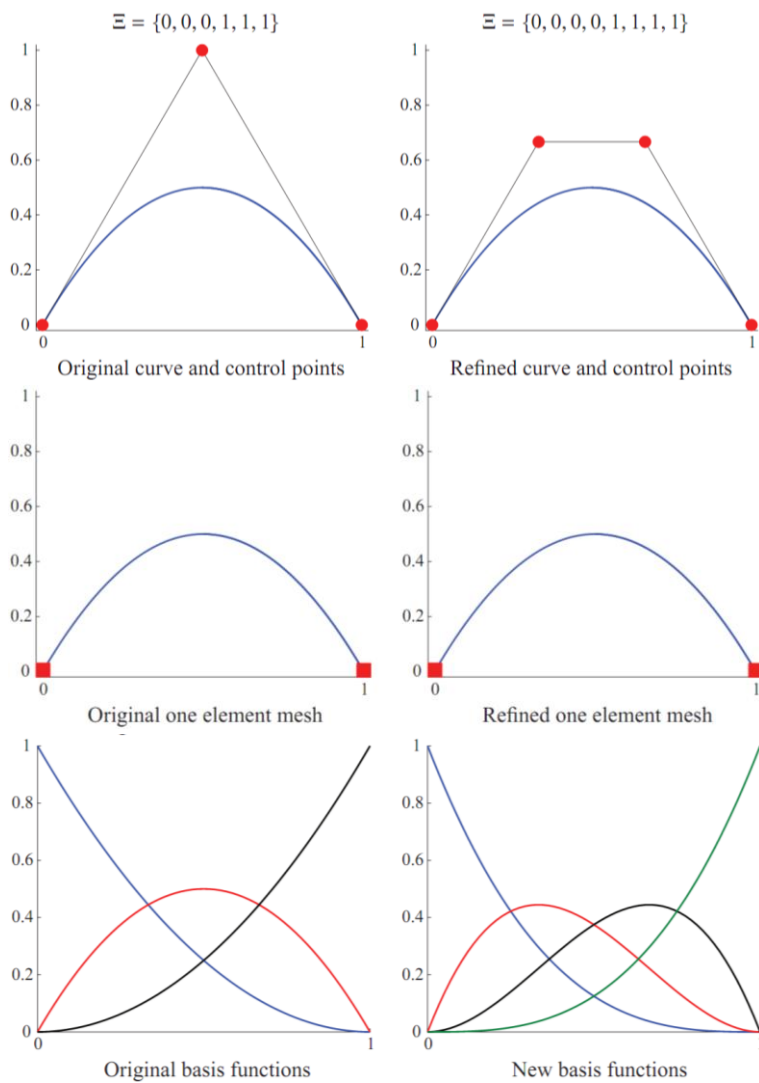


Figure 1.17. Order elevation. Control points are denoted by •. The knots, which define a mesh by partitioning the curve into elements, are denoted by ■.

Isogeometric Analysis

The knot vector of the original curve is:

$$\Xi = \{0,0,0,1,1,1\}$$

The control points, mesh and basis functions of the unrefined curve are shown on the left.

This time, no new knot values are added, but the multiplicity of the knots is increased by one.

The new curve, shown on the right, is geometrically and parametrically, identical to the original curve, but:

- the control points are changed (increased by one) and
- the basis is richer. The basis functions' number increased by one.

It is important to mention that despite the fact that there is one more control point and one more basis function than in the unrefined case, the mesh wasn't changed. The number of isogeometric elements still remains equal to one.

This process may be repeated to enrich the solution space by adding more basis functions of the same order while leaving the curve unchanged. Figure 1.18 shows the more advanced case of a global refinement of the curve from Figure 1.17.

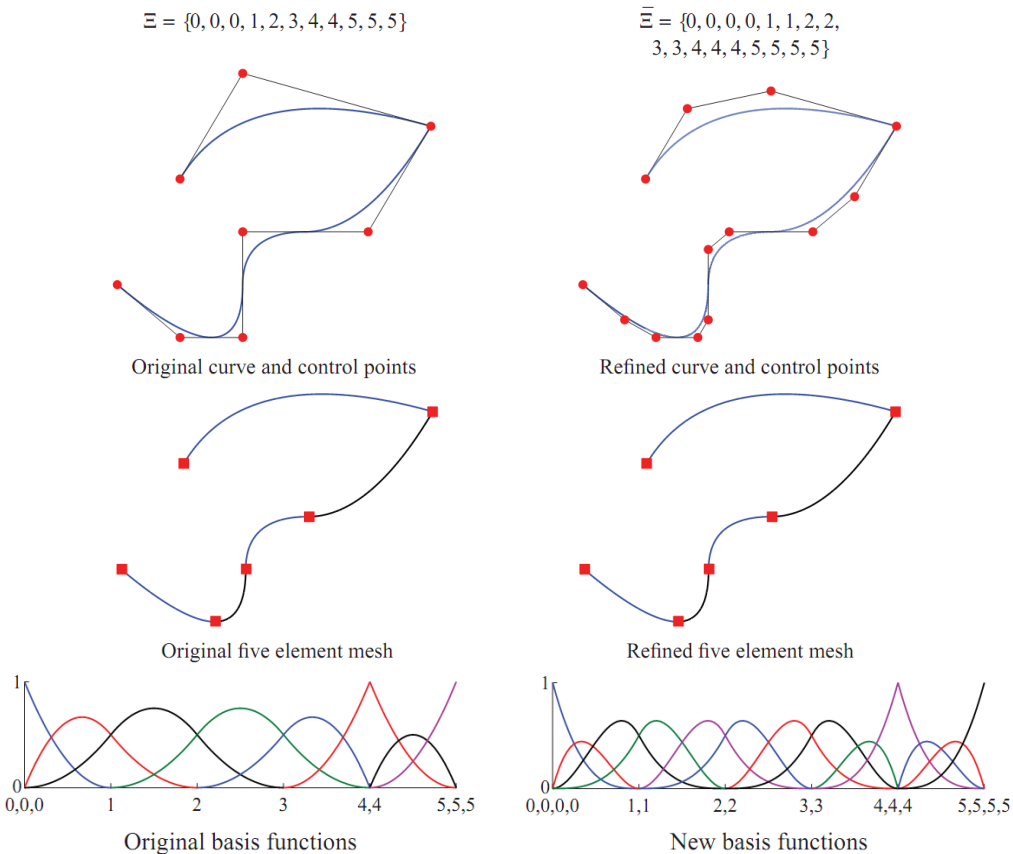


Figure 1.18. Order Elevation. Control points are denoted by •. The knots, which define a mesh by partitioning the curve into elements, are denoted by ■.

Isogeometric Analysis

Order elevation clearly has similarities with the classical p-refinement strategy in finite element analysis as it increases the polynomial order of the basis. The major difference is that p-refinement always begins with a basis that is C^0 everywhere, while order elevation is compatible with any combination of continuities that exist in the unrefined B-Spline mesh. This flexibility leads to a new higher-order technique that is unique to IGA.

1.2 NURBS

1.2.1 NURBS Basis Functions

NURBS is a Non-Uniform Rational Basis SPLine. IGA uses NURBS (Non-Uniform Rational Basis SPLines) as shape functions. With this mathematical model (commonly used in computer graphics), I can generate curves and surfaces and handle with great flexibility and precision both analytic and freeform shapes. NURBS are built from B-SPLines (Basis Smooth Polynomial Lines). Using NURBS, I gain the ability to represent exactly a wide array of objects that cannot be exactly represented by polynomials and non-rational B-SPLines. They are invaluable in designing meshes, proving theorems and a large range of other activities related to IGA.

I get the control points \mathbf{B}_i for the NURBS curve $C(\xi)$ by performing exactly the same projective transformation to the (projective) control points \mathbf{B}_i^w of the B-SPLine (projective) curve $\mathbf{C}^w(\xi)$. With a projective B-SPLine curve and its associated projective control points in hand, The NURBS curve's control points are obtained by the following relations:

$$(\mathbf{B}_i)_j = \frac{(\mathbf{B}_i^w)_j}{w_i} \text{ with } j=1, \dots, d \quad (1.18.a)$$

$$w_i = (\mathbf{B}_i^w)_{d+1} \quad (1.18.b)$$

where $(\mathbf{B}_i)_j$ is the j^{th} component of the vector \mathbf{B}_i and w_i is referred to as the i^{th} weight.

Considering the weighting function

$$W(\xi) = \sum_{i=1}^n \{N_{i,p}(\xi) \cdot w_i\} \quad (1.39)$$

where $N_{i,p}(\xi)$ is the standard B-SPLine basis function,

the NURBS curve is defined by the following equation:

$$[C(\xi)]_j = \frac{[C^w(\xi)]_j}{W(\xi)} \text{ where } j=1, \dots, d \quad (1.20)$$

As $\mathbf{C}^w(\xi)$ and $W(\xi)$ are both piecewise polynomial functions, the curve $C(\xi)$ is a piecewise rational function, which within an element is a polynomial divided by another polynomial. In the NURBS setting, the two polynomials have the same order, frequently called as the order of the NURBS curve. In fact, it is the order of the B-Spline from which it was generated.

To achieve an affine transformation of a NURBS object, I apply the affine transformation directly to its control points while leaving the weights fixed. Though each weight is associated with a specific control point, it is important that we do not think of it as a component of the control point. This is an easy mistake to make.

Part of the B-Splines' power is the ability to change their shape by adjusting the control points. It is important to manipulate NURBS in exactly the same way. For this purpose, I will construct a basis for the NURBS space from knot vectors, in order to build curves, surfaces and solids from linear combinations of basis functions and control points.

The weighting function $W(\xi) = \sum_{i=1}^n \{N_{i,p}(\xi) \cdot w_i\}$ is a scalar, piecewise polynomial function

for the $d+1$ component of the projective curve. From the geometric point of view, it is used to project a B-Spline curve from R^{d+1} into R^d . From the algebraic point of view, it is used to construct a basis for the NURBS space directly in order to build geometries and meshes in R^d while does not care about the projective geometry. This NURBS basis is a piecewise rational function and is equal to:

$$R_i^p(\xi) = \frac{N_{i,p}(\xi) \cdot w_i}{W(\xi)} = \frac{N_{i,p}(\xi) \cdot w_i}{\sum_{i=1}^n \{N_{i,p}(\xi) \cdot w_i\}} \quad (1.21)$$

where:

- p is the polynomial order and
- $i=1, \dots, n$ where n is the number of control points.

Combining NURBS basis functions (equation 1.21) with control points, I can produce the NURBS curve equal to:

$$\mathbf{C}(\xi) = \sum_{i=1}^n \{R_i^p(\xi) \cdot \mathbf{B}_i\} \quad (1.22)$$

NURBS Surfaces are defined in terms of rational basis functions. The corresponding relation is the following.

$$R_{i,j}^{p,q}(\xi, \eta) = \frac{N_{i,p}(\xi) \cdot M_{j,q}(\eta) \cdot w_{i,j}}{\sum_{i=1}^n \sum_{j=1}^m N_{i,p}(\xi) \cdot M_{j,q}(\eta) \cdot w_{i,j}} \quad (1.23)$$

Isogeometric Analysis

NURBS Solids are defined in terms of rational basis functions. The corresponding relation is the following.

$$R_{i,j,k}^{p,q,r}(\xi, \eta, \zeta) = \frac{N_{i,p}(\xi) \cdot M_{j,q}(\eta) \cdot L_{k,r}(\zeta) \cdot w_{i,j,k}}{\sum_{i=1}^n \sum_{j=1}^m \sum_{k=1}^l N_{i,p}(\xi) \cdot M_{j,q}(\eta) \cdot L_{k,r}(\zeta) \cdot w_{i,j,k}} \quad (1.24)$$

These rational basis functions bear much in common with their polynomial progenitors. Particularly, the continuity of the functions, as well as their support, follows directly from the knot vectors exactly as before. The basis still constitutes a partition of unity and it is pointwise nonnegative. These properties taken together again result in a strong convex hull property for the NURBS functions.

Lastly, it is worth mentioning that the weights play an important role in defining the basis, but they are divorced from any explicit geometric interpretation in this setting. So, I am free to choose control points independently from their associated weights.

If the weights are all equal, then:

$$R_i^p(\xi) = N_{i,p}(\xi)$$

and the curve is again a polynomial. That is why B-SPLines are a special case of NURBS.

1.2.2 Derivatives of NURBS Basis Functions

I can calculate the derivatives of NURBS basis functions using the following equation.

$$\frac{dR_i^p(\xi)}{d\xi} = w_i \cdot \frac{W(\xi) \cdot \frac{dN_{i,p}(\xi)}{d\xi} - \frac{dW(\xi)}{d\xi} \cdot N_{i,p}(\xi)}{(W(\xi))^2} \quad (1.25)$$

where

$$\frac{dW(\xi)}{d\xi} = \sum_{i=1}^n \left\{ \frac{dN_{i,p}(\xi)}{d\xi} \cdot w_i \right\} \quad (1.26)$$

I can calculate higher-order derivatives of these rational functions in terms of lower-order derivatives as:

$$\frac{d^k R_i^p(\xi)}{d\xi^k} = \frac{A_i^k(\xi) - \sum_{j=1}^k \binom{k}{j} \cdot W^{(j)}(\xi) \cdot \frac{d^{k-j} R_i^p(\xi)}{d\xi^{k-j}}}{W(\xi)} \quad (1.27)$$

where

$$A_i^k(\xi) = w_i \cdot \frac{d^k N_{i,p}(\xi)}{d\xi^k} \quad (1.28)$$

$$W^{(k)}(\xi) = \frac{d^k W(\xi)}{d\xi^k} \quad (1.29)$$

$$\binom{k}{j} = \frac{k!}{j!(k-j)!} \quad (1.30)$$

1.3 Multiple Patches

In Isogeometric Analysis (**IGA**), the B-SPLine parameter space is local to the entire patch rather than element. The B-SPLine mapping (a single map) takes a patch of multiple elements in the parameter space into the physical space, but the mapping itself is global to the whole patch, rather than to elements.

Patches play the role of subdomains within which element types and material models are assumed to be uniform. Many simple domains can be represented by a single patch. **Internal knots** partition the patch into elements.

Figure 1.19 depicts a 3D patch, which consists of 6 isogeometric elements.

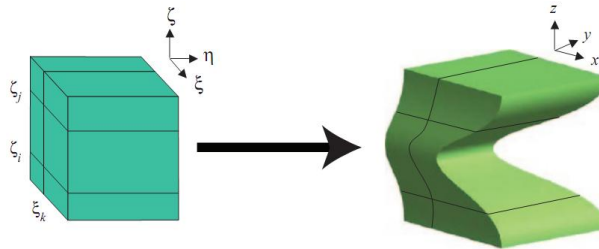


Figure 1.19. Parameter (6 elements) and physical space (6 isogeometric elements). (IGA)

It is almost the case to describe domains with multiple NURBS patches. I have to use multiple patches when:

- different material models are to be used in different parts of the domain.
- different physical models are to be used in different parts of the domain.
- different subdomains are to be assembled in parallel on a multiple processor machine.
- problem's geometry is complex. The tensor product structure of the parameter space of a patch makes it poorly suited for representing complex and multiply connected domains. Such geometries can be handled quite simply by using multiple patches.

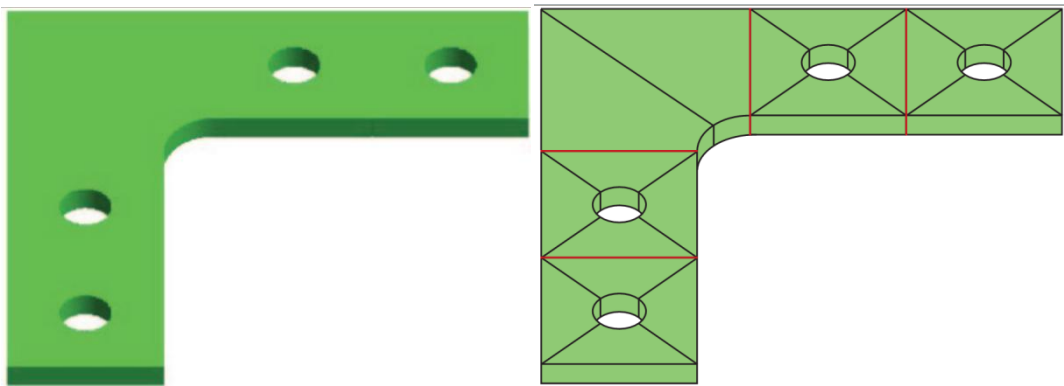


Figure 1.20. Structure (on left) and its isogeometric element mesh (on right).
Physical Space.

Figure 1.20 shows the initial structure, which has not quite simple geometry, on the left and the corresponding finite element mesh on the right. We see the physical space. Mesh contains totally 5 patches. Patch boundaries are shown in red. The four of them have identical features and contain 4 3D isogeometric elements each. The different fifth patch consists of two isogeometric elements. Element boundaries are shown in black.

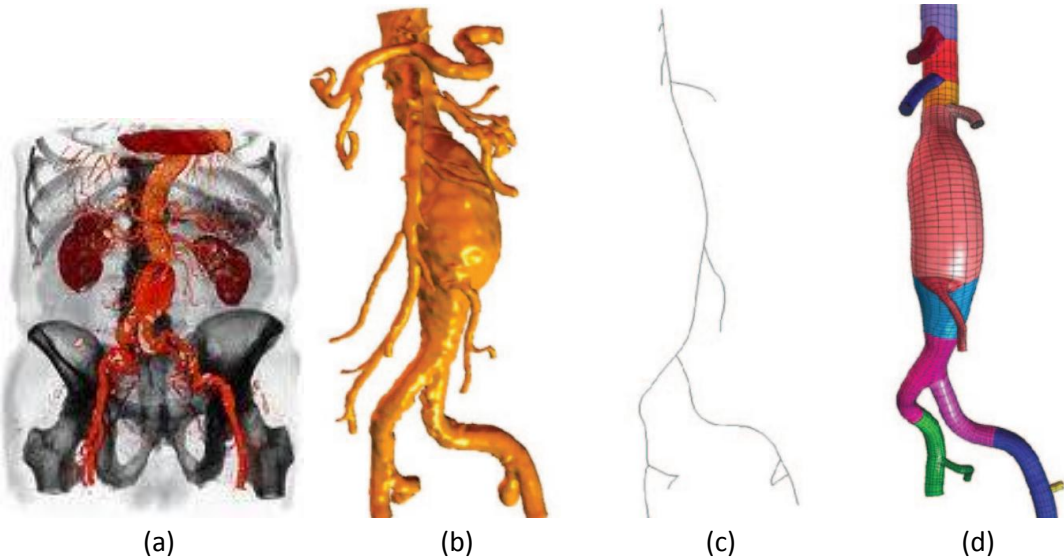


Figure 1.21. Flow in a patient-specific abdominal aorta with aneurysm.

Abdominal aortic aneurysm (also known as AAA, pronounced "triple-a") is a localized dilatation (ballooning) of the abdominal aorta exceeding the normal diameter by more than 50 percent, and is the most common form of aortic aneurysm. It is a very complicated simulation problem due to its complex geometry. Figure 1.21.a shows real problem, while Figure 1.21.b the corresponding imaging data. The skeleton of the NURBS mesh is depicted at Figure 1.21.c. Lastly, we can see the NURBS mesh. We can observe 15 different patches.

1.4 NURBS Mesh Generation

NURBS mesh generation includes the following steps:

1. Basic Features' Selection.
2. Polynomial Orders' Selection.
3. Knot Vectors' Selection.
4. Control Points' Selection.

1.4.1 Basic Features' Selection

In order to generate a NURBS mesh, it is strongly recommended to define at first the following major features:

1. Corners and other points to be interpolated.

Corners are a natural place to begin as the parameter space is a cube. There is no loss of generality in assuming it to be a cube, because dividing an entire knot vector by a constant does not change the resulting geometry in any way at all. That is why the knot vectors may be always normalized such that the parameter space is the unit cube. As I use open knot vectors, the basis should interpolate the corners. By indentifying them, I can find quickly and easily a few control points.

2. Edges and other lines of reduced continuity.

The next thing to look for is any place where the continuity is obviously decreased. The most obvious thing would be a crease in the geometry, as for example a sharp edge other than the image of one of the edges of the parametric cube.

3. Geometric primitives and lower-dimensional NURBS objects.

The third step is to identify simple objects that I already know how to construct. There might be templates for these geometrical primitives, such as polynomials or conic sections. As I use open knot vector, each face of the NURBS patch will actually be a NURBS surface and each edge of those surfaces is a NURBS curve. Thus, I can be on the lookout for 1D objects that I may already know how to model.

4. Extrusions, surfaces of revolution, symmetries or other tensor-product-like features.

The last step is to look for places in which a NURBS curve or surface has been swept along a patch defined by another NURBS curve. Such extrusions are very common in engineering design and identifying them makes the job of modeling much easier by effectively reducing a 3D problem into two problems of lower dimension.

1.4.2 Polynomial Orders' Selection

The first thing to determine is what polynomial orders will be needed. In general, a basis principle is to use the lowest polynomial order possible in each of the parametric directions. Analysis may frequently demand higher orders than geometric design, but it is best to work with the lowest order possible during design. For example, higher-order functions may be needed to avoid locking in structural analysis.

1.4.3 Knot Vectors' Selection

In order to select the knot vectors, I have to decide how many elements are necessary and what level of continuity is required across each element boundary. For most case, integer knot values are perfectly sufficient. If a knot vector in [0,1] is preferable for some reason, I may proceed by assigning integer values and simply divide by the greatest value once I am finished. This has no bearing on the resulting geometry.

1.4.4 Control Points' Selection

Only when I have selected:

- basic features
- polynomial orders and
- knot vectors

I am in the position to assign the actual control points.

The easiest place to start is normally the corners of an object as they will be interpolated. If have to simulate a 3D structure, I will take into consideration that solid geometry is an extrusion formed by a NURBS surface being swept along a NURBS curve. So, I can start by using the template to construct the surface to be extruded.

1.5 Comparison between IGA and FEA

1.5.1 Code Architecture

For comparison purposes, I will present at first the architecture of a classical FEA code.

The following Figure depicts the flowchart of a classical finite element code. Such a code can be converted to a single-patch isogeometric analysis code by replacing the routines shown in green.

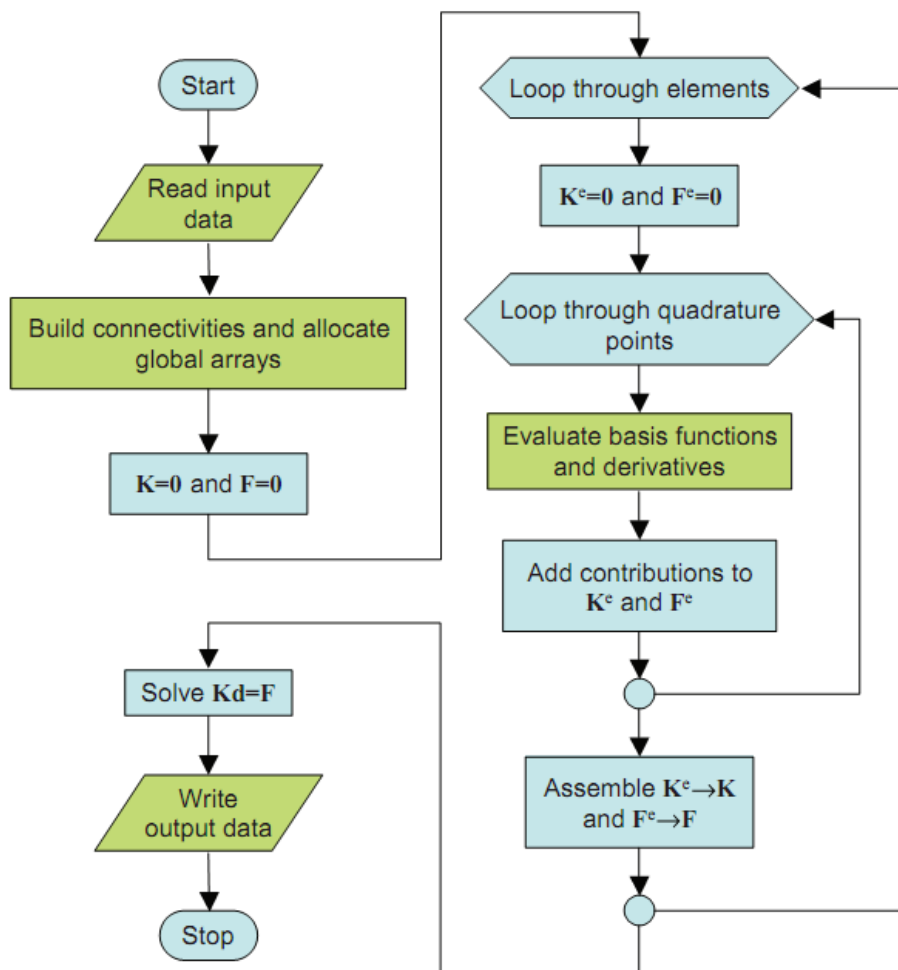


Figure 1.22. Flowchart of a classical FEA code.

The program begins with the data defining the boundary value problem, the mesh, and all of the geometrical data being read from files. Once these data have been read, the connectivity information can be generated (though sometimes this will be read in from an external file as well) and the memory is allocated for all of the major global arrays, which are subsequently initialized to zero. Once these pre-processing steps are completed, assembly of the system begins.

There is a loop through all of the elements in the mesh. Within each element, the element stiffness matrix and element force vector are initialized and then the code enters a loop through the quadrature points.

At each quadrature point, a routine is called that will evaluate all of the basis functions and any necessary derivatives. It is helpful to think of this routine as a black box. If I know the number of local basis functions, it is not important what those functions are or how they are evaluated. It is only important that I have a routine from which I can obtain those values when they are needed. With these values in hand, I proceed to build the local stiffness matrix and force vector.

After I have been through each quadrature point and fully assembled the local arrays, I use the connectivity information to add their contributions to the global stiffness matrix and force vector, and then move on to the next element.

After all of the elements are assembled, the global arrays are complete. I solve then the system and write the result to a file (postprocess).

To convert an existing file element code to a single-patch isogeometric analysis code, the only portions of the code that require modification are the ones shown in green in Figure 1.22. The input will change as the file format will depend on the specific element technology being used. The precise forms of the connectivity arrays and the global matrices also depend on the basis. The structured nature of the NURBS mesh means that these arrays can be calculated automatically from the knot vectors and polynomial orders. Next, the “black box” that evaluated the basis functions must be updated to evaluate the NURBS functions. The type of information about the basis that it provides to the routine that calls it is exactly the same, but that information should now correspond to the NURBS basis. Lastly, the output must be written and the format of that output will be specific to the NURBS basis.

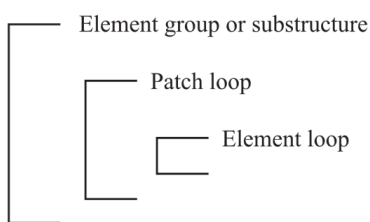


Figure 1.23. Program architecture of the assembly algorithm in IGA.

The patch loop does not have a direct analog in finite element analysis, although it might be considered analogous to a macro-element loop. If each patch consists of a single element, I have the assembly algorithm that is standard in FEA.

Figure 1.24 depicts the flowchart of a multi-patch IGA code. The routines in green represent differences from the single-patch code.

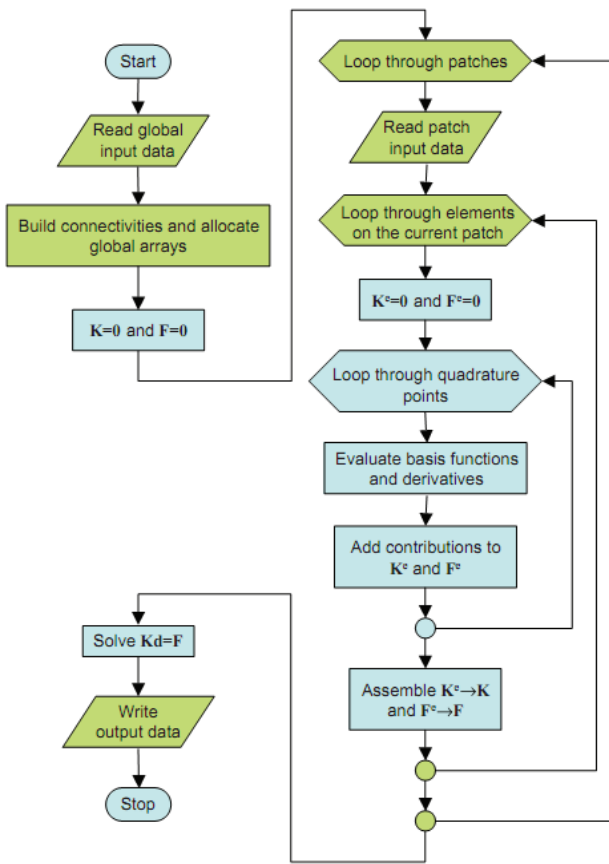


Figure 1.24. Flowchart of a multi-patch IGA code.

A multi-patch IGA code can be made to conform to flowchart in Figure 1.22. In practice, however, it makes more sense to consider the slight modification shown in Figure 1.24. In this case, I begin by inputting enough global information to build the global connectivities. This information includes the polynomial orders and the knot vectors for each of the patches, but it does not require the control points. I can save time and memory by not reading the control points until they are needed. Again, the knot vectors and polynomial orders are all that is required. Global arrays are allocated and initialized as before.

At this point the code enters a loop through the patches. The reason for making this loop explicit is that the control points defining the geometry are relevant to only a patch at a time. I can input this information within the loop, relating only the information relevant to the patch I am currently working with. I now loop through the elements on the current patch. Everything then proceeds exactly as before until after the global system is solved. Lastly, the output is written to files, typically in a format that makes it easy to identify control variables with the patch that they correspond to and so this routine will be specific to the multiple-patch setting.

The only other potential source of complexity is if local refinement is to be applied. This can either be implemented during assembly or within the solver. In either case, modifications of the appropriate routine will be required.

1.5.2 Similarities and Differences

Similarities

Isogeometric Analysis and classical Finite Element Analysis appear many similarities. These similarities are the followings.

- Isoparametric concept.
- Galerkin's method.
- Code architecture.
- Compactly supported basis.
- Bandwidth of matrices.
- Partition of unity.
- Affine covariance.
- Patch tests are satisfied.

Differences

Isogeometric Analysis and classical Finite Element Analysis appear many differences as well. These differences are described below.

- Geometry.
 - IGA. Exact Geometry.
IGA employs the exact geometry at all levels of discretization. This geometric exactness not only affects the accuracy of computed solutions, but even the analysis process as a whole as refinement requires no external description of the geometry.
 - FEA. Approximate Geometry.
FEA uses piecewise polynomial approximations, even for such common objects as conic sections.
- Points.
 - IGA. Control points.
 - FEA. Nodal points.

Isogeometric Analysis

- Variables.
 - IGA. Control variables.
 - FEA. Nodal variables.
- Basis.
 - IGA. Basis does not interpolate control points and variables. NURBS basis. Pointwise positive.
 - FEA. Basis interpolates control points and variables. Polynomial basis. Not necessarily positive.
- Continuity.
 - IGA. High, easily controlled continuity.
 - FEA. C^0 -continuity, always fixed.
- Refinement.
 - IGA. hpk-refinement space.
 - FEA. hp-refinement space.
- Convex hull property.
 - IGA. Convex hull property.
 - FEA. No convex hull property.
- In the presence of discontinuous data.
 - IGA. Variation diminishing.
 - FEA. Oscillatory.

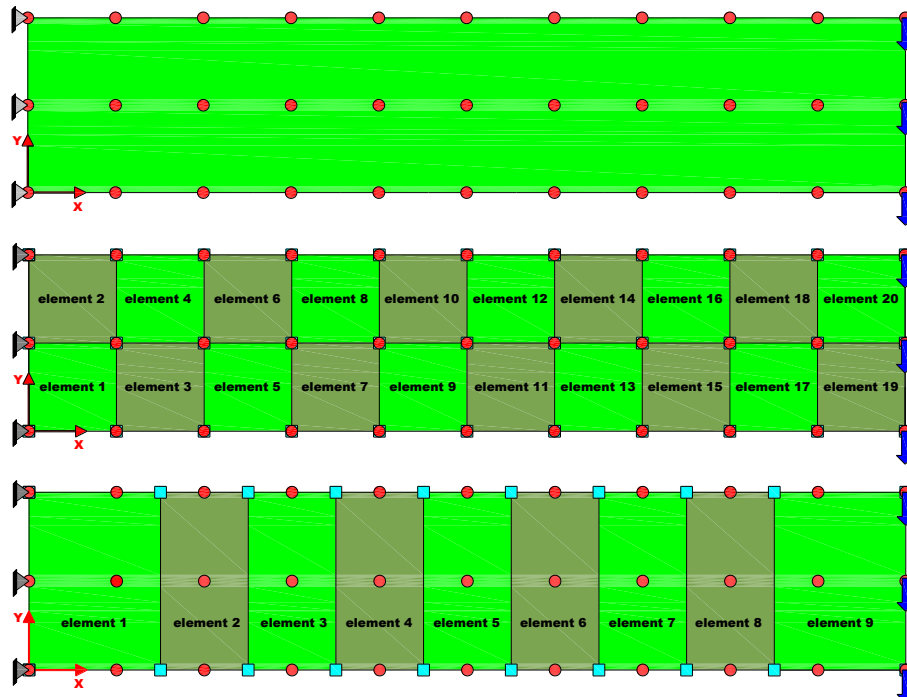


NATIONAL TECHNICAL UNIVERSITY OF ATHENS
SCHOOL OF CIVIL ENGINEERING
DEPARTMENT OF STRUCTURAL ENGINEERING
STATIC & ASEISMIC RESEARCH LABORATORY
ACADEMIC YEAR 2010-2011

MSc in ANALYSIS & DESIGN of EARTHQUAKE RESISTANCE STRUCTURE

ISOGEOMETRIC ANALYSIS WITH B-SPLINES & NURBS

CHAPTER 2 Applications

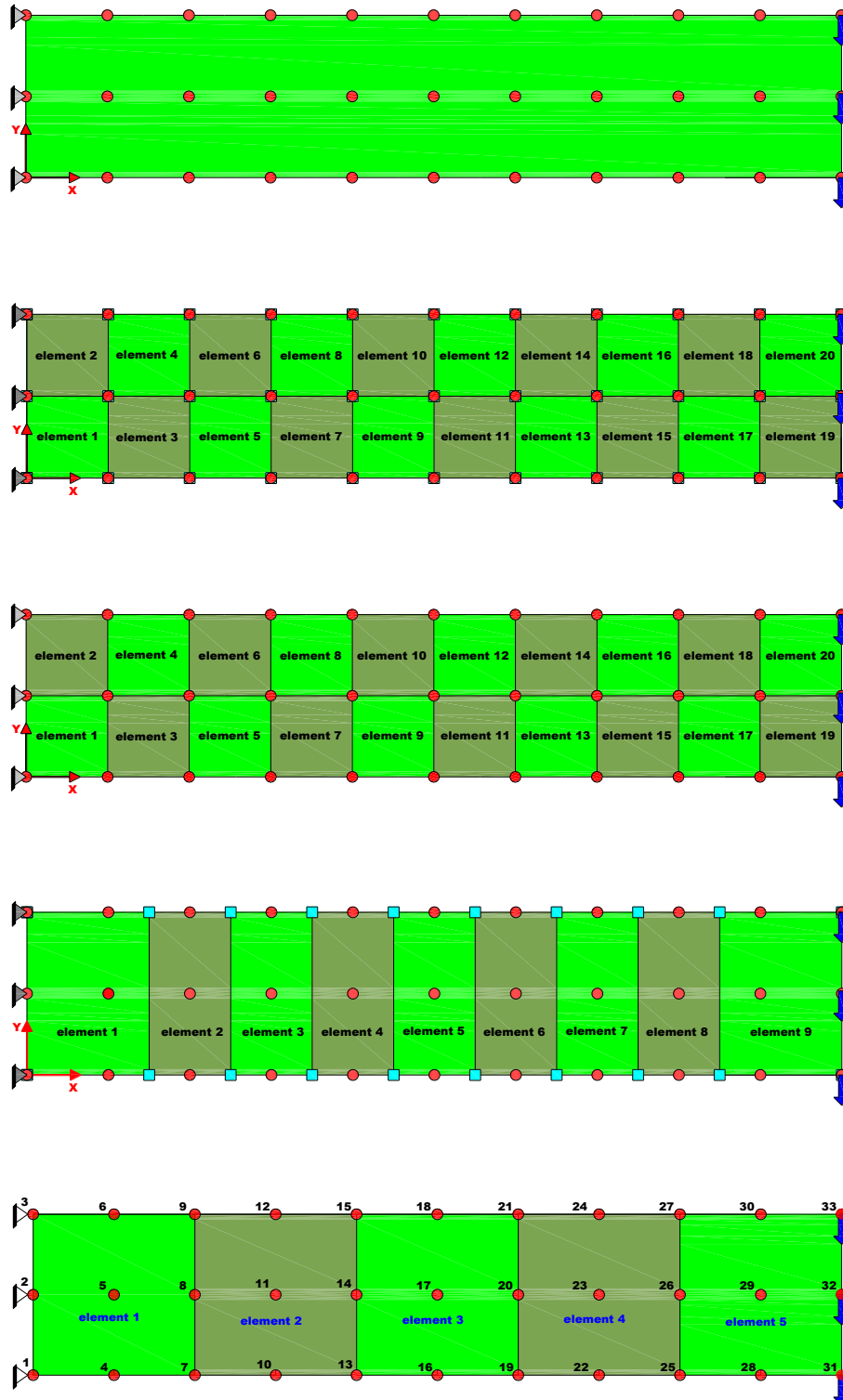


CONTENTS

2.1 Introduction (2D Problem)	59
2.2 Control Points/ Nodes: 33 & Shape Functions: Linear	60
2.2.1 Isogeometric Analysis	60
• Axis ξ	62
• Axis η	69
• Combinations Axes ξ, η ($\Xi \times H$).....	71
• Control Net.....	72
• Index Space	73
• Parameter Space	74
• Physical Space	75
• Elasticity Matrix [E]	77
• Deformation Matrix [B].....	77
• Local Stiffness Matrix [k^e].....	80
• Total Stiffness Matrix [K]	86
• Control Points' External Forces {P}.....	87
• Control Points' Displacements {U}	87
• Stress Field at Gauss Points	89
2.2.2 Finite Element Analysis	92
• 2D 4-sided 4-noded Finite Element.....	95
• Shape Functions	95
• Elasticity Matrix [E]	96
• Deformation Matrix [B].....	96
• Local Stiffness Matrix [k^e].....	97
• Control Net.....	99
• Parameter Space	100
• Physical Space	100
• Total Stiffness Matrix [K]	101
• Nodes' External Forces {P}	101
• Nodes' Displacements {U}.....	101
• Stress Field at Gauss Points	104
2.2.3 Comparison	109
• Shape Functions	110
• Control/ Node Net.....	111
• Parameter Space	111
• Physical Space	112
• Total Stiffness Matrix [K]	113
• Control Points'/ Nodes' Displacements {U}	114
• Stress Field at Gauss Points	116

2.3 Control Points/ Nodes: 33 & Shape Functions: Quadratic	117
2.3.1 Isogeometric Analysis	117
• Axis ξ	119
• Axis η	128
• Combinations Axes ξ, η ($\Xi \times H$).....	132
• Control Net.....	133
• Index Space	134
• Parameter Space	135
• Physical Space	136
• Elasticity Matrix [E]	138
• Deformation Matrix [B].....	138
• Local Stiffness Matrix [k^e].....	141
• Total Stiffness Matrix [K]	147
• Control Points' External Forces {P}.....	148
• Control Points' Displacements {U}	148
• Stress Field at Gauss Points	150
2.3.2 Finite Element Analysis	154
• Isoparametric 2D 4-sided 9-noded (Lagrange) Finite Element.....	155
• Shape Functions	155
• Elasticity Matrix [E]	156
• Deformation Matrix [B].....	156
• Local Stiffness Matrix [k^e].....	156
• Control Net.....	158
• Parameter Space	159
• Physical Space	159
• Total Stiffness Matrix [K]	160
• Nodes' External Forces {P}	160
• Nodes' Displacements {U}.....	160
• Stress Field at Gauss Points	163
2.3.3 Comparison	166
• Shape Functions	167
• Control/ Node Net.....	168
• Parameter Space	168
• Physical Space	169
• Total Stiffness Matrix [K]	170
• Control Points'/ Nodes' Displacements {U}	171
• Stress Field at Gauss Points	173

Isogeometric Analysis



2.

APPLICATIONS

2.1 Introduction (2D Problem)

Geometry

- height: $H=3\text{m}$
- length: $L=15\text{m}$
- thickness: $t=0,01\text{m}$

Material (Steel)

- elastic modulus: $E=210\text{GPa}=2,1 \cdot 10^8\text{kPa}$
- Poisson's ratio: $\nu=0,3$

Load

- concentrated: $P=1.000\text{kN}$
- location: extreme right edge

Boundary conditions

- fixed
- location: extreme left edge

Analysis

- static
- linear

Problem

- 2D

I will analyze the cantilever applying both IGA (IsoGeometric Analysis) and FEA (Finite Element Analysis), compare the two methods and explain differences and similarities.

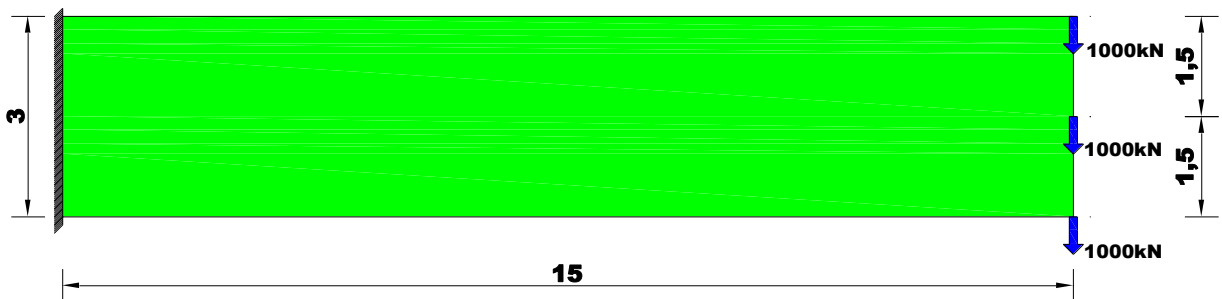


Figure 2.1. Cantilever Profile (Geometry. Boundary. Load.)

2.2 Control Points/ Nodes: 33 & Shape Functions: Linear.

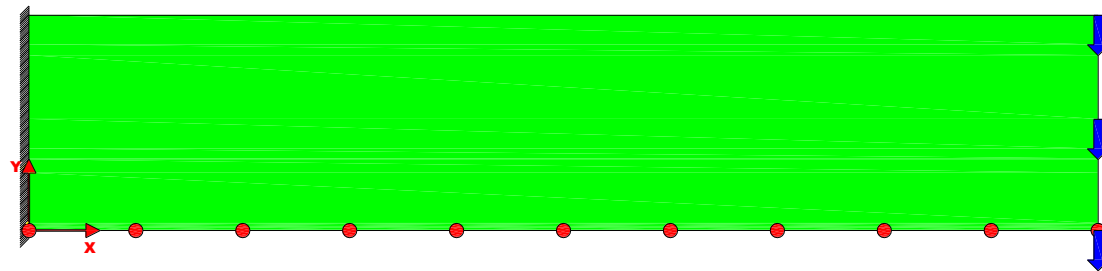
2.2.1. Isogeometric Analysis

I use the following analysis parameters:

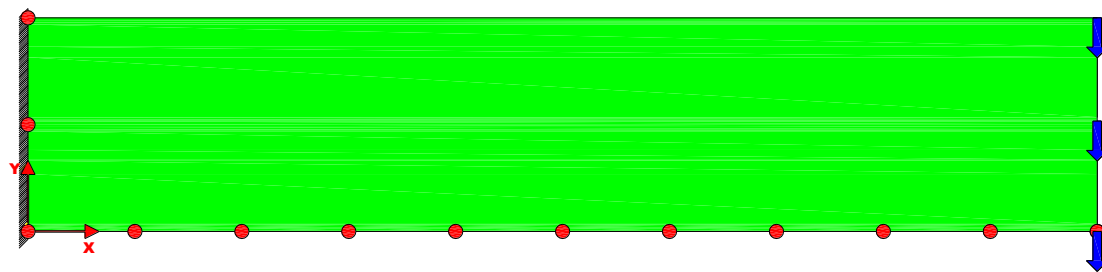
- The parametric axis ξ (parameter space) is parallel to cantilever's length (physical space), means horizontal. Its direction is from left to right.
- The parametric axis η (parameter space) is parallel to cantilever's height (physical space), means vertical. Its direction is from bottom to cantilever's top.
- $n \cdot m = 33$ control points. There are 3 ($m=3$ for axis η) groups of 11 ($n=11$ for axis ξ) control points equally spaced across cantilever's length in three different distances from its bottom. It is important to underline that the number of control points (C.P.) is equal to the B-SPLine's number. Cartesian coordinate system's origin is the extreme left and bottom corner.
- $p=q=1$. I choose linear Basis SPLine functions ($p=1$ Hughes, $K=p+1=1+1=2$ Fisher).

Method	IGA
Patches	1
Isogeometric Elements ($\Xi \times H$)	20
Horizontal Spans (Ξ)	10
Vertical Spans (H)	2
Control Points	33
Control Points (Ξ)	11
Control Points (H)	3
p	1
q	1
Gauss Points	5x5

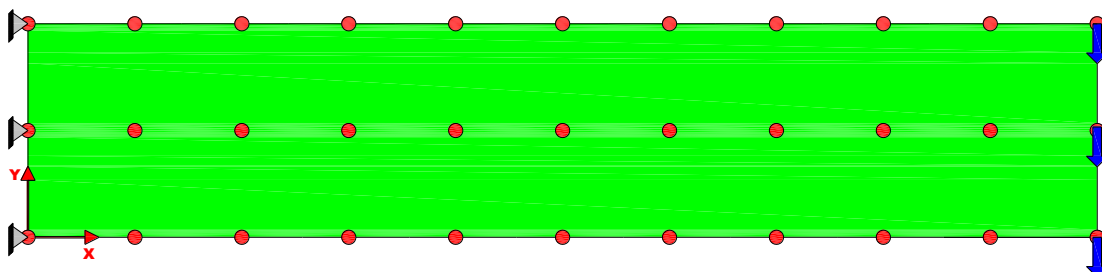
Figure 2.2.a. Analysis Parameters. IGA.



$n=11$ Control Points (Ξ)



$n=11$ Control Points (Ξ)
 $m=3$ Control Points (H)



$n=11$ Control Points (Ξ)
 $m=3$ Control Points (H)
 $n \cdot m = 11 \cdot 3 = 33$ Control Points ($\Xi \times H$)

Figure 2.2.b. Cantilever Profile (Cartesian Axes. Control Points.)

Axis ξ

Basis SPLine functions

The axis ξ is parallel to cantilever's horizontal side (length).

- $n=11$ (control points).
- $p=1$ (linear Basis SPLine functions, 2 control points per horizontal span).
- $n+p+1=11+1+1=13$ knot values.

The open uniform knot vector Ξ contains the following knot values:

- The extreme knots $-1, 1$ repeated $p+1=1+1=2$ times $\rightarrow 4$ knot values. Remaining, not recurrent: $13-4=9$ knot values $\rightarrow 9+2=11$ knots. \rightarrow I will separate the interval $[-1, 1]$ into $11-1=10$ equal spans. Notice that spans' number is equal to $n-p=11-1=10$.

$$\frac{1-(-1)}{10} = \frac{2}{10} = 0,2$$

$$\Xi = -1 \quad -1 \quad -0.8 \quad -0.6 \quad -0.4 \quad -0.2 \quad 0 \quad 0.2 \quad 0.4 \quad 0.6 \quad 0.8 \quad 1 \quad 1$$

The corresponding linear Basis SPLine functions to knot vector Ξ are 11 (one for every control point). The support of each linear BSPLine is two spans.

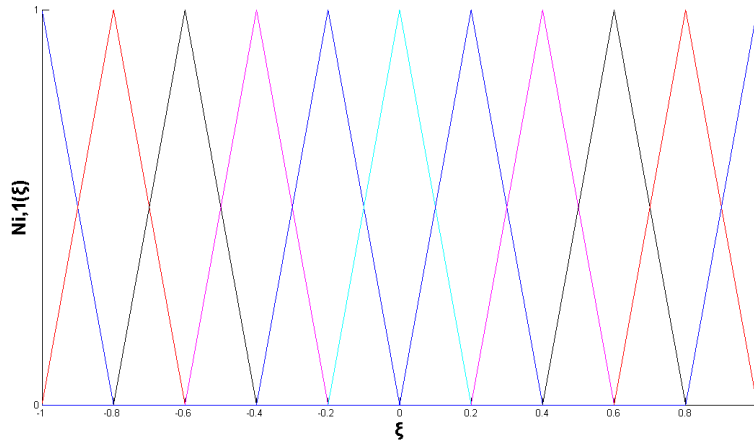


Figure 2.3. Linear Basis SPLine functions for open, uniform knot vector
 $\Xi=\{-1,-1,-0.8,-0.6,-0.4,-0.2,0,0.2,0.4,0.6,0.8,1,1\}$.

According to Hughes:

$$N_{i,0}(\xi) = \begin{cases} 1 & \text{if } \xi_i \leq \xi < \xi_{i+1} \\ 0 & \text{otherwise} \end{cases}$$

Isogeometric Analysis

For p=1,2,3,...:

$$N_{i,p}(\xi) = \frac{\xi - \xi_i}{\xi_{i+p} - \xi_i} \cdot N_{i,p-1}(\xi) + \frac{\xi_{i+p+1} - \xi}{\xi_{i+p+1} - \xi_{i+1}} \cdot N_{i+1,p-1}(\xi)$$

where i=1,...,n.

I prefer to use the polynomial constant K=p+1 than p. The corresponding relations are equal to:

$$N_{i,1}(\xi) = \begin{cases} 1 & \text{if } \xi_i \leq \xi < \xi_{i+1} \\ 1 & \text{if } i=n \text{ and } \xi = \xi_{n+1} \\ 0 & \text{otherwise} \end{cases}$$

$$N_{i,k}(\xi) = \frac{\xi - \xi_i}{\xi_{i+k-1} - \xi_i} \cdot N_{i,k-1}(\xi) + \frac{\xi_{i+k} - \xi}{\xi_{i+k} - \xi_{i+1}} \cdot N_{i+1,k-1}(\xi)$$

where i=1,...,n and k=2,...,K.

The derivative of BSpline function, $N'_{i,k}$, is given by:

$$N'_{i,k}(\xi) = \frac{k-1}{\xi_{i+k-1} - \xi_i} \cdot N_{i,k-1}(\xi) - \frac{k-1}{\xi_{i+k} - \xi_{i+1}} \cdot N_{i+1,k-1}(\xi)$$

It is very important to mention that index i refers to knots and not to knot values. Because the denominators in the second relation can be zero, the convention 0/0=0 is used; in other words 0x(.)=0 even if (.) is undefined. When i=n, the second term is omitted.

Gauss Points (coordinates, weight factors)

The polynomial Legendre $P_n(x)$ is a polynomial of order n.

$$P_n(x) = \frac{1}{2^n \cdot n!} \cdot \frac{d^n}{dx^n} \left[x^2 - 1 \right]^n$$

As far as concern the first 6 ($n = 0 \div 5$) Legendre polynomials, they are equal to:

n	0	1	2	3	4	5
$P_n(x)$	1	x	$\frac{1}{2} \cdot 3x^2 - 1$	$\frac{1}{2} \cdot 5x^3 - 3x$	$\frac{1}{8} \cdot 35x^4 - 30x^2 + 3$	$\frac{1}{8} \cdot 63x^5 - 70x^3 + 15x$

Figure 2.4. The first six Legendre polynomials.

Isogeometric Analysis

I use 5 Gauss Points for every horizontal span. The corresponding coordinates ξ_i , $i=1 \div 5$ are the five roots of Legendre polynomial $P_5(x)$.

$$\frac{1}{8} \cdot 63\xi^5 - 70\xi^3 + 15\xi = 0 \Rightarrow \xi_i = \begin{cases} 0 \\ \pm \frac{\sqrt{245-14\sqrt{70}}}{21} = \pm 0.53846 \\ \pm \frac{\sqrt{245+14\sqrt{70}}}{21} = \pm 0.90617 \end{cases}$$

In the following figure, we can see the curves $P_n(x)$ -x for the first 6 polynomials $n = 0 \div 5$. It is obvious why I have chosen the Legendre polynomials.

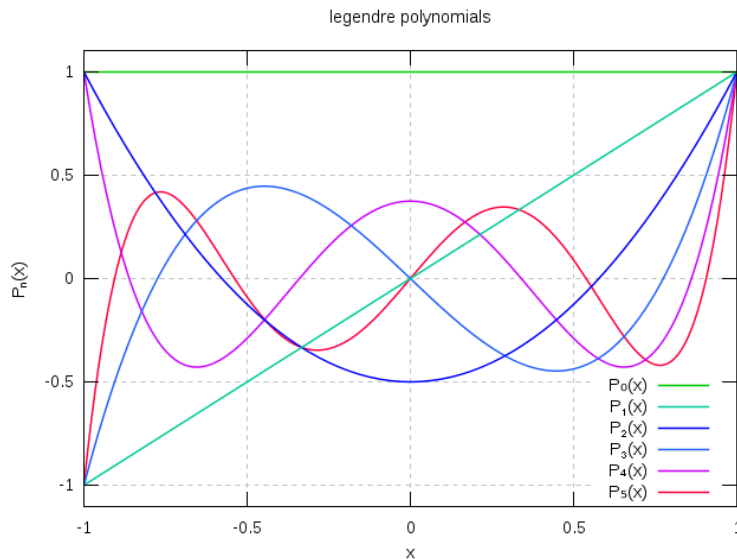


Figure 2.5. Legendre Polynomials.

It is worth mentioning the recursive relation Bonnête.

$$n \cdot P_n(x) = 2n-1 \cdot x \cdot P_{n-1}(x) - n-1 \cdot P_{n-2}(x)$$

I calculate integrals using numerical integration. That's why I use Gauss Points. Previously, I explained how I calculate Gauss Points' coordinates. Now, I will explain how I calculate the corresponding weight factors.

$$\int_{-1}^1 f(\xi) d\xi = \sum_{i=1}^n [w_i \cdot f(\xi_i)] \quad \text{where} \quad w_i = \frac{2}{(1-\xi_i^2) \cdot [P_n'(\xi_i)]^2}$$

For example, I will calculate the weight factor of Gauss Point $\xi_2=0.90617$.

$$\begin{aligned}
 P_5'(\xi) &= \frac{1}{8} \cdot 63\xi^5 - 70\xi^3 + 15\xi \\
 P_5'(\xi) &= \frac{1}{8} \cdot 63 \cdot 5 \cdot \xi^4 - 70 \cdot 3 \cdot \xi^2 + 15 = \frac{1}{8} \cdot 315 \cdot \xi^4 - 210 \cdot \xi^2 + 15 \\
 P_5'(\xi_2) &= P_5'(-0.90617) = \frac{1}{8} \cdot 315 \cdot 0.90617^4 - 210 \cdot 0.90617^2 + 15 = 6.86965 \\
 w_2 &= \frac{2}{(1-\xi_2^2) \cdot [P_n(\xi_2)]^2} = \frac{2}{(1-0.90617^2) \cdot 6.86965^2} = 0.2369
 \end{aligned}$$

Number of points, n	Points, x_i	Weights, w_i
1	0	2
2	$\pm 1/\sqrt{3}$	1
3	0	$\frac{5}{9}$
	$\pm \sqrt{3/5}$	$\frac{5}{9}$
4	$\pm \sqrt{(3 - 2\sqrt{6/5})/7}$	$\frac{18+\sqrt{30}}{36}$
	$\pm \sqrt{(3 + 2\sqrt{6/5})/7}$	$\frac{18-\sqrt{30}}{36}$
5	0	$\frac{128}{225}$
	$\pm \frac{1}{3} \sqrt{5 - 2\sqrt{10/7}}$	$\frac{322+13\sqrt{70}}{900}$
	$\pm \frac{1}{3} \sqrt{5 + 2\sqrt{10/7}}$	$\frac{322-13\sqrt{70}}{900}$

Figure 2.6. Gauss Points' coordinate and weight factor.

Each point's coordinate and weight factor is equal to (local numbering, span [-1,1]):

G.P.	ξ_i'	w_i
4	-0.90617	0.23692
5	-0.53846	0.47862
1	0	0.56888
3	0.53846	0.47862
2	0.90617	0.23692

Notice that:

$$\sum_{i=1}^5 w_i = 2$$

I use 5 Gauss Points for every horizontal span. The horizontal interval [-1,1] has 10 spans, so $10 \cdot 5 = 50$ G.P. These points are shown as yellow rhombi in Figure 2.7, while knots as cyan circles.

Isogeometric Analysis

I assume a local ξ for every span with its center in the span's middle. Then, from Gauss Points' local coordinates ξ'_i , I calculate the global ones ξ_i . Let's calculate the coordinate ξ_i of G.P. 2 for span 1 (extreme left span).

$$\begin{aligned} \frac{\xi'_{G.P.2} - -1}{1 - -1} &= \frac{\xi_{G.P.2} - -1}{-0.8 - -1} \Rightarrow \frac{0.9062 + 1}{1 + 1} = \frac{\xi_{G.P.2} + 1}{-0.8 + 1} \Rightarrow \\ \frac{1.9062}{2} &= \frac{\xi_{G.P.2} + 1}{0.2} \Rightarrow \xi_{G.P.2} = \frac{1.9062}{2} \cdot 0.2 - 1 \Rightarrow \\ \boxed{\xi_{G.P.2} = -0.80938} \end{aligned}$$

Generally, the coordinate ξ_j of Gauss Point j in the span (ξ_i, ξ_{i+1}) is equal to:

$$\begin{aligned} \frac{\xi'_{G.P.j} - -1}{1 - -1} &= \frac{\xi_{G.P.j} - \xi_i}{\xi_{i+1} - \xi_i} \Rightarrow \frac{\xi'_{G.P.j} + 1}{2} = \frac{\xi_{G.P.j} - \xi_i}{\xi_{i+1} - \xi_i} \Rightarrow \\ \xi_{G.P.j} &= \frac{\xi'_{G.P.j} + 1}{2} \cdot \frac{\xi_{i+1} - \xi_i}{2} + \xi_i = \xi'_{G.P.j} \cdot \frac{\xi_{i+1} - \xi_i}{2} + \frac{\xi_{i+1} - \xi_i}{2} + \frac{2 \cdot \xi_i}{2} \Rightarrow \\ \boxed{\xi_{G.P.j} = \xi'_{G.P.j} \cdot \frac{\xi_{i+1} - \xi_i}{2} + \frac{\xi_{i+1} + \xi_i}{2}} \end{aligned}$$

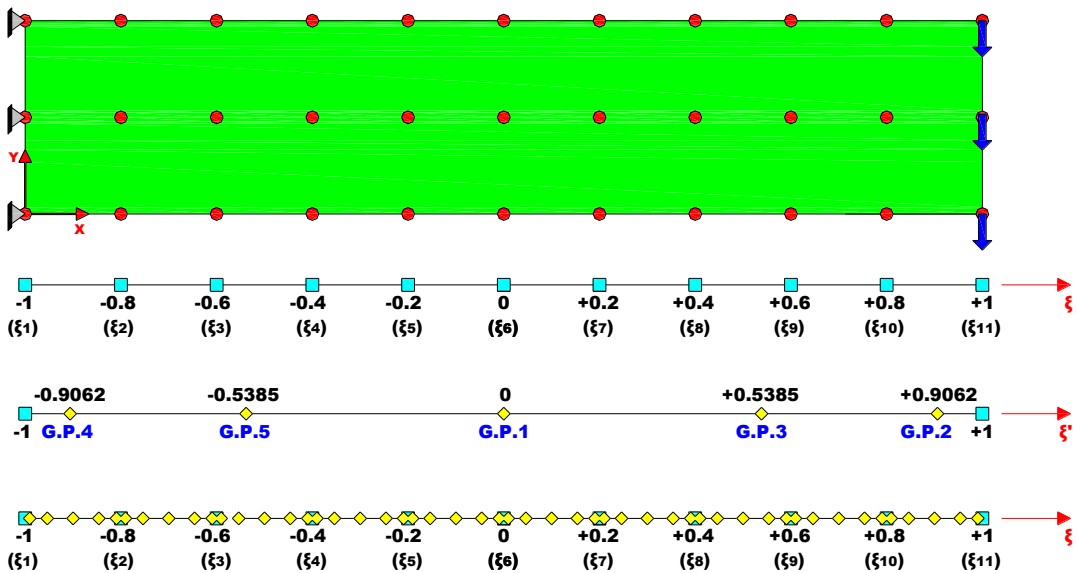


Figure 2.7. Gauss Points (parametric axis ξ).

B-SPLines' value at Gauss Points

I calculate the linear BSpline functions' ($N_{i,1}(\xi)$) values ($p=1, K=2$) at the position ξ_i of 50 Gauss Points in horizontal parametric axis ξ and their corresponding first derivatives

$$N'_{i,1}(\xi) = \frac{\partial N_{i,1}}{\partial \xi}.$$

$N_{i,1}(\xi)$ (2x5,p=1)	axis ξ				
	horizontal span 1				
$N_{1,1}(\xi)$	0,5	0,0469	0,2308	0,9531	0,7692
$N_{2,1}(\xi)$	0,5	0,9531	0,7692	0,0469	0,2308
horizontal span 2					
	G.P.6 (1)	G.P.7 (2)	G.P.8 (3)	G.P.9 (4)	G.P.10 (5)
$N_{2,1}(\xi)$	0,5	0,0469	0,2308	0,9531	0,7692
$N_{3,1}(\xi)$	0,5	0,9531	0,7692	0,0469	0,2308
horizontal span 3					
	G.P.11 (1)	G.P.12 (2)	G.P.13 (3)	G.P.14 (4)	G.P.15 (5)
$N_{3,1}(\xi)$	0,5	0,0469	0,2308	0,9531	0,7692
$N_{4,1}(\xi)$	0,5	0,9531	0,7692	0,0469	0,2308
horizontal span 4					
	G.P.16 (1)	G.P.17 (2)	G.P.18 (3)	G.P.19 (4)	G.P.20 (5)
$N_{4,1}(\xi)$	0,5	0,0469	0,2308	0,9531	0,7692
$N_{5,1}(\xi)$	0,5	0,9531	0,7692	0,0469	0,2308
horizontal span 5					
	G.P.21 (1)	G.P.22 (2)	G.P.23 (3)	G.P.24 (4)	G.P.25 (5)
$N_{5,1}(\xi)$	0,5	0,0469	0,2308	0,9531	0,7692
$N_{6,1}(\xi)$	0,5	0,9531	0,7692	0,0469	0,2308
horizontal span 6					
	G.P.26 (1)	G.P.27 (2)	G.P.28 (3)	G.P.29 (4)	G.P.30 (5)
$N_{6,1}(\xi)$	0,5	0,0469	0,2308	0,9531	0,7692
$N_{7,1}(\xi)$	0,5	0,9531	0,7692	0,0469	0,2308
horizontal span 7					
	G.P.31 (1)	G.P.32 (2)	G.P.33 (3)	G.P.34 (4)	G.P.35 (5)
$N_{7,1}(\xi)$	0,5	0,0469	0,2308	0,9531	0,7692
$N_{8,1}(\xi)$	0,5	0,9531	0,7692	0,0469	0,2308
horizontal span 8					
	G.P.36 (1)	G.P.37 (2)	G.P.38 (3)	G.P.39 (4)	G.P.40 (5)
$N_{8,1}(\xi)$	0,5	0,0469	0,2308	0,9531	0,7692
$N_{9,1}(\xi)$	0,5	0,9531	0,7692	0,0469	0,2308
horizontal span 9					
	G.P.41 (1)	G.P.42 (2)	G.P.43 (3)	G.P.44 (4)	G.P.45 (5)
$N_{9,1}(\xi)$	0,5	0,0469	0,2308	0,9531	0,7692
$N_{10,1}(\xi)$	0,5	0,9531	0,7692	0,0469	0,2308
horizontal span 10					
	G.P.46 (1)	G.P.47 (2)	G.P.48 (3)	G.P.49 (4)	G.P.50 (5)
$N_{10,1}(\xi)$	0,5	0,0469	0,2308	0,9531	0,7692
$N_{11,1}(\xi)$	0,5	0,9531	0,7692	0,0469	0,2308

Figure 2.8. Basis SPLine functions' values at Gauss Points of interval $\xi [-1,1]$
 $(N_{1,1} \div N_{11,1}, \xi_{G.P.1} \div \xi_{G.P.50}, p=1)$

We can see the connection between local and global numbering in Figure 2.8. The local numbers are in brackets.

$N'_{i,1}(\xi)$ (2x5,p=1)	axis ξ				
horizontal span 1					
	G.P.1 (1)	G.P.2 (2)	G.P.3 (3)	G.P.4 (4)	G.P.5 (5)
$N'_{1,1}(\xi)$	-5	-5	-5	-5	-5
$N'_{2,1}(\xi)$	5	5	5	5	5
horizontal span 2					
	G.P.6 (1)	G.P.7 (2)	G.P.8 (3)	G.P.9 (4)	G.P.10 (5)
$N'_{2,1}(\xi)$	-5	-5	-5	-5	-5
$N'_{3,1}(\xi)$	5	5	5	5	5
horizontal span 3					
	G.P.11 (1)	G.P.12 (2)	G.P.13 (3)	G.P.14 (4)	G.P.15 (5)
$N'_{3,1}(\xi)$	-5	-5	-5	-5	-5
$N'_{4,1}(\xi)$	5	5	5	5	5
horizontal span 4					
	G.P.16 (1)	G.P.17 (2)	G.P.18 (3)	G.P.19 (4)	G.P.20 (5)
$N'_{4,1}(\xi)$	-5	-5	-5	-5	-5
$N'_{5,1}(\xi)$	5	5	5	5	5
horizontal span 5					
	G.P.21 (1)	G.P.22 (2)	G.P.23 (3)	G.P.24 (4)	G.P.25 (5)
$N'_{5,1}(\xi)$	-5	-5	-5	-5	-5
$N'_{6,1}(\xi)$	5	5	5	5	5
horizontal span 6					
	G.P.26 (1)	G.P.27 (2)	G.P.28 (3)	G.P.29 (4)	G.P.30 (5)
$N'_{6,1}(\xi)$	-5	-5	-5	-5	-5
$N'_{7,1}(\xi)$	5	5	5	5	5
horizontal span 7					
	G.P.31 (1)	G.P.32 (2)	G.P.33 (3)	G.P.34 (4)	G.P.35 (5)
$N'_{7,1}(\xi)$	-5	-5	-5	-5	-5
$N'_{8,1}(\xi)$	5	5	5	5	5
horizontal span 8					
	G.P.36 (1)	G.P.37 (2)	G.P.38 (3)	G.P.39 (4)	G.P.40 (5)
$N'_{8,1}(\xi)$	-5	-5	-5	-5	-5
$N'_{9,1}(\xi)$	5	5	5	5	5
horizontal span 9					
	G.P.41 (1)	G.P.42 (2)	G.P.43 (3)	G.P.44 (4)	G.P.45 (5)
$N'_{9,1}(\xi)$	-5	-5	-5	-5	-5
$N'_{10,1}(\xi)$	5	5	5	5	5
horizontal span 10					
	G.P.46 (1)	G.P.47 (2)	G.P.48 (3)	G.P.49 (4)	G.P.50 (5)
$N'_{10,1}(\xi)$	-5	-5	-5	-5	-5
$N'_{11,1}(\xi)$	5	5	5	5	5

Figure 2.9. Basis SPLine first derivative's values at Gauss Points of interval $\xi [-1,1]$
 $(N'_{1,1} \div N'_{11,1}, \xi_{G.P.1} \div \xi_{G.P.50}, p=1)$

We can see the connection between local and global numbering in Figure 2.8. The local numbers are in brackets.

Axis η

Basis SPLine functions

The axis η is parallel to cantilever's vertical side (height).

- $m=3$ (control points).
- $q=1$ (linear Basis SPLine functions, 2 control points per vertical span).
- $m+q+1=3+1+1=5$ knot values.

The open uniform knot vector H contains the following knot values:

- The extreme knots $-1, 1$ repeated $p+1=1+1=2$ times $\rightarrow 4$ knot values. Remaining, not recurrent: $5-4=1$ knot value $\rightarrow 1+2=3$ knots. \rightarrow I will separate the interval $[-1, 1]$ into $3-1=2$ equal spans. Notice that spans' number is equal to $m-q=3-1=2$.

$$\frac{1 - (-1)}{2} = \frac{2}{2} = 1$$

$$H = -1 \quad 0 \quad 1$$

The corresponding linear Basis SPLine functions to knot vector H are 3 (one for every control point). The support of each linear BSPLine is two spans.

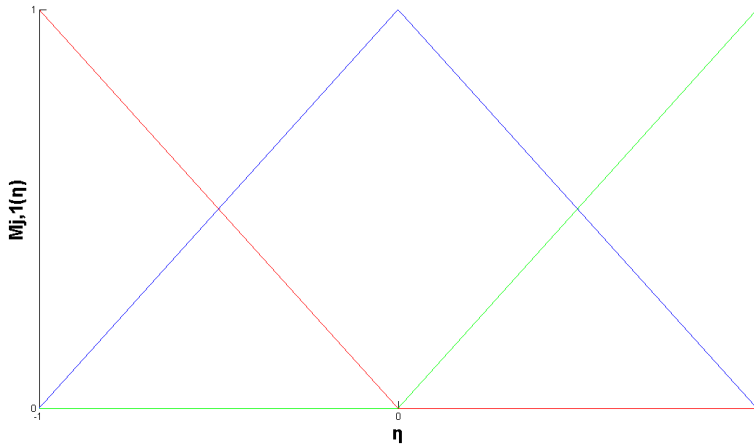


Figure 2.10. Linear Basis SPLine functions for open, uniform knot vector $H=\{-1,0,1\}$.

Gauss Points (coordinates, weight factors)

I use 5 Gauss Points for every vertical span. Each point's coordinate and weight factor is equal to (local numbering, span $[-1,1]$):

G.P.	η'_i	w_i
4	-0.90617	0.23692
5	-0.53846	0.47862
1	0	0.56888
3	0.53846	0.47862
2	0.90617	0.23692

Notice that: $\sum_{i=1}^5 w_i = 2$.

The vertical interval $[-1,1]$ has 2 spans, so $2 \cdot 5 = 10$ G.P. These points are shown as yellow rhombi in Figure 2.11, while knots as cyan circles.

I assume a local η for every span with its center in the span's middle. Then, from Gauss Points' local coordinates η'_i , I calculate the global ones η_i . Let's calculate the coordinate η_i of G.P. 2 for span 1 (lower span).

$$\begin{aligned} \frac{\eta_{G.P.2} - -1}{1 - -1} &= \frac{\eta_{G.P.2} - -1}{0 - -1} \Rightarrow \frac{0.9062 + 1}{1 + 1} = \frac{\eta_{G.P.2} + 1}{1} \Rightarrow \\ \frac{1.9062}{2} &= \frac{\eta_{G.P.2} + 1}{1} \Rightarrow \eta_{G.P.2} = \frac{1.9062}{2} - 1 \Rightarrow \\ \boxed{\eta_{G.P.2} = -0.0469} \end{aligned}$$

Generally, the coordinate η_j of Gauss Point j in the span (η_i, η_{i+1}) is equal to:

$$\eta_{G.P.j} = \eta'_{G.P.j} \cdot \frac{\eta_{i+1} - \eta_i}{2} + \frac{\eta_{i+1} + \eta_i}{2}$$

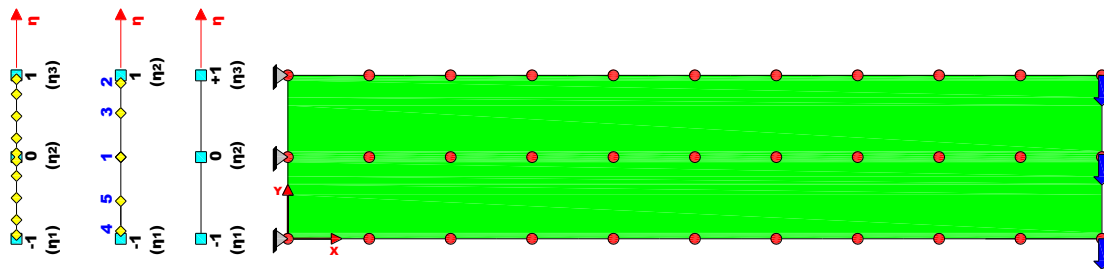


Figure 2.11. Gauss Points (parametric axis η).

B-SPLines' value at Gauss Points

I calculate the linear BSpline functions' ($M_{j,1}(\eta)$) values ($q=1, K=2$) at the position η_j of 10 Gauss Points in vertical parametric axis η and their corresponding first derivatives

$$M'_{j,1}(\eta) = \frac{\partial M_{j,1}(\eta)}{\partial \eta}.$$

Isogeometric Analysis

$M_{1,1}(\eta)$ (2x5,q=1)	axis η				
vertical span 1					
	G.P.1 (1)	G.P.2 (2)	G.P.3 (3)	G.P.4 (4)	G.P.5 (5)
$M_{1,1}(\eta)$	0,5	0,0469	0,2308	0,9531	0,7692
vertical span 2					
	G.P.6 (1)	G.P.7 (2)	G.P.8 (3)	G.P.9 (4)	G.P.10 (5)
$M_{2,1}(\eta)$	0,5	0,0469	0,2308	0,9531	0,7692
$M_{3,1}(\eta)$	0,5	0,9531	0,7692	0,0469	0,2308

Figure 2.12. Basis SPLine functions' values at Gauss Points of interval η [-1,1]
 $(M_{1,1} \div M_{3,1}, \eta_{G.P.1} \div \eta_{G.P.10}, q=1)$

$M'_{j,1}(\eta)$ (2x5,q=1)	axis η				
vertical span 1					
	G.P.1 (1)	G.P.2 (2)	G.P.3 (3)	G.P.4 (4)	G.P.5 (5)
$M'_{1,1}(\eta)$	-1	-1	-1	-1	-1
vertical span 2					
	G.P.6 (1)	G.P.7 (2)	G.P.8 (3)	G.P.9 (4)	G.P.10 (5)
$M'_{2,1}(\eta)$	-1	-1	-1	-1	-1
$M'_{3,1}(\eta)$	1	1	1	1	1

Figure 2.13. Basis SPLine first derivative's values at Gauss Points of interval η [-1,1]
 $(M'_{1,1} \div M'_{3,1}, \eta_{G.P.1} \div \eta_{G.P.10}, q=1)$

Combination Axes ξ, η ($\Xi \times H$)

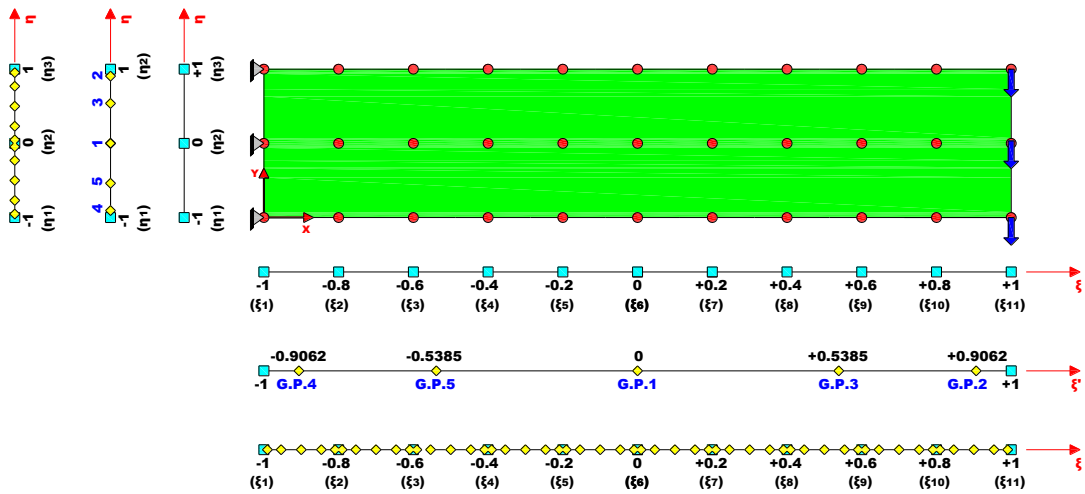


Figure 2.14. Gauss Points (parameter space $\Xi \times H$).

I combine the 50 Gauss Points in the axis ξ with the 10 Gauss Points in the axis η and I produce the $50 \times 10 = 500$ Gauss Points of the 2D plane stress cantilever.

Control Net

I choose 33 control points with the following features.

		axis X										
		X _{C.P.}										
local numbering			element 1	element 2	element 3	element 4	element 5	element 6	element 7	element 8	element 9	element 10
	C.P.1		0	0	1,5	1,5	3	3	4,5	4,5	6	6
	C.P.2		0	0	1,5	1,5	3	3	4,5	4,5	6	6
	C.P.3		1,5	1,5	3	3	4,5	4,5	6	6	7,5	7,5
	C.P.4		1,5	1,5	3	3	4,5	4,5	6	6	7,5	7,5
			element 11	element 12	element 13	element 14	element 15	element 16	element 17	element 18	element 19	element 20
	C.P.1		7,5	7,5	9	9	10,5	10,5	12	12	13,5	13,5
	C.P.2		7,5	7,5	9	9	10,5	10,5	12	12	13,5	13,5
	C.P.3		9	9	10,5	10,5	12	12	13,5	13,5	15	15
	C.P.4		9	9	10,5	10,5	12	12	13,5	13,5	15	15

Figure 2.15.a. Control Points' Cartesian coordinate X. (physical space)

		axis Y										
		Y _{C.P.}										
local numbering			element 1	element 2	element 3	element 4	element 5	element 6	element 7	element 8	element 9	element 10
	C.P.1		0	1,5	0	1,5	0	1,5	0	1,5	0	1,5
	C.P.2		1,5	3	1,5	3	1,5	3	1,5	3	1,5	3
	C.P.3		0	1,5	0	1,5	0	1,5	0	1,5	0	1,5
	C.P.4		1,5	3	1,5	3	1,5	3	1,5	3	1,5	3
			element 11	element 12	element 13	element 14	element 15	element 16	element 17	element 18	element 19	element 20
	C.P.1		0	1,5	0	1,5	0	1,5	0	1,5	0	1,5
	C.P.2		1,5	3	1,5	3	1,5	3	1,5	3	1,5	3
	C.P.3		0	1,5	0	1,5	0	1,5	0	1,5	0	1,5
	C.P.4		1,5	3	1,5	3	1,5	3	1,5	3	1,5	3

Figure 2.15.b. Control Points' Cartesian coordinate Y. (physical space)

		Weight Factor										
		W _{C.P.}										
local numbering			element 1	element 2	element 3	element 4	element 5	element 6	element 7	element 8	element 9	element 10
	C.P.1		1	1	1	1	1	1	1	1	1	1
	C.P.2		1	1	1	1	1	1	1	1	1	1
	C.P.3		1	1	1	1	1	1	1	1	1	1
	C.P.4		1	1	1	1	1	1	1	1	1	1
			element 11	element 12	element 13	element 14	element 15	element 16	element 17	element 18	element 19	element 20
	C.P.1		1	1	1	1	1	1	1	1	1	1
	C.P.2		1	1	1	1	1	1	1	1	1	1
	C.P.3		1	1	1	1	1	1	1	1	1	1
	C.P.4		1	1	1	1	1	1	1	1	1	1

Figure 2.15.c. Control Points' weight factor W. (physical space)

Control Points don't partition the structure into isogeometric elements, but they are the coefficients (multiplicative factors) of the corresponding B-Splines that form its geometry. In this particular problem, the cantilever has linear geometry as its boundaries are straight lines. That's why control points' weight factor is equal to 1.

In Figure 2.16 we can see the corresponding control net.

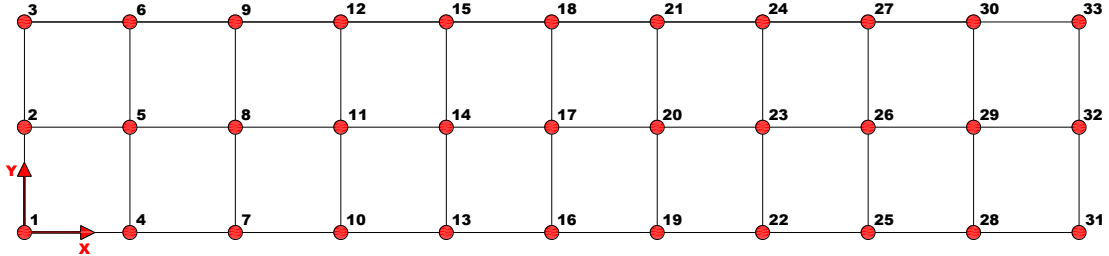


Figure 2.16. Control Net. (physical space)

Index Space

I present every knot value in index space. The most important is that we can see which knot vector's region is used by each isogeometric element. With darker green I represent the overlapping.

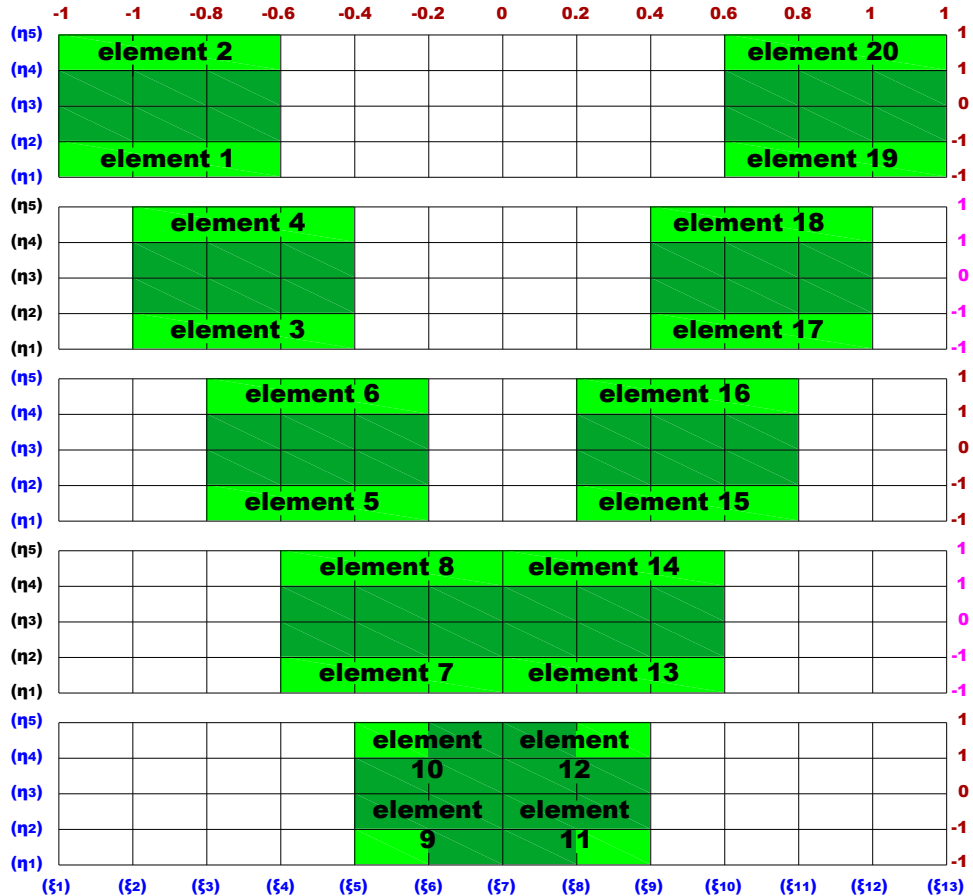
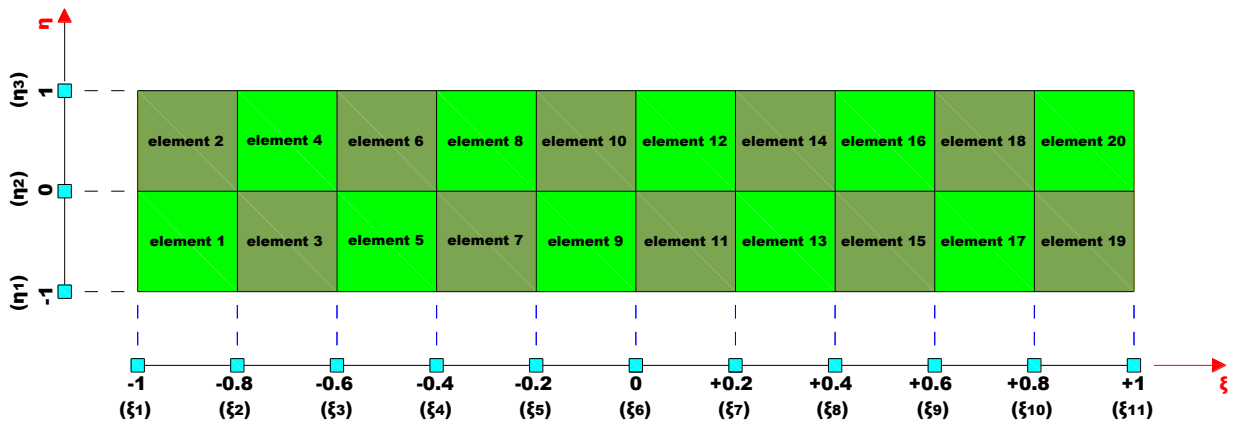


Figure 2.17. Index Space.

Parameter Space

I present every knot and not every knot value in parameter space. For example, extreme knot value -1 repeated $p+1=1+1=2$ times, but it has the same position, means it corresponds to one knot. In Figure 2.18 we can see the chosen mesh of isogeometric elements. It is very important to underline that knots and not control points partition the cantilever into isogeometric elements.

The 11 1D knots (ξ) partition the interval $[-1,1]$ of parametric axis ξ into 10 horizontal spans. The 3 1D knots (η) partition the interval $[-1,1]$ of parametric axis η into 2 vertical spans. Combining the two axes, we have the cantilever's mesh in the parameter space, which consists of $10 \times 2 = 20$ isogeometric elements.



**Figure 2.18.a. Parameter Space.
Knots partition cantilever into isogeometric elements.**

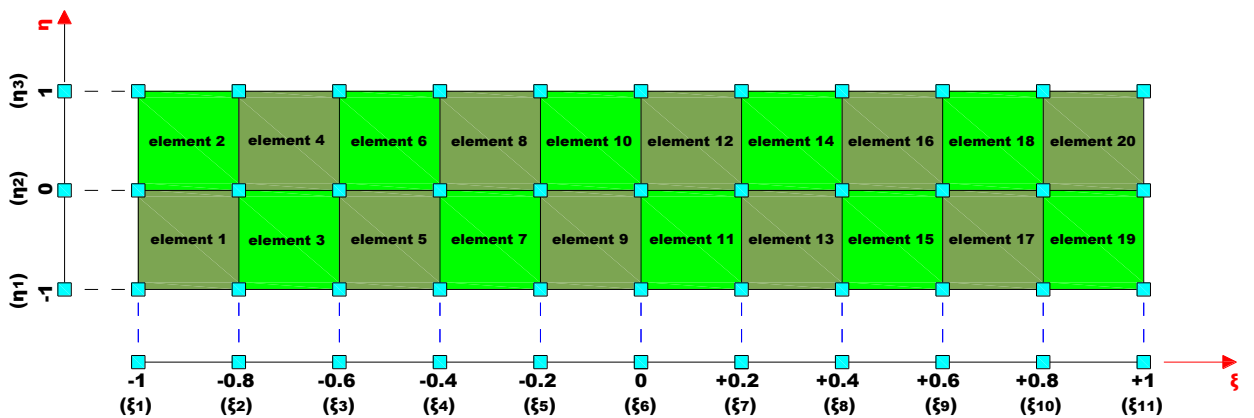


**Figure 2.18.b. Parameter Space.
Mesh of isogeometric elements.**

Physical Space

With the mesh of isogeometric elements in parameter space in hand, I can form the corresponding mesh in physical space. I follow the next procedure, where control points' numbering is local:

- I calculate knots' X Cartesian (physical) coordinates from their parametric ones. Supposing the knot $i (\xi_i, \eta_i)$, I have that:

$$X_i = X_{\xi_i} = X_{C.P.1} \cdot N_{1,1}(\xi_i) + \dots + X_{C.P.11} \cdot N_{11,1}(\xi_i)$$

Applying this relation for every knot:

$$X_{\xi_1} = X_{C.P.1} \cdot N_{1,1}(\xi_1) + \dots + X_{C.P.11} \cdot N_{11,1}(\xi_1) = X_{C.P.1} \cdot 1 = X_{C.P.1} = 0$$

Similarly,

$$X_{\xi_2} = X_{C.P.2} = 1,5m$$

$$X_{\xi_3} = X_{C.P.3} = 3m$$

$$X_{\xi_4} = X_{C.P.4} = 4,5m$$

$$X_{\xi_5} = X_{C.P.5} = 6m$$

$$X_{\xi_6} = X_{C.P.6} = 7,5m$$

$$X_{\xi_7} = X_{C.P.7} = 9m$$

$$X_{\xi_8} = X_{C.P.8} = 10,5m$$

$$X_{\xi_9} = X_{C.P.9} = 12m$$

$$X_{\xi_{10}} = X_{C.P.10} = 13,5m$$

$$X_{\xi_{11}} = X_{C.P.11} = 15m$$

- I calculate knots' Y Cartesian (physical) coordinates from their parametric ones. Supposing the knot $i (\xi_i, \eta_i)$, I have that:

$$Y_i = Y_{\eta_i} = Y_{C.P.1} \cdot M_{1,1}(\eta_i) + \dots + Y_{C.P.3} \cdot M_{3,1}(\eta_i)$$

Applying this relation for every knot:

$$Y_{\eta_1} = Y_{C.P.1} \cdot M_{1,1}(\eta_1) + \dots + Y_{C.P.3} \cdot M_{3,1}(\eta_1) = Y_{C.P.1} \cdot 1 = Y_{C.P.1} = 0$$

Similarly,

$$Y_{\eta_2} = Y_{C.P.2} = 1.5m$$

$$Y_{\eta_3} = Y_{C.P.3} = 3m$$

Isogeometric Analysis

- As I know for every knot its Cartesian coordinates (X, Y), I can draw them in cantilever's geometry (physical space). We can see the knots as cyan rhombi in Figure 2.19.
- Finally, I connect the knots with their adjacent ones. We can see the knot lines as black lines in Figure 2.19.

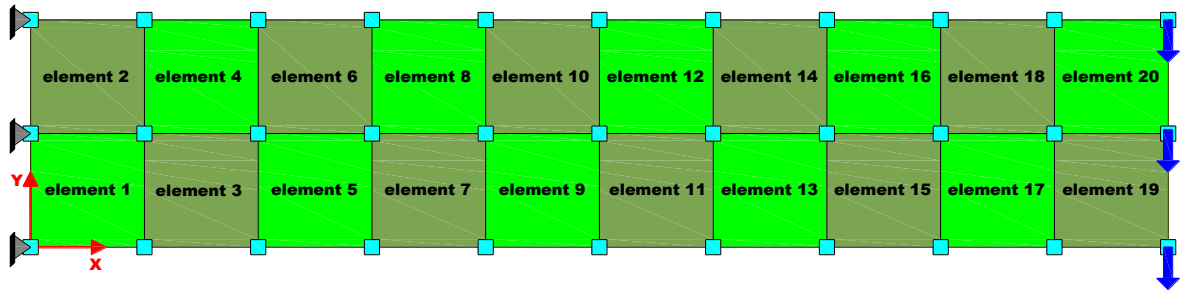


Figure 2.19. Physical Space. Mesh. Knots.

Figure 2.20 shows both knots (cyan rhombi) and control points (red circles) in the physical space. We observe that knots coincide with control points. There are as many knots as control points. That is why the Basis SPLine functions are linear ($p=q=1, K=2$).

Knots and not control points partition cantilever into 20 2D isogeometric elements. Although, the stiffness matrix refers to control points, so I form the equilibrium equation for them.

$$\mathbf{F} = \mathbf{K} \cdot \mathbf{U} \Rightarrow \mathbf{U} = \mathbf{K}^{-1} \cdot \mathbf{F}$$

Displacements' vector \mathbf{U} refers to control points. For this particular problem, there are 33 control points, so the above equation is written as follows:

$$\underset{66 \times 1}{\mathbf{F}} = \underset{66 \times 66}{\mathbf{K}} \cdot \underset{66 \times 1}{\mathbf{U}} \Rightarrow \underset{66 \times 1}{\mathbf{U}} = \underset{66 \times 66}{\mathbf{K}^{-1}} \cdot \underset{66 \times 1}{\mathbf{F}}$$

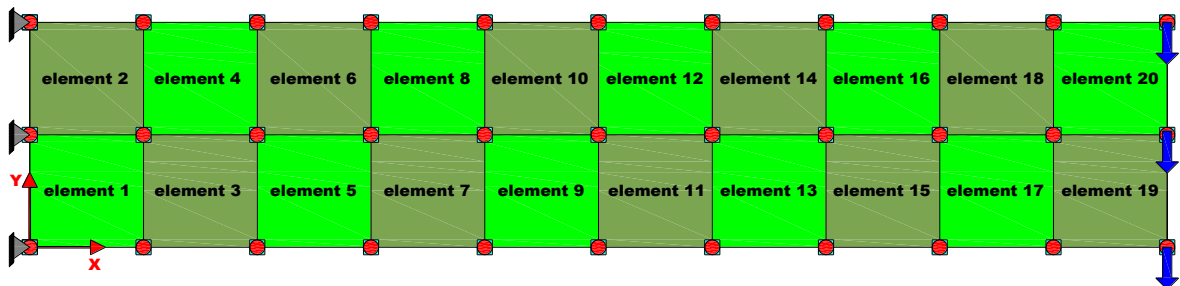


Figure 2.20. Physical Space. Mesh. Knots and Control Points.

Elasticity Matrix [E]

As it is a plane stress problem, the elasticity matrix [E] for every isogeometric element is equal to:

$$E_{3 \times 3} = \frac{E}{1-v^2} \cdot \begin{bmatrix} 1 & v & 0 \\ v & 1 & 0 \\ 0 & 0 & \frac{1-v}{2} \end{bmatrix}$$

Every isogeometric element has the same elasticity modulus $E = 210\text{GPa} = 2,1 \cdot 10^8 \text{kPa}$ and Poisson's ratio $v = 0,3$, so they have all the same elasticity matrix [E], which is equal to:

$$E_{3 \times 3} = 230.769.231 \cdot \begin{bmatrix} 1 & 0.3 & 0 \\ 0.3 & 1 & 0 \\ 0 & 0 & 0.35 \end{bmatrix} \text{kPa} \Rightarrow$$

$$E_{3 \times 3} = \begin{bmatrix} 230.769.231 & 69.230.769 & 0 \\ 69.230.769 & 230.769.231 & 0 \\ 0 & 0 & 80.769.231 \end{bmatrix} \text{kPa}$$

Deformation Matrix [B]

NURBS (Non-Uniform Rational B-SPLines) and not B-SPLines are used as shape functions. This NURBS basis is given by:

$$R_i^p(\xi) = \frac{\sum_{i=1}^n N_{i,p}(\xi) \cdot w_i}{\sum_{i=1}^n N_{i,p}(\xi)}$$

where:

- $i=1,\dots,n$
- n : control points' number
- p : B-SPLines' polynomial order
- $N_{i,p}(\xi)$: the corresponding Basis SPLine to control point i
- w_i : control point's i weight factor
- $R_i^p(\xi)$: the corresponding Non-Uniform Rational Basis SPLine to control point i with polynomial order p

Isogeometric Analysis

The Non-Uniform Rational Basis SPLine's derivative is equal to:

$$\frac{\partial R_i^p \xi}{\partial \xi} = \frac{\frac{\partial N_{i,p} \xi \cdot w_i}{\partial \xi} \cdot \sum_{i=1}^n N_{i,p} \xi \cdot w_i - N_{i,p} \xi \cdot w_i \cdot \frac{\partial \left(\sum_{i=1}^n N_{i,p} \xi \cdot w_i \right)}{\partial \xi}}{\left(\sum_{i=1}^n N_{i,p} \xi \cdot w_i \right)^2} \Rightarrow$$

$$\frac{\partial R_i^p \xi}{\partial \xi} = \frac{\frac{\partial N_{i,p} \xi}{\partial \xi} \cdot w_i \cdot \sum_{i=1}^n N_{i,p} \xi \cdot w_i - N_{i,p} \xi \cdot w_i \cdot \sum_{i=1}^n \frac{\partial N_{i,p} \xi}{\partial \xi} \cdot w_i}{\left(\sum_{i=1}^n N_{i,p} \xi \cdot w_i \right)^2} \Rightarrow$$

$$\frac{\partial R_i^p \xi}{\partial \xi} = \frac{\frac{\partial N_{i,p} \xi}{\partial \xi} \cdot w_i - N_{i,p} \xi \cdot w_i \cdot \sum_{i=1}^n \frac{\partial N_{i,p} \xi}{\partial \xi} \cdot w_i}{\sum_{i=1}^n N_{i,p} \xi \cdot w_i - \left(\sum_{i=1}^n N_{i,p} \xi \cdot w_i \right)^2}$$

The problem is 2D, so I have to calculate Rational Surfaces which are defined analogously in terms of the rational basis functions:

$$R_{i,j}^{p,q} \xi, \eta = \frac{N_{i,p} \xi \cdot M_{j,q} \eta \cdot w_{i,j}}{\sum_{i=1}^n \sum_{j=1}^m N_{i,p} \xi \cdot M_{j,q} \eta \cdot w_{i,j}}$$

where:

- $i=1,\dots,n$ (axis ξ)
- $j=1,\dots,m$ (axis η)
- n : control points' number (axis ξ)
- m : control points' number (axis η)
- p : B-SPLines' polynomial order (axis ξ)
- q : B-SPLines' polynomial order (axis η)
- $N_{i,p} \xi$: the corresponding Basis SPLine to control point i (axis ξ)
- $M_{j,q} \xi$: the corresponding Basis SPLine to control point j (axis η)
- $w_{i,j}$: control point's weight factor (2D, $\exists x, h$)
- $R_{i,j}^{p,q} \xi, \eta$: the corresponding Rational Surface to control point (i,j)

In this case, the weights are all equal, so:

$$R_i^p \xi = \frac{N_{i,p} \xi \cdot w_i}{\sum_{i=1}^n N_{i,p} \xi \cdot w_i} = \frac{N_{i,p} \xi}{\sum_{i=1}^n N_{i,p} \xi} = \frac{N_{i,p} \xi}{1} = N_{i,p} \xi$$

and the curve is again a polynomial. B-SPLines are a special case of NURBS.

Similarly,

$$R_{i,j}^{p,q} \xi, \eta = \frac{N_{i,p} \xi \cdot M_{j,q} \eta \cdot w_{i,j}}{\sum_{i=1}^n \sum_{j=1}^m N_{i,p} \xi \cdot M_{j,q} \eta \cdot w_{i,j}} = \frac{N_{i,p} \xi \cdot M_{j,q} \eta}{\sum_{i=1}^n \sum_{j=1}^m N_{i,p} \xi \cdot M_{j,q} \eta} = \frac{N_{i,p} \xi \cdot M_{j,q} \eta}{1} \Rightarrow$$

$$R_{i,j}^{p,q} \xi, \eta = N_{i,p} \xi \cdot M_{j,q} \eta$$

The corresponding partial derivatives are equal to:

$$\frac{\partial R_{i,j}^{p,q} \xi, \eta}{\partial \xi} = \frac{\partial N_{i,p} \xi}{\partial \xi} \cdot M_{j,q} \eta$$

$$\frac{\partial R_{i,j}^{p,q} \xi, \eta}{\partial \eta} = N_{i,p} \xi \cdot \frac{\partial M_{j,q} \eta}{\partial \eta}$$

For every isogeometric element, I calculate:

- Jacobian matrix

$$\begin{bmatrix} J & \xi, \eta \\ 2x2 & \end{bmatrix} = \begin{bmatrix} D_N & \xi, \eta \\ 2x4 & \end{bmatrix} \cdot \begin{bmatrix} XY \\ 4x2 \end{bmatrix}$$

where:

$$\begin{bmatrix} D_N & \xi, \eta \\ 2x4 & \end{bmatrix} = \begin{bmatrix} \frac{\partial R_{1,1}^{1,1} \xi, \eta}{\partial \xi} & \frac{\partial R_{1,2}^{1,1} \xi, \eta}{\partial \xi} & \frac{\partial R_{2,1}^{1,1} \xi, \eta}{\partial \xi} & \frac{\partial R_{2,2}^{1,1} \xi, \eta}{\partial \xi} \\ \frac{\partial R_{1,1}^{1,1} \xi, \eta}{\partial \eta} & \frac{\partial R_{1,2}^{1,1} \xi, \eta}{\partial \eta} & \frac{\partial R_{2,1}^{1,1} \xi, \eta}{\partial \eta} & \frac{\partial R_{2,2}^{1,1} \xi, \eta}{\partial \eta} \end{bmatrix}$$

$$\begin{bmatrix} XY \\ 4x2 \end{bmatrix} = \begin{bmatrix} X_{C.P.1} & Y_{C.P.1} \\ X_{C.P.2} & Y_{C.P.2} \\ X_{C.P.3} & Y_{C.P.3} \\ X_{C.P.4} & Y_{C.P.4} \end{bmatrix}$$

C.P.1, ..., C.P.4 are the corresponding 4 control points to every isogeometric element with local numbering.

- Deformation matrix

$$\begin{aligned} \left[\begin{array}{c|ccccc} \mathbf{B}_1 & \xi, \eta \\ \hline & 3 \times 4 \end{array} \right] &= \frac{1}{\det \mathbf{J}} \cdot \begin{bmatrix} \mathbf{J}_{22} & -\mathbf{J}_{12} & 0 & 0 \\ 0 & 0 & -\mathbf{J}_{21} & \mathbf{J}_{11} \\ -\mathbf{J}_{21} & \mathbf{J}_{11} & \mathbf{J}_{22} & -\mathbf{J}_{12} \end{bmatrix} \\ \left[\begin{array}{c|cccccc} \mathbf{B}_2 & \xi, \eta \\ \hline & 4 \times 8 \end{array} \right] &= \begin{bmatrix} \frac{\partial R_{1,1}^{1,1}}{\partial \xi} \xi, \eta & 0 & \frac{\partial R_{1,2}^{1,1}}{\partial \xi} \xi, \eta & 0 & \frac{\partial R_{2,1}^{1,1}}{\partial \xi} \xi, \eta & 0 & \frac{\partial R_{2,2}^{1,1}}{\partial \xi} \xi, \eta & 0 \\ \frac{\partial R_{1,1}^{1,1}}{\partial \eta} \xi, \eta & 0 & \frac{\partial R_{1,2}^{1,1}}{\partial \eta} \xi, \eta & 0 & \frac{\partial R_{2,1}^{1,1}}{\partial \eta} \xi, \eta & 0 & \frac{\partial R_{2,2}^{1,1}}{\partial \eta} \xi, \eta & 0 \\ 0 & \frac{\partial R_{1,1}^{1,1}}{\partial \xi} \xi, \eta & 0 & \frac{\partial R_{1,2}^{1,1}}{\partial \xi} \xi, \eta & 0 & \frac{\partial R_{2,1}^{1,1}}{\partial \xi} \xi, \eta & 0 & \frac{\partial R_{2,2}^{1,1}}{\partial \xi} \xi, \eta \\ 0 & \frac{\partial R_{1,1}^{1,1}}{\partial \eta} \xi, \eta & 0 & \frac{\partial R_{1,2}^{1,1}}{\partial \eta} \xi, \eta & 0 & \frac{\partial R_{2,1}^{1,1}}{\partial \eta} \xi, \eta & 0 & \frac{\partial R_{2,2}^{1,1}}{\partial \eta} \xi, \eta \end{bmatrix} \end{aligned}$$

The deformation matrix is equal to:

$$\left[\begin{array}{c|c} \mathbf{B} & \xi, \eta \\ \hline & 3 \times 8 \end{array} \right] = \left[\begin{array}{c|c} \mathbf{B}_1 & \xi, \eta \\ \hline & 3 \times 4 \end{array} \right] \cdot \left[\begin{array}{c|c} \mathbf{B}_2 & \xi, \eta \\ \hline & 4 \times 8 \end{array} \right] \Rightarrow$$

$$\left[\begin{array}{c|cccccc} \mathbf{B} & \xi, \eta \\ \hline & 3 \times 8 \end{array} \right] = \begin{bmatrix} \frac{\partial R_{1,1}^{1,1}}{\partial \xi} & 0 & \frac{\partial R_{1,1}^{1,1}}{\partial \xi} & 0 & \frac{\partial R_{2,1}^{1,1}}{\partial \xi} & 0 & \frac{\partial R_{2,2}^{1,1}}{\partial \xi} & 0 \\ 0 & \frac{\partial R_{1,1}^{1,1}}{\partial \eta} & 0 & \frac{\partial R_{1,2}^{1,1}}{\partial \eta} & 0 & \frac{\partial R_{2,1}^{1,1}}{\partial \eta} & 0 & \frac{\partial R_{2,2}^{1,1}}{\partial \eta} \\ \frac{\partial R_{1,1}^{1,1}}{\partial \xi} & \frac{\partial R_{1,1}^{1,1}}{\partial \xi} & \frac{\partial R_{1,2}^{1,1}}{\partial \xi} & \frac{\partial R_{1,2}^{1,1}}{\partial \xi} & \frac{\partial R_{2,1}^{1,1}}{\partial \xi} & \frac{\partial R_{2,1}^{1,1}}{\partial \xi} & \frac{\partial R_{2,2}^{1,1}}{\partial \xi} & \frac{\partial R_{2,2}^{1,1}}{\partial \xi} \\ \frac{\partial R_{1,1}^{1,1}}{\partial \eta} & \frac{\partial R_{1,1}^{1,1}}{\partial \eta} & \frac{\partial R_{1,2}^{1,1}}{\partial \eta} & \frac{\partial R_{1,2}^{1,1}}{\partial \eta} & \frac{\partial R_{2,1}^{1,1}}{\partial \eta} & \frac{\partial R_{2,1}^{1,1}}{\partial \eta} & \frac{\partial R_{2,2}^{1,1}}{\partial \eta} & \frac{\partial R_{2,2}^{1,1}}{\partial \eta} \end{bmatrix}$$

Local Stiffness Matrix [ke]

I calculate isogeometric element's local stiffness matrix using Gauss quadrature. I choose 5x5 quadrature rule, means 25 Gauss Points for every element.

$$\left[\begin{array}{c|c} \mathbf{k}^e & \\ \hline & 8 \times 8 \end{array} \right] = \sum_{i=1}^{25} \left\{ \left[\begin{array}{c|cc} \mathbf{B}^e & \xi_i, \eta_i \\ \hline & 8 \times 3 \end{array} \right]^T \cdot \mathbf{E} \cdot \left[\begin{array}{c|cc} \mathbf{B}^e & \xi_i, \eta_i \\ \hline & 3 \times 8 \end{array} \right] \cdot \mathbf{t} \cdot \det \left[\begin{array}{c|cc} \mathbf{J} & \xi_i, \eta_i \\ \hline & \end{array} \right] \cdot w_i \right\}$$

The weight factor of Gauss Point i is equal to $w_i = \frac{w}{n-p} \cdot \frac{\xi_i}{m-q}$.

where (n-p), (m-q) is the number of horizontal (parametric axis ξ), vertical (parametric axis η) spans respectively. I divide with (n-p), (m-q) in order to:

$$\sum_{i=1}^{500} w_i = 2 \text{ (global numbering)}$$

I used totally (25 Gauss Points per element)·(20 elements)=500 Gauss Points.

Let's follow the previous procedure for Gauss Point 1 of isogeometric element 1. We can see this Gauss Point in the following Figure 2.21. It is the one in the green circle.

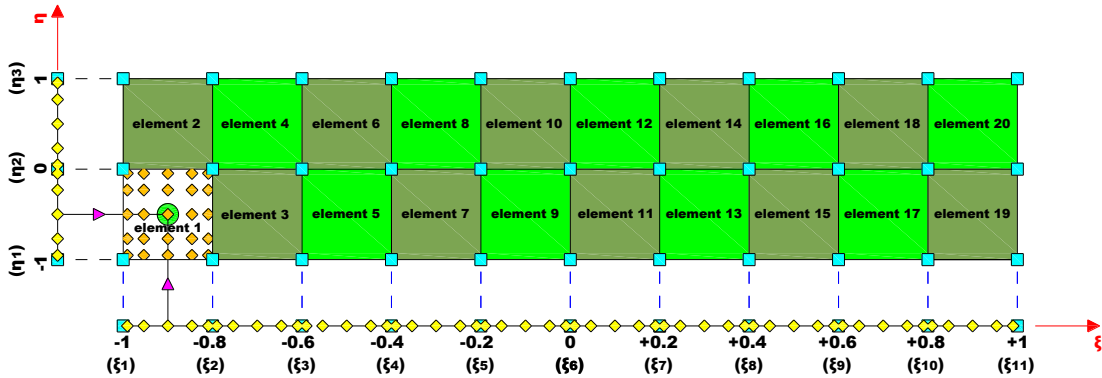


Figure 2.21. Gauss Point 1 of isogeometric element 1. (Parameter Space)

For element 1 (horizontal span 1 + vertical span 1),

$N_{i,1}(\xi)$ (2x5,p=1)	axis ξ				
	horizontal span 1				
	G.P.1 (1)	G.P.2 (2)	G.P.3 (3)	G.P.4 (4)	G.P.5 (5)
$N_{1,2}(\xi)$	0,5	0,0469	0,2308	0,9531	0,7692
$N_{2,2}(\xi)$	0,5	0,9531	0,7692	0,0469	0,2308

Figure 2.22.a. Basis SPLine functions for horizontal span 1. Parametric axis ξ . Values at Gauss Points.

$N'_{i,1}(\xi)$ (2x5,p=1)	axis ξ				
	horizontal span 1				
	G.P.1 (1)	G.P.2 (2)	G.P.3 (3)	G.P.4 (4)	G.P.5 (5)
$N'_{1,2}(\xi)$	-5	-5	-5	-5	-5
$N'_{2,2}(\xi)$	5	5	5	5	5

Figure 2.22.b. First derivative of basis SPLine functions for horizontal span 1. Parametric axis ξ . Values at Gauss Points.

$M_{j,1}(\eta)$ (2x5,q=1)	axis η				
vertical span 1					
	G.P.1 (1)	G.P.2 (2)	G.P.3 (3)	G.P.4 (4)	G.P.5 (5)
$M_{1,1}(\eta)$	0,5	0,0469	0,2308	0,9531	0,7692
$M_{2,1}(\eta)$	0,5	0,9531	0,7692	0,0469	0,2308

Figure 2.22.c. Basis SPLine functions for vertical span 1. Parametric axis η . Values at Gauss Points.

$M'_{j,1}(\eta)$ (2x5,q=1)	axis η				
vertical span 1					
	G.P.1 (1)	G.P.2 (2)	G.P.3 (3)	G.P.4 (4)	G.P.5 (5)
$M'_{1,1}(\eta)$	-1	-1	-1	-1	-1
$M'_{2,1}(\eta)$	1	1	1	1	1

Figure 2.22.d. First derivative of basis SPLine functions for vertical span 1. Parametric axis η . Values at Gauss Points.

$$XY = \begin{bmatrix} X_{C.P.1} & Y_{C.P.1} \\ X_{C.P.2} & Y_{C.P.2} \\ X_{C.P.3} & Y_{C.P.3} \\ X_{C.P.4} & Y_{C.P.4} \end{bmatrix} = \begin{bmatrix} 0 & 0 \\ 0 & 1,5 \\ 1,5 & 0 \\ 1,5 & 1,5 \end{bmatrix}$$

With BSPLines $N_{i,1} \xi, M_{j,1} \eta$ and their derivatives $(\frac{\partial N_{i,1}}{\partial \xi}, \frac{\partial M_{i,1}}{\partial \eta})$ in hand, I calculate corresponding NURBS' values at Gauss Point 1 (isogeometric element 1).

$$\boxed{R_{i,j}^{p,q} \xi, \eta = N_{i,p} \xi \cdot M_{j,q} \eta} \Rightarrow R_{i,j}^{1,1} \xi_{G.P.1}, \eta_{G.P.1} = N_{i,1} \xi_{G.P.1} \cdot M_{j,1} \eta_{G.P.1}$$

$$\boxed{\frac{\partial R_{i,j}^{p,q} \xi, \eta}{\partial \xi} = \frac{\partial N_{i,p}}{\partial \xi} \cdot M_{j,q} \eta} \Rightarrow \frac{\partial R_{i,j}^{1,1} \xi_{G.P.1}, \eta_{G.P.1}}{\partial \xi} = \frac{\partial N_{i,1}}{\partial \xi} \cdot M_{j,1} \eta_{G.P.1}$$

$$\boxed{\frac{\partial R_{i,j}^{p,q} \xi, \eta}{\partial \eta} = N_{i,p} \xi \cdot \frac{\partial M_{j,q}}{\partial \eta}} \Rightarrow \frac{\partial R_{i,j}^{1,1} \xi_{G.P.1}, \eta_{G.P.1}}{\partial \eta} = N_{i,1} \xi_{G.P.1} \cdot \frac{\partial M_{j,1}}{\partial \eta} \eta_{G.P.1}$$

Control Point 1 ($i=1, j=1$)

$$R_{1,1}^{1,1} \xi_{G.P.1}, \eta_{G.P.1} = N_{1,1} \xi_{G.P.1} \cdot M_{1,1} \eta_{G.P.1}$$

$$\frac{\partial R_{1,1}^{1,1} \xi_{G.P.1}, \eta_{G.P.1}}{\partial \xi} = \frac{\partial N_{1,1}}{\partial \xi} \xi_{G.P.1} \cdot M_{1,1} \eta_{G.P.1}$$

$$\frac{\partial R_{1,1}^{1,1} \xi_{G.P.1}, \eta_{G.P.1}}{\partial \eta} = N_{1,1} \xi_{G.P.1} \cdot \frac{\partial M_{1,1}}{\partial \eta} \eta_{G.P.1}$$

Isogeometric Analysis

Control Point 2 (i=1, j=2)

$$R_{1,2}^{1,1} \xi_{G.P.1}, \eta_{G.P.1} = N_{1,1} \xi_{G.P.1} \cdot M_{2,1} \eta_{G.P.1}$$

$$\frac{\partial R_{1,2}^{1,1} \xi_{G.P.1}, \eta_{G.P.1}}{\partial \xi} = \frac{\partial N_{1,1} \xi_{G.P.1}}{\partial \xi} \cdot M_{2,1} \eta_{G.P.1}$$

$$\frac{\partial R_{1,2}^{1,1} \xi_{G.P.1}, \eta_{G.P.1}}{\partial \eta} = N_{1,1} \xi_{G.P.1} \cdot \frac{\partial M_{2,1} \eta_{G.P.1}}{\partial \eta}$$

Control Point 3 (i=2, j=1)

$$R_{2,1}^{1,1} \xi_{G.P.1}, \eta_{G.P.1} = N_{2,1} \xi_{G.P.1} \cdot M_{1,1} \eta_{G.P.1}$$

$$\frac{\partial R_{2,1}^{1,1} \xi_{G.P.1}, \eta_{G.P.1}}{\partial \xi} = \frac{\partial N_{2,1} \xi_{G.P.1}}{\partial \xi} \cdot M_{1,1} \eta_{G.P.1}$$

$$\frac{\partial R_{2,1}^{1,1} \xi_{G.P.1}, \eta_{G.P.1}}{\partial \eta} = N_{2,1} \xi_{G.P.1} \cdot \frac{\partial M_{1,1} \eta_{G.P.1}}{\partial \eta}$$

Control Point 4 (i=2, j=2)

$$R_{2,2}^{1,1} \xi_{G.P.1}, \eta_{G.P.1} = N_{2,1} \xi_{G.P.1} \cdot M_{2,1} \eta_{G.P.1}$$

$$\frac{\partial R_{2,2}^{1,1} \xi_{G.P.1}, \eta_{G.P.1}}{\partial \xi} = \frac{\partial N_{2,1} \xi_{G.P.1}}{\partial \xi} \cdot M_{2,1} \eta_{G.P.1}$$

$$\frac{\partial R_{2,2}^{1,1} \xi_{G.P.1}, \eta_{G.P.1}}{\partial \eta} = N_{2,1} \xi_{G.P.1} \cdot \frac{\partial M_{2,1} \eta_{G.P.1}}{\partial \eta}$$

		element 1	G.P.1 (index\xi=1, index\eta=1)		
i	j		R _{i,j} ^{1,1}	dR _{i,j} ^{1,1} /d\xi	dR _{i,j} ^{1,1} /d\eta
		Control Point	N _{i,p} (\xi)*M _{j,q} (\eta)	N' _{i,p} (\xi)*M _{j,q} (\eta)	N _{i,p} (\xi)*M' _{j,q} (\eta)
1	1	C.P.1	0,25	-2,5	-0,5
1	2	C.P.2	0,25	-2,5	0,5
2	1	C.P.3	0,25	2,5	-0,5
2	2	C.P.4	0,25	2,5	0,5
		SUM	1	0	0

Figure 2.23. NUR-B-SPLINE Surfaces and their derivatives. Parameter space $\Xi \times H$. Values at Gauss Points.

$$\left[D_N \begin{matrix} \xi_1, \eta_1 \\ 2 \times 4 \end{matrix} \right] = \left[\begin{array}{cccc} \frac{\partial R_{1,1}^{1,1} \xi_1, \eta_1}{\partial \xi} & \frac{\partial R_{1,2}^{1,1} \xi_1, \eta_1}{\partial \xi} & \frac{\partial R_{2,1}^{1,1} \xi_1, \eta_1}{\partial \xi} & \frac{\partial R_{2,2}^{1,1} \xi_1, \eta_1}{\partial \xi} \\ \frac{\partial R_{1,1}^{1,1} \xi_1, \eta_1}{\partial \eta} & \frac{\partial R_{1,2}^{1,1} \xi_1, \eta_1}{\partial \eta} & \frac{\partial R_{2,1}^{1,1} \xi_1, \eta_1}{\partial \eta} & \frac{\partial R_{2,2}^{1,1} \xi_1, \eta_1}{\partial \eta} \end{array} \right] = \begin{bmatrix} -2,5 & -2,5 & 2,5 & 2,5 \\ -0,5 & 0,5 & -0,5 & 0,5 \end{bmatrix}$$

$$\begin{bmatrix} J & \xi_1, \eta_1 \\ 2x2 & 2x4 \end{bmatrix} = \begin{bmatrix} D_N & \xi_1, \eta_1 \\ 2x4 & 2x4 \end{bmatrix} \cdot \begin{bmatrix} X & Y \\ 4x2 & 4x2 \end{bmatrix} = \begin{bmatrix} -2,5 & -2,5 & 2,5 & 2,5 \\ -0,5 & 0,5 & -0,5 & 0,5 \end{bmatrix} \cdot \begin{bmatrix} 0 & 0 \\ 0 & 1,5 \\ 1,5 & 0 \\ 1,5 & 1,5 \end{bmatrix} = \begin{bmatrix} 7,5 & 0 \\ 0 & 1,5 \end{bmatrix}$$

$$\begin{bmatrix} B_1 & \xi_1, \eta_1 \\ 3x4 & 3x4 \end{bmatrix} = \frac{1}{\det[J]} \cdot \begin{bmatrix} J_{22} & -J_{12} & 0 & 0 \\ 0 & 0 & -J_{21} & J_{11} \\ -J_{21} & J_{11} & J_{22} & -J_{12} \end{bmatrix} = \frac{1}{11,25} \cdot \begin{bmatrix} 1,5 & 0 & 0 & 0 \\ 0 & 0 & 0 & 7,5 \\ 0 & 7,5 & 1,5 & 0 \end{bmatrix}$$

\Rightarrow

$$\begin{bmatrix} B_1 & \xi_1, \eta_1 \\ 3x4 & 3x4 \end{bmatrix} = \begin{bmatrix} 0,1333 & 0 & 0 & 0 \\ 0 & 0 & 0 & 0,6667 \\ 0 & 0,6667 & 0,1333 & 0 \end{bmatrix}$$

$$\begin{bmatrix} B_2 & \xi_1, \eta_1 \\ 4x8 & 4x8 \end{bmatrix} = \begin{bmatrix} \frac{\partial R_{1,1}^{1,1}}{\partial \xi} & 0 & \frac{\partial R_{1,2}^{1,1}}{\partial \xi} & 0 & \frac{\partial R_{1,3}^{1,1}}{\partial \xi} & 0 & \frac{\partial R_{1,4}^{1,1}}{\partial \xi} & 0 \\ \frac{\partial R_{1,1}^{1,1}}{\partial \eta} & 0 & \frac{\partial R_{1,2}^{1,1}}{\partial \eta} & 0 & \frac{\partial R_{1,3}^{1,1}}{\partial \eta} & 0 & \frac{\partial R_{1,4}^{1,1}}{\partial \eta} & 0 \\ 0 & \frac{\partial R_{1,1}^{1,1}}{\partial \xi} & 0 & \frac{\partial R_{1,2}^{1,1}}{\partial \xi} & 0 & \frac{\partial R_{1,3}^{1,1}}{\partial \xi} & 0 & \frac{\partial R_{1,4}^{1,1}}{\partial \xi} \\ 0 & \frac{\partial R_{1,1}^{1,1}}{\partial \eta} & 0 & \frac{\partial R_{1,2}^{1,1}}{\partial \eta} & 0 & \frac{\partial R_{1,3}^{1,1}}{\partial \eta} & 0 & \frac{\partial R_{1,4}^{1,1}}{\partial \eta} \end{bmatrix}$$

\Rightarrow

$$\begin{bmatrix} B_2 & \xi_1, \eta_1 \\ 4x8 & 4x8 \end{bmatrix} = \begin{bmatrix} -2,5 & 0 & -2,5 & 0 & 2,5 & 0 & 2,5 & 0 \\ -0,5 & 0 & 0,5 & 0 & -0,5 & 0 & 0,5 & 0 \\ 0 & -2,5 & 0 & -2,5 & 0 & 2,5 & 0 & 2,5 \\ 0 & -0,5 & 0 & 0,5 & 0 & -0,5 & 0 & 0,5 \end{bmatrix}$$

The deformation matrix (isogeometric element 1, Gauss Point 1) is equal to:

$$\begin{bmatrix} B & \xi_1, \eta_1 \\ 3x8 & 3x8 \end{bmatrix} = \begin{bmatrix} B_1 & \xi_1, \eta_1 \\ 3x4 & 3x4 \end{bmatrix} \cdot \begin{bmatrix} B_2 & \xi_1, \eta_1 \\ 4x8 & 4x8 \end{bmatrix}$$

$$\Rightarrow$$

$$\begin{bmatrix} B & \xi_1, \eta_1 \\ 3x8 & 3x8 \end{bmatrix} = \begin{bmatrix} 0,3333 & 0 & 0,3333 & 0 & -0,3333 & 0 & -0,3333 & 0 \\ 0 & -0,3333 & 0 & 0,3333 & 0 & -0,3333 & 0 & 0,3333 \\ -0,3333 & 0,3333 & 0,3333 & 0,3333 & -0,3333 & -0,3333 & 0,3333 & -0,3333 \end{bmatrix}$$

Isogeometric Analysis

		B(ξ, η)							
		u C.P.1	v C.P.1	u C.P.2	v C.P.2	u C.P.4	v C.P.4	u C.P.5	v C.P.5
element 1	ϵ_x	-0,3333	0	-0,3333	0	0,3333	0	0,3333	0
	ϵ_y	0	-0,3333	0	0,3333	0	-0,3333	0	0,3333
	γ_{xy}	-0,3333	-0,3333	0,3333	-0,3333	-0,3333	0,3333	0,3333	0,3333

Figure 2.24. Deformation Matrix. Isogeometric Element 1. Gauss Point 1. Global numbering of Control Points.

The weight factor of Gauss Point 1 (isogeometric element 1) is equal to:

$$w_1 = \frac{w}{n-p} \cdot \frac{\xi_1}{m-q} = \frac{0,56888}{11-1} \cdot \frac{0,56888}{3-1} \Rightarrow w_1 = 0,01618$$

The local stiffness matrix (isogeometric element 1, Gauss Point 1) is equal to:

$$k_{G.P.1}^{\text{ell}} = \left[\begin{array}{c|cc} B^{\text{ell}} & \xi_1, \eta_1 \\ \hline 8x3 & 3x3 \end{array} \right]^T \cdot E \cdot \left[\begin{array}{c|cc} B^{\text{ell}} & \xi_1, \eta_1 \\ \hline 3x3 & 3x8 \end{array} \right] \cdot t \cdot \det \left[\begin{array}{c|cc} J & \xi_1, \eta_1 \\ \hline 3x8 & 3x8 \end{array} \right] \cdot w_1$$

		local [k] (Isogeometric Element 1. Gauss Point 1. Global numbering of C.P.)								
		C.P.1		C.P.2		C.P.4		C.P.5		
		u (m)	v (m)	u (m)	v (m)	u (m)	v (m)	u (m)	v (m)	
element 1	C.P.1	F _x (kN)	63.015	30.341	30.341	2.334	-30.341	-2.334	-63.015	-30.341
	C.P.1	F _y (kN)	30.341	63.015	-2.334	-30.341	2.334	30.341	-30.341	-63.015
element 1	C.P.2	F _x (kN)	30.341	-2.334	63.015	-30.341	-63.015	30.341	-30.341	2.334
	C.P.2	F _y (kN)	2.334	-30.341	-30.341	63.015	30.341	-63.015	-2.334	30.341
element 1	C.P.4	F _x (kN)	-30.341	2.334	-63.015	30.341	63.015	-30.341	30.341	-2.334
	C.P.4	F _y (kN)	-2.334	30.341	30.341	-63.015	-30.341	63.015	2.334	-30.341
element 1	C.P.5	F _x (kN)	-63.015	-30.341	-30.341	-2.334	30.341	2.334	63.015	30.341
	C.P.5	F _y (kN)	-30.341	-63.015	2.334	30.341	-2.334	-30.341	30.341	63.015

Figure 2.25. Stiffness Matrix. Isogeometric Element 1. Gauss Point 1. Global numbering of Control Points. Excel.

		local [k] (Isogeometric Element 1. Gauss Point 1. Global numbering of C.P.)								
		C.P.1		C.P.2		C.P.4		C.P.5		
		u (m)	v (m)	u (m)	v (m)	u (m)	v (m)	u (m)	v (m)	
element 1	C.P.1	F _x (kN)	63.015	30.341	30.341	2.334	-30.341	-2.334	-63.015	-30.341
	C.P.1	F _y (kN)	30.341	63.015	-2.334	-30.341	2.334	30.341	-30.341	-63.015
element 1	C.P.2	F _x (kN)	30.341	-2.334	63.015	-30.341	-63.015	30.341	-30.341	2.334
	C.P.2	F _y (kN)	2.334	-30.341	-30.341	63.015	30.341	-63.015	-2.334	30.341
element 1	C.P.4	F _x (kN)	-30.341	2.334	-63.015	30.341	63.015	-30.341	30.341	-2.334
	C.P.4	F _y (kN)	-2.334	30.341	30.341	-63.015	-30.341	63.015	2.334	-30.341
element 1	C.P.5	F _x (kN)	-63.015	-30.341	-30.341	-2.334	30.341	2.334	63.015	30.341
	C.P.5	F _y (kN)	-30.341	-63.015	2.334	30.341	-2.334	-30.341	30.341	63.015

Figure 2.26. Stiffness Matrix. Isogeometric Element 1. Gauss Point 1. Global numbering of Control Points. MatLab.

Isogeometric Analysis

I follow the same procedure for the rest 24 Gauss Points of isogeometric element 1.

Isogeometric Element's 1 local stiffness matrix is equal to:

$$k^e = \sum_{i=1}^{25} k_{G.P.i}^e = \sum_{i=1}^{25} \left[B^e \quad \xi_i, \eta_i \right]^T \cdot E \cdot \left[B^e \quad \xi_i, \eta_i \right] \cdot t \cdot \det \left[J \quad \xi_i, \eta_i \right] \cdot w_i$$

		local [k] (kN/m) (Isogeometric Element 1. Global numbering of C.P.)							
		C.P.1		C.P.2		C.P.4		C.P.5	
		u (m)	v (m)	u (m)	v (m)	u (m)	v (m)	u (m)	v (m)
C.P.1	F_x (kN)	1.038.462	375.000	115.385	28.846	-634.615	-28.846	-519.231	-375.000
	F_y (kN)	375.000	1.038.462	-28.846	-634.615	28.846	115.385	-375.000	-519.231
C.P.2	F_x (kN)	115.385	-28.846	1.038.462	-375.000	-519.231	375.000	-634.615	28.846
	F_y (kN)	28.846	-634.615	-375.000	1.038.462	375.000	-519.231	-28.846	115.385
C.P.4	F_x (kN)	-634.615	28.846	-519.231	375.000	1.038.462	-375.000	115.385	-28.846
	F_y (kN)	-28.846	115.385	375.000	-519.231	-375.000	1.038.462	28.846	-634.615
C.P.5	F_x (kN)	-519.231	-375.000	-634.615	-28.846	115.385	28.846	1.038.462	375.000
	F_y (kN)	-375.000	-519.231	28.846	115.385	-28.846	-634.615	375.000	1.038.462

**Figure 2.27. Stiffness Matrix. Isogeometric Element 1.
Global numbering of Control Points. MatLab.**

Total Stiffness Matrix [K]

I calculate the local (numbering) Stiffness Matrix for every Isogeometric Element. Then, I form the total Stiffness Matrix of the structure.

Total Stiffness Matrix [kN/m]					
1	2	3	4	5	6
2	1	2	3	4	5
3	2	1	2	3	4
4	3	2	1	2	3
5	4	3	2	1	2
6	5	4	3	2	1

Figure 2.28. Total Stiffness Matrix. (66x66)

Two Degrees of Freedom correspond to every Control Point, the horizontal u and the vertical v displacement. The cantilever's total Stiffness Matrix is a symmetric square matrix with dimensions 66x66, as there are 33 Control Points and $33 \cdot 2 = 66$ Degrees of Freedom.

Control Points' External Forces {P}

I calculate the External Load Vector (66x1) and I reorder it.

$$\underset{(66 \times 1)}{F_{tot}} = \begin{bmatrix} 0 & \dots & 0 & -1000 & 0 & -1000 & 0 & -1000 \end{bmatrix}^T$$

$$\underset{(66 \times 1)}{F_{tot,m}} = \begin{bmatrix} F_f \\ F_s \end{bmatrix} = \begin{bmatrix} 0 & \dots & 0 & -1000 & 0 & -1000 & 0 & -1000 \\ 0 & & & & (60 \times 1) & & & \\ & & & & & 0 & & \\ & & & & & & (6 \times 1) & \end{bmatrix}^T$$

Control Points' Displacements {U}

I reorder the Total Stiffness Matrix and the External Load Vector and then I form the balance equation. I symbolize the unknown displacements with subscript f and the known ones (fixed Control Points) with s.

$$F_{tot,m} = [K_{tot,m}] \cdot U_{tot,m} \Rightarrow \begin{bmatrix} F_f \\ F_s \end{bmatrix}_{60 \times 1} = \begin{bmatrix} K_{ff} & K_{fs} \\ K_{sf} & K_{ss} \end{bmatrix}_{60 \times 60 \times 6} \cdot \begin{bmatrix} U_f \\ U_s \end{bmatrix}_{6 \times 1} \Rightarrow$$

$$\begin{bmatrix} 0 \\ \dots \\ 0 \\ -1000 \\ 0 \\ -1000 \\ 0 \\ -1000 \\ 0 \\ -1000 \\ 0 \\ 0 \end{bmatrix}_{60 \times 1} = \begin{bmatrix} [K_{ff}]_{60 \times 60} & [K_{fs}]_{60 \times 6} \\ [K_{sf}]_{6 \times 60} & [K_{ss}]_{6 \times 6} \end{bmatrix} \cdot \begin{bmatrix} U_f \\ U_s \end{bmatrix}_{6 \times 1} \Rightarrow \begin{bmatrix} [K_{ff}]_{60 \times 60} & [K_{fs}]_{60 \times 6} \\ [K_{sf}]_{6 \times 60} & [K_{ss}]_{6 \times 6} \end{bmatrix} \cdot \begin{bmatrix} 0 \\ \dots \\ 0 \\ -1000 \\ 0 \\ -1000 \\ 0 \\ -1000 \\ 0 \\ -1000 \\ 0 \\ 0 \end{bmatrix}_{60 \times 1}$$

Figure 2.29 shows Control Points' horizontal and vertical displacement.

The maximum horizontal displacement is equal to 9,5cm and corresponds to C.P.31 (-9,5cm) and C.P.33 (9,5cm).

The maximum vertical displacement is equal to 65,1cm and corresponds to C.P.31 (-65,1cm) and C.P.33 (-65,1cm). Negative value displays that maximum displacement's direction is the negative direction of axis Y, means these Control Points move downstairs as expected.

		horizontal u (cm)	vertical v (cm)
C.P.	1	0,0	0,0
C.P.	2	0,0	0,0
C.P.	3	0,0	0,0
C.P.	4	-1,8	-1,2
C.P.	5	0,0	-0,9
C.P.	6	1,8	-1,2
C.P.	7	-3,4	-4,0
C.P.	8	0,0	-3,7
C.P.	9	3,4	-4,0
C.P.	10	-4,8	-8,2
C.P.	11	0,0	-8,0
C.P.	12	4,8	-8,2
C.P.	13	-6,1	-13,9
C.P.	14	0,0	-13,7
C.P.	15	6,1	-13,9
C.P.	16	-7,1	-20,6
C.P.	17	0,0	-20,5
C.P.	18	7,1	-20,6
C.P.	19	-8,0	-28,4
C.P.	20	0,0	-28,3
C.P.	21	8,0	-28,4
C.P.	22	-8,7	-36,9
C.P.	23	0,0	-36,8
C.P.	24	8,7	-36,9
C.P.	25	-9,1	-45,9
C.P.	26	0,0	-45,9
C.P.	27	9,1	-45,9
C.P.	28	-9,4	-55,4
C.P.	29	0,0	-55,4
C.P.	30	9,4	-55,4
C.P.	31	-9,5	-65,1
C.P.	32	0,0	-65,0
C.P.	33	9,5	-65,1
max		9,5	0,0
min		-9,5	-65,1

Figure 2.29. Control Points' displacements.

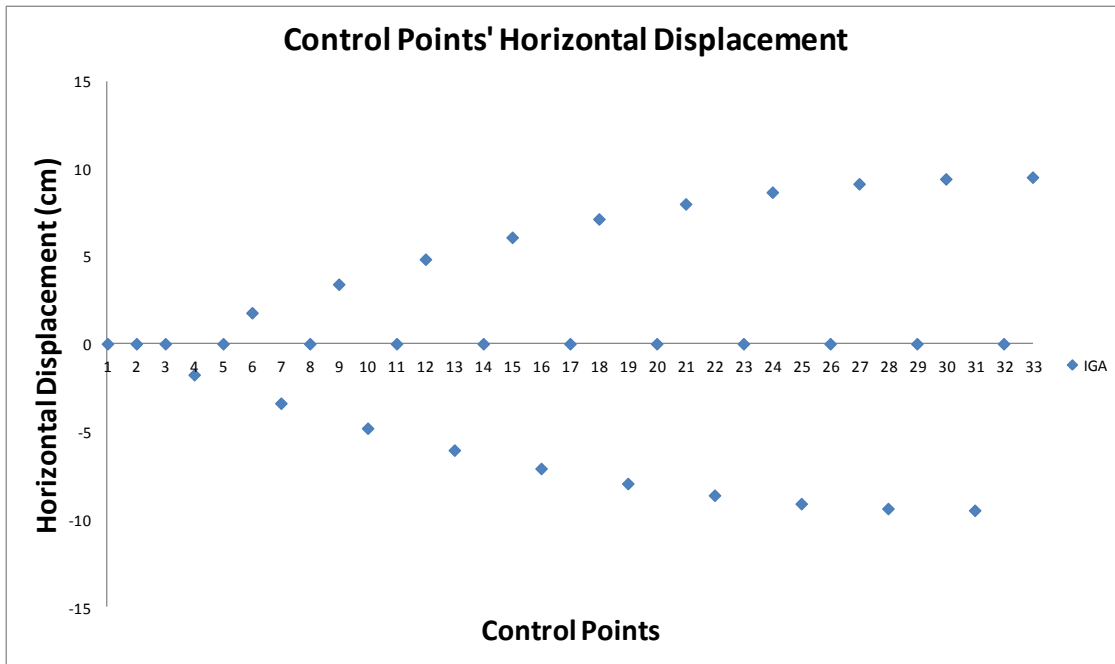


Figure 2.30.a. Control Points' horizontal displacement.

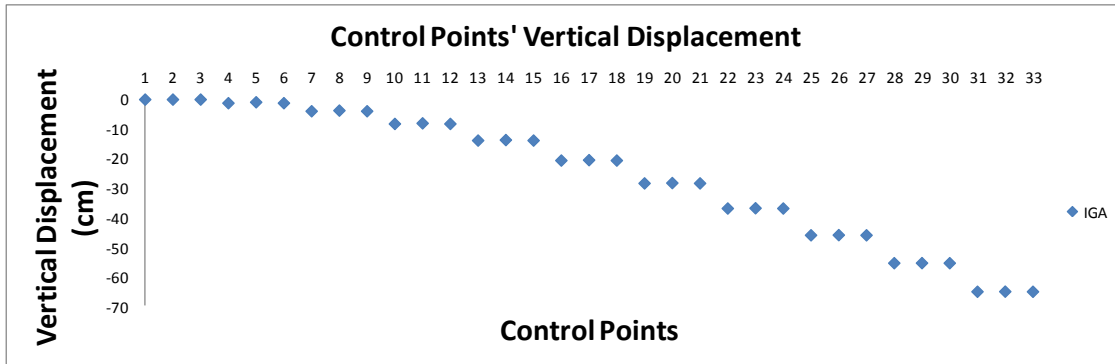


Figure 2.30.b. Control Points' vertical displacement.

Stress Field at Gauss Points

As I know Control Points' displacements, I can calculate the stress field at Isogeometric Elements' Gauss Points.

$$\sigma_{\xi_i, \eta_i} = E \cdot \varepsilon_{\xi_i, \eta_i} = E \cdot [B_{\xi_i, \eta_i}] \cdot d$$

where:

- $\sigma_{\xi_i, \eta_i} = \begin{cases} \sigma_X & \xi_i, \eta_i \\ \sigma_Y & \xi_i, \eta_i \\ \tau_{XY} & \xi_i, \eta_i \end{cases}$: stress field at Gauss Point i (plane stress problem)

Isogeometric Analysis

- $E_{3x3} = \frac{E}{1-v^2} \cdot \begin{bmatrix} 1 & v & 0 \\ v & 1 & 0 \\ 0 & 0 & \frac{1-v}{2} \end{bmatrix}$ (plane stress problem)
- $\varepsilon_{\xi_i, \eta_i} = \begin{bmatrix} \varepsilon_x & \xi_i, \eta_i \\ \varepsilon_y & \xi_i, \eta_i \\ \gamma_{xy} & \xi_i, \eta_i \end{bmatrix}_{3x1}$: strain field at Gauss Point i
- d_{8x1} : This displacement vector refers to displacements of Isogeometric Element's Control Points (local numbering).

Let's calculate the corresponding stress field to Gauss Point 1 of Isogeometric Element 1.

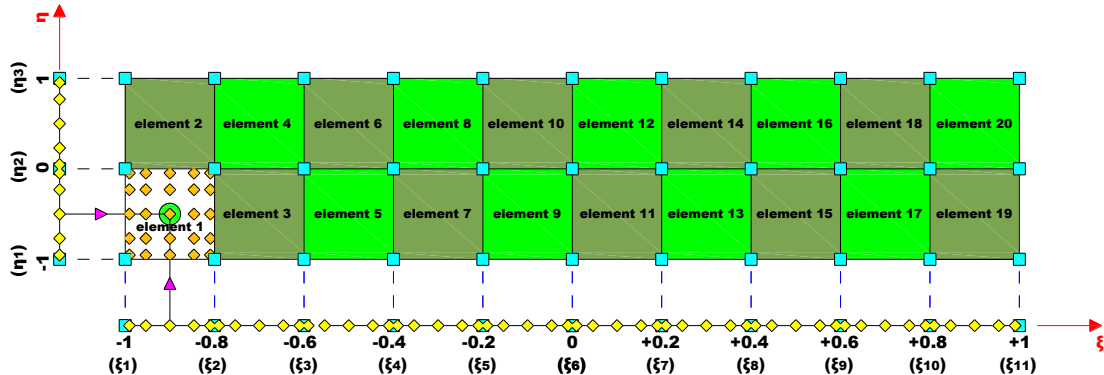


Figure 2.31. Gauss Point 1 of Isogeometric Element 1. (Parameter Space)

		$\{d\} (m)$
C.P.1	$u (m)$	0
	$v (m)$	0
C.P.2	$u (m)$	0
	$v (m)$	0
C.P.4	$u (m)$	-0,018
	$v (m)$	-0,012
C.P.5	$u (m)$	0
	$v (m)$	-0,009

Figure 2.32. Control Points' vertical and horizontal displacement.
Isogeometric Element 1.

$$\sigma_{\xi_1, \eta_1} = E \cdot [B_{\xi_1, \eta_1}] \cdot d = \begin{Bmatrix} -1.288,132 \\ -169,330 \\ -100,000 \end{Bmatrix} \text{ kPa} \Rightarrow \sigma_{\xi_1, \eta_1} = \begin{Bmatrix} -1.288,13 \\ -169,33 \\ -100,00 \end{Bmatrix} \text{ MPa}$$

Isogeometric Analysis

	element 1			element 2			element 3			element 4			element 5		
	σ_{xx} (MPa)	σ_{yy} (MPa)	τ_{xy} (MPa)	σ_{xx} (MPa)	σ_{yy} (MPa)	τ_{xy} (MPa)	σ_{xx} (MPa)	σ_{yy} (MPa)	τ_{xy} (MPa)	σ_{xx} (MPa)	σ_{yy} (MPa)	τ_{xy} (MPa)	σ_{xx} (MPa)	σ_{yy} (MPa)	τ_{xy} (MPa)
G.P.1	-1.288,13	-169,33	-100,00	1.288,13	169,33	-100,00	-1.134,45	30,75	-100,00	1.134,45	-30,75	-100,00	-1.004,23	-5,58	-100,00
G.P.2	-55,99	200,31	-24,33	2.520,27	538,97	-175,67	4,42	372,41	-122,01	2.273,32	310,92	-77,99	-5,88	293,92	-104,27
G.P.3	-555,97	50,32	-55,04	2.020,29	388,98	-144,96	-457,71	233,77	-113,08	1.811,19	172,28	-86,92	-410,99	172,39	-102,54
G.P.4	-2.520,27	-538,97	-175,67	55,99	-200,31	-24,33	-2.273,32	-310,92	-77,99	-4,42	-372,41	-122,01	-2.002,58	-305,09	-95,73
G.P.5	-2.020,29	-388,98	-144,96	555,97	-50,32	-55,04	-1.811,19	-172,28	-86,92	457,71	-233,77	-113,08	-1.597,47	-183,55	-97,46
G.P.6	-1.223,27	46,87	331,25	1.223,27	-46,87	331,25	-1.153,31	-32,13	298,60	1.153,31	32,13	298,60	-1.007,89	-17,79	249,42
G.P.7	8,87	416,51	406,92	2.455,41	322,77	255,58	-14,44	309,53	276,60	2.292,18	373,79	320,61	-9,54	281,72	245,15
G.P.8	-491,11	266,52	376,21	1.955,43	172,78	286,28	-476,57	170,89	285,53	1.830,05	235,15	311,68	-414,65	160,19	246,88
G.P.9	-2.455,41	-322,77	255,58	-8,87	-416,51	406,92	-2.292,18	-373,79	320,61	14,44	-309,53	276,60	-2.006,24	-317,29	253,69
G.P.10	-1.955,43	-172,78	286,28	491,11	-266,52	376,21	-1.830,05	-235,15	311,68	476,57	-170,89	285,53	-1.601,13	-195,76	251,96
G.P.11	-1.249,59	-40,86	156,26	1.249,59	40,86	156,26	-1.145,66	-6,62	136,86	1.145,66	6,62	136,86	-1.006,41	-12,83	107,63
G.P.12	-17,45	328,78	231,93	2.481,73	410,50	80,59	-6,79	335,05	114,85	2.284,53	348,28	158,86	-8,06	286,67	103,36
G.P.13	-517,43	178,79	201,22	1.981,75	260,51	111,29	-468,92	196,41	123,78	1.822,39	209,64	149,93	-413,17	165,14	105,10
G.P.14	-2.481,73	-410,50	80,59	17,45	-328,78	231,93	-2.284,53	-348,28	158,86	6,79	-335,05	114,85	-2.004,75	-312,34	111,90
G.P.15	-1.981,75	-260,51	111,29	517,43	-178,79	201,22	-1.822,39	-209,64	149,93	468,92	-196,41	123,78	-1.599,64	-190,80	110,17
G.P.16	-1.352,99	-385,53	-531,25	1.352,99	385,53	-531,25	-1.115,59	93,62	-498,60	1.115,59	-93,62	-498,60	-1.000,57	6,62	-449,42
G.P.17	-120,85	-15,89	-455,58	2.585,13	755,17	-606,92	23,28	435,28	-520,61	2.254,46	248,04	-476,60	-2,22	306,12	-453,69
G.P.18	-620,83	-165,88	-486,28	2.085,15	605,18	-576,21	-438,85	296,64	-511,68	1.792,32	109,40	-485,53	-407,33	184,59	-451,96
G.P.19	-2.585,13	-755,17	-606,92	120,85	15,89	-455,58	-2.254,46	-248,04	-476,60	-23,28	-435,28	-520,61	-1.998,92	-292,88	-445,15
G.P.20	-2.085,15	-605,18	-576,21	620,83	165,88	-486,28	-1.792,32	-109,40	-485,53	438,85	-296,64	-511,68	-1.593,81	-171,35	-446,88
G.P.21	-1.326,67	-297,80	-356,26	1.326,67	297,80	-356,26	1.123,24	68,11	-336,86	1.123,24	-68,11	-336,86	-1.002,06	1,67	-307,63
G.P.22	-94,53	71,84	-280,59	2.558,81	667,44	-431,93	15,63	409,77	-358,86	2.262,11	273,55	-314,85	-3,71	301,17	-311,90
G.P.23	-594,51	-78,15	-311,29	2.058,83	517,45	-401,22	-446,50	271,13	-349,93	1.799,98	134,92	-323,78	-408,82	179,64	-310,17
G.P.24	-2.558,81	-667,44	-431,93	94,53	-71,84	-280,59	-2.262,11	-273,55	-314,85	-15,63	-409,77	-358,86	-2.000,40	-297,84	-303,36
G.P.25	-2.058,83	-517,45	-401,22	594,51	78,15	-311,29	-1.799,98	-134,92	-323,78	446,50	-271,13	-349,93	-1.595,29	-176,30	-305,10
max	8,87	416,51	406,92	2.585,13	755,17	406,92	23,28	435,28	320,61	2.292,18	373,79	320,61	-2,22	306,12	253,69
min	-2.585,13	-755,17	-606,92	-8,87	-416,51	-606,92	-2.292,18	-373,79	-520,61	-23,28	-435,28	-520,61	-2.006,24	-317,29	-453,69

Figure 2.33.a. Stress Field at Gauss Points.

Isogeometric Elements 1-5.

	element 6			element 7			element 8			element 9			element 10		
	σ_{xx} (MPa)	σ_{yy} (MPa)	τ_{xy} (MPa)	σ_{xx} (MPa)	σ_{yy} (MPa)	τ_{xy} (MPa)	σ_{xx} (MPa)	σ_{yy} (MPa)	τ_{xy} (MPa)	σ_{xx} (MPa)	σ_{yy} (MPa)	τ_{xy} (MPa)	σ_{xx} (MPa)	σ_{yy} (MPa)	τ_{xy} (MPa)
G.P.1	1.004,23	5,58	-100,00	-869,75	1,01	-100,00	869,75	-1,01	-100,00	-736,05	-0,19	-100,00	736,05	0,19	-100,00
G.P.2	2.002,58	305,09	-95,73	-3,35	260,94	-107,49	1.736,16	258,91	-92,51	-3,15	219,68	-106,91	1.468,95	220,06	-93,09
G.P.3	1.597,47	183,55	-97,46	-354,92	155,46	-104,45	1.384,59	153,44	-95,55	-300,54	130,46	-104,11	1.171,55	130,84	-95,89
G.P.4	5,88	-293,92	-104,27	-1.736,16	-258,91	-92,51	3,35	-260,94	-107,49	-1.468,95	-220,06	-93,09	3,15	-219,68	-106,91
G.P.5	410,99	-172,39	-102,54	-1.384,59	-153,44	-95,55	354,92	-155,46	-104,45	-1.171,55	-130,84	-95,89	300,54	-130,46	-104,11
G.P.6	1.007,89	17,79	249,42	-876,17	-20,39	203,24	876,17	20,39	203,24	-741,97	-19,93	156,52	741,97	19,93	156,52
G.P.7	2.006,24	317,29	253,69	-9,77	239,53	195,75	1.742,58	280,31	210,73	-9,07	199,94	149,61	1.474,87	239,80	163,42
G.P.8	1.601,13	195,76	251,96	-361,34	134,06	198,79	1.391,01	174,84	207,69	-306,47	110,72	152,41	1.177,47	150,58	160,62
G.P.9	9,54	-281,72	245,15	-1.742,58	-280,31	210,73	9,77	-239,53	195,75	-1.474,87	-239,80	163,42	9,07	-199,94	149,61
G.P.10	414,65	-160,19	246,88	-1.391,01	-174,84	207,69	361,34	-134,06	198,79	-1.177,47	-150,58	160,62	306,47	-110,72	152,41
G.P.11	1.006,41	12,83	107,63	-873,57	-11,70	80,19	873,57	11,70	80,19	-739,57	-11,92	52,43	739,57	11,92	52,43
G.P.12	2.004,75	312,34	111,90	-7,16	248,22	72,70	1.739,97	271,62	87,68	-6,67	207,95	45,52	1.472,47	231,79	59,34
G.P.13	1.599,64	190,80	110,17	-385,73	142,75	75,74	1.388,40	166,15	84,64	-304,06	118,73	48,32	1.175,07	142,57	56,53
G.P.14	8,06	-286,67	103,36	-1.739,97	-271,62	87,68	7,16	-248,22	72,70	-1.472,47	-231,79	59,34	6,67	-207,95	45,52
G.P.15	413,17	-165,14	105,10	-1.388,40	-166,15	84,64	358,73	-142,75	75,74	-1.175,07	-142,57	56,53	304,06	-118,73	48,32
G.P.16	1.000,57	-6,62	-449,42	-863,33	22,42	-403,24	863,33	-22,42	-403,24	-730,13	19,55	-356,52	730,13	-19,55	-356,52
G.P.17	1.998,92	292,88	-445,15	3,07	282,34	-410,73	1.729,74	237,50	-395,75	2,78	239,42	-363,42	1.463,03	200,32	-349,61
G.P.18	1.593,81	171,35	-446,88	-348,50	176,87	-407,69	1.378,17	132,03	-398,79	-294,62	150,20	-360,62	1.165,63	111,10	-352,41
G.P.19	2,22	-306,12	-453,69	-1.729,74	-237,50	-395,75	-3,07	-282,34	-410,73	-1.463,03	-200,32	-349,61	-2,78	-239,42	-363,42
G.P.20	407,33	-184,59	-451,96	-1.378,17	-132,03	-398,79	348,50	-176,87	-407,69	-1.165,63	-111,10	-352,41	294,62	-150,20	-360,62
G.P.21	1.002,06	-1,67	-307,63	-865,94	13,73	-280,19	865,94	-13,73	-280,19	-732,53	11,54	-252,43	732,53	-11,54	-252,43
G.P.22	2.000,40	297,84	-303,36	0,47	273,65	-287,68	1.732,34	246,19	-272,70	0,37	231,41	-259,34	1.465,43	208,33	-245,52
G.P.23	1.595,29	176,30	-305,10	-351,10	168,18	-284,64	1.380,77	140,72	-275,74	-297,03	142,19	-256,53	1.168,03	119,11	-248,32
G.P.24	3,71	-301,17	-311,90	-1.732,34	-246,19	-272,70	-0,47	-273,65	-287,68	-1.465,43	-208,33	-245,52	-0,37	-231,41	

Isogeometric Analysis

	element 11			element 12			element 13			element 14			element 15		
	σ_{xx} (MPa)	σ_{yy} (MPa)	τ_{xy} (MPa)	σ_{xx} (MPa)	σ_{yy} (MPa)	τ_{xy} (MPa)	σ_{xx} (MPa)	σ_{yy} (MPa)	τ_{xy} (MPa)	σ_{xx} (MPa)	σ_{yy} (MPa)	τ_{xy} (MPa)	σ_{xx} (MPa)	σ_{yy} (MPa)	τ_{xy} (MPa)
G.P.1	-602,20	0,06	-100,00	602,20	-0,06	-100,00	-468,40	-0,16	-100,00	468,40	0,16	-100,00	-334,48	0,84	-100,00
G.P.2	-2,51	179,97	-107,00	1.201,89	179,85	-93,00	-2,01	139,76	-107,07	934,78	140,07	-92,93	-1,15	100,84	-106,59
G.P.3	-245,85	106,97	-104,16	958,55	106,84	-95,84	-191,26	82,98	-104,20	745,53	83,30	-95,80	-136,41	60,26	-103,91
G.P.4	-1.201,89	-179,85	-93,00	2,51	-179,97	-107,00	-934,78	-140,07	-92,93	2,01	-139,76	-107,07	-667,80	-99,15	-93,41
G.P.5	-958,55	-106,84	-95,84	245,85	-106,97	-104,16	-745,53	-83,30	-95,80	191,26	-82,98	-104,20	-532,54	-58,58	-96,09
G.P.6	-608,20	-19,94	109,89	608,20	19,94	109,89	-474,46	-20,35	63,23	474,46	20,35	63,23	-340,12	-17,97	16,66
G.P.7	-8,51	159,97	102,89	1.207,89	199,84	116,89	-8,07	119,56	56,17	940,84	160,27	70,30	-6,80	82,03	10,08
G.P.8	-251,85	86,97	105,73	964,55	126,84	114,05	-197,32	62,79	59,03	751,59	103,49	67,43	-142,05	41,45	12,75
G.P.9	-1.207,89	-199,84	116,89	8,51	-159,97	102,89	-940,84	-160,27	70,30	8,07	-119,56	56,17	-673,44	-117,97	23,25
G.P.10	-964,55	-126,84	114,05	251,85	-86,97	105,73	-751,59	-103,49	67,43	197,32	-62,79	59,03	-538,19	-77,39	20,58
G.P.11	-605,76	-11,82	24,72	605,76	11,82	24,72	-472,00	-12,16	-3,00	472,00	12,16	-3,00	-337,83	-10,34	-30,68
G.P.12	-6,07	168,09	17,72	1.205,45	191,73	31,72	-5,61	127,76	-10,07	938,38	152,07	4,07	-4,51	89,66	-37,26
G.P.13	-249,42	95,08	20,56	962,11	118,73	28,88	-194,86	70,98	-7,20	749,13	95,30	1,20	-139,76	49,08	-34,59
G.P.14	-1.205,45	-191,73	31,72	6,07	-168,09	17,72	-938,38	-152,07	4,07	5,61	-127,76	-10,07	-671,15	-110,33	-24,09
G.P.15	-962,11	-118,73	28,88	249,42	-95,08	20,56	-749,13	-95,30	1,20	194,86	-70,98	-7,20	-535,90	-69,76	-26,76
G.P.16	-596,20	20,06	-309,89	596,20	-20,06	-309,89	-462,34	20,04	-263,23	462,34	-20,04	-263,23	-328,83	19,66	-216,66
G.P.17	3,49	199,97	-316,89	1.195,89	159,85	-302,89	4,04	159,95	-270,30	928,72	119,88	-256,17	4,49	119,66	-223,25
G.P.18	-239,85	126,96	-314,05	952,55	86,85	-305,73	-185,21	103,18	-267,43	739,47	63,11	-259,03	-130,76	79,08	-220,58
G.P.19	-1.195,89	-159,85	-302,89	-3,49	-199,97	-316,89	-928,72	-119,88	-256,17	-4,04	-159,95	-270,30	-662,15	-80,34	-210,08
G.P.20	-952,55	-86,85	-305,73	239,85	-126,96	-314,05	-739,47	-63,11	-259,03	185,21	-103,18	-267,43	-526,90	-39,76	-212,75
G.P.21	-598,64	11,94	-224,72	598,64	-11,94	-224,72	-464,80	11,84	-197,00	464,80	-11,84	-197,00	-331,12	12,02	-169,32
G.P.22	1,06	191,85	-231,72	1.198,33	167,96	-217,72	1,59	151,76	-204,07	931,18	128,07	-189,93	2,20	112,02	-175,91
G.P.23	-242,29	118,85	-228,88	954,98	94,96	-220,56	-187,66	94,98	-201,20	741,93	71,30	-192,80	-133,05	71,44	-173,24
G.P.24	-1.198,33	-167,96	-217,72	-1,06	-191,85	-231,72	-931,18	-128,07	-189,93	-1,59	-151,76	-204,07	-664,44	-87,97	-162,74
G.P.25	-954,98	-94,96	-220,56	242,29	-118,85	-228,88	-741,93	-71,30	-192,80	187,66	-94,98	-201,20	-529,19	-47,40	-165,41
max	3,49	199,97	116,89	1.207,89	199,84	116,89	4,04	159,95	70,30	940,84	160,27	70,30	4,49	119,66	23,25
min	-1.207,89	-199,84	-316,89	-3,49	-199,97	-316,89	-940,84	-160,27	-270,30	-4,04	-159,95	-270,30	-673,44	-117,97	-223,25

Figure 2.33.c. Stress Field at Gauss Points.

Isogeometric Elements 11-15.

	element 16			element 17			element 18			element 19			element 20		
	σ_{xx} (MPa)	σ_{yy} (MPa)	τ_{xy} (MPa)	σ_{xx} (MPa)	σ_{yy} (MPa)	τ_{xy} (MPa)	σ_{xx} (MPa)	σ_{yy} (MPa)	τ_{xy} (MPa)	σ_{xx} (MPa)	σ_{yy} (MPa)	τ_{xy} (MPa)	σ_{xx} (MPa)	σ_{yy} (MPa)	τ_{xy} (MPa)
G.P.1	334,48	-0,84	-100,00	-201,20	-4,64	-100,00	201,20	4,64	-100,00	-64,37	25,56	-100,00	64,37	-25,56	-100,00
G.P.2	667,80	99,15	-93,41	-2,23	55,05	-109,26	400,16	64,33	-90,74	7,36	47,08	-94,52	136,11	-4,04	-105,48
G.P.3	532,54	58,58	-96,09	-82,97	30,83	-105,50	319,42	40,11	-94,50	-21,75	38,35	-96,74	107,00	-12,77	-103,26
G.P.4	1,15	-100,84	-106,59	-400,16	-64,33	-90,74	2,23	-55,05	-109,26	-136,11	4,04	-105,48	-7,36	-47,08	-94,52
G.P.5	136,41	-60,26	-103,91	-319,42	-40,11	-94,50	82,97	-30,83	-105,50	-107,00	12,77	-103,26	21,75	-38,35	-96,74
G.P.6	340,12	17,97	16,66	-209,13	-31,10	-30,36	209,13	31,10	-30,36	-59,68	41,22	-74,89	59,68	-41,22	-74,89
G.P.7	673,44	117,97	23,25	-10,17	28,59	-39,62	408,10	90,79	-21,10	12,06	62,74	-69,41	131,42	-19,69	-80,37
G.P.8	538,19	77,39	20,58	-90,91	4,37	-35,87	327,36	66,57	-24,86	-17,05	54,00	-71,63	102,31	-28,43	-78,15
G.P.9	6,80	-82,03	10,08	-408,10	-90,79	-21,10	10,17	-28,59	-39,62	-131,42	19,69	-80,37	-12,06	-62,74	-69,41
G.P.10	142,05	-41,45	12,75	-327,36	-66,57	-24,86	90,91	-4,37	-35,87	-102,31	28,43	-78,15	17,05	-54,00	-71,63
G.P.11	337,83	10,34	-30,68	-205,91	-20,36	-58,62	205,91	20,36	-58,62	-61,58	34,86	-85,08	61,58	-34,86	-85,08
G.P.12	671,15	110,33	-24,09	-6,95	39,32	-67,88	404,88	80,05	-49,36	10,16	56,38	-79,60	133,32	-13,34	-90,56
G.P.13	535,90	69,76	-26,76	-87,68	15,10	-64,12	324,14	55,83	-53,12	-18,95	47,65	-81,82	104,21	-22,07	-88,34
G.P.14	4,51	-89,66	-37,26	-404,88	-80,05	-49,36	6,95	-39,32	-67,88	-133,32	13,34	-90,56	-10,16	-56,38	-79,60
G.P.15	139,76	-49,08	-34,59	-324,14	-55,83	-53,12	87,68	-15,10	-64,12	-104,21	22,07	-88,34	18,95	-47,65	-81,82
G.P.16	328,83	-19,66	-216,66	-193,26	21,82	-169,64	193,26	-21,82	-169,64	-69,07	9,90	-125,11	69,07	-9,90	-125,11
G.P.17	662,15	80,34	-210,08	5,71	81,51	-178,90	392,22	37,87	-160,38	2,67	31,42	-119,63	140,81	11,62	-130,59
G.P.18	526,90	39,76	-212,75	-75,03	57,29	-175,14	311,49	13,65	-164,13	-26,44	22,69	-121,85	111,70	2,89	-128,37
G.P.19	-4,49	-119,66	-223,25	-392,22	-37,87	-160,38	-5,71	-81,51	-178,90	-140,81	-11,62	-130,59	-2,67	-31,42	-119,63
G.P.20	130,76	-79,08	-220,58	-311,49	-13,65	-164,13	75,03	-57,29	-175,14	-111,70	-2,89	-128,37	26,44	-22,69	-121,85
G.P.21	331,12	-12,02	-169,32	-196,48	11,08	-141,38	196,48	-11,08	-141,38	-67,17	16,25	-114,92	67,17	-16,25	-114,92
G.P.22	664,44	87,97	-162,74	2,49	70,77	-150,64	395,44	48,61	-132,12	4,57	37,77	-109,44	138,91	5,27	-120,40
G.P.23	529,19	47,40	-165,41	-78,25	46,55	-146,88	314,71	24,39	-135,88	-24,54	29,04	-111,66	109,80	-3,46	-118,18
G.P.24	-2,20	-112,02	-175,91	-395,44	-48,61	-132,12	-2,49	-70,77	-150,64	-138,91	-5,27	-120,40	-4,57	-37,77	-109,44
G.P.25	133,05	-71,44	-173,24	-314,71	-24,39	-135,88	78,25	-46,55	-146,88	-109,80	3,46	-118,18	24,54	-29,04	-111,66
max	673,44	117,97	23,25	5,71	81,51	-21,10	408,10	90,79	-21,10	12,06	62,74	-69,41	140,81	11,62	-69,41
min	-4,49	-119,66	-223,25	-408,10	-90,79	-178,90	-5,71	-81,51	-178,90	-140,81	-11,62	-13			

		(Element, G.P.)	
σ_{XX} (MPa)	max	(2,17)	2.585,13
	min	(1,19)	-2.585,13
σ_{YY} (MPa)	max	(2,17)	755,17
	min	(1,19)	-755,17
τ_{XY} (MPa)	max	(1,7), (2,9)	406,92
	min	(1,19), (2,17)	-606,92

Figure 2.34. Maximum and Minimum Stress.

Figure 2.33 depicts stresses at Isogeometric Elements' Gauss Points, while Figure 2.34 shows maximum and minimum stress.

As expected, elements 1 and 2 (nearest to fixed boundary) suffer from larger stresses. It is a cantilever under concentrated load $P=3.000$ kN at free edge, so the upper horizontal side suffers from tension and the lower horizontal side suffers from compression. Maximum bending moment occurs at fixed edge.

$$M_{\max} = -P \cdot L = -3.000 \text{ kN} \cdot 15 \text{ m} = -45.000 \text{ kNm}$$

Element 2 (G.P.17, nearest to upper horizontal side) experience the largest tension. Tensile stresses are equal to:

$$\max \sigma_{XX}^+ = 2.585,13 \text{ MPa}$$

$$\max \sigma_{YY}^+ = 755,17 \text{ MPa}$$

Element 1 (G.P.19, nearest to lower horizontal side) experience the largest compression. Compressive stresses are equal to:

$$\max \sigma_{XX}^- = -2.585,13 \text{ MPa}$$

$$\max \sigma_{YY}^- = -755,17 \text{ MPa}$$

2.2.2. Finite Element Analysis

I will solve the same problem applying Finite Element Method. In order to reach a safe conclusion, I have maintained as many nodes (FEA) as control points (IGA), means I have used 33 nodes with the same global numbering. The two (FEA, IGA) outgoing stiffness matrices will have the same dimensions (66x66). The nodes have the same distance between each other along the length and the height.

As it is a plane stress problem, the two stiffness matrices have both 66 rows and 66 columns. ($2 \cdot 33 = 66$, 66×66).

I use the following analysis parameters:

- **Nodes: 33.** It is important to underline that number of Nodes is equal to shape functions' number. Cartesian coordinate system's origin is the extreme left and bottom corner.
- **Shape functions: Linear.** The shape functions are linear, as I used 4-noded Finite Elements.
- **20 2D 4-sided, 4-noded Finite Elements.** I have simulated the structure with 20 2D 4-sided 4-noded Finite Elements. Every element has the same geometry and nodes. So, the local stiffness matrix is the same. The parametric axis ξ (parameter space) is parallel to cantilever's length (physical space), means horizontal. Its direction is from left to right. The parametric axis η (parameter space) is parallel to cantilever's height (physical space), means vertical. Its direction is from bottom to cantilever's top. In FEA, the parameter space is local to every element.

Method	FEA
Finite Elements (Number)	20
Finite Elements (Type)	2D
	4-sided
	4-noded
	isoparametric
Gauss Points	5x5

Figure 2.35. Analysis Parameters.

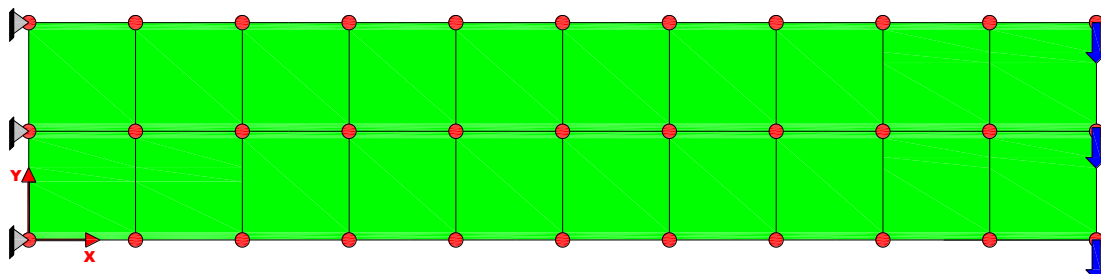
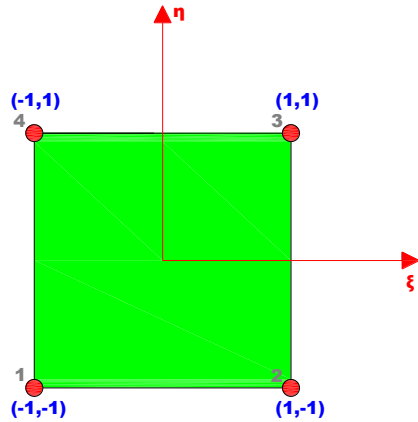


Figure 2.36. Cantilever Profile. (Cartesian Axes. Nodes.)

2D 4-sided 4-noded Finite Element

It is a plane stress problem. I have used isoparametric 2-D 4-sided 4-noded Finite Elements. Each element has 4 nodes and 2.4=8 degrees of freedom, as each node corresponds to 2 degrees of freedom, which are the horizontal displacement and the vertical displacement.



**Figure 2.37. Isoparametric 2D 4-sided 4-noded Finite Element.
Parameter Space. Local Numbering.**

Shape functions

The shape functions and their partial derivatives with respect to ξ , η are equal to:

$$\begin{aligned} N_1 &= \frac{1}{4} (1-\xi)(1-\eta) & N_{1,\xi} &= -\frac{1}{4} (1-\eta) & N_{1,\eta} &= -\frac{1}{4} (1-\xi) \\ N_2 &= \frac{1}{4} (1+\xi)(1-\eta) & N_{2,\xi} &= \frac{1}{4} (1-\eta) & N_{2,\eta} &= -\frac{1}{4} (1+\xi) \\ N_3 &= \frac{1}{4} (1+\xi)(1+\eta) & N_{3,\xi} &= \frac{1}{4} (1+\eta) & N_{3,\eta} &= \frac{1}{4} (1+\xi) \\ N_4 &= \frac{1}{4} (1-\xi)(1+\eta) & N_{4,\xi} &= -\frac{1}{4} (1+\eta) & N_{4,\eta} &= \frac{1}{4} (1-\xi) \end{aligned}$$

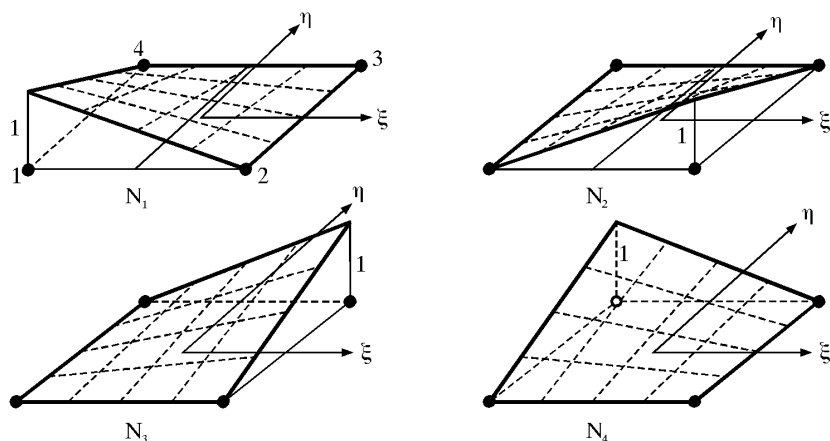


**Figure 2.38. Shape functions.
Isoparametric 2D 4-sided 4-noded Finite Element.**

For every element $e = 1 \div 20$, I follow the below procedure.

Elasticity Matrix [E]

As it is a plane stress problem, the elasticity matrix [E] is equal to:

$$E_{3 \times 3} = \frac{E}{1-v^2} \cdot \begin{bmatrix} 1 & v & 0 \\ v & 1 & 0 \\ 0 & 0 & \frac{1-v}{2} \end{bmatrix}$$

Deformation Matrix [B]

I calculate the deformation matrix.

$$\left[B_e \right]_{3 \times 8} = \left[B_{1,e} \right]_{3 \times 4} \cdot \left[B_{2,e} \right]_{4 \times 8}$$

where:

$$\left[B_{1,e} \right]_{3 \times 4} = \frac{1}{\det[J_e]} \cdot \begin{bmatrix} J_{e,22} & \xi, \eta & -J_{e,12} & \xi, \eta & 0 & 0 \\ 0 & 0 & 0 & -J_{e,21} & \xi, \eta & J_{e,11} & \xi, \eta \\ -J_{e,21} & \xi, \eta & J_{e,11} & \xi, \eta & J_{e,22} & \xi, \eta & -J_{e,12} & \xi, \eta \end{bmatrix}$$

$$\left[J_e \right]_{2 \times 2} = \left[D_N \right]_{2 \times 4} \cdot X Y_e = \begin{bmatrix} N_{1,\xi} & \xi, \eta & N_{2,\xi} & \xi, \eta & N_{3,\xi} & \xi, \eta & N_{4,\xi} & \xi, \eta \\ N_{1,\eta} & \xi, \eta & N_{2,\eta} & \xi, \eta & N_{3,\eta} & \xi, \eta & N_{4,\eta} & \xi, \eta \end{bmatrix} \cdot \begin{bmatrix} X_{1,e} & Y_{1,e} \\ X_{2,e} & Y_{2,e} \\ X_{3,e} & Y_{3,e} \\ X_{4,e} & Y_{4,e} \end{bmatrix} \Rightarrow$$

$$\left[J \right]_{2 \times 2} = \begin{bmatrix} -\frac{1}{4} & 1-\eta & \frac{1}{4} & 1-\eta & \frac{1}{4} & 1+\eta & -\frac{1}{4} & 1+\eta \\ -\frac{1}{4} & 1-\xi & -\frac{1}{4} & 1+\xi & \frac{1}{4} & 1+\xi & \frac{1}{4} & 1-\xi \end{bmatrix} \cdot \begin{bmatrix} X_{1,e} & Y_{1,e} \\ X_{2,e} & Y_{2,e} \\ X_{3,e} & Y_{3,e} \\ X_{4,e} & Y_{4,e} \end{bmatrix}$$

$X_{n,e}, Y_{n,e}$: Node's n (Finite Element e) Cartesian coordinates (local numbering)

$$\left[B_{2,e} \right]_{4 \times 8} = \begin{bmatrix} N_{1,\xi} & \xi, \eta & 0 & N_{2,\xi} & \xi, \eta & 0 & N_{3,\xi} & \xi, \eta & 0 & N_{4,\xi} & \xi, \eta & 0 \\ N_{1,\eta} & \xi, \eta & 0 & N_{2,\eta} & \xi, \eta & 0 & N_{3,\eta} & \xi, \eta & 0 & N_{4,\eta} & \xi, \eta & 0 \\ 0 & N_{1,\xi} & \xi, \eta & 0 & N_{2,\xi} & \xi, \eta & 0 & N_{3,\xi} & \xi, \eta & 0 & N_{4,\xi} & \xi, \eta & 0 \\ 0 & N_{1,\eta} & \xi, \eta & 0 & N_{2,\eta} & \xi, \eta & 0 & N_{3,\eta} & \xi, \eta & 0 & N_{4,\eta} & \xi, \eta & 0 \end{bmatrix} \Rightarrow$$

$$\Rightarrow \left[\begin{array}{c|ccccc} B_{2,e} & \xi, \eta \\ \hline 4x8 & \end{array} \right] = \begin{bmatrix} -\frac{1}{4} 1-\eta & 0 & \frac{1}{4} 1-\eta & 0 & \frac{1}{4} 1+\eta & 0 & -\frac{1}{4} 1+\eta & 0 \\ -\frac{1}{4} 1-\xi & 0 & -\frac{1}{4} 1+\xi & 0 & \frac{1}{4} 1+\xi & 0 & \frac{1}{4} 1-\xi & 0 \\ 0 & -\frac{1}{4} 1-\eta & 0 & \frac{1}{4} 1-\eta & 0 & \frac{1}{4} 1+\eta & 0 & -\frac{1}{4} 1+\eta \\ 0 & -\frac{1}{4} 1-\xi & 0 & -\frac{1}{4} 1+\xi & 0 & \frac{1}{4} 1+\xi & 0 & \frac{1}{4} 1-\xi \end{bmatrix}$$

Local Stiffness Matrix [k^e]

I produce the local stiffness matrix.

$$k_e = \int_{-1-1}^{1-1} \int_{8x3}^{1-1} [B_e \xi, \eta]^T \cdot E \cdot [B_e \xi, \eta] \cdot t \cdot \det[J_e \xi, \eta] d\xi d\eta$$

I have calculated the double integral using numerical integration (integration rule 5x5).

$$k_e = \sum_{i=1}^5 \sum_{j=1}^5 \left\{ w_i \cdot w_j \cdot [B_e \xi_i, \eta_j]_8^T \cdot E \cdot [B_e \xi_i, \eta_j]_{3x8} \cdot t \cdot \det[J_e \xi_i, \eta_j] \right\}$$

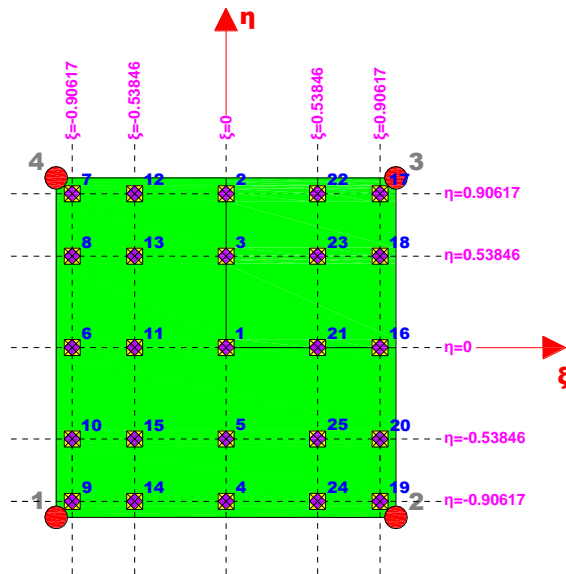


Figure 2.39. Gauss Points. (Local numbering.)
Isoparametric 2D 4-sided 4-noded Finite Element.

Isogeometric Analysis

The weight factors for the 25 five Gauss Points are equal to:

G.P.	ξ_i	w_i	η_j	w_j	$w_{ij} = w_i \cdot w_j$
1	0	0,56888	0	0,56888	0,32362
2	0	0,56888	0,90617	0,23692	0,13478
3	0	0,56888	0,53846	0,47862	0,27228
4	0	0,56888	-0,90617	0,23692	0,13478
5	0	0,56888	-0,53846	0,47862	0,27228
6	0,90617	0,23692	0	0,56888	0,13478
7	0,90617	0,23692	0,90617	0,23692	0,05613
8	0,90617	0,23692	0,53846	0,47862	0,11339
9	0,90617	0,23692	-0,90617	0,23692	0,05613
10	0,90617	0,23692	-0,53846	0,47862	0,11339
11	0,53846	0,47862	0	0,56888	0,27228
12	0,53846	0,47862	0,90617	0,23692	0,11339
13	0,53846	0,47862	0,53846	0,47862	0,22908
14	0,53846	0,47862	-0,90617	0,23692	0,11339
15	0,53846	0,47862	-0,53846	0,47862	0,22908
16	-0,90617	0,23692	0	0,56888	0,13478
17	-0,90617	0,23692	0,90617	0,23692	0,05613
18	-0,90617	0,23692	0,53846	0,47862	0,11339
19	-0,90617	0,23692	-0,90617	0,23692	0,05613
20	-0,90617	0,23692	-0,53846	0,47862	0,11339
21	-0,53846	0,47862	0	0,56888	0,27228
22	-0,53846	0,47862	0,90617	0,23692	0,11339
23	-0,53846	0,47862	0,53846	0,47862	0,22908
24	-0,53846	0,47862	-0,90617	0,23692	0,11339
25	-0,53846	0,47862	-0,53846	0,47862	0,22908

Each Finite Element has the same local Stiffness Matrix, which is the following:

		local [k] (kN/m) (Finite Element 1. Global numbering of Nodes.)							
		Node 1		Node 2		Node 4		Node 5	
		u (m)	v (m)	u (m)	v (m)	u (m)	v (m)	u (m)	v (m)
Node 1	F _x (kN)	1.038.462	375.000	115.385	28.846	-634.615	-28.846	-519.231	-375.000
	F _y (kN)	375.000	1.038.462	-28.846	-634.615	28.846	115.385	-375.000	-519.231
Node 2	F _x (kN)	115.385	-28.846	1.038.462	-375.000	-519.231	375.000	-634.615	28.846
	F _y (kN)	28.846	-634.615	-375.000	1.038.462	375.000	-519.231	-28.846	115.385
Node 4	F _x (kN)	-634.615	28.846	-519.231	375.000	1.038.462	-375.000	115.385	-28.846
	F _y (kN)	-28.846	115.385	375.000	-519.231	-375.000	1.038.462	28.846	-634.615
Node 5	F _x (kN)	-519.231	-375.000	-634.615	-28.846	115.385	28.846	1.038.462	375.000
	F _y (kN)	-375.000	-519.231	28.846	115.385	-28.846	-634.615	375.000	1.038.462

Figure 2.40. Stiffness Matrix. Finite Element 1.
Global numbering of Nodes.

Isogeometric Analysis

Control Net

Figure 2.41 shows Nodes' Cartesian coordinates.

		axis X										
		X _N	element 1	element 2	element 3	element 4	element 5	element 6	element 7	element 8	element 9	element 10
local numbering	Node 1	0	0	1,5	1,5	3	3	4,5	4,5	6	6	
	Node 2	0	0	1,5	1,5	3	3	4,5	4,5	6	6	
	Node 3	1,5	1,5	3	3	4,5	4,5	6	6	7,5	7,5	
	Node 4	1,5	1,5	3	3	4,5	4,5	6	6	7,5	7,5	
		element 11	element 12	element 13	element 14	element 15	element 16	element 17	element 18	element 19	element 20	
	Node 1	7,5	7,5	9	9	10,5	10,5	12	12	13,5	13,5	
	Node 2	7,5	7,5	9	9	10,5	10,5	12	12	13,5	13,5	
	Node 3	9	9	10,5	10,5	12	12	13,5	13,5	15	15	
	Node 4	9	9	10,5	10,5	12	12	13,5	13,5	15	15	

Figure 2.41.a. Nodes' Cartesian coordinate X. (physical space)

		axis Y										
		Y _N	element 1	element 2	element 3	element 4	element 5	element 6	element 7	element 8	element 9	element 10
local numbering	Node 1	0	1,5	0	1,5	0	1,5	0	1,5	0	1,5	
	Node 2	1,5	3	1,5	3	1,5	3	1,5	3	1,5	3	
	Node 3	0	1,5	0	1,5	0	1,5	0	1,5	0	1,5	
	Node 4	1,5	3	1,5	3	1,5	3	1,5	3	1,5	3	
		element 11	element 12	element 13	element 14	element 15	element 16	element 17	element 18	element 19	element 20	
	Node 1	0	1,5	0	1,5	0	1,5	0	1,5	0	1,5	
	Node 2	1,5	3	1,5	3	1,5	3	1,5	3	1,5	3	
	Node 3	0	1,5	0	1,5	0	1,5	0	1,5	0	1,5	
	Node 4	1,5	3	1,5	3	1,5	3	1,5	3	1,5	3	

Figure 2.41.b. Nodes' Cartesian coordinate Y. (physical space)

33 Nodes partition the structure into 20 Finite Elements.

In Figure 2.16 we can see the corresponding node net.

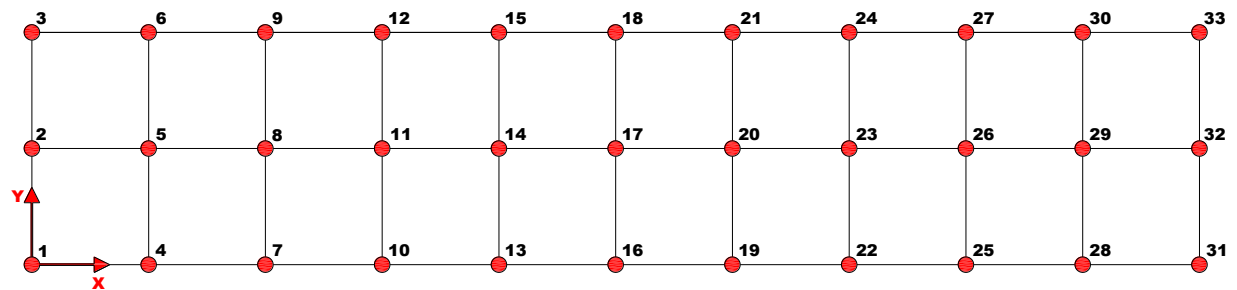
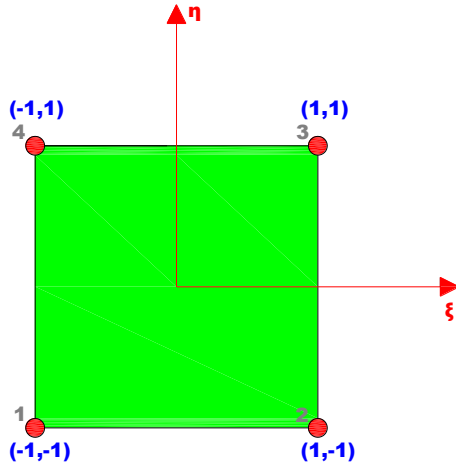


Figure 2.42. Node Net. (physical space)

Parameter Space



**Figure 2.43. Isoparametric 2D 4-sided 4-noded Finite Element.
Parameter Space. Local Numbering.**

Physical Space

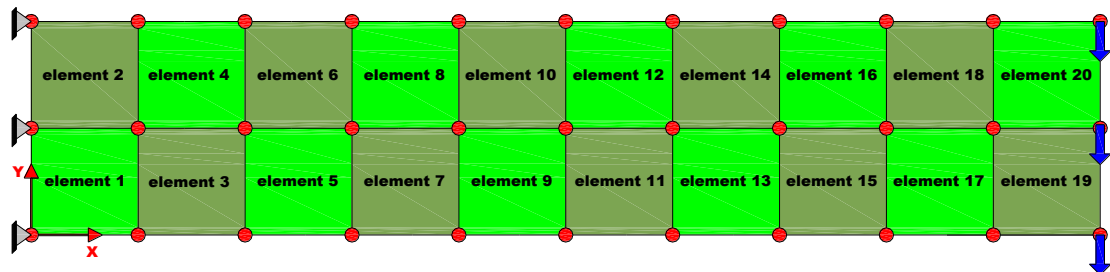


**Figure 2.44. Finite Element Mesh.
Nodes partition cantilever into finite elements.**

Figure 2.44 shows nodes (red circles) in the physical space. Nodes partition cantilever into 20 isoparametric 2D 4-sided 4-noded finite elements. The Total Stiffness Matrix refers to nodes, so I form the equilibrium equation for them.

$$\mathbf{F} = \mathbf{K} \cdot \mathbf{U} \Rightarrow \mathbf{U} = \mathbf{K}^{-1} \cdot \mathbf{F}$$

Displacements' vector \mathbf{U} refers to nodes. For this particular problem, there are 33 nodes, so the above equation is written as follows:

$$\underset{66 \times 1}{\mathbf{F}} = \underset{66 \times 66}{\mathbf{K}} \cdot \underset{66 \times 1}{\mathbf{U}} \Rightarrow \underset{66 \times 1}{\mathbf{U}} = \underset{66 \times 66}{\mathbf{K}^{-1}} \cdot \underset{66 \times 1}{\mathbf{F}}$$

Total Stiffness Matrix [K]

I calculate the local (numbering) Stiffness Matrix for every Finite Element. Then, I form the total Stiffness Matrix of the structure.

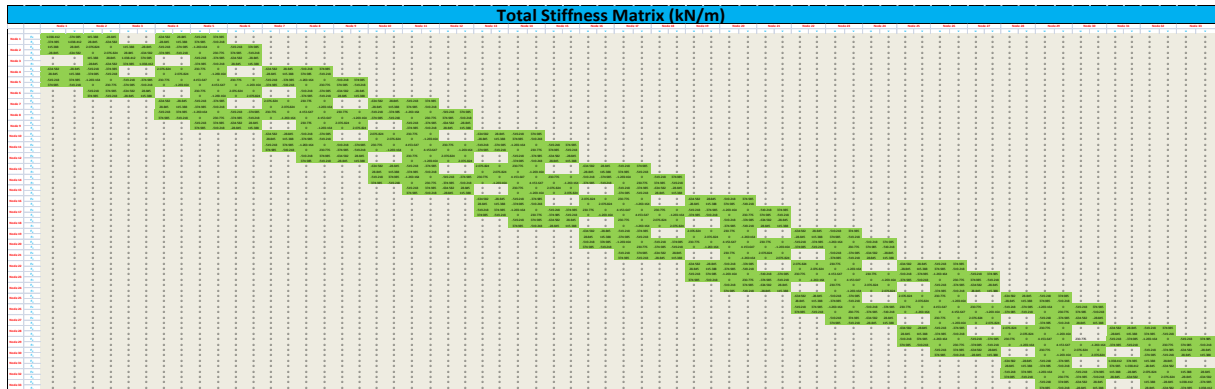


Figure 2.45. Total Stiffness Matrix. (66x66)

Two Degrees of Freedom correspond to every Node, the horizontal u and the vertical v displacement. The cantilever's total Stiffness Matrix is a symmetric square matrix with dimensions 66x66, as there are 33 Nodes and $33 \cdot 2 = 66$ Degrees of Freedom.

Nodes' External Forces {P}

I calculate the External Load Vector (66x1) and I reorder it.

$$\mathbf{F}_{\text{tot}} \underset{(66 \times 1)}{=} \begin{matrix} 0 & \dots & 0 & -1000 & 0 & -1000 & 0 & -1000 \end{matrix}^T$$

$$\mathbf{F}_{\text{tot,m}} \underset{(66 \times 1)}{=} \left\{ \begin{matrix} \mathbf{F}_f \\ \mathbf{F}_s \end{matrix} \right\} \underset{(6 \times 1)}{=} \left\{ \begin{matrix} 0 & \dots & 0 & -1000 & 0 & -1000 & 0 & -1000 \\ & & & & & & & \\ & & & & & & & \\ & & & & & & & \\ & & & & & & & \\ & & & & & & & \\ & & & & & & & \end{matrix}^T \right\} \underset{(60 \times 1)}{=}$$

Control Points' Displacements {U}

I reorder the Total Stiffness Matrix and the External Load Vector and then I form the balance equation. I symbolize the unknown displacements with subscript f and the known ones (fixed Nodes) with s.

$$F_{\text{tot,m}} = [K_{\text{tot,m}}] \cdot U_{\text{tot,m}} \Rightarrow \begin{Bmatrix} F_f \\ 60 \times 1 \\ F_s \\ 6 \times 1 \end{Bmatrix} = \begin{bmatrix} K_{ff} & K_{fs} \\ 60 \times 60 & 60 \times 6 \\ K_{sf} & K_{ss} \\ 6 \times 60 & 6 \times 6 \end{bmatrix} \cdot \begin{Bmatrix} U_f \\ 60 \times 1 \\ U_s \\ 6 \times 1 \end{Bmatrix}$$

$$\Rightarrow$$

$$\left\{ \begin{array}{c} 0 \\ \dots \\ 0 \\ -1000 \\ 0 \\ -1000 \\ 0 \\ 0 \\ -1000 \\ 60 \times 1 \\ 0 \\ 6 \times 1 \end{array} \right\} = \left[\begin{array}{cc} K_{ff} & K_{fs} \\ 60 \times 60 & 60 \times 6 \\ K_{sf} & K_{ss} \\ 6 \times 60 & 6 \times 6 \end{array} \right] \cdot \left\{ \begin{array}{c} U_f \\ 60 \times 1 \\ U_s \\ 6 \times 1 \end{array} \right\} \Rightarrow \left\{ \begin{array}{c} U_f \\ 60 \times 1 \\ K_{ff} \\ 60 \times 60 \end{array} \right\} \cdot \left\{ \begin{array}{c} 0 \\ \dots \\ 0 \\ -1000 \\ 0 \\ -1000 \\ 0 \\ -1000 \\ 60 \times 1 \end{array} \right\}$$

Figure 2.46 shows Nodes' horizontal and vertical displacement.

The maximum horizontal displacement is equal to 9,5cm and corresponds to:

- ❖ Node 31: $u=-9,5$ cm
- ❖ Node 33: $u=+9,5$ cm.

The maximum vertical displacement is equal to 65,1cm and corresponds to:

- ❖ Node 31: $v=-65,1$ cm
- ❖ Node 33: $v=-65,1$ cm.

Negative value displays that maximum displacement's direction is the negative direction of axis Y, means these Nodes move downstairs as expected.

		horizontal u (cm)	vertical v (cm)
Node	1	0,0	0,0
Node	2	0,0	0,0
Node	3	0,0	0,0
Node	4	-1,8	-1,2
Node	5	0,0	-0,9
Node	6	1,8	-1,2
Node	7	-3,4	-4,0
Node	8	0,0	-3,7
Node	9	3,4	-4,0
Node	10	-4,8	-8,2
Node	11	0,0	-8,0
Node	12	4,8	-8,2
Node	13	-6,1	-13,9
Node	14	0,0	-13,7
Node	15	6,1	-13,9
Node	16	-7,1	-20,6
Node	17	0,0	-20,5
Node	18	7,1	-20,6
Node	19	-8,0	-28,4
Node	20	0,0	-28,3
Node	21	8,0	-28,4
Node	22	-8,7	-36,9
Node	23	0,0	-36,8
Node	24	8,7	-36,9
Node	25	-9,1	-45,9
Node	26	0,0	-45,9
Node	27	9,1	-45,9
Node	28	-9,4	-55,4
Node	29	0,0	-55,4
Node	30	9,4	-55,4
Node	31	-9,5	-65,1
Node	32	0,0	-65,0
Node	33	9,5	-65,1
max		9,5	0,0
min		-9,5	-65,1

Figure 2.46. Nodes' displacements.

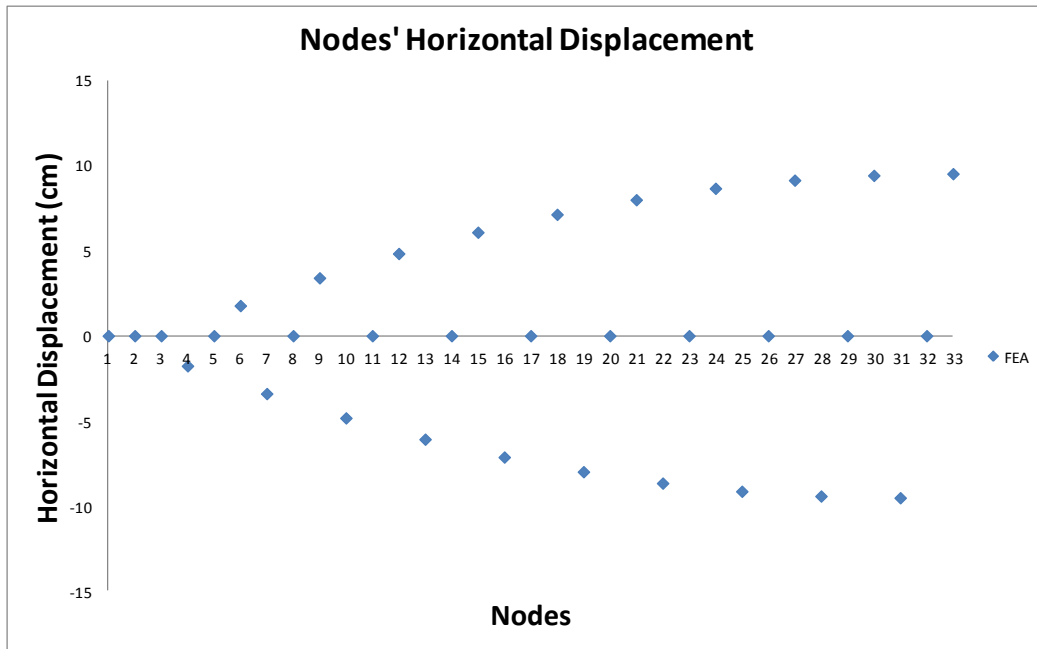


Figure 2.47.a. Nodes' horizontal displacement.

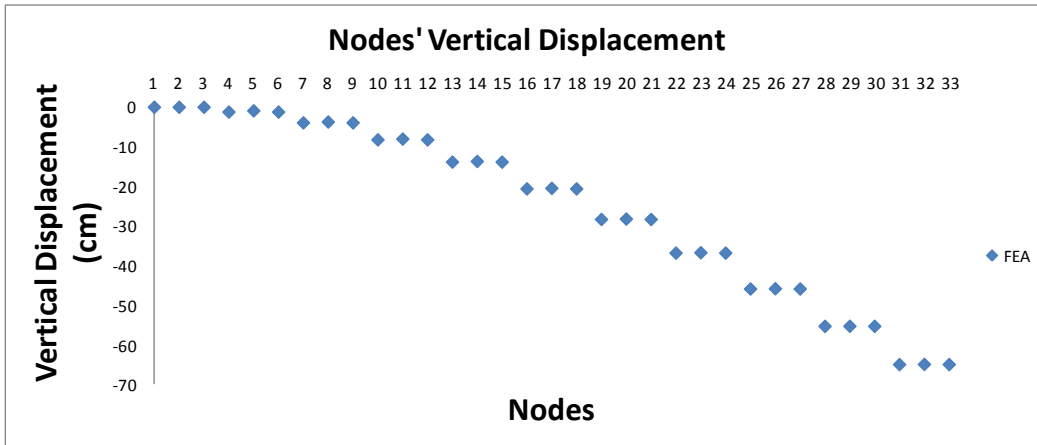


Figure 2.47.b. Nodes' vertical displacement.

Stress Field at Gauss Points

As I know Nodes' displacements, I can calculate the stress field at Finite Elements' Gauss Points.

$$\sigma_{\xi_i, \eta_i} = E \cdot \varepsilon_{\xi_i, \eta_i} = E \cdot [B_{\xi_i, \eta_i}] \cdot d$$

where:

Isogeometric Analysis

- $\sigma_{\xi_i, \eta_i} = \begin{Bmatrix} \sigma_X & \xi_i, \eta_i \\ \sigma_Y & \xi_i, \eta_i \\ \tau_{XY} & \xi_i, \eta_i \end{Bmatrix}_{3x1}$: stress field at Gauss Point i (plane stress problem)

- $E = \frac{E}{1-v^2} \cdot \begin{bmatrix} 1 & v & 0 \\ v & 1 & 0 \\ 0 & 0 & \frac{1-v}{2} \end{bmatrix}$ (plane stress problem)

- $\varepsilon_{\xi_i, \eta_i} = \begin{Bmatrix} \varepsilon_X & \xi_i, \eta_i \\ \varepsilon_Y & \xi_i, \eta_i \\ \gamma_{XY} & \xi_i, \eta_i \end{Bmatrix}_{3x1}$: strain field at Gauss Point i

- d : Displacement vector refers to displacements of Finite Element's Nodes (local numbering).

Let's calculate the corresponding stress field to Gauss Point 1 of Finite Element 1.

			{d} (m)
element 1	Node 1	u (m)	0
		v (m)	0
	Node 2	u (m)	0
		v (m)	0
	Node 4	u (m)	-0,018
		v (m)	-0,012
	Node 5	u (m)	0
		v (m)	-0,009

Figure 2.48. Nodes' vertical and horizontal displacement.
Finite Element 1.

$$\sigma_{\xi_1, \eta_1} = E \cdot [B_{\xi_1, \eta_1}] \cdot d = \begin{Bmatrix} -1.288.132 \\ -169.330 \\ -100.000 \end{Bmatrix} \text{ kPa} \Rightarrow \sigma_{\xi_1, \eta_1} = \begin{Bmatrix} -1.288,13 \\ -169,33 \\ -100,00 \end{Bmatrix} \text{ MPa}$$

Isogeometric Analysis

	element 1			element 2			element 3			element 4			element 5		
	σ_{xx} (MPa)	σ_{yy} (MPa)	τ_{xy} (MPa)	σ_{xx} (MPa)	σ_{yy} (MPa)	τ_{xy} (MPa)	σ_{xx} (MPa)	σ_{yy} (MPa)	τ_{xy} (MPa)	σ_{xx} (MPa)	σ_{yy} (MPa)	τ_{xy} (MPa)	σ_{xx} (MPa)	σ_{yy} (MPa)	τ_{xy} (MPa)
G.P.1	-1.288,13	-169,33	-100,00	1.288,13	169,33	-100,00	1.134,45	30,75	-100,00	1.134,45	-30,75	-100,00	-1.004,23	-5,58	-100,00
G.P.2	-55,99	200,31	-24,33	2.520,27	538,97	-175,67	4,42	372,41	-122,01	2.273,32	310,92	-77,99	-5,88	293,92	-104,27
G.P.3	-555,97	50,32	-55,04	2.020,29	388,98	-144,96	-457,71	233,77	-113,08	1.811,19	172,28	-86,92	-410,99	172,39	-102,54
G.P.4	-2.520,27	-538,97	-175,67	55,99	-200,31	-24,33	-2.273,32	-310,92	-77,99	-4,42	-372,41	-122,01	-2.002,58	-305,09	-95,73
G.P.5	2.020,29	-388,98	-144,96	555,97	-50,32	-55,04	1.811,19	-172,28	-86,92	457,71	-233,77	-113,08	-1.597,47	-183,55	-97,46
G.P.6	-1.223,27	46,87	331,25	1.223,27	-46,87	331,25	-1.153,31	-32,13	298,61	1.153,31	32,13	298,61	-1.007,89	-17,79	249,42
G.P.7	8,87	416,51	406,92	2.455,41	322,77	255,58	-14,44	309,53	276,60	2.292,18	373,79	320,61	-9,54	281,72	245,15
G.P.8	-491,11	266,52	376,21	1.955,43	172,78	286,28	-476,57	170,89	285,53	1.830,05	235,15	311,68	-414,66	160,19	246,88
G.P.9	-2.455,41	-322,77	255,58	-8,87	-416,51	406,92	-2.292,18	-373,79	320,61	14,44	-309,53	276,60	-2.006,24	-317,29	253,69
G.P.10	-1.955,43	-172,78	286,28	491,11	-266,52	376,21	-1.830,05	-235,15	311,68	476,57	-170,89	285,53	-1.601,13	-195,76	251,96
G.P.11	-1.249,59	-40,86	156,26	1.249,59	40,86	156,26	-1.145,66	-6,62	136,86	1.145,66	6,62	136,86	-1.006,41	-12,83	107,63
G.P.12	-17,45	328,78	231,93	2.481,73	410,50	80,59	-6,79	335,05	114,85	2.284,53	348,28	158,86	-8,06	286,67	103,36
G.P.13	-517,43	178,79	201,22	1.981,17	260,51	111,29	-468,92	196,41	123,78	1.822,39	209,64	149,94	-413,17	165,14	105,10
G.P.14	-2.481,73	-410,50	80,59	17,45	-328,78	231,93	-2.284,53	-348,28	158,86	6,79	-335,05	114,85	-2.004,75	-312,34	111,90
G.P.15	1.981,75	-260,51	111,29	517,43	-178,79	201,22	1.822,39	-209,64	149,94	468,92	-196,41	123,78	-1.599,64	-190,81	110,17
G.P.16	-1.352,99	-385,53	-531,25	1.352,99	385,53	-531,25	-1.115,59	93,62	-498,61	1.115,59	-93,62	-498,61	-1.000,57	6,62	-449,42
G.P.17	-120,85	-15,89	-455,58	2.585,13	755,17	-606,92	23,28	435,28	-520,61	2.254,46	248,04	-476,60	-2,22	306,12	-453,69
G.P.18	-620,83	-165,88	-486,28	2.085,15	605,18	-576,21	-438,85	296,64	-511,68	1.792,32	109,40	-485,53	-407,33	184,59	-451,96
G.P.19	-2.585,13	-755,17	-606,92	120,85	15,89	-455,58	-2.254,46	-248,04	-476,60	-23,28	-435,28	-520,61	-1.998,92	-292,88	-445,15
G.P.20	-2.085,15	-605,18	-576,21	620,83	165,88	-486,28	-1.792,32	-109,40	-485,53	438,85	-296,64	-511,68	-1.593,81	-171,35	-446,88
G.P.21	-1.326,67	-297,80	-356,26	1.326,67	297,80	-356,26	-1.123,24	68,11	-336,86	1.123,24	-68,11	-336,86	-1.002,06	1,67	-307,63
G.P.22	-94,53	71,84	-280,59	2.558,81	667,44	-431,93	15,63	409,77	-358,86	2.262,11	273,56	-314,85	-3,71	301,17	-311,90
G.P.23	-594,51	-78,15	-311,29	2.058,83	517,45	-401,22	-446,50	271,13	-349,94	1.799,98	134,92	-323,78	-408,82	179,64	-310,17
G.P.24	-2.558,81	-667,44	-431,93	94,53	-71,84	-280,59	-2.262,11	-273,56	-314,85	-15,63	-409,77	-358,86	-2.000,40	-297,84	-303,36
G.P.25	-2.058,83	-517,45	-401,22	594,51	78,15	-311,29	-1.799,98	-134,92	-323,78	446,50	-271,13	-349,94	-1.595,29	-176,30	-305,10
max	8,87	416,51	406,92	2.585,13	755,17	406,92	23,28	435,28	320,61	2.292,18	373,79	320,61	-2,22	306,12	253,69
min	-2.585,13	-755,17	-606,92	-8,87	-416,51	-606,92	-2.292,18	-373,79	-520,61	-23,28	-435,28	-520,61	-2.006,24	-317,29	-453,69

Figure 2.49.a. Stress Field at Gauss Points.

Finite Elements 1-5.

	element 6			element 7			element 8			element 9			element 10		
	σ_{xx} (MPa)	σ_{yy} (MPa)	τ_{xy} (MPa)	σ_{xx} (MPa)	σ_{yy} (MPa)	τ_{xy} (MPa)	σ_{xx} (MPa)	σ_{yy} (MPa)	τ_{xy} (MPa)	σ_{xx} (MPa)	σ_{yy} (MPa)	τ_{xy} (MPa)	σ_{xx} (MPa)	σ_{yy} (MPa)	τ_{xy} (MPa)
G.P.1	1.004,23	5,58	-100,00	-869,75	1,01	-100,00	869,75	-1,01	-100,00	-736,05	-0,19	-100,00	736,05	0,19	-100,00
G.P.2	2.002,58	305,09	-95,73	-3,35	260,94	-107,49	1.736,16	258,91	-92,51	-3,15	219,68	-106,91	1.468,95	220,06	-93,09
G.P.3	1.597,47	183,55	-97,46	-354,92	155,47	-104,45	1.384,59	153,44	-95,55	-300,54	130,46	-104,11	1.171,55	130,84	-95,89
G.P.4	5,88	-293,92	-104,27	-1.736,16	-258,91	-92,51	3,35	-260,94	-107,49	-1.468,95	-260,06	-93,09	3,15	-219,68	-106,91
G.P.5	410,99	-172,39	-102,54	-1.384,59	-153,44	-95,55	354,92	-155,47	-104,45	-1.171,55	-130,84	-95,89	300,54	-130,46	-104,11
G.P.6	1.007,89	17,79	249,42	-876,17	-20,39	203,24	876,17	20,39	203,24	-741,97	-19,93	156,52	741,97	19,93	156,52
G.P.7	2.006,24	317,29	253,69	-9,77	239,53	195,75	1.742,58	280,31	210,73	-9,07	199,94	149,61	1.474,87	239,80	163,42
G.P.8	1.601,13	195,76	251,96	-361,34	134,06	198,79	1.391,01	174,84	207,69	-306,40	110,72	152,41	1.177,47	150,58	160,62
G.P.9	9,54	-281,72	245,15	-1.742,58	-280,31	210,73	9,77	-239,53	195,75	-1.474,87	-239,80	163,42	9,07	-199,94	149,61
G.P.10	414,66	-160,19	246,88	-1.391,01	-174,84	207,69	361,34	-134,06	198,79	-1.177,47	-150,58	160,62	306,47	-110,72	152,41
G.P.11	1.006,41	12,83	107,63	-873,57	-11,70	80,19	873,57	11,70	80,19	-739,57	-11,92	52,43	739,57	11,92	52,43
G.P.12	2.004,75	312,34	111,90	-7,16	248,22	72,70	1.739,97	271,62	87,68	-6,67	207,95	45,52	1.472,47	231,79	59,34
G.P.13	1.599,64	190,81	110,17	-358,73	142,75	75,74	1.388,40	166,15	84,64	-304,06	118,73	48,32	1.175,07	142,57	56,53
G.P.14	8,06	-286,67	103,36	-1.739,97	-271,62	87,68	7,16	-248,22	72,70	-1.472,47	-231,79	59,34	6,67	-207,95	45,52
G.P.15	413,17	-165,14	105,10	-1.388,40	-166,15	84,64	358,73	-142,75	75,74	-1.175,07	-142,57	56,53	304,06	-118,73	48,32
G.P.16	1.000,57	-6,62	-449,42	-863,33	22,42	-403,24	863,33	-22,42	-403,24	-730,13	19,55	-356,52	730,13	-19,55	-356,52
G.P.17	1.998,92	292,88	-445,15	3,07	282,34	-410,73	1.729,74	237,51	-395,75	2,78	239,42	-363,42	1.463,03	200,32	-349,61
G.P.18	1.593,81	171,35	-446,88	-348,50	176,87	-407,69	1.378,17	132,03	-398,79	-294,62	150,20	-360,62	1.165,63	111,10	-352,41
G.P.19	2,22	-306,12	-453,69	-1.729,74	-237,51	-395,75	-3,07	-282,34	-410,73	-1.463,03	-200,32	-349,61	-2,78	-239,42	-363,42
G.P.20	407,33	-184,59	-451,96	-1.378,17	-132,03	-398,79	348,50	-176,87	-407,69	1.165,63	-111,10	-352,41	294,62	-150,20	-360,62
G.P.21	1.002,06	-1,67	-307,63	-865,94	13,73	-280,19	865,94	-13,73	-280,19	-732,53	11,54	-252,43	732,53	-11,54	-252,43
G.P.22	2.000,40	297,84	-303,36	0,47	273,65	-287,68	1.732,34	246,19	-272,70	0,37	231,41	-259,34	1.465,43	208,33	-245,52
G.P.23	1.595,29	176,30	-305,10	-351,10	168,18	-284,64	1.380,77	140,72	-275,74	-297,03	142,19	-256,53	1.168,03	119,11	-248,32
G.P.24	3,71	-301,17	-311,90	-1.732,34	-246,19	-272,70	-0,47	-273,65	-287,68	-1.465,43	-208,33	-245,52	-0,37	-231,41</td	

Isogeometric Analysis

	element 11			element 12			element 13			element 14			element 15		
	σ_{xx} (MPa)	σ_{yy} (MPa)	τ_{xy} (MPa)	σ_{xx} (MPa)	σ_{yy} (MPa)	τ_{xy} (MPa)	σ_{xx} (MPa)	σ_{yy} (MPa)	τ_{xy} (MPa)	σ_{xx} (MPa)	σ_{yy} (MPa)	τ_{xy} (MPa)	σ_{xx} (MPa)	σ_{yy} (MPa)	τ_{xy} (MPa)
G.P.1	-602,20	0,06	-100,00	602,20	-0,06	-100,00	-468,40	-0,16	-100,00	468,40	0,16	-100,00	-334,48	0,84	-100,00
G.P.2	-2,51	179,97	-107,00	1.201,89	179,85	-93,00	-2,01	139,76	-107,07	934,78	140,07	-92,93	-1,15	100,84	-106,59
G.P.3	-245,85	106,97	-104,16	958,55	106,84	-95,84	-191,26	82,98	-104,20	745,53	83,30	-95,80	-136,41	60,26	-103,91
G.P.4	-1.201,89	-179,85	-93,00	2,51	-179,97	-107,00	-934,78	-140,07	-92,93	2,01	-139,76	-107,07	-667,80	-99,15	-93,41
G.P.5	-958,55	-106,84	-95,84	245,85	-106,97	-104,16	-745,53	-83,30	-95,80	191,26	-82,98	-104,20	-532,54	-58,58	-96,09
G.P.6	-608,20	-19,94	109,89	608,20	19,94	109,89	-474,46	-20,35	63,23	474,46	20,35	63,23	-340,12	-17,97	16,66
G.P.7	-8,51	159,97	102,89	1.207,89	199,84	116,89	-8,07	119,56	56,17	940,84	160,27	70,30	-6,80	82,03	10,08
G.P.8	-251,85	86,97	105,73	964,55	126,84	114,05	-197,32	62,79	59,03	751,59	103,49	67,43	-142,05	41,45	12,75
G.P.9	-1.207,89	-199,84	116,89	8,51	-159,97	102,89	-940,84	-160,27	70,30	8,07	-119,56	56,17	-673,44	-117,97	23,25
G.P.10	-964,55	-126,84	114,05	251,85	-86,97	105,73	-751,59	-103,49	67,43	197,32	-62,79	59,03	-538,19	-77,39	20,58
G.P.11	-605,77	-11,82	24,72	605,77	11,82	24,72	-472,00	-12,16	-3,00	472,00	12,16	-3,00	-337,83	-10,34	-30,68
G.P.12	-6,07	168,09	17,72	1.205,45	191,73	31,72	-5,61	127,76	-10,07	938,38	152,07	4,07	-4,51	89,66	-37,26
G.P.13	-249,42	95,08	20,56	962,11	118,73	28,88	-194,86	70,98	-7,20	749,13	95,30	1,20	-139,76	49,08	-34,59
G.P.14	-1.205,45	-191,73	31,72	6,07	-168,09	17,72	-938,38	-152,07	4,07	5,61	-127,76	-10,07	-671,15	-110,33	-24,09
G.P.15	-962,11	-118,73	28,88	249,42	-95,08	20,56	-749,13	-95,30	1,20	194,86	-70,98	-7,20	-535,90	-69,76	-26,76
G.P.16	-596,20	20,06	-309,89	596,20	-20,06	-309,89	-462,34	20,04	-263,24	462,34	-20,04	-263,24	-328,83	19,66	-216,66
G.P.17	3,49	199,97	-316,89	1.195,89	159,85	-302,89	4,04	159,95	-270,30	928,72	119,88	-256,17	4,49	119,66	-223,25
G.P.18	-239,85	126,96	-314,05	952,55	86,85	-305,73	-185,21	103,18	-267,43	739,47	63,11	-259,04	-130,76	79,08	-220,58
G.P.19	-1.195,89	-159,85	-302,89	-3,49	-199,97	-316,89	-928,72	-119,88	-256,17	-4,04	-159,95	-270,30	-662,15	-80,34	-210,08
G.P.20	-952,55	-86,85	-305,73	239,85	-126,96	-314,05	-739,47	-63,11	-259,04	185,21	-103,18	-267,43	-526,90	-39,76	-212,75
G.P.21	-598,64	11,94	-224,72	598,64	-11,94	-224,72	-464,80	11,84	-197,00	464,80	-11,84	-197,00	-331,12	12,02	-169,32
G.P.22	1,06	191,85	-231,72	1.198,33	167,96	-217,72	1,59	151,76	-204,07	931,18	128,08	-189,93	2,20	112,02	-175,91
G.P.23	-242,29	118,85	-228,88	954,98	94,96	-220,56	-187,66	94,98	-201,20	741,93	71,30	-192,80	-133,05	71,44	-173,24
G.P.24	1.198,33	-167,96	-217,72	-1,06	-191,85	-231,72	-931,18	-128,08	-189,93	-1,59	-151,76	-204,07	-664,44	-87,97	-162,74
G.P.25	-954,98	-94,96	-220,56	242,29	-118,85	-228,88	-741,93	-71,30	-192,80	187,66	-94,98	-201,20	-529,19	-47,40	-165,41
max	3,49	199,97	116,89	1.207,89	199,84	116,89	4,04	159,95	70,30	940,84	160,27	70,30	4,49	119,66	23,25
min	-1.207,89	-199,84	-316,89	-3,49	-199,97	-316,89	-940,84	-160,27	-270,30	-4,04	-159,95	-270,30	-673,44	-117,97	-223,25

Figure 2.49.c. Stress Field at Gauss Points.

Finite Elements 11-15.

	element 16			element 17			element 18			element 19			element 20		
	σ_{xx} (MPa)	σ_{yy} (MPa)	τ_{xy} (MPa)	σ_{xx} (MPa)	σ_{yy} (MPa)	τ_{xy} (MPa)	σ_{xx} (MPa)	σ_{yy} (MPa)	τ_{xy} (MPa)	σ_{xx} (MPa)	σ_{yy} (MPa)	τ_{xy} (MPa)	σ_{xx} (MPa)	σ_{yy} (MPa)	τ_{xy} (MPa)
G.P.1	334,48	-0,84	-100,00	-201,20	-4,64	-100,00	201,20	4,64	-100,00	-64,37	25,56	-100,00	64,37	-25,56	-100,00
G.P.2	667,80	99,15	-93,41	-2,23	55,05	-109,26	400,16	64,33	-90,74	7,36	47,08	-94,52	136,11	-4,04	-105,48
G.P.3	532,54	58,58	-96,09	-82,97	30,83	-105,50	319,43	40,11	-94,50	-21,75	38,35	-96,74	107,00	-12,77	-103,26
G.P.4	1,15	-100,84	-106,59	-400,16	-64,33	-90,74	2,23	-55,05	-109,26	-136,11	4,04	-105,48	-7,36	-47,08	-94,52
G.P.5	136,41	-60,26	-103,91	-319,43	-40,11	-94,50	82,97	-30,83	-105,50	-107,00	12,77	-103,26	21,75	-38,35	-96,74
G.P.6	340,12	17,97	16,66	-209,13	-31,10	-30,36	209,13	31,10	-30,36	-59,68	41,22	-74,89	59,68	-41,22	-74,89
G.P.7	673,44	117,97	23,25	-10,17	28,59	-39,62	408,10	90,79	-21,10	12,06	62,74	-69,41	131,42	-19,69	-80,37
G.P.8	538,19	77,39	20,58	-90,91	4,37	-35,87	327,36	66,57	-24,86	-17,05	54,00	-71,63	102,31	-28,43	-78,15
G.P.9	6,80	-82,03	10,08	-408,10	-90,79	-21,10	10,17	-28,59	-39,62	-131,42	19,69	-80,37	-12,06	-62,74	-69,41
G.P.10	142,05	-41,45	12,75	-327,36	-66,57	-24,86	90,91	-4,37	-35,87	-102,31	28,43	-78,15	17,05	-54,00	-71,63
G.P.11	337,83	10,34	-30,68	-205,91	-20,36	-58,62	205,91	20,36	-58,62	-61,58	34,86	-85,08	61,58	-34,86	-85,08
G.P.12	671,15	110,33	-24,09	-6,95	39,32	-67,88	404,88	80,05	-49,36	10,16	56,38	-79,60	133,32	-13,34	-90,56
G.P.13	535,90	69,76	-26,76	-87,68	15,10	-64,12	324,14	55,83	-53,12	-18,95	47,65	-81,82	104,21	-22,07	-88,34
G.P.14	4,51	-89,66	-37,26	-404,88	-80,05	-49,36	6,95	-39,32	-67,88	-133,32	13,34	-90,56	-10,16	-56,38	-79,60
G.P.15	139,76	-49,08	-34,59	-324,14	-55,83	-53,12	87,68	-15,10	-64,12	-104,21	22,07	-88,34	18,95	-47,65	-81,82
G.P.16	328,83	-19,66	-216,66	-193,26	21,82	-169,64	193,26	-21,82	-169,64	-69,07	9,90	-125,11	69,07	-9,90	-125,11
G.P.17	662,15	80,34	-210,08	5,71	81,51	-178,90	392,22	37,87	-160,38	2,67	31,42	-119,63	140,81	11,62	-130,59
G.P.18	526,90	39,76	-212,75	-75,03	57,29	-175,14	311,49	13,65	-164,13	-26,44	22,69	-121,85	111,70	2,89	-128,37
G.P.19	-4,49	-119,66	-223,25	-392,22	-37,87	-160,38	-5,71	-81,51	-178,90	-140,81	-11,62	-130,59	-2,67	-31,42	-119,63
G.P.20	130,76	-79,08	-220,58	-311,49	-13,65	-164,13	75,03	-57,29	-175,14	-111,70	-2,89	-128,37	26,44	-22,69	-121,85
G.P.21	331,12	-12,02	-169,32	-196,48	11,08	-141,38	196,48	-11,08	-141,38	-67,17	16,25	-114,92	67,17	-16,25	-114,92
G.P.22	664,44	87,97	-162,74	2,49	70,77	-150,64	395,44	48,61	-132,12	4,57	37,77	-109,44	138,91	5,27	-120,40
G.P.23	529,19	47,40	-165,41	-78,25	46,55	-146,88	314,71	24,39	-135,88	-24,54	29,04	-111,66	109,80	-3,46	-118,18
G.P.24	-2,20	-112,02	-175,91	-395,44	-48,61	-132,12	-2,49	-70,77	-150,64	-138,91	-5,27	-120,40	-4,57	-37,77	-109,44
G.P.25	133,05	-71,44	-173,24	-314,71	-24,39	-135,88	78,25	-46,55	-146,88	-109,80	3,46	-118,18	24,54	-29,04	-111,66
max	673,44	117,97	23,25	5,71	81,51	-21,10	408,10	90,79	-21,10	12,06	62,74	-69,41	140,81	11,62	-69,41
min	-4,49	-119,66	-223,25	-408,10	-90,79	-178,90	-5,71	-81,51	-178,90	-140,81	-11,62	-130,			

		(Element, G.P.)	
σ_{xx} (MPa)	max	(3,17), (4,17)	2.585,13
	min	(1,19), (2,19)	-2.585,13
σ_{yy} (MPa)	max	(3,17), (4,17)	755,17
	min	(1,19), (2,19)	-755,17
τ_{xy} (MPa)	max	(1,7), (2,7), (3,9), (4,9)	406,92
	min	(1,19), (2,19), (3,17), (4,17)	-606,92

Figure 2.50. Maximum and Minimum Stress.

Figure 2.49 depicts stresses at Finite Elements' Gauss Points, while Figure 2.50 shows maximum and minimum stress.

As expected (just like IGA showed), elements 1 and 2 (nearest to fixed boundary) suffer from larger stresses. It is a cantilever under concentrated load $P=3.000$ kN at free edge, so the upper horizontal side suffers from tension and the lower horizontal side suffers from compression. Maximum bending moment occurs at fixed edge.

$$M_{\max} = -P \cdot L = -3.000 \text{ kN} \cdot 15 \text{ m} = -45.000 \text{ kNm}$$

Element 2 (G.P.17, nearest to upper horizontal side) experience the largest tension. Tensile stresses are equal to:

$$\max \sigma_{xx}^+ = 2.585,13 \text{ MPa}$$

$$\max \sigma_{yy}^+ = 755,17 \text{ MPa}$$

Element 1 (G.P.19, nearest to lower horizontal side) experience the largest compression. Compressive stresses are equal to:

$$\max \sigma_{xx}^- = -2.585,13 \text{ MPa}$$

$$\max \sigma_{yy}^- = -755,17 \text{ MPa}$$

2.2.3. Comparison

Comparing two methods' results, I will reach interesting conclusions.

- IsoGeometric Analysis (IGA)

Method	IGA
Patches	1
Isogeometric Elements (Ξ_H)	20
Horizontal Spans (Ξ)	10
Vertical Spans (H)	2
Control Points	33
Control Points (Ξ)	11
Control Points (H)	3
p	1
q	1
Gauss Points	5x5

Figure 2.51.a. Analysis Parameters. IGA.

- Finite Element Analysis (FEA)

Method	FEA
Finite Elements (Number)	20
Finite Elements (Type)	2D
	4-sided
	4-noded
	isoparametric
Gauss Points	5x5

Figure 2.51.b. Analysis Parameters. FEA.

Particularly, I will compare:

- B-SPLine Functions (IGA) with Shape Functions (FEA).
- Control Net (IGA) with Node Net (FEA).
- Parameter Space (Mesh).
- Physical Space (Mesh).
- Total Stiffness Matrix.
- Control Points' Displacements (IGA) with Nodes' Displacements (FEA).
- Stress Field at Gauss Points.

Shape Functions

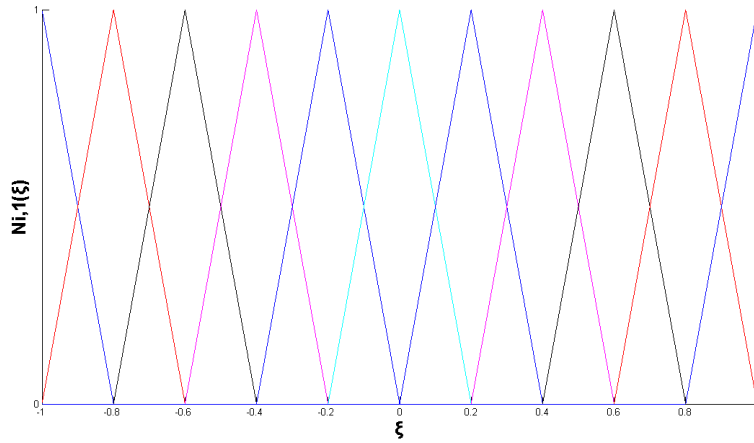


Figure 2.52.a. Linear Basis SPLine Functions for open, uniform knot vector
 $\Xi = \{-1, -1, -0.8, -0.6, -0.4, -0.2, 0, 0.2, 0.4, 0.6, 0.8, 1, 1\}$.

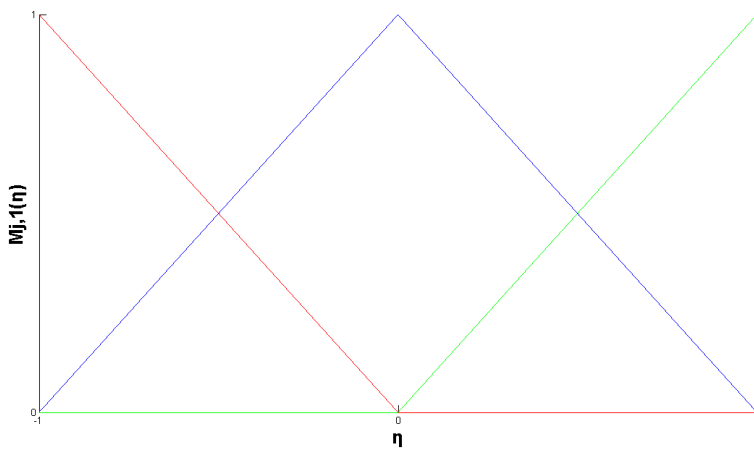


Figure 2.52.b. Linear Basis SPLine Functions for open, uniform knot vector
 $H = \{-1, -1, 0, 1, 1\}$.

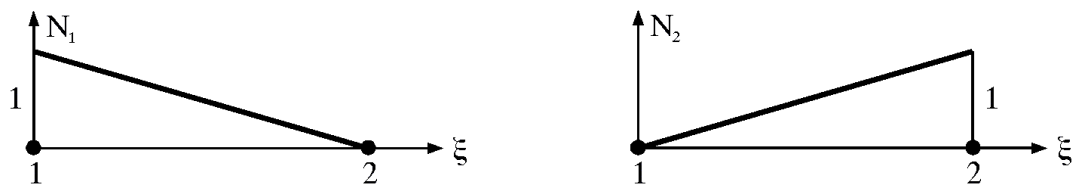


Figure 2.52.c. Shape Functions. Isoparametric 2-Noded Truss Finite Element.

For $p=1$, IGA's B-SPLine Functions are exactly the same with FEA's Shape Functions.

Control/ Node Net

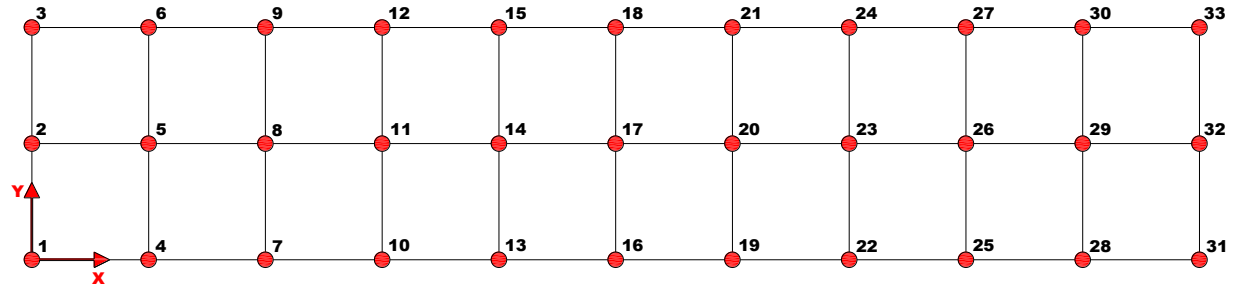


Figure 2.53.a. Control Net. Physical space.

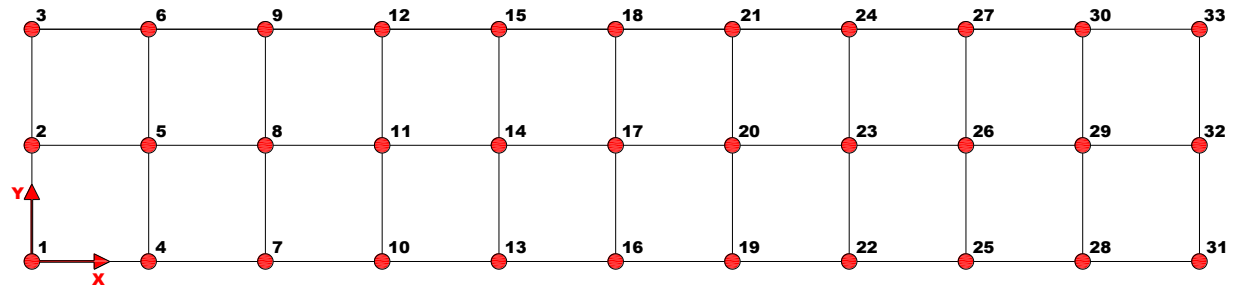


Figure 2.53.b. Node Net. Physical Space.

I choose as many Nodes as Control Points in order to have the same number of Degrees of Freedom. They have the same geometric features.

Parameter Space

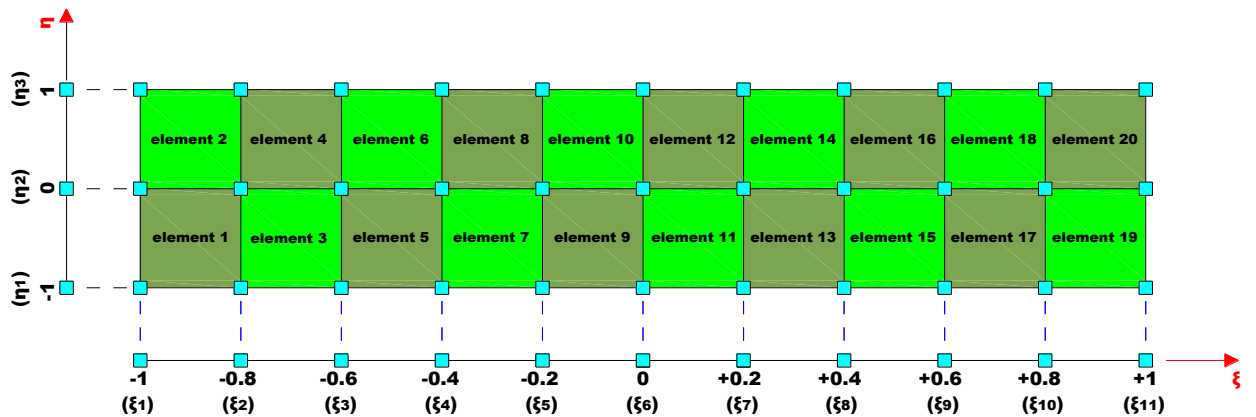
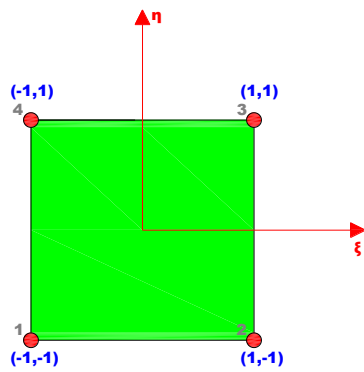


Figure 2.54.a. Isogeometric Elements' Mesh. Parameter Space.



**Figure 2.54.b. Isoparametric 2D 4-sided 4-noded Finite Element.
Parameter Space. Local Numbering.**

In classical Finite Element Analysis (FEA), the parameter space ("reference/ parent element") is local to individual elements and is mapped into a single element in the physical space. Each finite element has its own mapping from the reference element.

In Isogeometric Analysis (IGA), the B-SPLine parameter space is local to the entire patch rather than element. The B-SPLine mapping (a single map) takes a patch of multiple elements in the parameter space into the physical space, but the mapping itself is global to the whole patch, rather than to the elements.

Physical Space

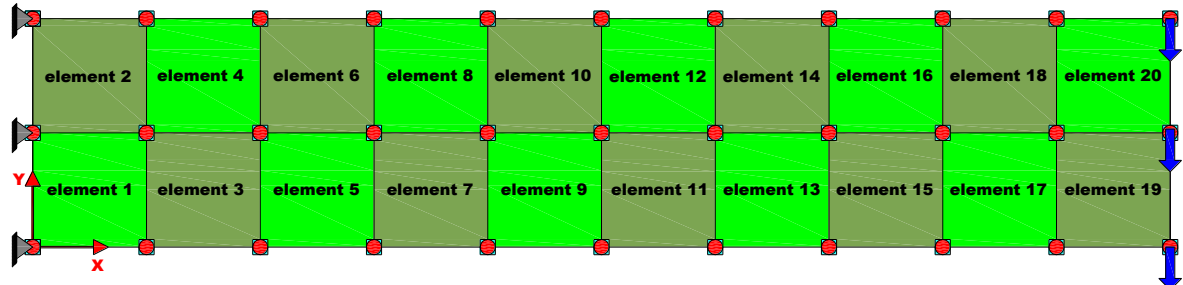


Figure 2.55.a. Physical Space. Mesh. Knots and Control Points.

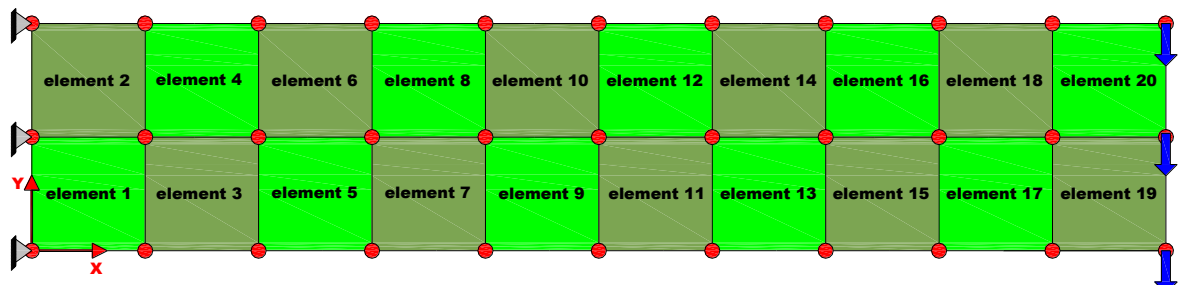


Figure 2.55.b. Physical Space. Mesh. Nodes.

Figure 2.55.a. shows both knots (cyan rhombi) and control points (red circles) in the physical space. We observe that knots coincide with control points. There are as many knots as control points. That is why the Basis SPLine functions are linear ($p=1, K=2$).

Figure 2.55.b. shows nodes (red circles) in the physical space. We observe that Finite Element Mesh is exactly the same with Isogeometric Element Mesh. The reason is that:

1. the Basis SPLine Functions (IGA) and Shape Functions (FEA) are linear and exactly the same.
2. I have chosen Node Net exactly the same with Control Net, means that Control Points and Nodes have exactly the same geometric features.

It is important to mention that Nodes partition structure into Finite Elements and Knots (and not Control Points) partition structure into Isogeometric Elements.

Total Stiffness Matrix [K]

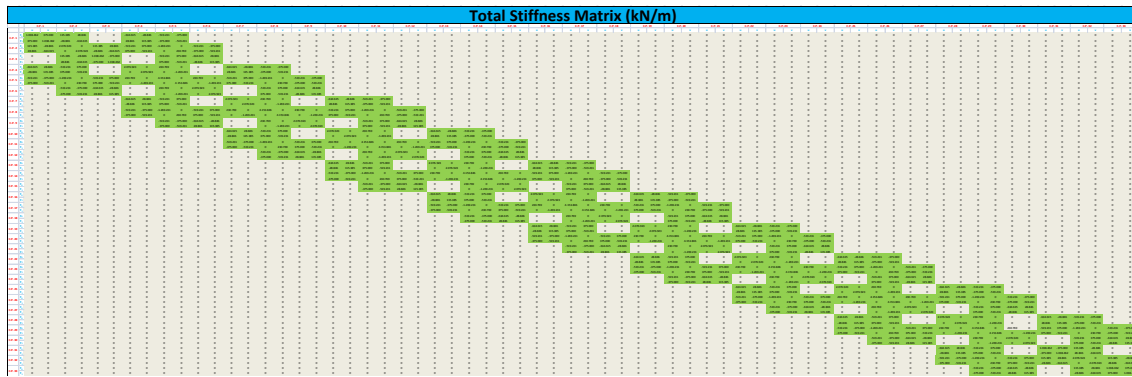


Figure 2.56.a. Total Stiffness Matrix. (66x66). IGA.

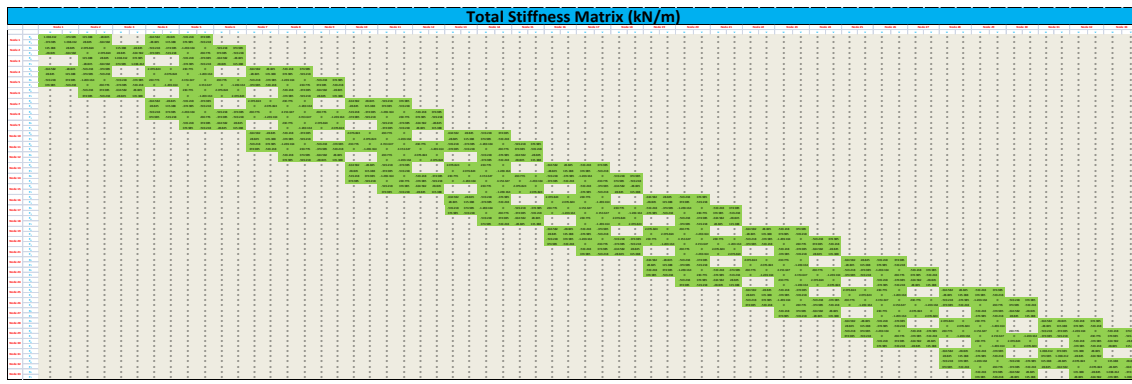


Figure 2.56.b. Total Stiffness Matrix. (66x66). FEA.

We can see that the two matrices are exactly the same, as expected. The reason is that:

3. the Basis SPLine Functions (IGA) and Shape Functions (FEA) are linear and exactly the same.
4. I choose Node Net exactly the same with Control Net, means that Control Points and Nodes have exactly the same geometric features.

C.P./ Nodes' Displacements {U}

	horizontal u (cm)	vertical v (cm)		horizontal u (cm)	vertical v (cm)
C.P.	Node				
C.P. 1	Node 1	0,0	0,0	0,0	0,0
C.P. 2	Node 2	0,0	0,0	0,0	0,0
C.P. 3	Node 3	0,0	0,0	0,0	0,0
C.P. 4	Node 4	-1,8	-1,2	-1,8	-1,2
C.P. 5	Node 5	0,0	-0,9	0,0	-0,9
C.P. 6	Node 6	1,8	-1,2	1,8	-1,2
C.P. 7	Node 7	-3,4	-4,0	-3,4	-4,0
C.P. 8	Node 8	0,0	-3,7	0,0	-3,7
C.P. 9	Node 9	3,4	-4,0	3,4	-4,0
C.P. 10	Node 10	-4,8	-8,2	-4,8	-8,2
C.P. 11	Node 11	0,0	-8,0	0,0	-8,0
C.P. 12	Node 12	4,8	-8,2	4,8	-8,2
C.P. 13	Node 13	-6,1	-13,9	-6,1	-13,9
C.P. 14	Node 14	0,0	-13,7	0,0	-13,7
C.P. 15	Node 15	6,1	-13,9	6,1	-13,9
C.P. 16	Node 16	-7,1	-20,6	-7,1	-20,6
C.P. 17	Node 17	0,0	-20,5	0,0	-20,5
C.P. 18	Node 18	7,1	-20,6	7,1	-20,6
C.P. 19	Node 19	-8,0	-28,4	-8,0	-28,4
C.P. 20	Node 20	0,0	-28,3	0,0	-28,3
C.P. 21	Node 21	8,0	-28,4	8,0	-28,4
C.P. 22	Node 22	-8,7	-36,9	-8,7	-36,9
C.P. 23	Node 23	0,0	-36,8	0,0	-36,8
C.P. 24	Node 24	8,7	-36,9	8,7	-36,9
C.P. 25	Node 25	-9,1	-45,9	-9,1	-45,9
C.P. 26	Node 26	0,0	-45,9	0,0	-45,9
C.P. 27	Node 27	9,1	-45,9	9,1	-45,9
C.P. 28	Node 28	-9,4	-55,4	-9,4	-55,4
C.P. 29	Node 29	0,0	-55,4	0,0	-55,4
C.P. 30	Node 30	9,4	-55,4	9,4	-55,4
C.P. 31	Node 31	-9,5	-65,1	-9,5	-65,1
C.P. 32	Node 32	0,0	-65,0	0,0	-65,0
C.P. 33	Node 33	9,5	-65,1	9,5	-65,1
max		9,5	0,0	max	9,5
min		-9,5	-65,1	min	-9,5

Figure 2.57. Control Points', Nodes' displacements.

They are exactly the same, as expected.

Isogeometric Analysis

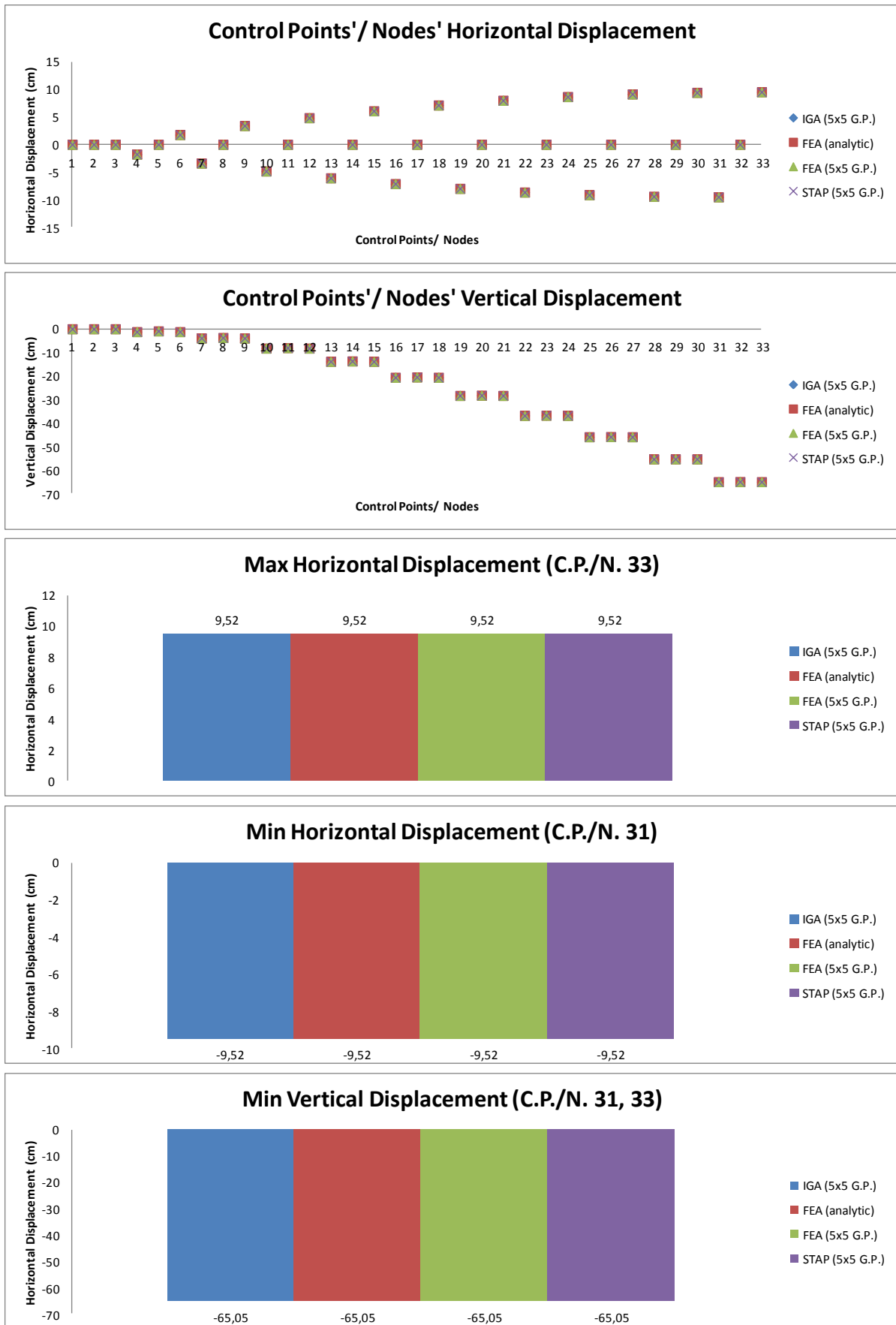


Figure 2.58. Comparison. IGA. FEA (CantiFEA/analytic and quadrature. STAP).

Stress Field at Gauss Points

		(Isogeometric Element, G.P.)	
		max	min
σ_{xx} (MPa)	max	(2,17)	2.585,13
	min	(1,19)	-2.585,13
σ_{yy} (MPa)	max	(2,17)	755,17
	min	(1,19)	-755,17
τ_{xy} (MPa)	max	(1,7), (2,9)	406,92
	min	(1,19), (2,17)	-606,92

Figure 2.58.a. Maximum and Minimum Stress. IGA.

		(Finite Element, G.P.)	
		max	min
σ_{xx} (MPa)	max	(2,17)	2.585,13
	min	(1,19)	-2.585,13
σ_{yy} (MPa)	max	(2,17)	755,17
	min	(1,19)	-755,17
τ_{xy} (MPa)	max	(1,7), (2,9)	406,92
	min	(1,19), (2,17)	-606,92

Figure 2.58.b. Maximum and Minimum Stress. FEA.

They are exactly the same, as expected.

2.3 Control Points/ Nodes: 33 & Shape Functions: Quadratic.

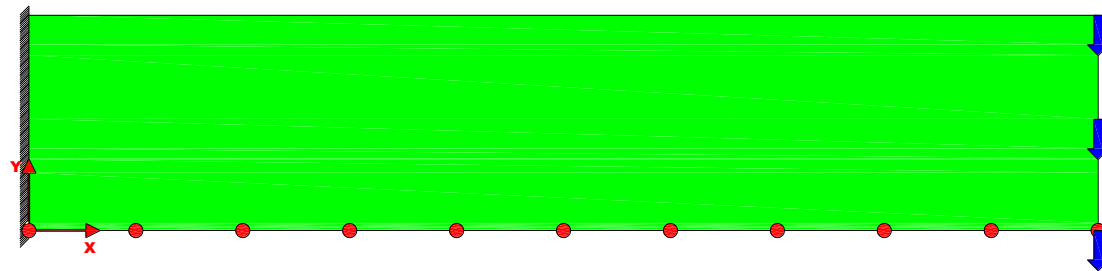
2.3.1. Isogeometric Analysis

I use the following analysis parameters:

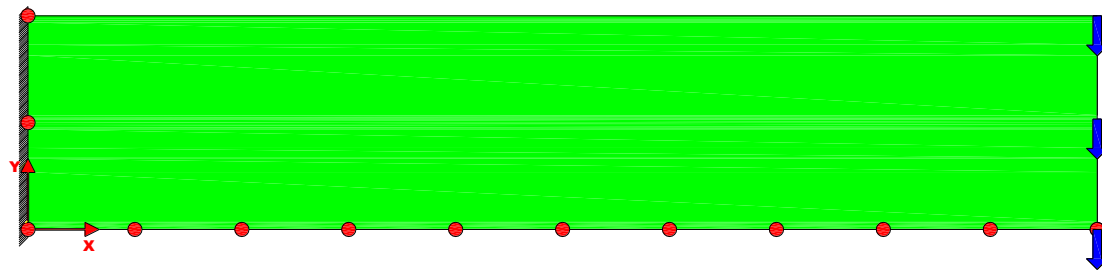
- The parametric axis ξ (parameter space) is parallel to cantilever's length (physical space), means horizontal. Its direction is from left to right.
- The parametric axis η (parameter space) is parallel to cantilever's height (physical space), means vertical. Its direction is from bottom to cantilever's top.
- $n \cdot m = 33$ control points. There are 3 ($m=3$ for axis η) groups of 11 ($n=11$ for axis ξ) control points equally spaced across cantilever's length in three different distances from its bottom. It is important to underline that number of control points (C.P.) is equal to B-Spline's number. Cartesian coordinate system's origin is the extreme left and bottom corner.
- $p=q=2$. I choose quadratic Basis SPLine functions ($p=2$ Hughes, $K=p+2=1+2=3$ Fisher).

Method	IGA
Patches	1
Isogeometric Elements ($\Xi \times H$)	9
Horizontal Spans (Ξ)	9
Vertical Spans (H)	1
Control Points	33
Control Points (Ξ)	11
Control Points (H)	3
p	2
q	2
Gauss Points	5x5

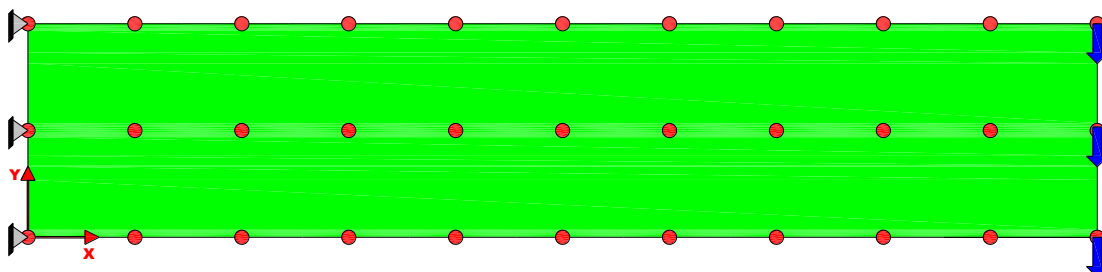
Figure 2.59.a. Analysis Parameters. IGA.



n=11 Control Points (Ξ)



n=11 Control Points (Ξ)
m=3 Control Points (H)



n=11 Control Points (Ξ)
m=3 Control Points (H)
n•m=11•3=33 Control Points ($\Xi \times H$)

Figure 2.59.b Cantilever Profile (Cartesian Axes. Control Points.)

Axis ξ

Basis SPLine functions

The axis ξ is parallel to cantilever's horizontal side (length).

- $n=11$ (control points).
- $p=2$ (quadratic Basis SPLine functions, 3 control points per horizontal span).
- $n+p+1=11+2+1=14$ knot values.

The open uniform knot vector Ξ contains the following knot values:

- The extreme knots $-1, 1$ repeated $p+1=2+1=3$ times $\rightarrow 6$ knot values. Remaining, not recurrent: $14-6=8$ knot values $\rightarrow 8+2=10$ knots. \rightarrow I will separate the interval $[-1, 1]$ into $10-1=9$ equal spans. Notice that spans' number is equal to $n-p=11-2=9$.

$$\frac{1 - -1}{9} = \frac{2}{9}$$

$$\Xi = \left\{ -1, -1, -1, -\frac{7}{9}, -\frac{5}{9}, -\frac{3}{9}, -\frac{1}{9}, \frac{1}{9}, \frac{3}{9}, \frac{5}{9}, \frac{7}{9}, 1, 1, 1 \right\}$$

The corresponding quadratic Basis SPLine functions to knot vector Ξ are 10 (one for every control point). The support of each quadratic B-SPLine is three spans.

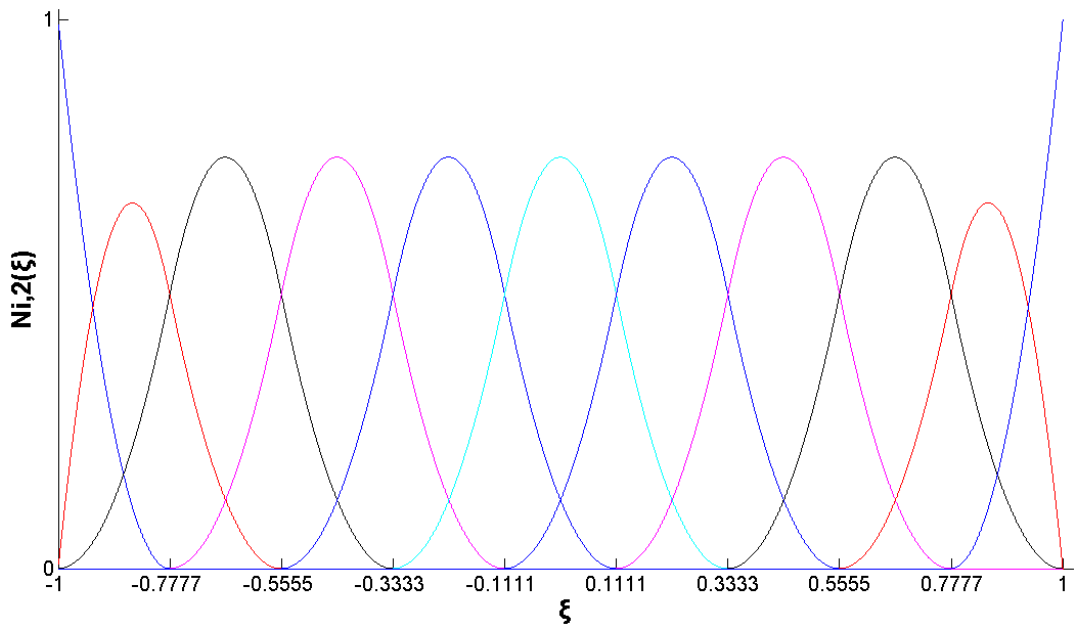


Figure 2.60. Quadratic Basis SPLine functions for open, uniform knot vector $\Xi=\{-1,-1,-1,-0.7777,-0.5555,-0.3333,-0.1111,0.1111,0.3333,0.5555,0.7777,1,1,1\}$.

Gauss Points (coordinates, weight factors)

I use 5 Gauss Points for every horizontal span.

Number of points, n	Points, x_i	Weights, w_i
1	0	2
2	$\pm 1/\sqrt{3}$	1
	0	$\frac{5}{9}$
3	$\pm \sqrt{3/5}$	$\frac{5}{9}$
	$\pm \sqrt{(3 - 2\sqrt{6/5})/7}$	$\frac{18 + \sqrt{30}}{36}$
4	$\pm \sqrt{(3 + 2\sqrt{6/5})/7}$	$\frac{18 - \sqrt{30}}{36}$
	0	$\frac{128}{225}$
	$\pm \frac{1}{3} \sqrt{5 - 2\sqrt{10}/7}$	$\frac{322 + 13\sqrt{70}}{900}$
5	$\pm \frac{1}{3} \sqrt{5 + 2\sqrt{10}/7}$	$\frac{322 - 13\sqrt{70}}{900}$

Figure 2.61. Gauss Points' coordinate and weight factor.

Each point's coordinate and weight factor is equal to (local numbering, span [-1,1]):

G.P.	ξ'_i	w_i
4	-0.90617	0.23692
5	-0.53846	0.47862
1	0	0.56888
3	0.53846	0.47862
2	0.90617	0.23692

Notice that:

$$\sum_{i=1}^5 w_i = 2$$

I use 5 Gauss Points for every horizontal span. The horizontal interval [-1,1] has 9 spans, so $9 \cdot 5 = 45$ G.P. These points are shown as yellow rhombi in Figure 2.62, while knots as cyan circles.

I assume a local ξ for every span with its center in the span's middle. Then, from Gauss Points' local coordinates ξ'_i , I calculate the global ones ξ_i . Let's calculate the coordinate ξ_i of G.P. 2 for span 1 (extreme left span).

$$\frac{\xi'_{G.P.2} - -1}{1 - -1} = \frac{\xi_{G.P.2} - -1}{-0.7777 - -1} \Rightarrow \frac{0.9062 + 1}{1 + 1} = \frac{\xi_{G.P.2} + 1}{-0.7777 + 1} \Rightarrow$$

$$\frac{1.9062}{2} = \frac{\xi_{G.P.2} + 1}{0.2223} \Rightarrow \xi_{G.P.2} = \frac{1.9062}{2} \cdot 0.2222 - 1 \Rightarrow$$

$$\boxed{\xi_{G.P.2} = -0.7882}$$

Generally, the coordinate ξ_j of Gauss Point j in the span (ξ_i, ξ_{i+1}) is equal to:

$$\frac{\xi'_{G.P.j} - -1}{1 - -1} = \frac{\xi_{G.P.j} - \xi_i}{\xi_{i+1} - \xi_i} \Rightarrow \frac{\xi'_{G.P.j} + 1}{2} = \frac{\xi_{G.P.j} - \xi_i}{\xi_{i+1} - \xi_i} \Rightarrow$$

$$\xi_{G.P.j} = \frac{\xi'_{G.P.j} + 1}{2} \cdot \xi_{i+1} - \xi_i + \xi_i = \xi'_{G.P.j} \cdot \frac{\xi_{i+1} - \xi_i}{2} + \frac{\xi_{i+1} - \xi_i}{2} + \frac{2 \cdot \xi_i}{2} \Rightarrow$$

$$\boxed{\xi_{G.P.j} = \xi'_{G.P.j} \cdot \frac{\xi_{i+1} - \xi_i}{2} + \frac{\xi_{i+1} + \xi_i}{2}}$$

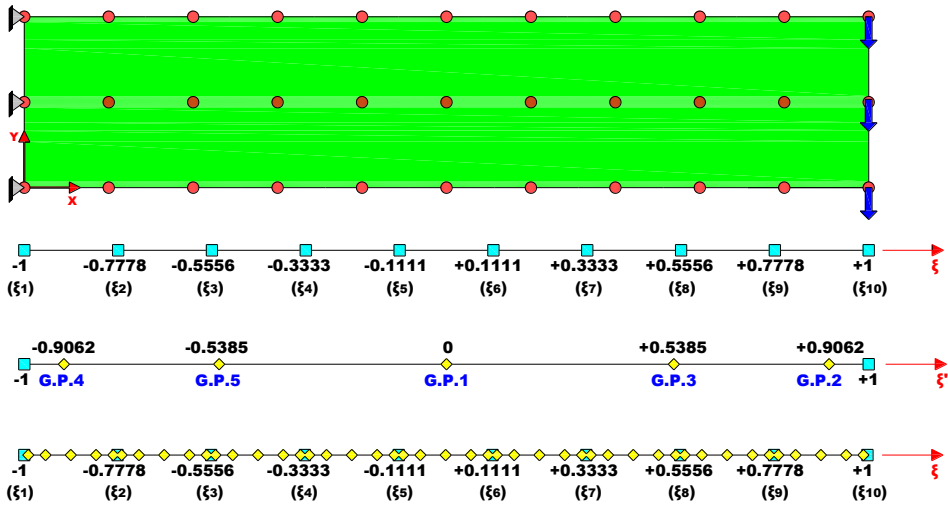


Figure 2.62. Gauss Points (parametric axis ξ).

B-SPLines' value at Gauss Points

I calculate the quadratic B-Spline functions' ($N_{i,2}(\xi)$) values ($p=2, K=3$) at the position ξ_i of 45 Gauss Points in horizontal parametric axis ξ and their corresponding first derivatives

$$N'_{i,2}(\xi) = \frac{\partial N_{i,2}}{\partial \xi}.$$

Isogeometric Analysis

Figure 2.63 shows respectively constant ($p=0$, $K=1$), linear ($p=1$, $K=2$), quadratic ($p=2$, $K=3$) BSPLines' values for the horizontal interval $[-1, 1]$ (axis ξ).

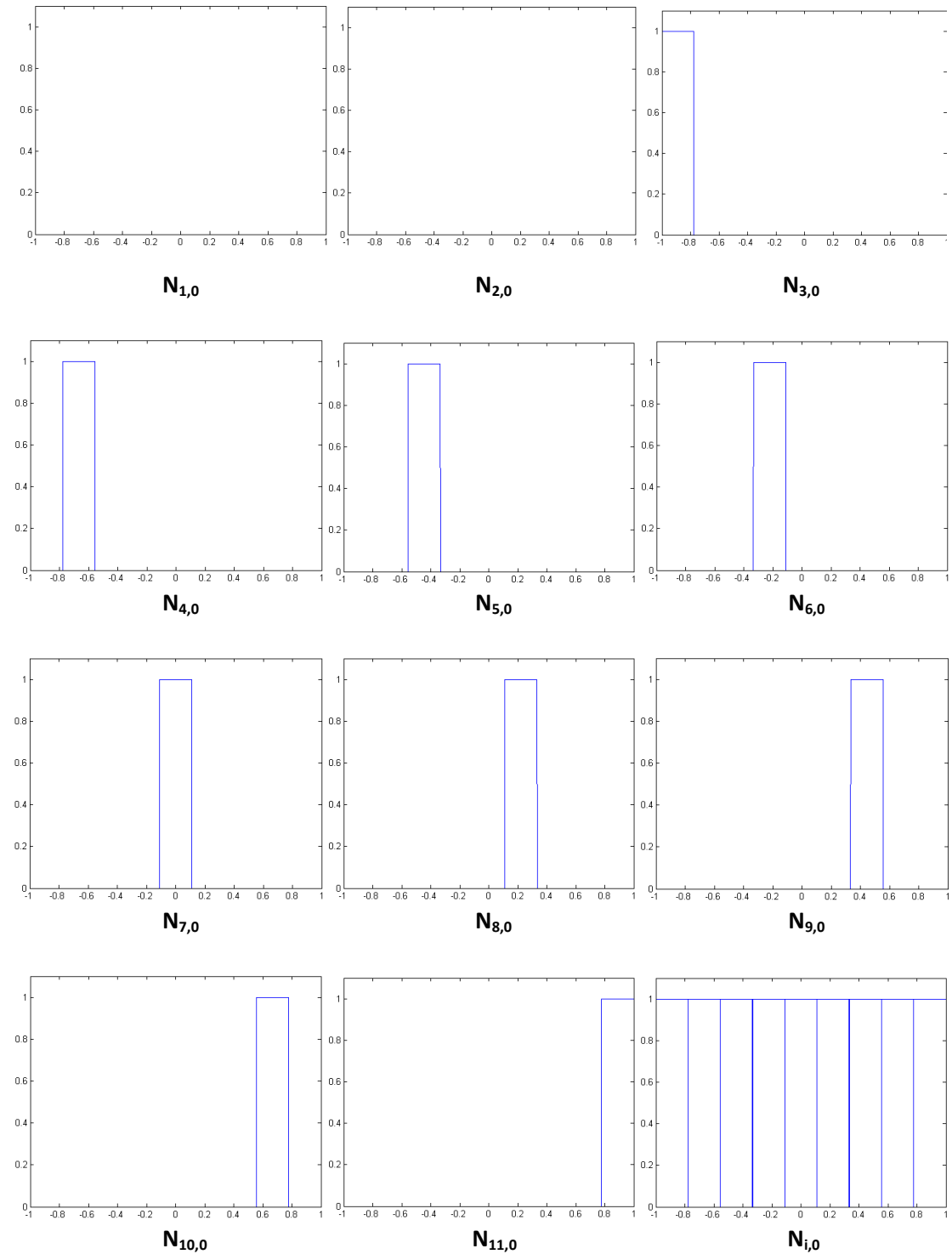


Figure 2.63.a. B-SPLines (Constant, $p=0$, $K=1$) (Ξ)

Isogeometric Analysis

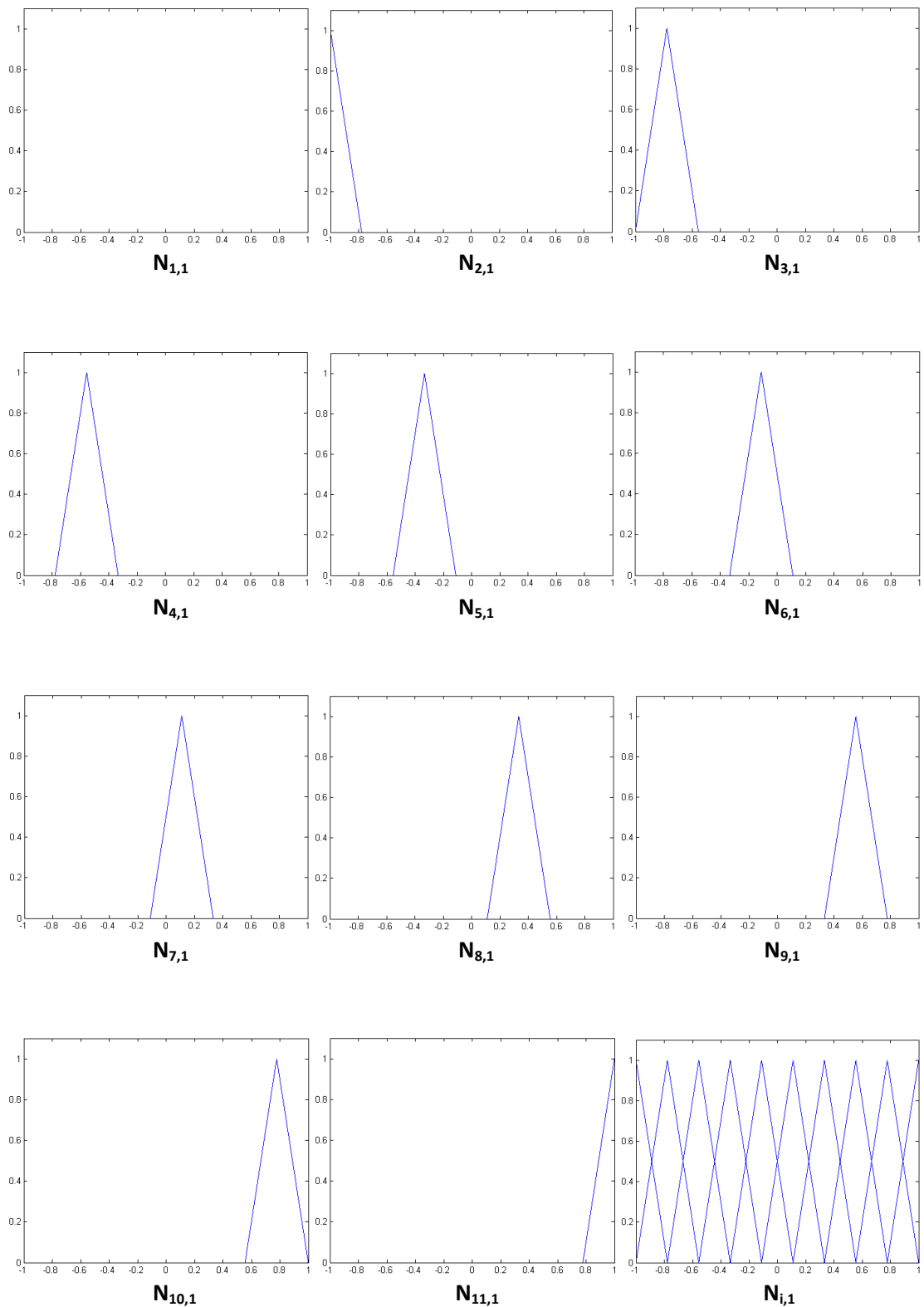


Figure 2.63.b. B-SPLines (Linear, p=1, K=2) (Ξ)

Isogeometric Analysis

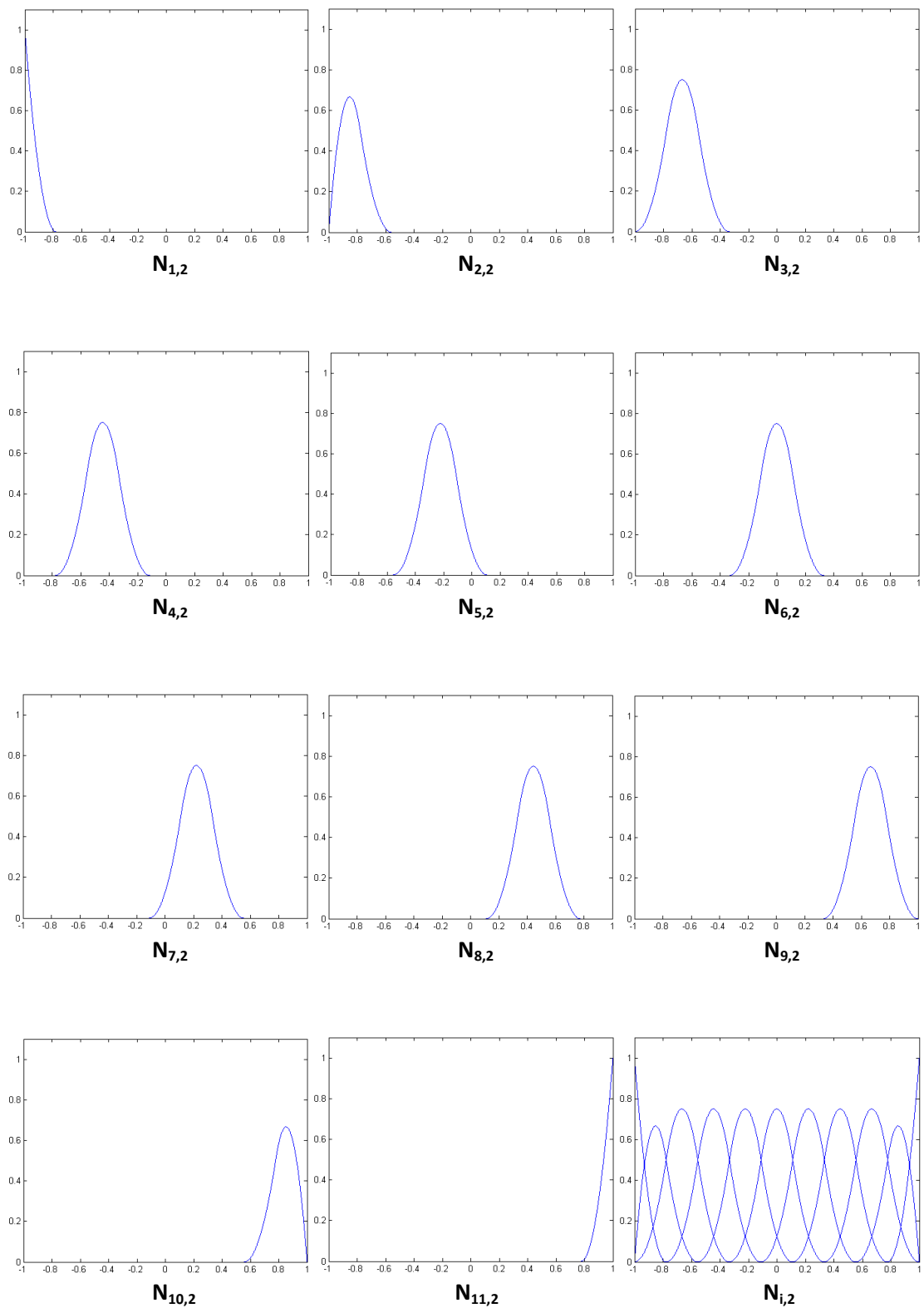


Figure 2.63.c. B-SPLines (Quadratic, p=2, K=3) (Ξ)

Isogeometric Analysis

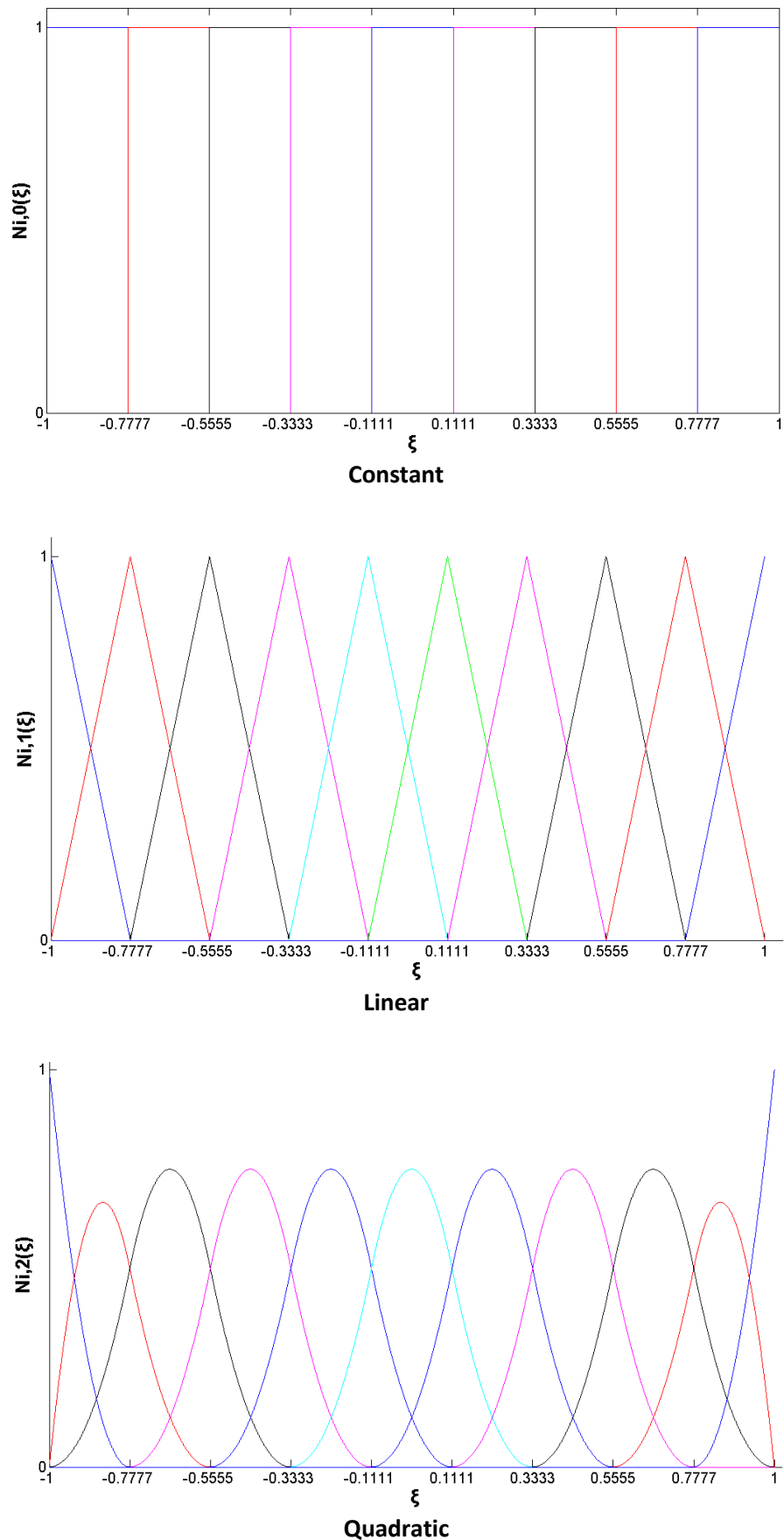


Figure 2.63.d. BSPLines (Ξ)

$N_{i,2}(\xi)$ (3x5,p=2)	axis ξ				
horizontal span 1					
$N_{1,2}(\xi)$	G.P.1 (1)	G.P.2 (2)	G.P.3 (3)	G.P.4 (4)	G.P.5 (5)
0,2500	0,0022	0,0533	0,9084	0,5917	
$N_{2,2}(\xi)$	0,6250	0,5436	0,6509	0,0905	0,3817
$N_{3,2}(\xi)$	0,1250	0,4542	0,2959	0,0011	0,0266
horizontal span 2					
	G.P.6 (1)	G.P.7 (2)	G.P.8 (3)	G.P.9 (4)	G.P.10 (5)
$N_{2,2}(\xi)$	0,1250	0,0011	0,0266	0,4542	0,2959
$N_{3,2}(\xi)$	0,7500	0,5447	0,6775	0,5447	0,6775
$N_{4,2}(\xi)$	0,1250	0,4542	0,2959	0,0011	0,0266
horizontal span 3					
	G.P.11 (1)	G.P.12 (2)	G.P.13 (3)	G.P.14 (4)	G.P.15 (5)
$N_{3,2}(\xi)$	0,1250	0,0011	0,0266	0,4542	0,2959
$N_{4,2}(\xi)$	0,7500	0,5447	0,6775	0,5447	0,6775
$N_{5,2}(\xi)$	0,1250	0,4542	0,2959	0,0011	0,0266
horizontal span 4					
	G.P.16 (1)	G.P.17 (2)	G.P.18 (3)	G.P.19 (4)	G.P.20 (5)
$N_{4,2}(\xi)$	0,1250	0,0011	0,0266	0,4542	0,2959
$N_{5,2}(\xi)$	0,7500	0,5447	0,6775	0,5447	0,6775
$N_{6,2}(\xi)$	0,1250	0,4542	0,2959	0,0011	0,0266
horizontal span 5					
	G.P.21 (1)	G.P.22 (2)	G.P.23 (3)	G.P.24 (4)	G.P.25 (5)
$N_{5,2}(\xi)$	0,1250	0,0011	0,0266	0,4542	0,2959
$N_{6,2}(\xi)$	0,7500	0,5447	0,6775	0,5447	0,6775
$N_{7,2}(\xi)$	0,1250	0,4542	0,2959	0,0011	0,0266
horizontal span 6					
	G.P.26 (1)	G.P.27 (2)	G.P.28 (3)	G.P.29 (4)	G.P.30 (5)
$N_{6,2}(\xi)$	0,1250	0,0011	0,0266	0,4542	0,2959
$N_{7,2}(\xi)$	0,7500	0,5447	0,6775	0,5447	0,6775
$N_{8,2}(\xi)$	0,1250	0,4542	0,2959	0,0011	0,0266
horizontal span 7					
	G.P.31 (1)	G.P.32 (2)	G.P.33 (3)	G.P.34 (4)	G.P.35 (5)
$N_{7,2}(\xi)$	0,1250	0,0011	0,0266	0,4542	0,2959
$N_{8,2}(\xi)$	0,7500	0,5447	0,6775	0,5447	0,6775
$N_{9,2}(\xi)$	0,1250	0,4542	0,2959	0,0011	0,0266
horizontal span 8					
	G.P.36 (1)	G.P.37 (2)	G.P.38 (3)	G.P.39 (4)	G.P.40 (5)
$N_{8,2}(\xi)$	0,1250	0,0011	0,0266	0,4542	0,2959
$N_{9,2}(\xi)$	0,7500	0,5447	0,6775	0,5447	0,6775
$N_{10,2}(\xi)$	0,1250	0,4542	0,2959	0,0011	0,0266
horizontal span 9					
	G.P.41 (1)	G.P.42 (2)	G.P.43 (3)	G.P.44 (4)	G.P.45 (5)
$N_{9,2}(\xi)$	0,1250	0,0011	0,0266	0,4542	0,2959
$N_{10,2}(\xi)$	0,6250	0,0905	0,3817	0,5436	0,6509
$N_{11,2}(\xi)$	0,2500	0,9084	0,5917	0,0022	0,0533

Figure 2.63. Basis SPLine functions' values at Gauss Points of interval ξ [-1,1]
 $(N_{1,2} \div N_{11,2}, \xi_{G.P.1} \div \xi_{G.P.45}, p=2)$

We can see the connection between local and global numbering in Figure 2.63. The local numbers are in brackets.

$N'_{i,2}(\xi)$ (3x5,p=2)	axis ξ				
element 1					
$N'_{1,2}(\xi)$	G.P.1 (1)	G.P.2 (2)	G.P.3 (3)	G.P.4 (4)	G.P.5 (5)
-4,5000	-0,4222	-2,0769	-8,5778	-6,9231	
$N'_{2,2}(\xi)$	2,2500	-3,8667	-1,3847	8,3667	5,8847
$N'_{3,2}(\xi)$	2,2500	4,2889	3,4616	0,2111	1,0384
element 2					
$N'_{2,2}(\xi)$	G.P.6 (1)	G.P.7 (2)	G.P.8 (3)	G.P.9 (4)	G.P.10 (5)
-2,2500	-0,2111	-1,0384	-4,2889	-3,4616	
$N'_{3,2}(\xi)$	0,0000	-4,0778	-2,4231	4,0778	2,4231
$N'_{4,2}(\xi)$	2,2500	4,2889	3,4616	0,2111	1,0384
element 3					
$N'_{3,2}(\xi)$	G.P.11 (1)	G.P.12 (2)	G.P.13 (3)	G.P.14 (4)	G.P.15 (5)
-2,2500	-0,2111	-1,0384	-4,2889	-3,4616	
$N'_{4,2}(\xi)$	0,0000	-4,0778	-2,4231	4,0778	2,4231
$N'_{5,2}(\xi)$	2,2500	4,2889	3,4616	0,2111	1,0384
element 4					
$N'_{4,2}(\xi)$	G.P.16 (1)	G.P.17 (2)	G.P.18 (3)	G.P.19 (4)	G.P.20 (5)
-2,2500	-0,2111	-1,0384	-4,2889	-3,4616	
$N'_{5,2}(\xi)$	0,0000	-4,0778	-2,4231	4,0778	2,4231
$N'_{6,2}(\xi)$	2,2500	4,2889	3,4616	0,2111	1,0384
element 5					
$N'_{5,2}(\xi)$	G.P.21 (1)	G.P.22 (2)	G.P.23 (3)	G.P.24 (4)	G.P.25 (5)
-2,2500	-0,2111	-1,0384	-4,2889	-3,4616	
$N'_{6,2}(\xi)$	0,0000	-4,0778	-2,4231	4,0778	2,4231
$N'_{7,2}(\xi)$	2,2500	4,2889	3,4616	0,2111	1,0384
element 6					
$N'_{6,2}(\xi)$	G.P.26 (1)	G.P.27 (2)	G.P.28 (3)	G.P.29 (4)	G.P.30 (5)
-2,2500	-0,2111	-1,0384	-4,2889	-3,4616	
$N'_{7,2}(\xi)$	0,0000	-4,0778	-2,4231	4,0778	2,4231
$N'_{8,2}(\xi)$	2,2500	4,2889	3,4616	0,2111	1,0384
element 7					
$N'_{7,2}(\xi)$	G.P.31 (1)	G.P.32 (2)	G.P.33 (3)	G.P.34 (4)	G.P.35 (5)
-2,2500	-0,2111	-1,0384	-4,2889	-3,4616	
$N'_{8,2}(\xi)$	0,0000	-4,0778	-2,4231	4,0778	2,4231
$N'_{9,2}(\xi)$	2,2500	4,2889	3,4616	0,2111	1,0384
element 8					
$N'_{8,2}(\xi)$	G.P.36 (1)	G.P.37 (2)	G.P.38 (3)	G.P.39 (4)	G.P.40 (5)
-2,2500	-0,2111	-1,0384	-4,2889	-3,4616	
$N'_{9,2}(\xi)$	0,0000	-4,0778	-2,4231	4,0778	2,4231
$N'_{10,2}(\xi)$	2,2500	4,2889	3,4616	0,2111	1,0384
element 9					
$N'_{9,2}(\xi)$	G.P.41 (1)	G.P.42 (2)	G.P.43 (3)	G.P.44 (4)	G.P.45 (5)
-2,2500	-0,2111	-1,0384	-4,2889	-3,4616	
$N'_{10,2}(\xi)$	-2,2500	-8,3667	-5,8847	8,3667	1,3847
$N'_{11,2}(\xi)$	4,5000	8,5778	6,9231	0,4222	2,0769

Figure 2.64. Basis SPLINE first derivative's values at Gauss Points of interval $\xi [-1,1]$
 $(N'_{1,2} \div N'_{11,2}, \xi_{G.P.1} \div \xi_{G.P.50}, p=2)$

We can see the connection between local and global numbering in Figure 2.64. The local numbers are in brackets.

Axis η

Basis SPLine functions

The axis η is parallel to cantilever's vertical side (height).

- $m=3$ (control points).
- $q=2$ (quadratic Basis SPLine functions, 3 control points per vertical span).
- $m+q+1=3+2+1=6$ knot values.

The open uniform knot vector H contains the following knot values:

- The extreme knots -1, 1 repeated $q+1=2+1=3$ times $\rightarrow 6$ knot values. Remaining, not recurrent: $6-6=0$ knot value $\rightarrow 0+2=2$ knots. \rightarrow I will separate the interval $[-1, 1]$ into $2-1=1$ span. Notice that spans' number is equal to $m-q=3-2=1$.

$$\frac{1 - -1}{1} = \frac{2}{1} = 2$$

$$H = -1 \quad 1$$

The corresponding quadratic Basis SPLine functions to knot vector H are 3 (one for every control point). The support of each quadratic BSPLine is three spans.

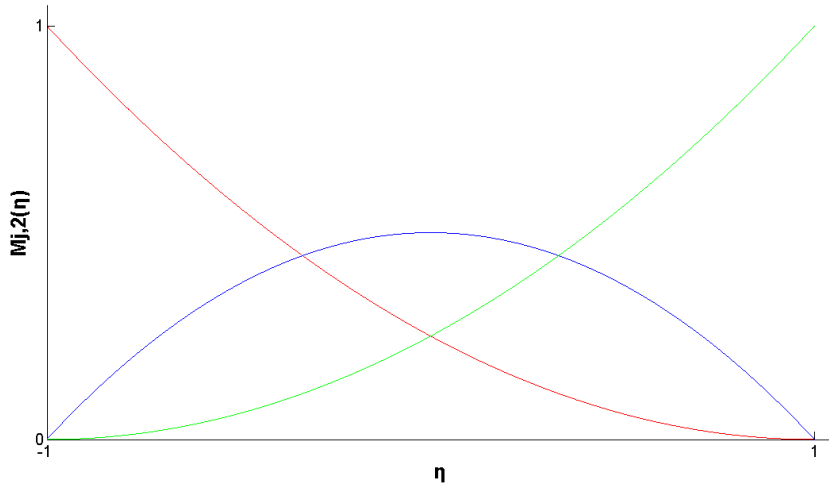


Figure 2.65. Quadratic Basis SPLine functions for open, uniform knot vector $H=\{-1,1\}$.

Gauss Points (coordinates, weight factors)

I use 5 Gauss Points for every vertical span. Each point's coordinate and weight factor is equal to (local numbering, span $[-1,1]$):

G.P.	η'_i	w_i
4	-0.90617	0.23692
5	-0.53846	0.47862
1	0	0.56888
3	0.53846	0.47862
2	0.90617	0.23692

Notice that: $\sum_{i=1}^5 w_i = 2$.

The vertical interval $[-1,1]$ has 1 spans, so $1 \cdot 5 = 5$ G.P. These points are shown as yellow rhombi in Figure 2.66, while knots as cyan circles.

I assume a local η for every span with its center in the span's middle. Then, from Gauss Points' local coordinates η'_i , I calculate the global ones η_i . Let's calculate the coordinate η_i of G.P. 2 for span 1.

$$\frac{\eta_{G.P.2} - -1}{1 - -1} = \frac{\eta_{G.P.2} - -1}{1 - -1} \Rightarrow \eta_{G.P.2} = \eta_{G.P.2} \Rightarrow$$

$\eta_{G.P.2} = 0.9062$

Generally, the coordinate η_j of Gauss Point j in the span (η_i, η_{i+1}) is equal to:

$$\eta_{G.P.j} = \eta'_{G.P.j} \cdot \frac{\eta_{i+1} - \eta_i}{2} + \frac{\eta_{i+1} + \eta_i}{2}$$

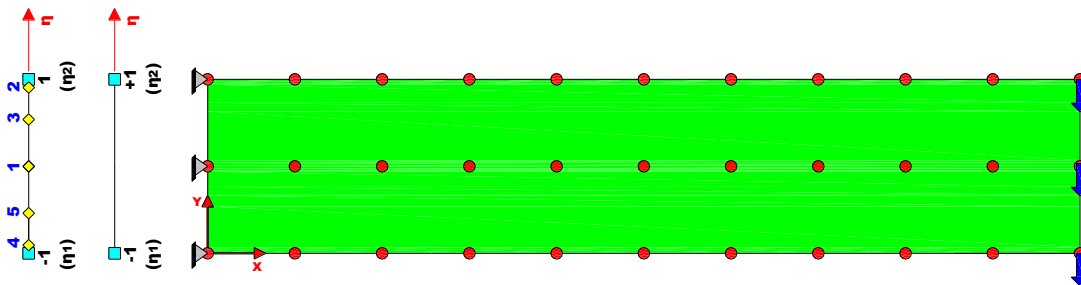


Figure 2.66. Gauss Points (parametric axis η).

B-SPLines' value at Gauss Points

I calculate the quadratic B-Spline functions' ($M_{j,2}(\eta)$) values ($q=2, K=3$) at the position η_j of 5 Gauss Points in vertical parametric axis η and their corresponding first derivatives

$$M'_{j,2}(\eta) = \frac{\partial M_{j,2}(\eta)}{\partial \eta}.$$

Isogeometric Analysis

Figure 2.67 shows respectively constant ($q=0$, $K=1$), linear ($q=1$, $K=2$), quadratic ($q=2$, $K=3$) BSPLines' values for the vertical interval $[-1, 1]$ (axis η).

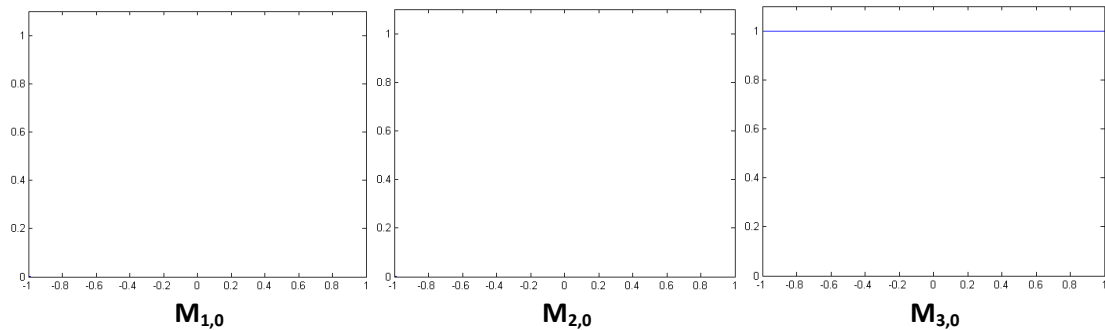


Figure 2.67.a. B-SPLines (Constant, $q=0$, $K=1$) (H)

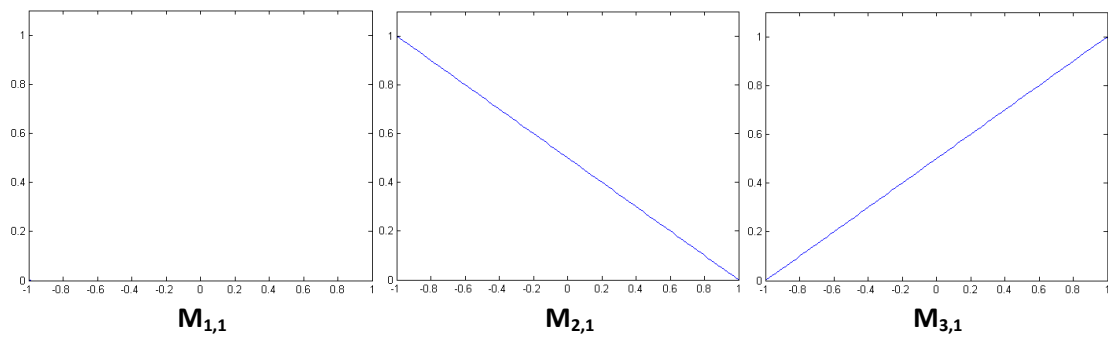


Figure 2.67.b. B-SPLines (Linear, $q=1$, $K=2$) (H)

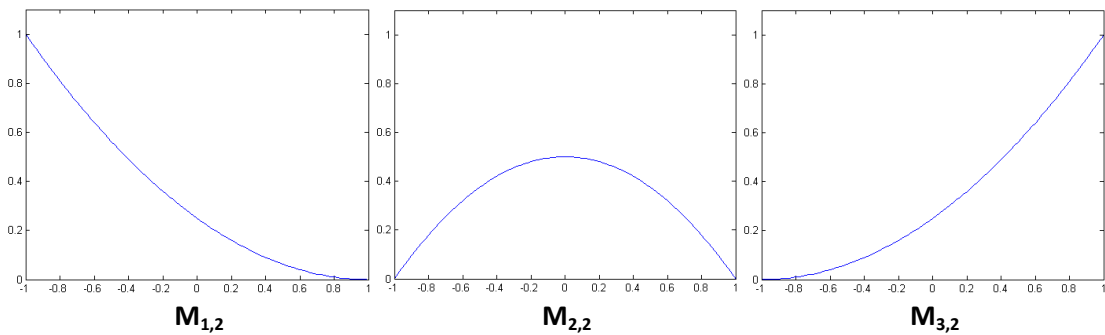


Figure 2.67.c. B-SPLines (Quadratic, $q=2$, $K=3$) (H)

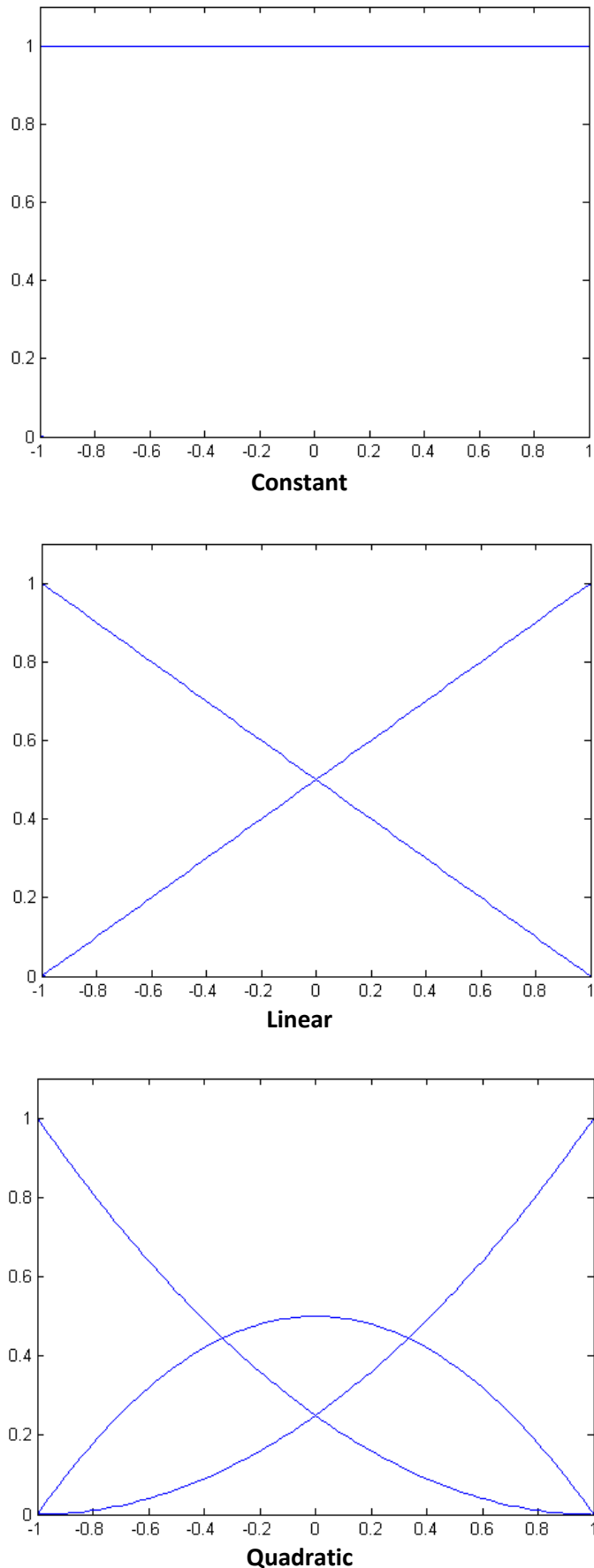


Figure 2.67.d. B-SPLines (H)

$M_{j,2}(\eta)$ (3x5,q=2)	axis η				
	vertical span 1				
	G.P.1	G.P.2	G.P.3	G.P.4	G.P.5
$M_{1,2}(\eta)$	0,25000	0,00220	0,05330	0,90840	0,59170
$M_{2,2}(\eta)$	0,50000	0,08940	0,35500	0,08940	0,35500
$M_{3,2}(\eta)$	0,25000	0,90840	0,59170	0,00220	0,05330

 Figure 2.68. Basis SPLine functions' values at Gauss Points of interval $\eta [-1,1]$

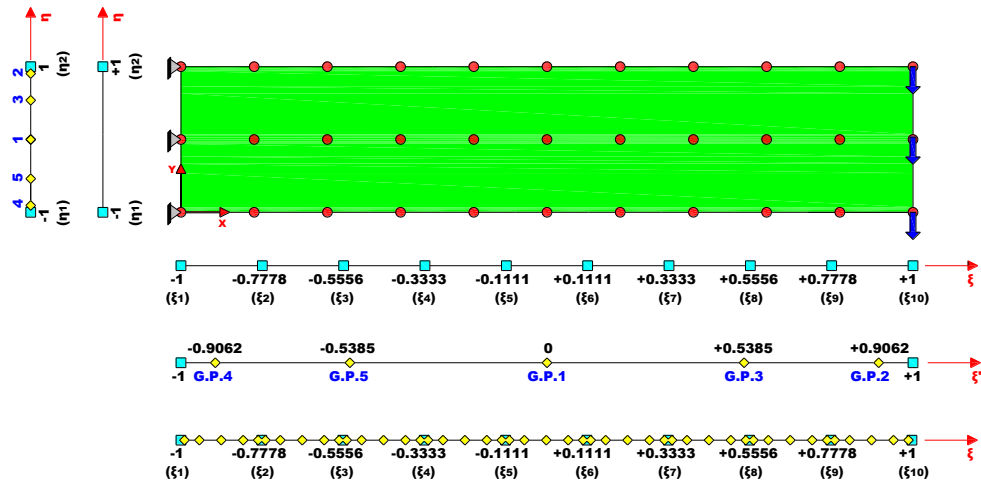
$$(M_{1,2} \div M_{3,2}, \eta_{G.P.1} \div \eta_{G.P.5}, q=2)$$

$M'_{j,2}(\eta)$ (3x5,q=2)	axis η				
	vertical span 1				
	G.P.1	G.P.2	G.P.3	G.P.4	G.P.5
$M'_{1,2}(\eta)$	-0,50000	-0,04690	-0,23080	-0,95310	-0,76920
$M'_{2,2}(\eta)$	0,00000	-0,90620	-0,53850	0,90620	0,53850
$M'_{3,2}(\eta)$	0,50000	0,95310	0,76920	0,04690	0,23080

 Figure 2.69. Basis SPLine first derivative's values at Gauss Points of interval $\eta [-1,1]$

$$(M'_{1,2} \div M'_{3,2}, \eta_{G.P.1} \div \eta_{G.P.5}, q=2)$$

Combination Axes $\xi, \eta (\Xi \times H)$


 Figure 2.70. Gauss Points (parameter space $\Xi \times H$).

I combine the 45 Gauss Points in the axis ξ with the 5 Gauss Points in the axis η and I produce the $45 \times 5 = 225$ Gauss Points of the 2D plane stress cantilever.

Control Net

I choose 33 control points with the following features.

		axis X									
		X _{C.P.}									
local numbering	C.P.1	element 1	element 2	element 3	element 4	element 5	element 6	element 7	element 8	element 9	element 10
		0	0	1,5	1,5	3	3	4,5	4,5	6	6
	C.P.2	0	0	1,5	1,5	3	3	4,5	4,5	6	6
		1,5	1,5	3	3	4,5	4,5	6	6	7,5	7,5
	C.P.3	1,5	1,5	3	3	4,5	4,5	6	6	7,5	7,5
		1,5	1,5	3	3	4,5	4,5	6	6	7,5	7,5
	element 11 element 12 element 13 element 14 element 15 element 16 element 17 element 18 element 19 element 20										
	C.P.1	7,5	7,5	9	9	10,5	10,5	12	12	13,5	13,5
		7,5	7,5	9	9	10,5	10,5	12	12	13,5	13,5
	C.P.2	9	9	10,5	10,5	12	12	13,5	13,5	15	15
		9	9	10,5	10,5	12	12	13,5	13,5	15	15

Figure 2.71.a. Control Points' Cartesian coordinate X. (physical space)

		axis Y									
		Y _{C.P.}									
local numbering	C.P.1	element 1	element 2	element 3	element 4	element 5	element 6	element 7	element 8	element 9	element 10
		0	1,5	0	1,5	0	1,5	0	1,5	0	1,5
	C.P.2	1,5	3	1,5	3	1,5	3	1,5	3	1,5	3
		0	1,5	0	1,5	0	1,5	0	1,5	0	1,5
	C.P.3	1,5	3	1,5	3	1,5	3	1,5	3	1,5	3
		0	1,5	0	1,5	0	1,5	0	1,5	0	1,5
	element 11 element 12 element 13 element 14 element 15 element 16 element 17 element 18 element 19 element 20										
	C.P.1	0	1,5	0	1,5	0	1,5	0	1,5	0	1,5
		1,5	3	1,5	3	1,5	3	1,5	3	1,5	3
	C.P.2	0	1,5	0	1,5	0	1,5	0	1,5	0	1,5
		1,5	3	1,5	3	1,5	3	1,5	3	1,5	3

Figure 2.7171.b. Control Points' Cartesian coordinate Y. (physical space)

		Weight Factor									
		W _{C.P.}									
local numbering	C.P.1	element 1	element 2	element 3	element 4	element 5	element 6	element 7	element 8	element 9	element 10
		1	1	1	1	1	1	1	1	1	1
	C.P.2	1	1	1	1	1	1	1	1	1	1
		1	1	1	1	1	1	1	1	1	1
	C.P.3	1	1	1	1	1	1	1	1	1	1
		1	1	1	1	1	1	1	1	1	1
	element 11 element 12 element 13 element 14 element 15 element 16 element 17 element 18 element 19 element 20										
	C.P.1	1	1	1	1	1	1	1	1	1	1
		1	1	1	1	1	1	1	1	1	1
	C.P.2	1	1	1	1	1	1	1	1	1	1
		1	1	1	1	1	1	1	1	1	1
	C.P.3	1	1	1	1	1	1	1	1	1	1
		1	1	1	1	1	1	1	1	1	1
	C.P.4	1	1	1	1	1	1	1	1	1	1

Figure 2.71.c. Control Points' weight factor W. (physical space)

Control Points don't partition the structure into isogeometric elements, but they are the coefficients (multiplicative factors) of the corresponding B-Splines that form its geometry. In this particular problem, the cantilever has linear geometry as its boundaries are straight lines. That's why control points' weight factor is equal to 1.

In Figure 2.16 we can see the corresponding control net.

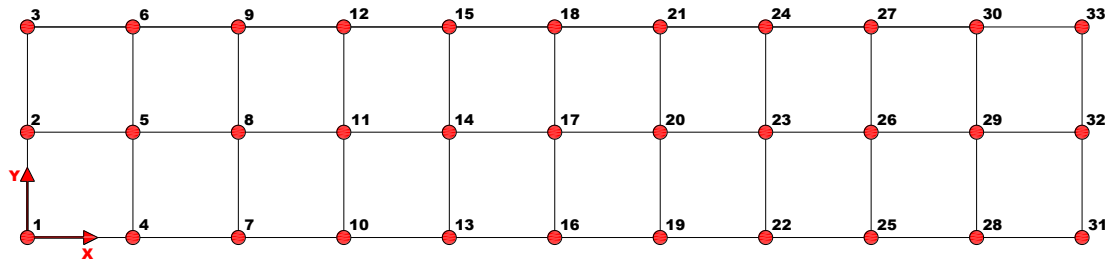


Figure 2.72. Control Net. (physical space)

Index Space

I present every knot value in index space. The most important is that we can see which knot vector's region is used by each isogeometric element. With darker green I represent the overlapping.

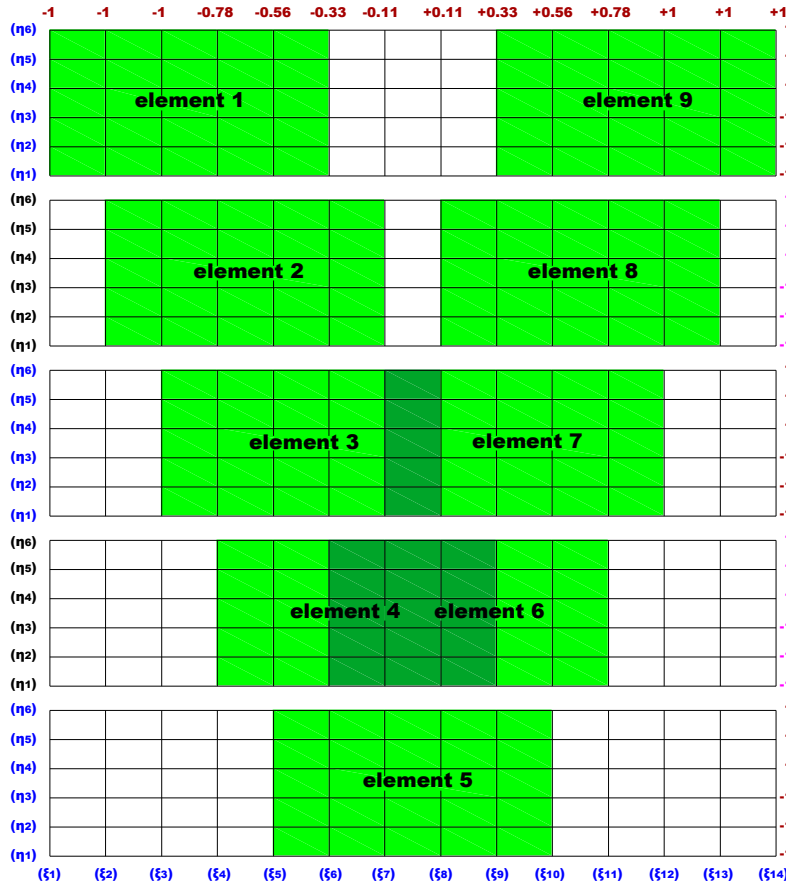


Figure 2.73. Index Space.

Parameter Space

I present every knot and not every knot value in parameter space. For example, extreme knot value -1 repeated $p+1=2+1=3$ times, but it has the same position, means it corresponds to one knot. In Figure 2.74 we can see the chosen mesh of isogeometric elements. It is very important to underline that knots and not control points partition the cantilever into isogeometric elements.

The 10 1D knots (ξ) partition the interval [-1,1] of parametric axis ξ into 9 horizontal spans. The 2 1D knots (η) partition the interval [-1,1] of parametric axis η into 1 vertical span. Combining the two axes, we have the cantilever's mesh in the parameter space, which consists of $9 \times 1 = 9$ isogeometric elements.

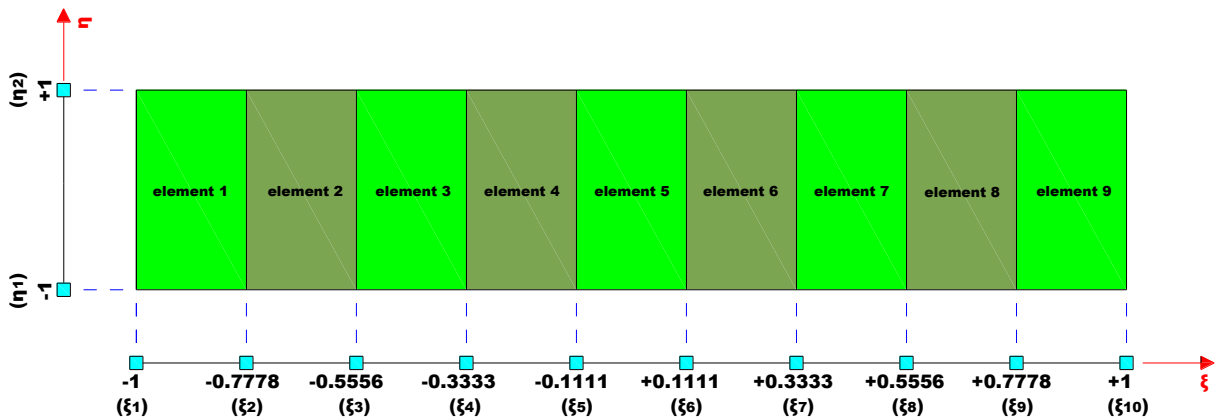


Figure 2.74.a. Parameter Space.
Knots partition cantilever into isogeometric elements.

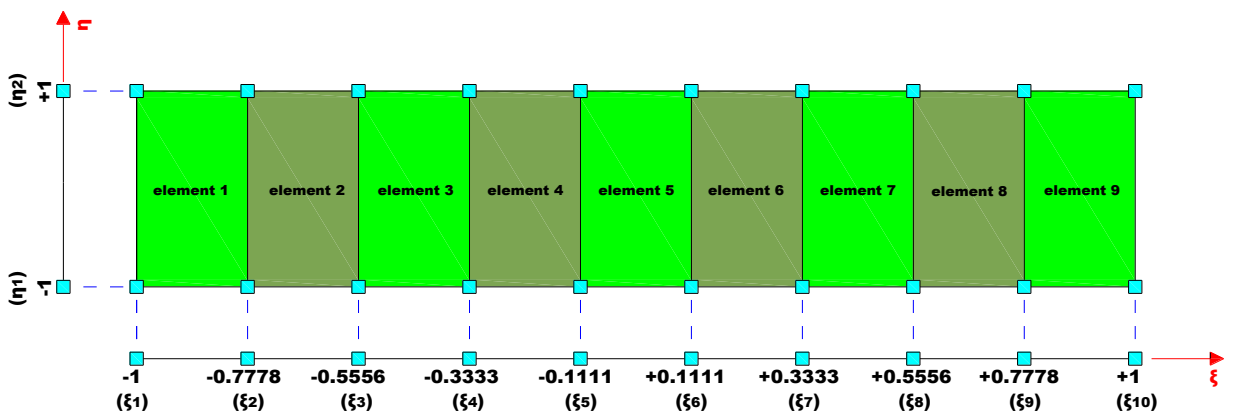


Figure 2.74.b. Parameter Space.
Mesh of isogeometric elements.

Physical Space

With the mesh of isogeometric elements in parameter space in hand, I can form the corresponding mesh in physical space. I follow the next procedure, where control points' numbering is local:

- I calculate knots' X Cartesian (physical) coordinates from their parametric ones. Supposing the knot $i (\xi_i, \eta_i)$, I have that:

$$X_i = X_{\xi_i} = X_{C.P.1} \cdot N_{1,2}(\xi_i) + \dots + X_{C.P.11} \cdot N_{11,2}(\xi_i)$$

Applying this relation for every knot:

$$X_{\xi_1} = X_{C.P.1} \cdot N_{1,2}(\xi_1) + \dots + X_{C.P.11} \cdot N_{11,2}(\xi_1) = X_{C.P.1} \cdot 1 = X_{C.P.1} = 0$$

Similarly,

$$\begin{aligned} X_{\xi_2} &= X_{C.P.2} \cdot 0,5 + X_{C.P.3} \cdot 0,5 = \frac{X_{C.P.2} + X_{C.P.3}}{2} = \frac{1,5 + 3}{2} = 2,25 \text{m} \\ X_{\xi_3} &= \frac{X_{C.P.3} + X_{C.P.4}}{2} = 3,75 \text{m} \text{ and } X_{\xi_4} = \frac{X_{C.P.4} + X_{C.P.5}}{2} = 5,25 \text{m} \\ X_{\xi_5} &= \frac{X_{C.P.5} + X_{C.P.6}}{2} = 6,75 \text{m} \text{ and } X_{\xi_6} = \frac{X_{C.P.6} + X_{C.P.7}}{2} = 8,25 \text{m} \\ X_{\xi_7} &= \frac{X_{C.P.7} + X_{C.P.8}}{2} = 9,75 \text{m} \text{ and } X_{\xi_8} = \frac{X_{C.P.8} + X_{C.P.9}}{2} = 11,25 \text{m} \\ X_{\xi_9} &= \frac{X_{C.P.9} + X_{C.P.10}}{2} = 12,75 \text{m} \text{ and } X_{\xi_{10}} = \frac{X_{C.P.10} + X_{C.P.11}}{2} = 14,25 \text{m} \\ X_{\xi_{11}} &= X_{C.P.11} = 15 \text{m} \end{aligned}$$

- I calculate knots' Y Cartesian (physical) coordinates from their parametric ones. Supposing the knot $i (\xi_i, \eta_i)$, I have that:

$$Y_i = Y_{\eta_i} = Y_{C.P.1} \cdot M_{1,2}(\eta_i) + \dots + Y_{C.P.3} \cdot M_{3,2}(\eta_i)$$

Applying this relation for every knot:

$$Y_{\eta_1} = Y_{C.P.1} \cdot M_{1,1}(\eta_1) + \dots + Y_{C.P.3} \cdot M_{11,1}(\eta_1) = Y_{C.P.1} \cdot 1 = Y_{C.P.1} = 0$$

Similarly,

$$Y_{\eta_2} = Y_{C.P.3} = 3 \text{m}$$

- As I know for every knot its Cartesian coordinates (X, Y), I can draw them in physical space. We can see the knots as cyan rhombi in Figure 2.75.
- Finally, I connect the knots with their adjacent ones. We can see the knot lines as black lines in Figure 2.75.

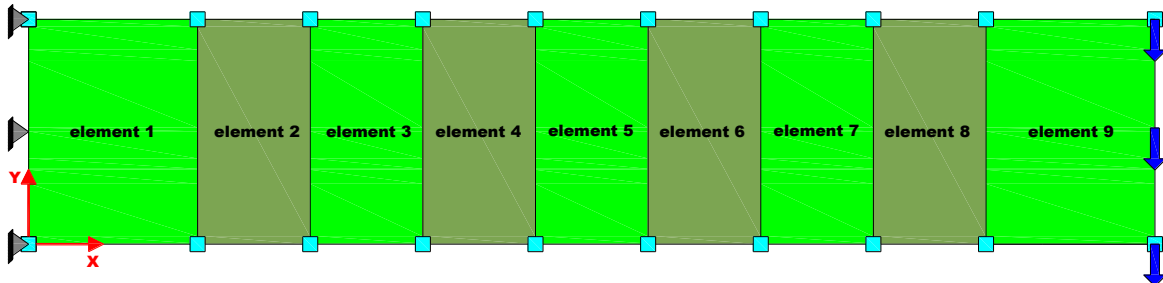


Figure 2.75. Physical Space. Mesh. Knots.

Figure 2.76 shows both knots (cyan rhombi) and control points (red circles) in the physical space. We observe that knots don't coincide with control points as happened in the case of linear B-SPLines. That's why Basis SPLine functions are not linear, but quadratic ($p=q=2$, $K=3$) and the overlapping is smaller for extreme elements 1 and 9 than for intermediate ones.

Knots and not control points partition cantilever into 9 2D isogeometric elements. Although, the stiffness matrix refers to control points, so I form the equilibrium equation for them.

$$\mathbf{F} = \mathbf{K} \cdot \mathbf{U} \Rightarrow \mathbf{U} = \mathbf{K}^{-1} \cdot \mathbf{F}$$

Displacements' vector \mathbf{U} refers to control points. For this particular problem, there are 33 control points, so the above equation is written as follows:

$$\begin{matrix} \mathbf{F} & = & \mathbf{K} & \cdot & \mathbf{U} \\ 66 \times 1 & & 66 \times 66 & & 66 \times 1 \end{matrix} \Rightarrow \begin{matrix} \mathbf{U} & = & \mathbf{K}^{-1} & \cdot & \mathbf{F} \\ 66 \times 1 & & 66 \times 66 & & 66 \times 1 \end{matrix}$$

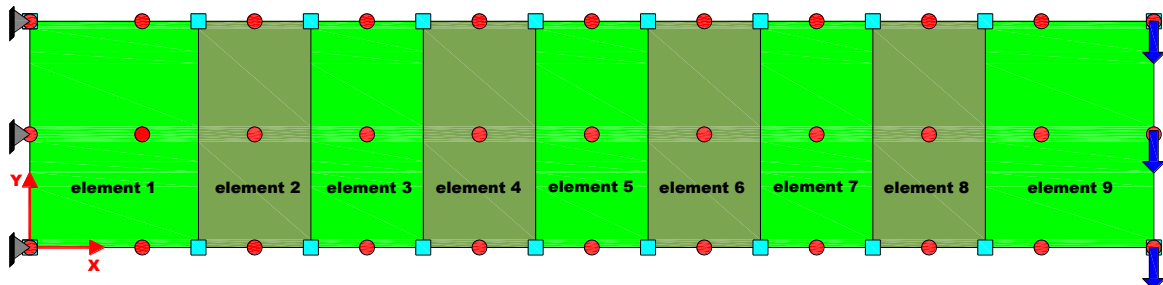


Figure 2.76. Physical Space. Mesh. Knots and Control Points.

Elasticity Matrix [E]

As it is a plane stress problem, the elasticity matrix [E] for every isogeometric element is equal to:

$$E_{3 \times 3} = \frac{E}{1-v^2} \cdot \begin{bmatrix} 1 & v & 0 \\ v & 1 & 0 \\ 0 & 0 & \frac{1-v}{2} \end{bmatrix}$$

Every isogeometric element has the same elasticity modulus $E = 210\text{GPa} = 2,1 \cdot 10^8 \text{kPa}$ and Poisson's ratio $v = 0,3$, so they have all the same elasticity matrix [E], which is equal to:

$$E_{3 \times 3} = 230.769.231 \cdot \begin{bmatrix} 1 & 0.3 & 0 \\ 0.3 & 1 & 0 \\ 0 & 0 & 0.35 \end{bmatrix} \text{kPa} \Rightarrow$$

$$E_{3 \times 3} = \begin{bmatrix} 230.769.231 & 69.230.769 & 0 \\ 69.230.769 & 230.769.231 & 0 \\ 0 & 0 & 80.769.231 \end{bmatrix} \text{kPa}$$

Deformation Matrix [B]

NURBS (Non-Uniform Rational B-SPLines) and not B-SPLines are used as shape functions. This NURBS basis is given by:

$$R_i^p(\xi) = \frac{\sum_{i=1}^n N_{i,p}(\xi) \cdot w_i}{\sum_{i=1}^n N_{i,p}(\xi)}$$

where:

- $i=1,\dots,n$
- n : control points' number
- p : B-SPLines' polynomial order
- $N_{i,p}(\xi)$: the corresponding Basis SPLine to control point i
- w_i : control point's i weight factor
- $R_i^p(\xi)$: the corresponding Non-Uniform Rational Basis SPLine to control point i with polynomial order p

Isogeometric Analysis

The Non-Uniform Rational Basis SPLine's derivative is equal to:

$$\frac{\partial R_i^p \xi}{\partial \xi} = \frac{\frac{\partial N_{i,p} \xi \cdot w_i}{\partial \xi} \cdot \sum_{i=1}^n N_{i,p} \xi \cdot w_i - N_{i,p} \xi \cdot w_i \cdot \frac{\partial \left(\sum_{i=1}^n N_{i,p} \xi \cdot w_i \right)}{\partial \xi}}{\left(\sum_{i=1}^n N_{i,p} \xi \cdot w_i \right)^2} \Rightarrow$$

$$\frac{\partial R_i^p \xi}{\partial \xi} = \frac{\frac{\partial N_{i,p} \xi}{\partial \xi} \cdot w_i \cdot \sum_{i=1}^n N_{i,p} \xi \cdot w_i - N_{i,p} \xi \cdot w_i \cdot \sum_{i=1}^n \frac{\partial N_{i,p} \xi}{\partial \xi} \cdot w_i}{\left(\sum_{i=1}^n N_{i,p} \xi \cdot w_i \right)^2} \Rightarrow$$

$$\frac{\partial R_i^p \xi}{\partial \xi} = \frac{\frac{\partial N_{i,p} \xi}{\partial \xi} \cdot w_i - N_{i,p} \xi \cdot w_i \cdot \sum_{i=1}^n \frac{\partial N_{i,p} \xi}{\partial \xi} \cdot w_i}{\sum_{i=1}^n N_{i,p} \xi \cdot w_i - \left(\sum_{i=1}^n N_{i,p} \xi \cdot w_i \right)^2}$$

The problem is 2D, so I have to calculate Rational Surfaces which are defined analogously in terms of the rational basis functions:

$$R_{i,j}^{p,q} \xi, \eta = \frac{N_{i,p} \xi \cdot M_{j,q} \eta \cdot w_{i,j}}{\sum_{i=1}^n \sum_{j=1}^m N_{i,p} \xi \cdot M_{j,q} \eta \cdot w_{i,j}}$$

where:

- $i=1, \dots, n$ (axis ξ)
- $j=1, \dots, m$ (axis η)
- n : control points' number (axis ξ)
- m : control points' number (axis η)
- p : B-SPLines' polynomial order (axis ξ)
- q : B-SPLines' polynomial order (axis η)
- $N_{i,p} \xi$: the corresponding Basis SPLine to control point i (axis ξ)
- $M_{j,q} \xi$: the corresponding Basis SPLine to control point j (axis η)
- $w_{i,j}$: control point's weight factor (2D, $\Xi \times H$)
- $R_{i,j}^{p,q} \xi, \eta$: the corresponding Rational Surface to control point (i,j)

In this case, the weights are all equal, so:

$$R_i^p \xi = \frac{N_{i,p} \xi \cdot w_i}{\sum_{i=1}^n N_{i,p} \xi \cdot w_i} = \frac{N_{i,p} \xi}{\sum_{i=1}^n N_{i,p} \xi} = \frac{N_{i,p} \xi}{1} = N_{i,p} \xi$$

Isogeometric Analysis

and the curve is again a polynomial. B-SPLines are a special case of NURBS.

Similarly,

$$R_{i,j}^{p,q} \xi, \eta = \frac{N_{i,p} \xi \cdot M_{j,q} \eta \cdot w_{i,j}}{\sum_{i=1}^n \sum_{j=1}^m N_{i,p} \xi \cdot M_{j,q} \eta \cdot w_{i,j}} = \frac{N_{i,p} \xi \cdot M_{j,q} \eta}{\sum_{i=1}^n \sum_{j=1}^m N_{i,p} \xi \cdot M_{j,q} \eta} = \frac{N_{i,p} \xi \cdot M_{j,q} \eta}{1} \Rightarrow$$

$$R_{i,j}^{p,q} \xi, \eta = N_{i,p} \xi \cdot M_{j,q} \eta$$

The corresponding partial derivatives are equal to:

$$\frac{\partial R_{i,j}^{p,q} \xi, \eta}{\partial \xi} = \frac{\partial N_{i,p} \xi}{\partial \xi} \cdot M_{j,q} \eta$$

$$\frac{\partial R_{i,j}^{p,q} \xi, \eta}{\partial \eta} = N_{i,p} \xi \cdot \frac{\partial M_{j,q} \eta}{\partial \eta}$$

For every isogeometric element, I calculate:

- Jacobian matrix

$$\begin{bmatrix} J & \xi, \eta \\ 2x2 & \end{bmatrix} = \begin{bmatrix} D_N & \xi, \eta \\ 2x9 & \end{bmatrix} \cdot \begin{bmatrix} X & Y \\ 9x2 & \end{bmatrix}$$

where:

$$\begin{bmatrix} D_N & \xi, \eta \\ 2x9 & \end{bmatrix} = \begin{bmatrix} \frac{\partial R_{1,1}^{2,2}}{\partial \xi} & \frac{\partial R_{1,2}^{2,2}}{\partial \xi} & \frac{\partial R_{1,3}^{2,2}}{\partial \xi} & \frac{\partial R_{2,1}^{2,2}}{\partial \xi} & \frac{\partial R_{2,2}^{2,2}}{\partial \xi} & \frac{\partial R_{2,3}^{2,2}}{\partial \xi} & \frac{\partial R_{3,1}^{2,2}}{\partial \xi} & \frac{\partial R_{3,2}^{2,2}}{\partial \xi} & \frac{\partial R_{3,3}^{2,2}}{\partial \xi} \\ \frac{\partial R_{1,1}^{2,2}}{\partial \eta} & \frac{\partial R_{1,2}^{2,2}}{\partial \eta} & \frac{\partial R_{1,3}^{2,2}}{\partial \eta} & \frac{\partial R_{2,1}^{2,2}}{\partial \eta} & \frac{\partial R_{2,2}^{2,2}}{\partial \eta} & \frac{\partial R_{2,3}^{2,2}}{\partial \eta} & \frac{\partial R_{3,1}^{2,2}}{\partial \eta} & \frac{\partial R_{3,2}^{2,2}}{\partial \eta} & \frac{\partial R_{3,3}^{2,2}}{\partial \eta} \end{bmatrix}$$

$$\begin{bmatrix} X & Y \\ 9x2 & \end{bmatrix} = \begin{bmatrix} X_{C.P.1} & Y_{C.P.1} \\ X_{C.P.2} & Y_{C.P.2} \\ X_{C.P.3} & Y_{C.P.3} \\ X_{C.P.4} & Y_{C.P.4} \\ X_{C.P.5} & Y_{C.P.5} \\ X_{C.P.6} & Y_{C.P.6} \\ X_{C.P.7} & Y_{C.P.7} \\ X_{C.P.8} & Y_{C.P.8} \\ X_{C.P.9} & Y_{C.P.9} \end{bmatrix}$$

C.P.1, ..., C.P.9 are the corresponding 9 control points to every isogeometric element with local numbering.

- Deformation matrix

$$\begin{aligned} \left[\begin{array}{c|cc} \mathbf{B}_1 & \xi, \eta \\ \hline 3 \times 4 & \end{array} \right] &= \frac{1}{\det \mathbf{J}} \cdot \begin{bmatrix} \mathbf{J}_{22} & -\mathbf{J}_{12} & 0 & 0 \\ 0 & 0 & -\mathbf{J}_{21} & \mathbf{J}_{11} \\ -\mathbf{J}_{21} & \mathbf{J}_{11} & \mathbf{J}_{22} & -\mathbf{J}_{12} \end{bmatrix} \\ \left[\begin{array}{c|cc} \mathbf{B}_2 & \xi, \eta \\ \hline 4 \times 18 & \end{array} \right] &= \begin{bmatrix} \frac{\partial R_{1,1}^{2,2}}{\partial \xi} & 0 & \frac{\partial R_{1,2}^{2,2}}{\partial \xi} & 0 & \frac{\partial R_{1,3}^{2,2}}{\partial \xi} & 0 & \frac{\partial R_{2,1}^{2,2}}{\partial \xi} & 0 & \frac{\partial R_{2,2}^{2,2}}{\partial \xi} & 0 & \frac{\partial R_{2,3}^{2,2}}{\partial \xi} & 0 & \frac{\partial R_{3,1}^{2,2}}{\partial \xi} & 0 & \frac{\partial R_{3,2}^{2,2}}{\partial \xi} & 0 & \frac{\partial R_{3,3}^{2,2}}{\partial \xi} & 0 \\ \frac{\partial R_{1,1}^{2,2}}{\partial \eta} & 0 & \frac{\partial R_{1,2}^{2,2}}{\partial \eta} & 0 & \frac{\partial R_{1,3}^{2,2}}{\partial \eta} & 0 & \frac{\partial R_{2,1}^{2,2}}{\partial \eta} & 0 & \frac{\partial R_{2,2}^{2,2}}{\partial \eta} & 0 & \frac{\partial R_{2,3}^{2,2}}{\partial \eta} & 0 & \frac{\partial R_{3,1}^{2,2}}{\partial \eta} & 0 & \frac{\partial R_{3,2}^{2,2}}{\partial \eta} & 0 & \frac{\partial R_{3,3}^{2,2}}{\partial \eta} & 0 \\ 0 & \frac{\partial R_{1,1}^{2,2}}{\partial \xi} & 0 & \frac{\partial R_{1,2}^{2,2}}{\partial \xi} & 0 & \frac{\partial R_{1,3}^{2,2}}{\partial \xi} & 0 & \frac{\partial R_{2,1}^{2,2}}{\partial \xi} & 0 & \frac{\partial R_{2,2}^{2,2}}{\partial \xi} & 0 & \frac{\partial R_{2,3}^{2,2}}{\partial \xi} & 0 & \frac{\partial R_{3,1}^{2,2}}{\partial \xi} & 0 & \frac{\partial R_{3,2}^{2,2}}{\partial \xi} & 0 & \frac{\partial R_{3,3}^{2,2}}{\partial \xi} & 0 \\ 0 & \frac{\partial R_{1,1}^{2,2}}{\partial \eta} & 0 & \frac{\partial R_{1,2}^{2,2}}{\partial \eta} & 0 & \frac{\partial R_{1,3}^{2,2}}{\partial \eta} & 0 & \frac{\partial R_{2,1}^{2,2}}{\partial \eta} & 0 & \frac{\partial R_{2,2}^{2,2}}{\partial \eta} & 0 & \frac{\partial R_{2,3}^{2,2}}{\partial \eta} & 0 & \frac{\partial R_{3,1}^{2,2}}{\partial \eta} & 0 & \frac{\partial R_{3,2}^{2,2}}{\partial \eta} & 0 & \frac{\partial R_{3,3}^{2,2}}{\partial \eta} & 0 \end{bmatrix} \end{aligned}$$

The deformation matrix is equal to:

$$\left[\begin{array}{c|cc} \mathbf{B} & \xi, \eta \\ \hline 3 \times 18 & \end{array} \right] = \left[\begin{array}{c|cc} \mathbf{B}_1 & \xi, \eta \\ \hline 3 \times 4 & \end{array} \right] \cdot \left[\begin{array}{c|cc} \mathbf{B}_2 & \xi, \eta \\ \hline 4 \times 18 & \end{array} \right] \Rightarrow$$

$$\left[\begin{array}{c|cc} \mathbf{B} & \xi, \eta \\ \hline 3 \times 18 & \end{array} \right] = \begin{bmatrix} \frac{\partial R_{1,1}^{2,2}}{\partial \xi} & \frac{\partial R_{1,2}^{2,2}}{\partial \xi} & 0 & \frac{\partial R_{1,3}^{2,2}}{\partial \xi} & 0 & \frac{\partial R_{2,1}^{2,2}}{\partial \xi} & 0 & \frac{\partial R_{2,2}^{2,2}}{\partial \xi} & 0 & \frac{\partial R_{2,3}^{2,2}}{\partial \xi} & 0 & \frac{\partial R_{3,1}^{2,2}}{\partial \xi} & 0 & \frac{\partial R_{3,2}^{2,2}}{\partial \xi} & 0 & \frac{\partial R_{3,3}^{2,2}}{\partial \xi} & 0 \\ 0 & \frac{\partial R_{1,1}^{2,2}}{\partial \eta} & 0 & \frac{\partial R_{1,2}^{2,2}}{\partial \eta} & 0 & \frac{\partial R_{1,3}^{2,2}}{\partial \eta} & 0 & \frac{\partial R_{2,1}^{2,2}}{\partial \eta} & 0 & \frac{\partial R_{2,2}^{2,2}}{\partial \eta} & 0 & \frac{\partial R_{2,3}^{2,2}}{\partial \eta} & 0 & \frac{\partial R_{3,1}^{2,2}}{\partial \eta} & 0 & \frac{\partial R_{3,2}^{2,2}}{\partial \eta} & 0 & \frac{\partial R_{3,3}^{2,2}}{\partial \eta} & 0 \\ \frac{\partial R_{1,1}^{2,2}}{\partial \xi} & \frac{\partial R_{1,2}^{2,2}}{\partial \xi} & 0 & \frac{\partial R_{1,3}^{2,2}}{\partial \xi} & 0 & \frac{\partial R_{2,1}^{2,2}}{\partial \xi} & 0 & \frac{\partial R_{2,2}^{2,2}}{\partial \xi} & 0 & \frac{\partial R_{2,3}^{2,2}}{\partial \xi} & 0 & \frac{\partial R_{3,1}^{2,2}}{\partial \xi} & 0 & \frac{\partial R_{3,2}^{2,2}}{\partial \xi} & 0 & \frac{\partial R_{3,3}^{2,2}}{\partial \xi} & 0 \\ \frac{\partial R_{1,1}^{2,2}}{\partial \eta} & \frac{\partial R_{1,2}^{2,2}}{\partial \eta} & 0 & \frac{\partial R_{1,3}^{2,2}}{\partial \eta} & 0 & \frac{\partial R_{2,1}^{2,2}}{\partial \eta} & 0 & \frac{\partial R_{2,2}^{2,2}}{\partial \eta} & 0 & \frac{\partial R_{2,3}^{2,2}}{\partial \eta} & 0 & \frac{\partial R_{3,1}^{2,2}}{\partial \eta} & 0 & \frac{\partial R_{3,2}^{2,2}}{\partial \eta} & 0 & \frac{\partial R_{3,3}^{2,2}}{\partial \eta} & 0 \end{bmatrix}$$

Local Stiffness Matrix [k^e]

I calculate isogeometric element's local stiffness matrix using Gauss quadrature. I choose 5x5 quadrature rule, means 25 Gauss Points for every element.

$$\left[\begin{array}{c|cc} \mathbf{k}^e & \\ \hline 18 \times 18 & \end{array} \right] = \sum_{i=1}^{25} \left\{ \left[\begin{array}{c|cc} \mathbf{B}^e & \xi_i, \eta_i \\ \hline 18 \times 3 & \end{array} \right]^T \cdot \mathbf{E} \cdot \left[\begin{array}{c|cc} \mathbf{B}^e & \xi_i, \eta_i \\ \hline 3 \times 18 & \end{array} \right] \cdot \mathbf{t} \cdot \det \left[\begin{array}{c|cc} \mathbf{J} & \xi_i, \eta_i \\ \hline \end{array} \right] \cdot \mathbf{w}_i \right\}$$

The weight factor of Gauss Point i is equal to $w_i = \frac{w}{n-p} \cdot \frac{\xi_i}{m-q}$.

where (n-p), (m-q) is the number of horizontal (parametric axis ξ), vertical (parametric axis η) spans respectively. I divide with (n-p), (m-q) in order to:

$$\sum_{i=1}^{225} w_i = 2 \text{ (global numbering)}$$

I used totally (25 Gauss Points per element) · (9 elements) = 225 Gauss Points.

Isogeometric Analysis

Let's follow the previous procedure for Gauss Point 1 of isogeometric element 1. We can see this Gauss Point in the following Figure 2.77. It is the one in the green circle.

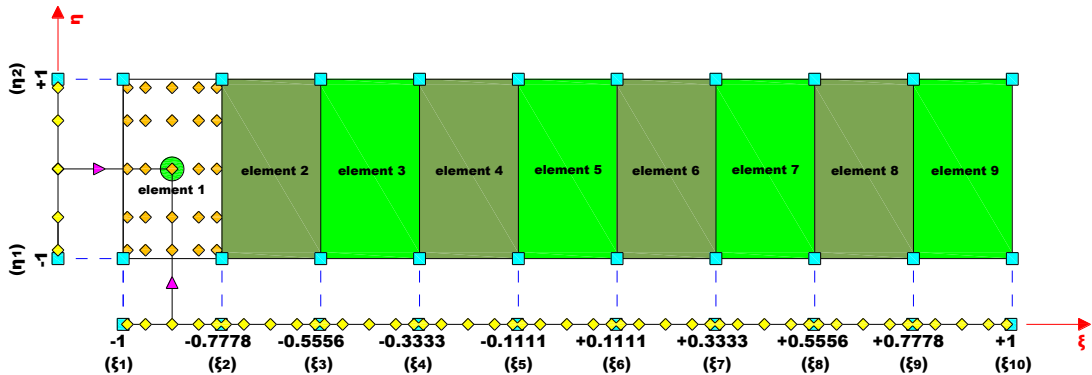


Figure 2.77. Gauss Point 1 of isogeometric element 1. (Parameter Space)

For element 1 (horizontal span 1 + vertical span 1),

$N_{i,2}(\xi)$ (3x5,p=2)	axis ξ				
	horizontal span 1				
	G.P.1 (1)	G.P.2 (2)	G.P.3 (3)	G.P.4 (4)	G.P.5 (5)
$N_{1,2}(\xi)$	0,2500	0,0022	0,0533	0,9084	0,5917
$N_{2,2}(\xi)$	0,6250	0,5436	0,6509	0,0905	0,3817
$N_{3,2}(\xi)$	0,1250	0,4542	0,2959	0,0011	0,0266

Figure 2.78.a. Basis SPLine functions for horizontal span 1. Parametric axis ξ . Values at Gauss Points.

$N'_{i,2}(\xi)$ (3x5,p=2)	axis ξ				
	element 1				
	G.P.1 (1)	G.P.2 (2)	G.P.3 (3)	G.P.4 (4)	G.P.5 (5)
$N'_{1,2}(\xi)$	-4,5000	-0,4222	-2,0769	-8,5778	-6,9231
$N'_{2,2}(\xi)$	2,2500	-3,8667	-1,3847	8,3667	5,8847
$N'_{3,2}(\xi)$	2,2500	4,2889	3,4616	0,2111	1,0384

Figure 2.78.b. First derivative of basis SPLine functions for horizontal span 1. Parametric axis ξ . Values at Gauss Points.

$M_{j,2}(\eta)$ (3x5,q=2)	axis η				
	vertical span 1				
	G.P.1	G.P.2	G.P.3	G.P.4	G.P.5
$M_{1,2}(\eta)$	0,25000	0,00220	0,05330	0,90840	0,59170
$M_{2,2}(\eta)$	0,50000	0,08940	0,35500	0,08940	0,35500
$M_{3,2}(\eta)$	0,25000	0,90840	0,59170	0,00220	0,05330

Figure 2.78.c. Basis SPLine functions for vertical span 1. Parametric axis η . Values at Gauss Points.

$M'_{j,2}(\eta)$ (3x5,q=2)	axis η				
	vertical span 1				
	G.P.1	G.P.2	G.P.3	G.P.4	G.P.5
$M'_{1,2}(\eta)$	-0,50000	-0,04690	-0,23080	-0,95310	-0,76920
$M'_{2,2}(\eta)$	0,00000	-0,90620	-0,53850	0,90620	0,53850
$M'_{3,2}(\eta)$	0,50000	0,95310	0,76920	0,04690	0,23080

Figure 2.78.d. First derivative of basis SPLine functions for vertical span 1.
Parametric axis η . Values at Gauss Points.

$$XY = \begin{bmatrix} X_{C.P.1} & Y_{C.P.1} \\ X_{C.P.2} & Y_{C.P.2} \\ X_{C.P.3} & Y_{C.P.3} \\ X_{C.P.4} & Y_{C.P.4} \\ X_{C.P.5} & Y_{C.P.5} \\ X_{C.P.6} & Y_{C.P.6} \\ X_{C.P.7} & Y_{C.P.7} \\ X_{C.P.8} & Y_{C.P.8} \\ X_{C.P.9} & Y_{C.P.9} \end{bmatrix} = \begin{bmatrix} 0 & 0 \\ 0 & 1,5 \\ 0 & 3 \\ 1,5 & 0 \\ 1,5 & 1,5 \\ 1,5 & 3 \\ 3 & 0 \\ 3 & 1,5 \\ 3 & 3 \end{bmatrix}$$

With BSPLines $N_{i,2} \xi, M_{j,2} \eta$ and their derivatives $(\frac{\partial N_{i,2}}{\partial \xi}, \frac{\partial M_{i,2}}{\partial \eta})$ in hand, I calculate corresponding NURBS' values at Gauss Point 1 (isogeometric element 1).

$$\boxed{R_{i,j}^{p,q} \xi, \eta = N_{i,p} \xi \cdot M_{j,q} \eta} \Rightarrow R_{i,j}^{2,2} \xi_{G.P.1}, \eta_{G.P.1} = N_{i,2} \xi_{G.P.1} \cdot M_{j,2} \eta_{G.P.1}$$

$$\boxed{\frac{\partial R_{i,j}^{p,q} \xi, \eta}{\partial \xi} = \frac{\partial N_{i,p} \xi}{\partial \xi} \cdot M_{j,q} \eta} \Rightarrow \frac{\partial R_{i,j}^{2,2} \xi_{G.P.1}, \eta_{G.P.1}}{\partial \xi} = \frac{\partial N_{i,2} \xi_{G.P.1}}{\partial \xi} \cdot M_{j,2} \eta_{G.P.1}$$

$$\boxed{\frac{\partial R_{i,j}^{p,q} \xi, \eta}{\partial \eta} = N_{i,p} \xi \cdot \frac{\partial M_{j,q} \eta}{\partial \eta}} \Rightarrow \frac{\partial R_{i,j}^{2,2} \xi_{G.P.1}, \eta_{G.P.1}}{\partial \eta} = N_{i,2} \xi_{G.P.1} \cdot \frac{\partial M_{j,2} \eta_{G.P.1}}{\partial \eta}$$

Control Point 1 ($i=1, j=1$)

$$R_{1,1}^{2,2} \xi_{G.P.1}, \eta_{G.P.1} = N_{1,2} \xi_{G.P.1} \cdot M_{1,2} \eta_{G.P.1}$$

$$\frac{\partial R_{1,1}^{2,2} \xi_{G.P.1}, \eta_{G.P.1}}{\partial \xi} = \frac{\partial N_{1,2} \xi_{G.P.1}}{\partial \xi} \cdot M_{1,2} \eta_{G.P.1}$$

$$\frac{\partial R_{1,1}^{2,2} \xi_{G.P.1}, \eta_{G.P.1}}{\partial \eta} = N_{1,2} \xi_{G.P.1} \cdot \frac{\partial M_{1,2} \eta_{G.P.1}}{\partial \eta}$$

Control Point 3 (i=1, j=3)

$$R_{1,3}^{2,2} \xi_{G.P.1}, \eta_{G.P.1} = N_{1,2} \xi_{G.P.1} \cdot M_{3,2} \eta_{G.P.1}$$

$$\frac{\partial R_{1,3}^{2,2} \xi_{G.P.1}, \eta_{G.P.1}}{\partial \xi} = \frac{\partial N_{1,2} \xi_{G.P.1}}{\partial \xi} \cdot M_{3,2} \eta_{G.P.1}$$

$$\frac{\partial R_{1,3}^{2,2} \xi_{G.P.1}, \eta_{G.P.1}}{\partial \eta} = N_{1,2} \xi_{G.P.1} \cdot \frac{\partial M_{3,2} \eta_{G.P.1}}{\partial \eta}$$

Control Point 6 (i=2, j=2)

$$R_{2,2}^{2,2} \xi_{G.P.1}, \eta_{G.P.1} = N_{2,2} \xi_{G.P.1} \cdot M_{2,2} \eta_{G.P.1}$$

$$\frac{\partial R_{2,2}^{2,2} \xi_{G.P.1}, \eta_{G.P.1}}{\partial \xi} = \frac{\partial N_{2,2} \xi_{G.P.1}}{\partial \xi} \cdot M_{2,2} \eta_{G.P.1}$$

$$\frac{\partial R_{2,2}^{2,2} \xi_{G.P.1}, \eta_{G.P.1}}{\partial \eta} = N_{2,2} \xi_{G.P.1} \cdot \frac{\partial M_{2,2} \eta_{G.P.1}}{\partial \eta}$$

Control Point 9 (i=3, j=3)

$$R_{3,3}^{2,2} \xi_{G.P.1}, \eta_{G.P.1} = N_{3,2} \xi_{G.P.1} \cdot M_{3,2} \eta_{G.P.1}$$

$$\frac{\partial R_{3,3}^{2,2} \xi_{G.P.1}, \eta_{G.P.1}}{\partial \xi} = \frac{\partial N_{3,2} \xi_{G.P.1}}{\partial \xi} \cdot M_{3,2} \eta_{G.P.1}$$

$$\frac{\partial R_{3,3}^{2,2} \xi_{G.P.1}, \eta_{G.P.1}}{\partial \eta} = N_{3,2} \xi_{G.P.1} \cdot \frac{\partial M_{3,2} \eta_{G.P.1}}{\partial \eta}$$

		element 1	G.P.1 (index $\xi=1$, index $\eta=1$)		
i	j		$R_{i,j}^{2,2}$	$dR_{i,j}^{2,2}/d\xi$	$dR_{i,j}^{2,2}/d\eta$
1	1	C.P.1	0,0625	-1,1250	-0,1250
1	2	C.P.2	0,1250	-2,2500	0,0000
1	3	C.P.3	0,0625	-1,1250	0,1250
2	1	C.P.4	0,1563	0,5625	-0,3125
2	2	C.P.5	0,3125	1,1250	0,0000
2	3	C.P.6	0,1563	0,5625	0,3125
3	1	C.P.7	0,0313	0,5625	-0,0625
3	2	C.P.8	0,0625	1,1250	0,0000
3	3	C.P.9	0,0313	0,5625	0,0625
		SUM	0,40625	-3,9375	-0,3125

Figure 2.79. NUR-B-Spline Surfaces and their derivatives. Parameter space $\Xi \times H$. Values at Gauss Points.

Isogeometric Analysis

$$\left[\begin{array}{c|ccccc} D_N & \xi_1, \eta_1 \\ \hline 2x9 & \frac{\partial R_{1,1}^{2,2}}{\partial \xi} & \frac{\partial R_{1,2}^{2,2}}{\partial \xi} & \frac{\partial R_{1,3}^{2,2}}{\partial \xi} & \frac{\partial R_{2,1}^{2,2}}{\partial \xi} & \frac{\partial R_{2,2}^{2,2}}{\partial \xi} & \frac{\partial R_{2,3}^{2,2}}{\partial \xi} & \frac{\partial R_{3,1}^{2,2}}{\partial \xi} & \frac{\partial R_{3,2}^{2,2}}{\partial \xi} & \frac{\partial R_{3,3}^{2,2}}{\partial \xi} \\ \hline \frac{\partial R_{1,1}^{2,2}}{\partial \eta} & \frac{\partial R_{1,2}^{2,2}}{\partial \eta} & \frac{\partial R_{1,3}^{2,2}}{\partial \eta} & \frac{\partial R_{2,1}^{2,2}}{\partial \eta} & \frac{\partial R_{2,2}^{2,2}}{\partial \eta} & \frac{\partial R_{2,3}^{2,2}}{\partial \eta} & \frac{\partial R_{3,1}^{2,2}}{\partial \eta} & \frac{\partial R_{3,2}^{2,2}}{\partial \eta} & \frac{\partial R_{3,3}^{2,2}}{\partial \eta} \end{array} \right] \Rightarrow$$

$$\left[\begin{array}{c|ccccc} D_N & \xi_1, \eta_1 \\ \hline 2x9 & -1,125 & -2,25 & -1,125 & 0,5625 & 1,125 & 0,5625 & 0,5625 & 1,125 & 0,5625 \\ \hline & -0,125 & 0 & 0,125 & -0,3125 & 0 & 0,3125 & -0,0625 & 0 & 0,0625 \end{array} \right]$$

$$\left[\begin{array}{c|cc} J & \xi_1, \eta_1 \\ \hline 2x2 & 10,13 & 0 \\ & 0 & 1,5 \end{array} \right] = \left[\begin{array}{c|cc} D_N & \xi_1, \eta_1 \\ \hline 2x9 & \end{array} \right] \cdot \left[\begin{array}{c|cc} X & Y \\ 9x2 & \end{array} \right] =$$

$$\left[\begin{array}{c|cc} B_1 & \xi_1, \eta_1 \\ \hline 3x4 & \end{array} \right] = \frac{1}{\det[J]} \cdot \left[\begin{array}{cccc} J_{22} & -J_{12} & 0 & 0 \\ 0 & 0 & -J_{21} & J_{11} \\ -J_{21} & J_{11} & J_{22} & -J_{12} \end{array} \right] = \left[\begin{array}{cccc} 0,0988 & 0 & 0 & 0 \\ 0 & 0 & 0 & 0,6667 \\ 0 & 0,6667 & 0,0988 & 0 \end{array} \right]$$

$$\left[\begin{array}{c|cc} B_2 & \xi_1, \eta_1 \\ \hline 4x18 & \end{array} \right] = \left[\begin{array}{cccccccccccccccc} \frac{\partial R_{1,1}^{2,2}}{\partial \xi} & 0 & \frac{\partial R_{1,2}^{2,2}}{\partial \xi} & 0 & \frac{\partial R_{1,3}^{2,2}}{\partial \xi} & 0 & \frac{\partial R_{2,1}^{2,2}}{\partial \xi} & 0 & \frac{\partial R_{2,2}^{2,2}}{\partial \xi} & 0 & \frac{\partial R_{2,3}^{2,2}}{\partial \xi} & 0 & \frac{\partial R_{3,1}^{2,2}}{\partial \xi} & 0 & \frac{\partial R_{3,2}^{2,2}}{\partial \xi} & 0 & \frac{\partial R_{3,3}^{2,2}}{\partial \xi} & 0 \\ \hline \frac{\partial R_{1,1}^{2,2}}{\partial \eta} & 0 & \frac{\partial R_{1,2}^{2,2}}{\partial \eta} & 0 & \frac{\partial R_{1,3}^{2,2}}{\partial \eta} & 0 & \frac{\partial R_{2,1}^{2,2}}{\partial \eta} & 0 & \frac{\partial R_{2,2}^{2,2}}{\partial \eta} & 0 & \frac{\partial R_{2,3}^{2,2}}{\partial \eta} & 0 & \frac{\partial R_{3,1}^{2,2}}{\partial \eta} & 0 & \frac{\partial R_{3,2}^{2,2}}{\partial \eta} & 0 & \frac{\partial R_{3,3}^{2,2}}{\partial \eta} & 0 \\ 0 & \frac{\partial R_{1,2}^{2,2}}{\partial \xi} & 0 & \frac{\partial R_{1,3}^{2,2}}{\partial \xi} & 0 & \frac{\partial R_{2,1}^{2,2}}{\partial \xi} & 0 & \frac{\partial R_{2,2}^{2,2}}{\partial \xi} & 0 & \frac{\partial R_{2,3}^{2,2}}{\partial \xi} & 0 & \frac{\partial R_{3,1}^{2,2}}{\partial \xi} & 0 & \frac{\partial R_{3,2}^{2,2}}{\partial \xi} & 0 & \frac{\partial R_{3,3}^{2,2}}{\partial \xi} & 0 \\ 0 & \frac{\partial R_{1,1}^{2,2}}{\partial \eta} & 0 & \frac{\partial R_{1,2}^{2,2}}{\partial \eta} & 0 & \frac{\partial R_{1,3}^{2,2}}{\partial \eta} & 0 & \frac{\partial R_{2,1}^{2,2}}{\partial \eta} & 0 & \frac{\partial R_{2,2}^{2,2}}{\partial \eta} & 0 & \frac{\partial R_{2,3}^{2,2}}{\partial \eta} & 0 & \frac{\partial R_{3,1}^{2,2}}{\partial \eta} & 0 & \frac{\partial R_{3,2}^{2,2}}{\partial \eta} & 0 \\ 0 & \frac{\partial R_{1,1}^{2,2}}{\partial \xi} & 0 & \frac{\partial R_{1,2}^{2,2}}{\partial \xi} & 0 & \frac{\partial R_{1,3}^{2,2}}{\partial \xi} & 0 & \frac{\partial R_{2,1}^{2,2}}{\partial \xi} & 0 & \frac{\partial R_{2,2}^{2,2}}{\partial \xi} & 0 & \frac{\partial R_{2,3}^{2,2}}{\partial \xi} & 0 & \frac{\partial R_{3,1}^{2,2}}{\partial \xi} & 0 & \frac{\partial R_{3,2}^{2,2}}{\partial \xi} & 0 \end{array} \right] \Rightarrow$$

$$\left[\begin{array}{c|cc} B_2 & \xi_1, \eta_1 \\ \hline 4x18 & \end{array} \right] = \left[\begin{array}{cccccccccccccccc} -1,13 & 0 & -2,25 & 0 & -1,13 & 0 & 0,56 & 0 & 1,13 & 0 & 0,56 & 0 & 0,56 & 0 & 1,13 & 0 & 0,56 & 0 \\ -0,13 & 0 & 0 & 0 & 0,13 & 0 & -0,31 & 0 & 0 & 0 & 0,31 & 0 & -0,06 & 0 & 0 & 0 & 0,06 & 0 \\ 0 & -1,13 & 0 & -2,25 & 0 & -1,13 & 0 & 0,56 & 0 & 1,13 & 0 & 0,56 & 0 & 0,56 & 0 & 1,13 & 0 & 0,56 \\ 0 & -0,13 & 0 & 0 & 0 & 0,13 & 0 & -0,31 & 0 & 0 & 0 & 0,31 & 0 & -0,06 & 0 & 0 & 0 & 0,06 \end{array} \right]$$

The deformation matrix (isogeometric element 1, Gauss Point 1) is equal to:

$$\left[\begin{array}{c|cc} B & \xi_1, \eta_1 \\ \hline 3x18 & \end{array} \right] = \left[\begin{array}{c|cc} B_1 & \xi_1, \eta_1 \\ \hline 3x4 & \end{array} \right] \cdot \left[\begin{array}{c|cc} B_2 & \xi_1, \eta_1 \\ \hline 4x18 & \end{array} \right] \Rightarrow$$

B(ξ, η)																			
	u C.P.1	v C.P.1	u C.P.2	v C.P.2	u C.P.3	v C.P.3	u C.P.4	v C.P.4	u C.P.5	v C.P.5	u C.P.6	v C.P.6	u C.P.7	v C.P.7	u C.P.8	v C.P.8	u C.P.9	v C.P.9	
element 1	$-0,1111$	0	-0,2222	0	-0,1111	0	0,0556	0	0,1111	0	0,0556	0	0,0556	0	0,1111	0	0,0556	0	
ϵ_x	0	-0,0833	0	0,0000	0	0,0833	0	-0,2083	0	0,0000	0	0,2083	0	-0,0417	0	0,0000	0	0,0417	
ϵ_y	0	0	-0,0833	0	0,0000	-0,2222	0,0833	-0,1111	-0,2083	0,0556	0,0000	0,1111	0,2083	0,0556	-0,0417	0,0556	0,0000	0,1111	0,0417
ϵ_{xy}	-0,0833	-0,1111	0,0000	-0,2222	0,0833	-0,1111	-0,2083	0,0556	0,0000	0,1111	0,2083	0,0556	-0,0417	0,0556	0,0000	0,1111	0,0417	0,0556	

Figure 2.80. Deformation Matrix. Isogeometric Element 1. Gauss Point 1. Global numbering of Control Points.

The weight factor of Gauss Point 1 (isogeometric element 1) is equal to:

$$w_1 = \frac{w \xi_1}{n-p} \cdot \frac{w \eta_1}{m-q} = \frac{0,56888}{11-2} \cdot \frac{0,56888}{3-2} \Rightarrow w_1 = 0,03595$$

Isogeometric Analysis

The local stiffness matrix (isogeometric element 1, Gauss Point 1) is equal to:

$$k_{G.P.1}^{\text{ell}} = \begin{bmatrix} B^{\text{ell}} & \xi_1, \eta_1 \end{bmatrix}_{18 \times 18}^T \cdot E \cdot \begin{bmatrix} B^{\text{ell}} & \xi_1, \eta_1 \end{bmatrix}_{3 \times 3} \cdot t \cdot \det \begin{bmatrix} J & \xi_1, \eta_1 \end{bmatrix}_{3 \times 18} \cdot w_1$$

		Excel																			
		local [k] (Isogeometric Element 1. Gauss Point 1. Global numbering of C.P.)																			
		C.P.1		C.P.2		C.P.3		C.P.4		C.P.5		C.P.6		C.P.7		C.P.8		C.P.9			
		u (m)	v (m)	u (m)	v (m)	u (m)	v (m)	u (m)	v (m)	u (m)	v (m)	u (m)	v (m)	u (m)	v (m)	u (m)	v (m)	u (m)	v (m)	u (m)	v (m)
element1	C.P.1	F _x (kN)	18.623	7.585	31.119	8.169	12.496	583	-122	6.710	-15.559	-4.084	-15.438	-10.794	-6.248	-292	-15.559	-4.084	-9.311	-3.793	
		F _y (kN)	7.585	14.198	7.002	10.892	-583	-3.306	8.460	19.157	-3.501	-5.446	-11.961	-24.603	292	1.653	-3.501	-5.446	-3.793	-7.099	
	C.P.2	F _x (kN)	31.119	7.002	62.237	0	31.119	-7.002	-15.559	17.504	-31.119	0	-15.559	-17.504	-15.559	3.501	-31.119	0	-15.559	-3.501	
		F _y (kN)	8.169	10.892	0	21.783	-8.169	10.892	20.422	-5.446	0	-10.892	-20.422	-5.446	4.084	-5.446	0	-10.892	-4.084	-5.446	
	C.P.3	F _x (kN)	12.496	-583	31.119	-8.169	18.623	-7.585	-15.438	10.794	-15.559	4.084	-122	-6.710	-9.311	3.793	-15.559	4.084	-6.248	292	
		F _y (kN)	583	-3.306	-7.002	10.892	-7.585	14.198	11.961	-24.603	3.501	-5.446	-8.460	19.157	3.793	-7.099	3.501	-5.446	-292	1.653	
	C.P.4	F _x (kN)	-122	8.460	-15.559	20.422	-15.438	11.961	23.035	-9.481	7.780	-10.211	-15.255	-729	7.719	-5.981	7.780	-10.211	61	-4.230	
		F _y (kN)	6.710	19.157	17.504	-5.446	10.794	-24.603	-9.481	56.062	2.723	729	-53.339	5.397	12.302	-8.752	2.723	-3.355	-9.579		
	C.P.5	F _x (kN)	-15.559	-3.501	-31.119	0	-15.559	3.501	7.780	-8.752	15.559	0	7.780	8.752	1.750	15.559	0	7.780	1.750		
		F _y (kN)	-4.084	-5.446	0	-10.892	4.084	-5.446	-10.211	2.723	0	5.446	10.211	2.723	-2.042	2.723	0	5.446	2.042	2.723	
	C.P.6	F _x (kN)	-15.438	-11.961	-15.559	-20.422	-122	-8.460	-15.255	729	7.780	10.211	23.035	9.481	61	4.230	7.780	10.211	7.719	5.981	
		F _y (kN)	-10.794	-24.603	-17.504	-5.446	-6.710	19.157	-729	-53.339	8.752	2.723	9.481	56.062	3.355	-9.579	8.752	2.723	5.397	12.302	
	C.P.7	F _x (kN)	-6.248	292	-15.559	4.084	-9.311	3.793	-7.099	-5.981	12.302	-1.750	2.723	4.230	-9.579	-1.896	3.549	-1.750	2.723	146	-827
		F _y (kN)	-292	1.653	3.501	-5.446	3.793	-7.099	-5.981	12.302	-1.750	2.723	4.230	-9.579	-1.896	3.549	-1.750	2.723	146	-827	
	C.P.8	F _x (kN)	-15.559	-3.501	-31.119	0	-15.559	3.501	7.780	-8.752	15.559	0	7.780	8.752	1.750	15.559	0	7.780	1.750		
		F _y (kN)	-4.084	-5.446	0	-10.892	4.084	-5.446	-10.211	2.723	0	5.446	10.211	2.723	-2.042	2.723	0	5.446	2.042	2.723	
	C.P.9	F _x (kN)	-9.311	-3.793	-15.559	-4.084	-6.248	-292	61	-3.355	7.780	2.042	7.719	5.397	3.124	146	7.780	2.042	4.656	1.896	
		F _y (kN)	-3.793	-7.099	-3.501	-5.446	292	1.653	-4.230	-9.579	1.750	2.723	5.981	12.302	-146	-827	1.750	2.723	1.896	3.549	

Figure 2.81. Stiffness Matrix. Isogeometric Element 1. Gauss Point 1. Global numbering of Control Points. Excel.

		MatLab																			
		local [k] (Isogeometric Element 1. Gauss Point 1. Global numbering of C.P.)																			
		C.P.1		C.P.2		C.P.3		C.P.4		C.P.5		C.P.6		C.P.7		C.P.8		C.P.9			
		u (m)	v (m)	u (m)	v (m)	u (m)	v (m)	u (m)	v (m)	u (m)	v (m)	u (m)	v (m)	u (m)	v (m)	u (m)	v (m)	u (m)	v (m)	u (m)	v (m)
element1	C.P.1	F _x (kN)	18.623	7.585	31.119	8.169	12.496	583	-122	6.710	-15.559	-4.084	-15.438	-10.794	-6.248	-292	-15.559	-4.084	-9.311	-3.793	
		F _y (kN)	7.585	14.198	7.002	10.892	-583	-3.306	8.460	19.157	-3.501	-5.446	-11.961	-24.603	292	1.653	-3.501	-5.446	-3.793	-7.099	
	C.P.2	F _x (kN)	31.119	7.002	62.237	0	31.119	-7.002	-15.559	17.504	-31.119	0	-15.559	-17.504	-15.559	3.501	-31.119	0	-15.559	-3.501	
		F _y (kN)	8.169	10.892	0	21.783	-8.169	10.892	20.422	-5.446	0	-10.892	-20.422	-5.446	4.084	-5.446	0	-10.892	-4.084	-5.446	
	C.P.3	F _x (kN)	12.496	-583	31.119	-8.169	18.623	-7.585	-15.438	10.794	-15.559	4.084	-122	-6.710	-9.311	3.793	-15.559	4.084	-6.248	292	
		F _y (kN)	583	-3.306	-7.002	10.892	-7.585	14.198	11.961	-24.603	3.501	-5.446	-8.460	19.157	3.793	-7.099	3.501	-5.446	-292	1.653	
	C.P.4	F _x (kN)	-122	8.460	-15.559	20.422	-15.438	11.961	23.035	-9.481	7.780	-10.211	-15.255	-729	7.719	-5.981	7.780	-10.211	61	-4.230	
		F _y (kN)	6.710	19.157	17.504	-5.446	10.794	-24.603	-9.481	56.062	-8.752	2.723	729	-53.339	-5.397	12.302	-8.752	2.723	-3.355	-9.579	
	C.P.5	F _x (kN)	-15.559	-3.501	-31.119	0	-15.559	3.501	7.780	-8.752	15.559	0	7.780	8.752	1.750	15.559	0	7.780	1.750		
		F _y (kN)	-4.084	-5.446	0	-10.892	4.084	-5.446	-10.211	2.723	0	5.446	10.211	2.723	-2.042	2.723	0	5.446	2.042	2.723	
	C.P.6	F _x (kN)	-15.438	-11.961	-15.559	-20.422	-122	-8.460	-15.255	729	7.780	10.211	23.035	9.481	61	4.230	7.780	10.211	7.719	5.981	
		F _y (kN)	-10.794	-24.603	-17.504	-5.446	-6.710	19.157	-729	-53.339	8.752	2.723	9.481	56.062	3.355	-9.579	8.752	2.723	5.397	12.302	
	C.P.7	F _x (kN)	-6.248	292	-15.559	4.084	-9.311	3.793	-7.099	-5.981	12.302	-1.750	2.723	4.230	-9.579	-1.896	3.549	-1.750	2.723	146	-827
		F _y (kN)	-292	1.653	3.501	-5.446	3.793	-7.099	-5.981	12.302	-1.750	2.723	4.230	-9.579	-1.896	3.549	-1.750	2.723	146	-827	
	C.P.8	F _x (kN)	-15.559	-3.501	-31.119	0	-15.559	3.501	7.780	-8.752	15.559	0	7.780	8.752	1.750	15.559	0	7.780	1.750		
		F _y (kN)	-4.084	-5.446	0	-10.892	4.084	-5.446	-10.211	2.723	0	5.446	10.211	2.723	-2.042	2.723	0	5.446	2.042	2.723	
	C.P.9	F _x (kN)	-9.311	-3.793	-15.559	-4.084	-6.248	-292	61	-3.355	7.780	2.042	7.719	5.397	3.124	146	7.780	2.042	4.656	1.896	
		F _y (kN)	-3.793	-7.099	-3.501	-5.446	292	1.653	-4.230	-9.579	1.750	2.723	5.981	12.302	-146	-827	1.750	2.723	1.896	3.549	

Figure 2.82. Stiffness Matrix. Isogeometric Element 1. Gauss Point 1. Global numbering of Control Points. MatLab.

I follow the same procedure for the rest 24 Gauss Points of isogeometric element 1.

Isogeometric Element's 1 local stiffness matrix is equal to:

Isogeometric Analysis

$$\left[\begin{matrix} k^e \\ 18 \times 18 \end{matrix} \right] = \sum_{i=1}^{25} \left[\begin{matrix} k_{G.P.i}^e \\ 18 \times 18 \end{matrix} \right] = \sum_{i=1}^{25} \left\{ \left[\begin{matrix} B^e & \xi_i, \eta_i \\ 18 \times 3 & \end{matrix} \right]^T \cdot \left[\begin{matrix} E \\ 3 \times 3 \end{matrix} \right] \cdot \left[\begin{matrix} B^e & \xi_i, \eta_i \\ 3 \times 18 & \end{matrix} \right] \cdot t \cdot \det \left[\begin{matrix} J & \xi_i, \eta_i \\ 3 \times 3 & \end{matrix} \right] \cdot w_i \right\}$$

MatLab																			
local [k] (Isogeometric Element 1. Global numbering of C.P.)																			
	C.P.1	C.P.2		C.P.3		C.P.4		C.P.5		C.P.6		C.P.7		C.P.8		C.P.9			
element1	u (m)	v (m)	u (m)	v (m)	u (m)	v (m)	u (m)	v (m)	u (m)	v (m)	u (m)	v (m)	u (m)	v (m)	u (m)	v (m)	u (m)	v (m)	
	Fx (kN)	910.590	375.000	257.860	19.230	20.140	9.620	-400.040	-24.040	-303.220	-208.330	-135.480	-104.170	-196.460	-4.810	-111.690	-41.670	-41.720	
	Fy (kN)	375.000	813.710	-19.230	-157.250	-9.620	-240.450	24.040	118.740	-208.330	-235.500	-104.170	-176.790	4.810	-35.010	-41.670	-55.970	-20.830	
	Fx (kN)	257.860	-19.230	672.880	0	257.860	19.230	-303.220	208.330	-232.290	0	-303.220	-208.330	-111.690	41.670	-126.480	0	-111.690	-41.670
	Fy (kN)	19.230	-157.250	0	730.510	-19.230	-157.250	208.330	-235.500	0	177.450	-208.330	-235.500	41.670	-55.970	0	-10.520	-41.670	-55.970
	Fx (kN)	20.140	-9.620	257.860	-19.230	910.590	-375.000	-135.480	104.170	-303.220	208.330	-400.040	24.040	-41.720	20.830	-111.690	41.670	-196.460	4.810
	Fy (kN)	9.620	-240.450	19.230	-157.250	-375.000	813.710	104.170	-176.790	208.330	-235.500	-24.040	118.740	20.830	-31.480	41.670	-55.970	-4.810	-35.010
	Fx (kN)	-400.040	24.040	-303.220	208.330	-135.480	104.170	755.840	-93.750	167.020	-4.810	-14.620	-2.400	25.610	-103.370	-54.500	-88.140	-40.600	-44.070
	Fy (kN)	-24.040	118.740	208.330	-235.500	104.170	-176.790	-93.750	793.290	4.810	-205.920	2.400	-269.490	-84.130	177.710	-78.530	-103.450	-39.260	-98.590
	Fx (kN)	303.220	-208.330	-232.290	0	-303.220	208.330	167.020	4.810	574.190	0	167.020	-4.810	-54.500	88.140	39.510	-54.500	-88.140	-58.140
	Fy (kN)	-208.330	-235.500	0	177.450	208.330	-235.500	-4.810	-205.920	0	729.720	4.810	-205.920	78.530	-103.450	0	182.580	-78.530	-103.450
	Fx (kN)	135.480	-104.170	-303.220	-208.330	-400.040	-24.040	-14.620	2.400	167.020	4.810	755.840	93.750	-40.600	44.070	-54.500	88.140	25.610	103.370
	Fy (kN)	-104.170	-176.790	-208.330	-235.500	24.040	118.740	-2.400	-269.490	-4.810	-205.920	93.750	793.290	39.260	-98.590	78.530	-103.450	84.130	177.710
	Fx (kN)	-196.460	4.810	-111.690	41.670	-41.720	20.830	25.610	-84.130	-54.500	78.530	-40.600	39.260	283.030	-93.750	110.110	-4.810	26.230	-2.400
	Fy (kN)	-4.810	-35.010	41.670	-55.970	20.830	-31.480	-103.370	177.710	88.140	-103.450	44.070	-98.590	-93.750	177.810	4.810	-840	2.400	-30.190
	Fx (kN)	-111.690	-41.670	-126.480	0	-111.690	41.670	-54.500	-78.530	59.310	0	-54.500	78.530	110.110	4.810	199.160	0	110.110	-4.810
	Fy (kN)	-41.670	-55.970	0	-10.520	41.670	-55.970	-88.140	-103.450	0	182.580	88.140	-103.450	-4.810	-840	0	148.450	4.810	-840
	Fx (kN)	-41.720	-20.830	-111.690	-41.670	-196.460	-4.810	-40.600	-39.260	-54.500	-78.530	25.610	84.130	26.230	2.400	110.110	4.810	283.030	93.750
	Fy (kN)	-3.793	-7.099	-3.501	-5.446	292	1.653	-4.230	-9.579	1.750	2.723	5.981	12.302	-146	-827	1.750	2.723	1.896	3.549

Figure 2.83. Stiffness Matrix. Isogeometric Element 1. Global numbering of Control Points. MatLab.

Total Stiffness Matrix [K]

I calculate the local (numbering) Stiffness Matrix for every Isogeometric Element. Then, I form the total Stiffness Matrix of the structure.

Figure 2.84. Total Stiffness Matrix. (66x66)

Two Degrees of Freedom correspond to every Control Point, the horizontal u and the vertical v displacement. The cantilever's total Stiffness Matrix is a symmetric square matrix with dimensions 66×66 , as there are 33 Control Points and $33 \cdot 2 = 66$ Degrees of Freedom.

Control Points' External Forces {P}

I calculate the External Load Vector (66x1) and I reorder it.

$$\underset{(66 \times 1)}{F_{\text{tot}}} = \begin{bmatrix} 0 & \dots & 0 & -1000 & 0 & -1000 & 0 & -1000 \end{bmatrix}^T$$

$$\underset{(66 \times 1)}{F_{\text{tot,m}}} = \begin{bmatrix} F_f \\ F_s \end{bmatrix} = \begin{bmatrix} 0 & \dots & 0 & -1000 & 0 & -1000 & 0 & -1000 \\ 0 \\ 0 \end{bmatrix}^T$$

Control Points' Displacements {U}

I reorder the Total Stiffness Matrix and the External Load Vector and then I form the balance equation. I symbolize the unknown displacements with subscript f and the known ones (fixed Control Points) with s.

$$F_{\text{tot,m}} = [K_{\text{tot,m}}] \cdot U_{\text{tot,m}} \Rightarrow \begin{bmatrix} F_f \\ F_s \end{bmatrix} = \begin{bmatrix} K_{ff} & K_{fs} \\ K_{sf} & K_{ss} \end{bmatrix} \cdot \begin{bmatrix} U_f \\ U_s \end{bmatrix} \Rightarrow$$

$$\begin{bmatrix} 0 \\ \dots \\ 0 \\ -1000 \\ 0 \\ -1000 \\ 0 \\ -1000 \\ 0 \\ -1000 \\ 0 \\ 0 \end{bmatrix}_{60 \times 1} = \begin{bmatrix} K_{ff} & K_{fs} \\ K_{sf} & K_{ss} \end{bmatrix} \cdot \begin{bmatrix} U_f \\ U_s \end{bmatrix}_{6 \times 1} \Rightarrow \begin{bmatrix} U_f \\ U_s \end{bmatrix}_{6 \times 1} = \begin{bmatrix} 0 \\ \dots \\ 0 \\ -1000 \\ 0 \\ -1000 \\ 0 \\ -1000 \\ 0 \\ -1000 \\ 0 \\ 0 \end{bmatrix}_{60 \times 1}$$

Figure 2.85 shows Control Points' horizontal and vertical displacement.

The maximum horizontal displacement is equal to 10,6cm and corresponds to C.P.31 (-10,6m) and C.P.33 (10,6cm).

The maximum vertical displacement is equal to 72,1cm and corresponds to C.P.31 (-72,1cm), C.P.32 (-72,1cm) and C.P.33 (-72,1cm). Negative value displays that maximum displacement's direction is the negative direction of axis Y, means these Control Points move downstairs as expected.

	horizontal u (cm)	vertical v (cm)
C.P. 1	0,0	0,0
C.P. 2	0,0	0,0
C.P. 3	0,0	0,0
C.P. 4	-1,9	-1,0
C.P. 5	0,0	-0,1
C.P. 6	1,9	-1,0
C.P. 7	-3,8	-4,1
C.P. 8	0,0	-3,7
C.P. 9	3,8	-4,1
C.P. 10	-5,4	-8,9
C.P. 11	0,0	-8,4
C.P. 12	5,4	-8,9
C.P. 13	-6,8	-15,1
C.P. 14	0,0	-14,7
C.P. 15	6,8	-15,1
C.P. 16	-7,9	-22,7
C.P. 17	0,0	-22,3
C.P. 18	7,9	-22,7
C.P. 19	-8,9	-31,3
C.P. 20	0,0	-31,0
C.P. 21	8,9	-31,3
C.P. 22	-9,7	-40,7
C.P. 23	0,0	-40,5
C.P. 24	9,7	-40,7
C.P. 25	-10,2	-50,8
C.P. 26	0,0	-50,7
C.P. 27	10,2	-50,8
C.P. 28	-10,5	-61,4
C.P. 29	0,0	-61,3
C.P. 30	10,5	-61,4
C.P. 31	-10,6	-72,1
C.P. 32	0,0	-72,1
C.P. 33	10,6	-72,1
max	10,6	0,0
min	-10,6	-72,1

Figure 2.85. Control Points' displacements.

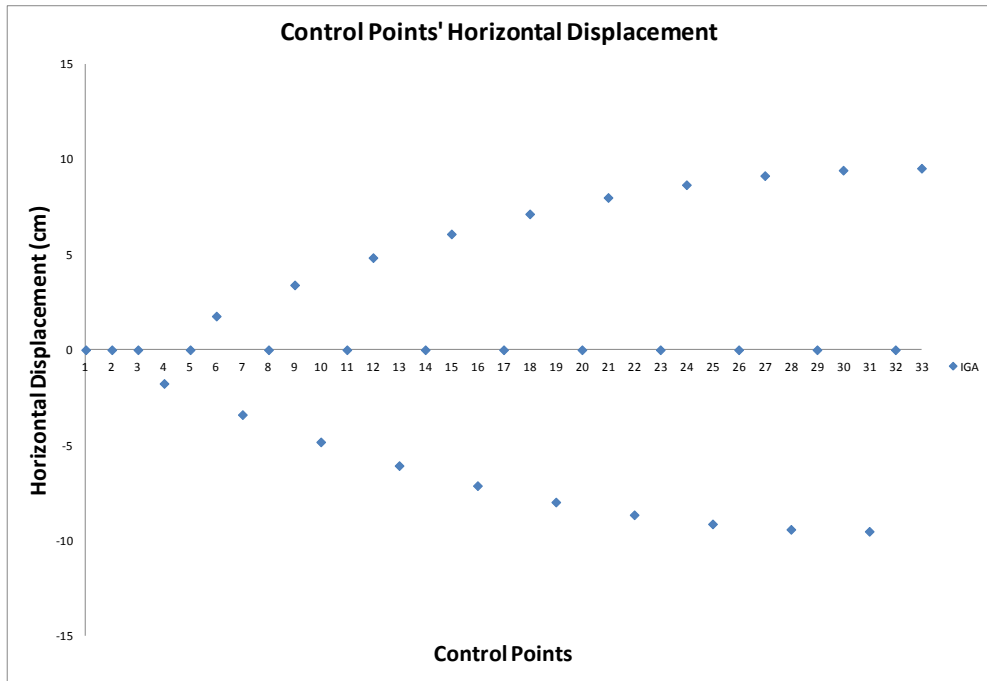


Figure 2.86.a. Control Points' horizontal displacement.

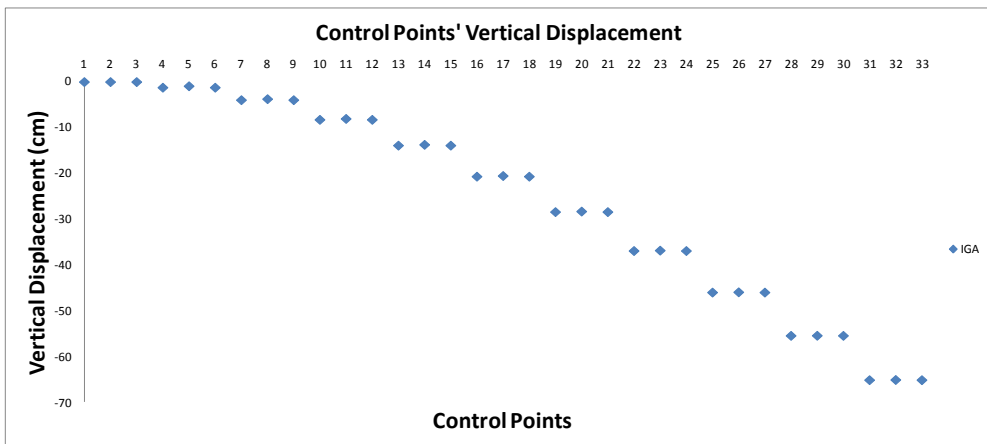


Figure 2.86.b. Control Points' vertical displacement.

Stress Field at Gauss Points

As I know Control Points' displacements, I can calculate the stress field at Isogeometric Elements' Gauss Points.

$$\sigma_{\xi_i, \eta_i} = E \cdot \varepsilon_{\xi_i, \eta_i} = E \cdot [B_{\xi_i, \eta_i}] \cdot d$$

where:

- $\sigma_{\xi_i, \eta_i} = \begin{cases} \sigma_X & \xi_i, \eta_i \\ \sigma_Y & \xi_i, \eta_i \\ \tau_{XY} & \xi_i, \eta_i \end{cases}$: stress field at Gauss Point i (plane stress problem)

Isogeometric Analysis

- $E_{3 \times 3} = \frac{E}{1-v^2} \cdot \begin{bmatrix} 1 & v & 0 \\ v & 1 & 0 \\ 0 & 0 & 1-v/2 \end{bmatrix}$ (plane stress problem)
- $\varepsilon_{\xi_i, \eta_i} = \varepsilon_X \xi_i, \eta_i - \varepsilon_Y \xi_i, \eta_i + \gamma_{XY} \xi_i, \eta_i^T$: strain field at Gauss Point i
- $d_{18 \times 1}$: This displacement vector refers to displacements of C.P. (local numbering).

Let's calculate the corresponding stress field to Gauss Point 1 of Isogeometric Element 1.

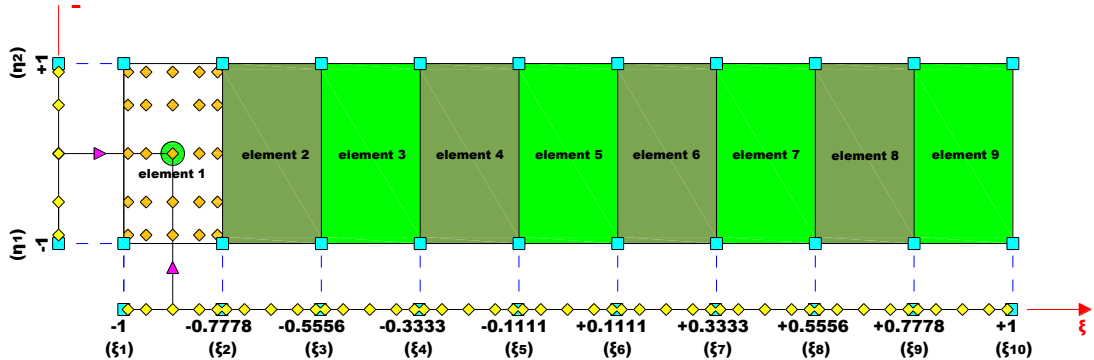


Figure 2.87. Gauss Point 1 of Isogeometric Element 1. (Parameter Space)

		(d) (m)
element 1	C.P.1	$u(m)$ 0,000 $v(m)$ 0,000
	C.P.2	$u(m)$ 0,000 $v(m)$ 0,000
	C.P.3	$u(m)$ 0,000 $v(m)$ 0,000
	C.P.4	$u(m)$ -0,019 $v(m)$ -0,010
	C.P.5	$u(m)$ 0,000 $v(m)$ -0,001
	C.P.6	$u(m)$ 0,019 $v(m)$ -0,010
	C.P.7	$u(m)$ -0,038 $v(m)$ -0,041
	C.P.8	$u(m)$ 0,000 $v(m)$ -0,037
	C.P.9	$u(m)$ 0,038 $v(m)$ -0,041

Figure 2.88. Control Points' vertical and horizontal displacement.
Isogeometric Element 1.

$$\sigma_{\xi_1, \eta_1} = E_{3 \times 3} \cdot [B]_{3 \times 18} \cdot d_{18 \times 1} = \begin{Bmatrix} 0 \\ 0 \\ 87.667 \end{Bmatrix} \text{ kPa} \Rightarrow \sigma_{\xi_1, \eta_1} = \begin{Bmatrix} 0 \\ 0 \\ 87.67 \end{Bmatrix} \text{ MPa}$$

Isogeometric Analysis

MPa	element 1			element 2			element 3			element 4			element 5		
	σ_{xx}	σ_{yy}	τ_{xy}												
G.P.1	0,00	0,00	87,67	0,00	0,00	-150,86	0,00	0,00	-89,47	0,00	0,00	-103,31	0,00	0,00	-100,52
G.P.2	2.395,53	-25,33	-6,42	2.218,12	51,53	-109,47	1.878,95	-19,14	-84,38	1.640,69	6,22	-86,07	1.355,93	-1,60	-87,40
G.P.3	1.423,47	-15,05	54,44	1.318,05	30,62	-136,25	1.116,51	-11,38	-87,67	974,93	3,70	-97,22	805,72	-0,95	-95,89
G.P.4	-2.395,53	25,33	-6,42	-2.218,12	-51,53	-109,47	-1.878,95	19,14	-84,38	-1.640,69	6,22	-86,07	-1.355,93	1,60	-87,40
G.P.5	-1.423,47	15,05	54,44	-1.318,05	-30,62	-136,25	-1.116,51	11,38	-87,67	-974,93	-3,70	-97,22	-805,72	0,95	-95,89
G.P.6	0,00	0,00	-190,23	0,00	0,00	-78,74	0,00	0,00	-121,23	0,00	0,00	-111,01	0,00	0,00	-112,90
G.P.7	2.388,40	-116,00	-120,47	2.010,00	33,34	-86,10	1.796,19	-10,12	-100,28	1.502,46	3,25	-98,63	1.237,35	-1,61	-98,66
G.P.8	1.419,23	-68,93	-165,60	1.194,38	19,81	-81,34	1.067,33	-6,01	-113,83	892,79	1,93	-106,64	735,26	-0,96	-107,87
G.P.9	-2.388,40	116,00	-120,47	-2.010,00	-33,34	-86,10	-1.796,19	10,12	-100,28	-1.502,46	-3,25	-98,63	-1.237,35	1,61	-98,66
G.P.10	-1.419,23	68,93	-165,60	-1.194,38	-19,81	-81,34	-1.067,33	6,01	-113,83	-892,79	-1,93	-106,64	-735,26	0,96	-107,87
G.P.11	0,00	0,00	24,38	0,00	0,00	-103,31	0,00	0,00	-106,36	0,00	0,00	-104,70	0,00	0,00	-105,13
G.P.12	2.367,20	-153,57	13,11	2.099,49	57,52	-90,88	1.828,13	-19,24	-91,85	1.559,05	6,13	-90,35	1.285,35	-1,99	-91,34
G.P.13	1.406,64	-91,25	20,40	1.247,56	34,18	-98,92	1.086,31	-11,44	-101,24	926,42	3,64	-99,63	763,78	-1,18	-100,26
G.P.14	-2.367,20	153,57	13,11	-2.099,49	-57,52	-90,88	-1.828,13	19,24	-91,85	-1.559,05	-6,13	-90,35	-1.285,35	1,99	-91,34
G.P.15	-1.406,64	91,25	20,40	-1.247,56	-34,18	-98,92	-1.086,31	11,44	-101,24	-926,42	-3,64	-99,63	-763,78	1,18	-100,26
G.P.16	0,00	0,00	-242,71	0,00	0,00	-261,96	0,00	0,00	-74,15	0,00	0,00	-122,01	0,00	0,00	-110,94
G.P.17	2.596,46	680,31	-424,63	2.384,45	-69,59	-171,81	1.975,31	17,15	-84,92	1.774,75	-4,68	-99,92	1.475,48	1,63	-98,94
G.P.18	1.542,87	404,25	-306,95	1.416,89	-43,35	-230,13	1.173,77	10,19	-77,95	1.054,59	-2,78	-114,21	876,76	0,97	-106,70
G.P.19	-2.596,46	-680,31	-424,63	-2.384,45	69,59	-171,81	-1.975,31	-17,15	-84,92	-1.774,75	4,68	-99,92	-1.475,48	-1,63	-98,94
G.P.20	-1.542,87	-404,25	-306,95	-1.416,89	41,35	-230,13	-1.173,77	-10,19	-77,95	-1.054,59	2,78	-114,21	-876,76	-0,97	-106,70
G.P.21	0,00	0,00	-55,15	0,00	0,00	-212,18	0,00	0,00	-78,38	0,00	0,00	-111,24	0,00	0,00	-103,96
G.P.22	2.492,07	319,98	206,85	2.322,00	-3,65	-141,81	1.934,57	-3,04	-82,72	1.720,85	1,42	-91,12	1.426,85	-0,07	-91,51
G.P.23	1.480,83	190,14	-108,71	1.379,78	-2,17	-187,34	1.149,56	-1,81	-79,91	1.022,56	0,84	-104,13	847,86	-0,04	-99,56
G.P.24	-2.492,07	-319,98	-206,85	-2.322,00	3,65	-141,81	-1.934,57	3,04	-82,72	-1.720,85	-1,42	-91,12	-1.426,85	0,07	-91,51
G.P.25	-1.480,83	-190,14	-108,71	-1.379,78	2,17	-187,34	-1.149,56	1,81	-79,91	-1.022,56	-0,84	-104,13	-847,86	0,04	-99,56
max	2.596,46	680,31	87,67	2.384,45	69,59	-78,74	1.975,31	19,24	-74,15	1.774,75	6,22	-86,07	1.475,48	1,99	-87,40
min	-2.596,46	-680,31	-424,63	-2.384,45	-69,59	-261,96	-1.975,31	-19,24	-121,23	-1.774,75	-6,22	-122,01	-1.475,48	-1,99	-112,90

Figure 2.89.a. Stress Field at Gauss Points. Isogeometric Elements 1-5.

	element 6			element 7			element 8			element 9		
	σ_{xx}	σ_{yy}	τ_{xy}									
G.P.1	0,00	0,00	-101,20	0,00	0,00	-100,69	0,00	0,00	-100,23	0,00	0,00	-107,53
G.P.2	1.089,02	-0,31	-86,30	812,17	1,50	-87,29	556,45	-1,17	-84,75	194,28	-6,91	-96,13
G.P.3	647,11	-0,18	-95,94	482,61	0,89	-95,96	330,65	-0,70	-94,77	115,45	-4,11	-103,50
G.P.4	-1.089,02	0,31	-86,30	-812,17	-1,50	-87,29	-556,45	1,17	-84,75	-194,28	6,91	-96,13
G.P.5	-647,11	0,18	-95,94	-482,61	-0,89	-95,96	-330,65	0,70	-94,77	-115,45	4,11	-103,50
G.P.6	0,00	0,00	-113,26	0,00	0,00	-112,77	0,00	0,00	-107,36	0,00	0,00	-99,32
G.P.7	966,11	2,17	-97,88	682,53	-4,95	-101,20	457,80	14,31	-88,16	82,31	1,01	-91,72
G.P.8	574,08	1,29	-107,83	405,57	-2,94	-108,68	272,03	8,50	-100,58	48,91	0,60	-96,63
G.P.9	-966,11	-2,17	-97,88	-682,53	4,95	-101,20	-457,80	-14,31	-88,16	-82,31	-1,01	-91,72
G.P.10	-574,08	-1,29	-107,83	-405,57	2,94	-108,68	-272,03	-8,50	-100,58	-48,91	-0,60	-96,63
G.P.11	0,00	0,00	-105,50	0,00	0,00	-104,90	0,00	0,00	-102,07	0,00	0,00	-101,73
G.P.12	1.015,93	1,00	-90,31	735,32	-1,70	-92,60	497,44	6,75	-84,39	120,22	-3,75	-92,82
G.P.13	603,69	0,59	-100,14	436,94	-1,01	-100,56	295,59	4,01	-95,83	71,44	-2,23	-98,58
G.P.14	-1.015,93	-1,00	-90,31	-735,32	1,70	-92,60	-497,44	-6,75	-84,39	-120,22	3,75	-92,82
G.P.15	-603,69	-0,59	-100,14	-436,94	1,01	-100,56	-295,59	-4,01	-95,83	-71,44	2,23	-98,58
G.P.16	0,00	0,00	-112,91	0,00	0,00	-113,17	0,00	0,00	-112,97	0,00	0,00	-110,84
G.P.17	1.212,34	-1,40	-98,51	940,24	2,69	-97,93	658,29	-6,02	-101,21	413,09	11,35	-92,36
G.P.18	720,39	-0,83	-107,83	558,71	1,60	-107,79	391,17	-3,58	-108,81	245,46	6,75	-104,32
G.P.19	-1.212,34	1,40	-98,51	-940,24	-2,69	-97,93	-658,29	6,02	-101,21	-413,09	-11,35	-92,36
G.P.20	-720,39	0,83	-107,83	-558,71	-1,60	-107,79	-391,17	3,58	-108,81	-245,46	-6,75	-104,32
G.P.21	0,00	0,00	-105,29	0,00	0,00	-105,14	0,00	0,00	-105,40	0,00	0,00	-112,26
G.P.22	1.162,25	-1,12	-90,69	888,46	2,84	-90,65	616,58	-5,33	-92,14	303,72	-1,52	-97,29
G.P.23	690,63	-0,67	-100,14	527,94	1,69	-100,03	366,38	-3,17	-100,72	180,48	-0,91	-106,97
G.P.24	-1.162,25	1,12	-90,69	-888,46	-2,84	-90,65	-616,58	5,33	-92,14	-303,72	1,52	-97,29
G.P.25	-690,63	0,67	-100,14	-527,94	-1,69	-100,03	-366,38	3,17	-100,72	-180,48	0,91	-106,97
max	1.212,34	2,17	-86,30	940,24	4,95	-87,29	658,29	14,31	-84,39	413,09	11,35	-91,72
min	-1.212,34	-2,17	-113,26	-940,24	-4,95	-113,17	-658,29	-14,31	-112,97	-413,09	-11,35	-112,90

Figure 2.89.b. Stress Field at Gauss Points. Isogeometric Elements 6-9.

		(Isogeometric Element, G.P.)	
	max	(1,17)	2.596,46
σ_{xx} (MPa)	min	(1,19)	-2.596,46
	max	(1,17)	680,31
σ_{yy} (MPa)	min	(1,19)	-680,31
	max	(1,1)	87,67
τ_{xy} (MPa)	min	(1,17), (1,19)	-424,63

Figure 2.90. Maximum and Minimum Stress.

Figure 2.89 depicts stresses at Isogeometric Elements' Gauss Points, while Figure 2.90 shows maximum and minimum stress.

As expected, element 1 (nearest to fixed boundary) suffer from larger stresses. It is a cantilever under concentrated load $P=3.000$ kN at free edge, so the upper horizontal side suffers from tension and the lower horizontal side suffers from compression. Maximum bending moment occurs at fixed edge.

$$M_{\max} = -P \cdot L = -3.000 \text{ kN} \cdot 15 \text{ m} = -45.000 \text{ kNm}$$

Element 1 (G.P.17, nearest to upper horizontal side) experience the largest tension. Tensile stresses are equal to:

$$\begin{aligned} \max \sigma_{xx}^+ &= 2.596,46 \text{ MPa} \\ \max \sigma_{yy}^+ &= 680,31 \text{ MPa} \end{aligned}$$

Element 1 (G.P.19, nearest to lower horizontal side) experience the largest compression. Compressive stresses are equal to:

$$\begin{aligned} \max \sigma_{xx}^- &= -2.596,46 \text{ MPa} \\ \max \sigma_{yy}^- &= -680,31 \text{ MPa} \end{aligned}$$

2.3.2. Finite Element Analysis

I will solve the same problem applying Finite Element Method. In order to reach a safe conclusion, I have maintained as many nodes (FEA) as control points (IGA), means I have used 33 nodes with the same global numbering. The two (FEA, IGA) outgoing stiffness matrices will have the same dimensions (66x66). The nodes have the same distance between each other along the length and the height.

As it is a plane stress problem, the two stiffness matrices have both 66 rows and 66 columns. ($2 \cdot 33 = 66$, 66×66).

I use the following analysis parameters:

- **n=33 Nodes.** It is important to underline that number of Nodes is equal to shape functions' number. Cartesian coordinate system's origin is the extreme left and bottom corner.
- **p=2.** The shape functions are quadratic, as I used 9-noded (Lagrange) Finite Elements.
- **9 2D 4-sided, 9-noded (Lagrange) Finite Elements.** I have simulated the structure with 9 2D 4-sided 9-noded (Lagrange) Finite Elements. Every element has the same geometry and nodes. So, the local stiffness matrix is the same. The parametric axis ξ (parameter space) is parallel to cantilever's length (physical space), means horizontal. Its direction is from left to right. The parametric axis η (parameter space) is parallel to cantilever's height (physical space), means vertical. Its direction is from bottom to cantilever's top. In FEA, the parameter space is local to every element.

Method	FEA
Finite Elements (Number)	9
Finite Elements (Type)	2D
	4-sided
	9-noded
	isoparametric
Gauss Points	5x5

Figure 2.91. Analysis Parameters.

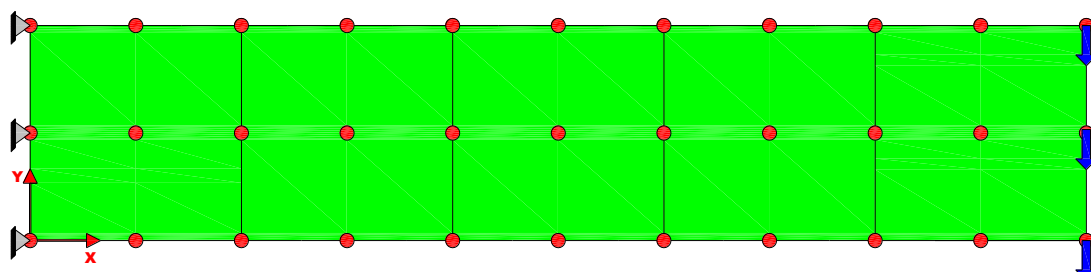
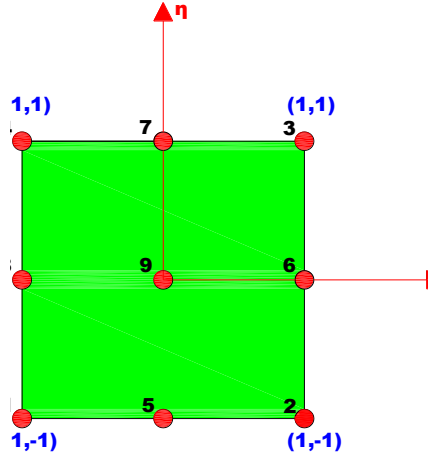


Figure 2.92. Cantilever Profile. (Cartesian Axes. Nodes.)

Isoparametric 2D 4-sided 9-noded (Lagrange) Finite Element

It is a plane stress problem. I have used isoparametric 2-D 4-sided 9-noded (Lagrange) Finite Elements. Each one has 9 nodes and $2 \cdot 9 = 18$ degrees of freedom, as each node corresponds to 2 degrees of freedom (horizontal and vertical displacement).



**Figure 2.93. Isoparametric 2D 4-sided 9-noded (Lagrange) Finite Element.
Parameter Space. Local Numbering.**

Shape functions

The shape functions and their partial derivatives with respect to ξ, η are equal to:

$$\begin{aligned}
 N_1 &= \frac{1}{4}\xi\eta(1-\xi)(1-\eta) & N_5 &= -\frac{1}{2}\eta(1-\xi^2)(1-\eta) \\
 N_2 &= -\frac{1}{4}\xi\eta(1+\xi)(1-\eta) & N_6 &= \frac{1}{2}\xi(1+\xi)(1-\eta^2) & N_9 &= 1-\xi^2(1-\eta^2) \\
 N_3 &= \frac{1}{4}\xi\eta(1+\xi)(1+\eta) & N_7 &= \frac{1}{2}\eta(1-\xi^2)(1+\eta) \\
 N_4 &= -\frac{1}{4}\xi\eta(1-\xi)(1+\eta) & N_8 &= -\frac{1}{2}\xi(1-\xi)(1-\eta^2)
 \end{aligned}$$

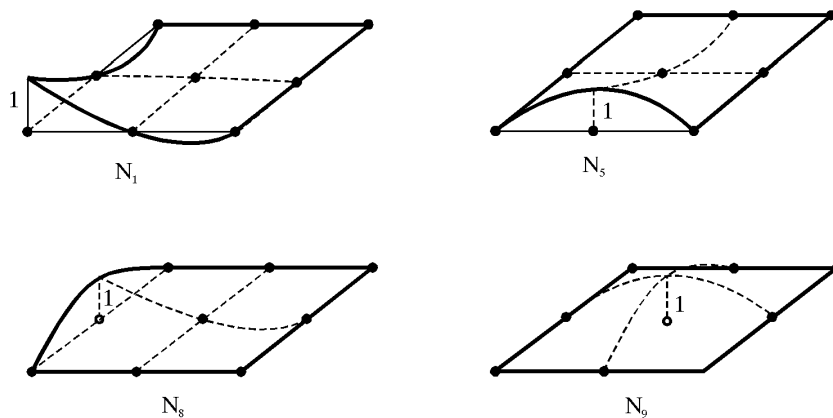


**Figure 2.94. Shape functions.
Isoparametric 2D Lagrange Finite Element.**

For every element $e = 1 \div 5$, I follow the below procedure.

Elasticity Matrix [E]

As it is a plane stress problem, the elasticity matrix [E] is equal to:

$$E_{3x3} = \frac{E}{1-v^2} \cdot \begin{bmatrix} 1 & v & 0 \\ v & 1 & 0 \\ 0 & 0 & \frac{1-v}{2} \end{bmatrix}$$

Deformation Matrix [B]

I calculate the deformation matrix.

$$\begin{bmatrix} B_e & \xi, \eta \end{bmatrix}_{3x18} = \begin{bmatrix} B_{1,e} & \xi, \eta \end{bmatrix}_{3x4} \cdot \begin{bmatrix} B_{2,e} & \xi, \eta \end{bmatrix}_{4x18}$$

where:

$$\begin{bmatrix} B_{1,e} & \xi, \eta \end{bmatrix}_{3x4} = \frac{1}{\det[J_e \quad \xi, \eta]} \cdot \begin{bmatrix} J_{e,22} & \xi, \eta & -J_{e,12} & \xi, \eta & 0 & 0 \\ 0 & 0 & -J_{e,21} & \xi, \eta & J_{e,11} & \xi, \eta \\ -J_{e,21} & \xi, \eta & J_{e,11} & \xi, \eta & J_{e,22} & \xi, \eta \\ -J_{e,12} & \xi, \eta & \end{bmatrix}$$

$$\begin{bmatrix} J_e & \xi, \eta \end{bmatrix}_{2x2} = \begin{bmatrix} D_N & \xi, \eta \end{bmatrix}_{2x9} \cdot X Y_e = \begin{bmatrix} N_{1,\xi} & \xi, \eta & N_{2,\xi} & \xi, \eta & \dots & N_{9,\xi} & \xi, \eta \\ N_{1,\eta} & \xi, \eta & N_{2,\eta} & \xi, \eta & \dots & N_{9,\eta} & \xi, \eta \end{bmatrix}_{9x2} \cdot \begin{bmatrix} X_{1,e} & Y_{1,e} \\ X_{2,e} & Y_{2,e} \\ \dots & \dots \\ X_{9,e} & Y_{9,e} \end{bmatrix}$$

$X_{n,e}, Y_{n,e}$: Node's n (Finite Element e) Cartesian coordinates (local numbering)

$$\begin{bmatrix} B_{2,e} & \xi, \eta \end{bmatrix}_{4x18} = \begin{bmatrix} N_{1,\xi} & \xi, \eta & 0 & N_{2,\xi} & \xi, \eta & 0 & \dots & \dots & N_{9,\xi} & \xi, \eta & 0 \\ N_{1,\eta} & \xi, \eta & 0 & N_{2,\eta} & \xi, \eta & 0 & \dots & \dots & N_{9,\eta} & \xi, \eta & 0 \\ 0 & N_{1,\xi} & \xi, \eta & 0 & N_{2,\xi} & \xi, \eta & \dots & \dots & 0 & N_{9,\xi} & \xi, \eta \\ 0 & N_{1,\eta} & \xi, \eta & 0 & N_{2,\eta} & \xi, \eta & \dots & \dots & 0 & N_{9,\eta} & \xi, \eta \end{bmatrix}$$

Local Stiffness Matrix [k^e]

I produce the local stiffness matrix.

$$k_{e, 18x18} = \int_{-1}^1 \int_{-1}^1 \begin{bmatrix} B_e & \xi, \eta \end{bmatrix}_{18x3}^T \cdot E_{3x3} \cdot \begin{bmatrix} B_e & \xi, \eta \end{bmatrix}_{3x18} \cdot \det[J_e \quad \xi, \eta] d\xi d\eta$$

Isogeometric Analysis

I have calculated the double integral using numerical integration (integration rule 5x5).

$$k_e = \sum_{i=1}^5 \sum_{j=1}^5 \left\{ w_i \cdot w_j \cdot \left[B_e \xi_i, \eta_j \right]_{18 \times 3}^T \cdot E \cdot \left[B_e \xi_i, \eta_j \right]_{3 \times 3} \cdot t \cdot \det \left[J_e \xi_i, \eta_j \right]_{3 \times 18} \right\}$$

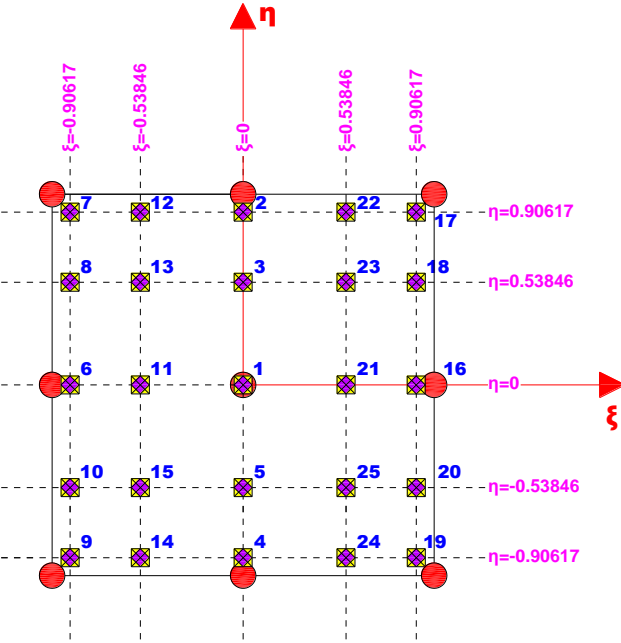


Figure 2.95. Gauss Points. (Local numbering.)
Isoparametric 2D 4-sided 9-noded (Lagrange) Finite Element.

Each Finite Element has the same local Stiffness Matrix, which is the following:

		local [k] (Isogeometric Element 1. Global numbering of Nodes.)																										
		Node 1			Node 7			Node 9			Node 3			Node 4			Node 8			Node 6			Node 2			Node 5		
		u (m)	v (m)	u (m)	v (m)	u (m)	v (m)	u (m)	v (m)	u (m)	v (m)	u (m)	v (m)	u (m)	v (m)	u (m)	v (m)	u (m)	v (m)	u (m)	v (m)	u (m)	v (m)	u (m)	v (m)			
element 1	Node 1	F _x (kN)	971.179	375.774	40.312	9.635	-34.741	-41.753	-143.399	-9.635	-696.880	-38.901	123.298	166.871	223.244	166.891	223.244	166.871	123.298	166.891	223.244	166.871	-554.122	-667.004				
	Node 1	F _y (kN)	375.774	971.179	-9.635	-143.399	-41.753	-34.741	9.635	40.312	38.121	71.109	166.891	223.244	166.871	123.298	-38.901	71.109	-38.120	223.244	-166.891	123.298	-166.871	-554.122	667.002			
Node 7	Node 7	F _x (kN)	40.312	-9.635	971.179	-375.774	-143.399	9.635	-34.741	41.753	-696.880	38.901	71.109	-38.120	223.244	-166.891	123.298	-166.871	223.244	-166.891	123.298	-166.871	-554.122	667.002				
	Node 7	F _y (kN)	9.635	-143.399	-375.774	971.178	-143.399	40.313	41.753	-34.741	38.121	71.108	38.902	-696.880	-166.871	123.299	-166.891	223.244	-166.871	123.299	-166.891	223.244	-166.871	-554.122	667.002			
Node 9	Node 9	F _x (kN)	-34.741	-41.753	-143.399	-9.635	971.178	375.774	40.313	9.635	-143.399	166.871	223.244	166.891	223.244	166.871	123.299	-38.902	38.120	-696.880	-166.871	123.299	166.871	-554.122	-667.001			
	Node 9	F _y (kN)	-41.753	-34.741	9.635	40.313	375.774	971.178	-9.635	-143.399	166.871	223.244	166.891	223.244	166.871	123.299	-38.902	38.120	71.108	166.891	223.244	-38.120	-667.001	-554.122				
Node 3	Node 3	F _x (kN)	-143.399	9.635	-34.741	41.753	40.313	-9.635	971.178	-375.774	-143.399	166.871	-38.901	123.299	-38.902	166.880	38.120	71.108	166.891	223.244	-38.120	166.890	667.002	-554.122	667.002			
	Node 3	F _y (kN)	-9.635	40.312	41.753	-34.741	9.635	-143.399	-375.774	971.179	-143.399	166.871	123.298	-166.891	223.244	-38.120	71.109	38.901	-166.890	223.244	-166.891	123.298	-166.890	667.002	-554.122	667.002		
Node 4	Node 4	F _x (kN)	-696.880	38.121	-38.121	223.244	166.871	223.244	-166.871	2.650.245	0	268.085	0	-554.122	-666.922	-266.350	0	-554.122	666.923	328.378	-1	0	-2.996.392	-1	-2.996.392			
	Node 4	F _y (kN)	-38.901	71.109	38.901	71.108	166.891	123.299	-166.891	123.298	0	3.447.738	-667.082	-554.122	0	268.085	667.083	-554.122	0	667.083	-554.122	0	-1	-2.996.392	-1	-2.996.392		
Node 8	Node 8	F _x (kN)	123.298	166.891	71.109	38.902	71.108	-38.902	123.299	-166.891	-554.122	-667.082	3.447.722	0	0	-554.122	667.081	268.085	0	-2.996.376	1	0	-2.996.376	1	-2.996.376			
	Node 8	F _y (kN)	166.871	223.244	-38.120	-696.880	38.120	-696.880	-166.871	223.244	-666.922	-554.122	0	2.650.239	666.920	-554.122	0	-266.350	0	-2.996.376	1	0	-2.996.376	1	-2.996.376			
Node 6	Node 6	F _x (kN)	223.244	166.871	223.244	-166.871	-696.880	38.120	-696.880	-38.120	-266.350	0	-554.122	666.920	2.650.239	0	-554.122	-666.922	-328.373	1	0	-2.996.376	1	-2.996.376				
	Node 6	F _y (kN)	166.891	223.298	-166.891	123.299	166.891	71.108	38.901	-554.122	667.083	268.085	0	-554.122	-667.082	3.447.722	0	-554.122	-667.082	-554.122	1	0	-2.996.392	-1	-2.996.392			
Node 2	Node 2	F _x (kN)	71.109	-38.901	123.298	-166.891	123.299	166.891	71.108	38.901	-554.122	667.083	268.085	0	-554.122	-667.082	3.447.738	0	-554.122	-667.082	3.447.738	0	-2.996.392	-1	-2.996.392			
	Node 2	F _y (kN)	38.121	-696.880	-166.871	223.244	166.871	223.244	-38.121	-696.880	666.923	-554.122	0	-266.350	-666.922	-554.122	0	2.650.245	-1	-328.378	0	8.866.009	0	8.866.009				
Node 5	Node 5	F _x (kN)	-554.122	-667.004	-554.122	667.002	-554.122	-667.001	-554.122	667.002	-554.122	-667.002	-1	-2.996.392	1	-328.373	1	-2.996.392	-1	-328.378	0	8.866.009	0	8.866.009				
	Node 5	F _y (kN)	-667.004	-554.122	667.002	-554.122	-667.001	-554.122	667.002	-554.122	-667.002	-1	-2.996.392	1	-328.373	1	-2.996.392	-1	-328.378	0	8.866.009	0	8.866.009					

Figure 2.96. Stiffness Matrix. Finite Element 1.
Global numbering of Nodes.

Control Net

Figure 2.97 shows Nodes' Cartesian coordinates.

local numbering	X_N	axis X				
		element 1	element 2	element 3	element 4	element 5
Node 1		0	3	6	9	12
Node 2		3	6	9	12	15
Node 3		3	6	9	12	15
Node 4		0	3	6	9	12
Node 5		1,5	4,5	7,5	10,5	13,5
Node 6		3	6	9	12	15
Node 7		1,5	4,5	7,5	10,5	13,5
Node 8		0	3	6	9	12
Node 9		1,5	4,5	7,5	10,5	13,5

Figure 2.97.a. Nodes' Cartesian coordinate X. (physical space)

local numbering	Y_N	axis Y				
		element 1	element 2	element 3	element 4	element 5
Node 1		0	0	0	0	0
Node 2		0	0	0	0	0
Node 3		3	3	3	3	3
Node 4		3	3	3	3	3
Node 5		0	0	0	0	0
Node 6		1,5	1,5	1,5	1,5	1,5
Node 7		3	3	3	3	3
Node 8		1,5	1,5	1,5	1,5	1,5
Node 9		1,5	1,5	1,5	1,5	1,5

Figure 2.97.b. Nodes' Cartesian coordinate Y. (physical space)

33 Nodes partition the structure into 5 Lagrange Finite Elements.

In Figure 2.98 we can see the corresponding node net.

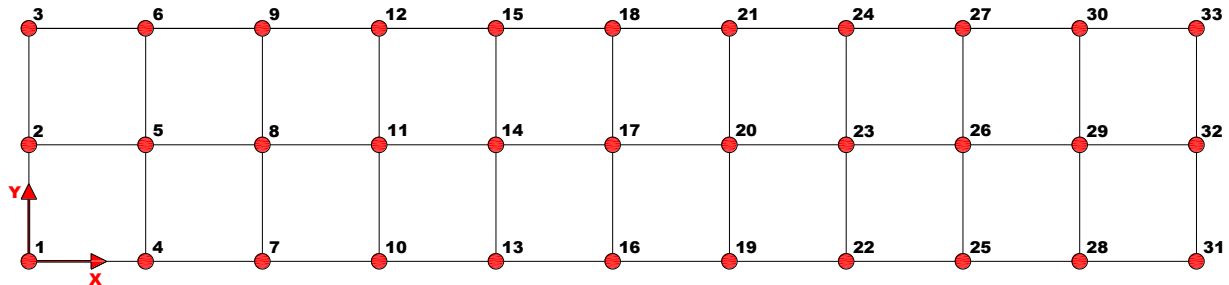


Figure 2.98. Node Net. (physical space)

Parameter Space

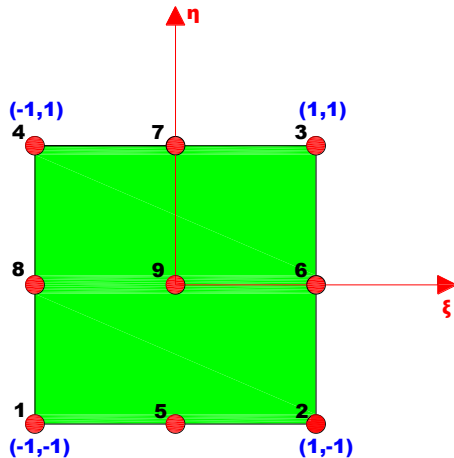


Figure 2.99. Isoparametric 2D 4-sided 9-noded (Lagrange) Finite Element. Parameter Space. Local Numbering.

Physical Space

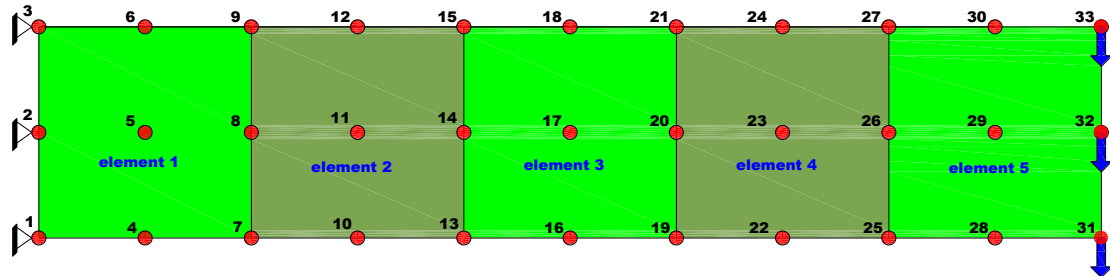


Figure 2.100. Finite Element Mesh. Nodes partition cantilever into finite elements.

Figure 2.100 shows nodes (red circles) in the physical space. Nodes partition cantilever into 5 isoparametric 2D 4-sided 9-noded finite elements. The Total Stiffness Matrix refers to nodes, so I form the equilibrium equation for them.

$$\mathbf{F} = \mathbf{K} \cdot \mathbf{U} \Rightarrow \mathbf{U} = \mathbf{K}^{-1} \cdot \mathbf{F}$$

Displacements' vector \mathbf{U} refers to nodes. For this particular problem, there are 33 nodes, so the above equation is written as follows:

$$\underset{66 \times 1}{\mathbf{F}} = \underset{66 \times 66}{\mathbf{K}} \cdot \underset{66 \times 1}{\mathbf{U}} \Rightarrow \underset{66 \times 1}{\mathbf{U}} = \underset{66 \times 66}{\mathbf{K}^{-1}} \cdot \underset{66 \times 1}{\mathbf{F}}$$

Total Stiffness Matrix [K]

I calculate the local (numbering) Stiffness Matrix for every Finite Element. Then, I form the total Stiffness Matrix of the structure.

Figure 2.101. Total Stiffness Matrix. (66x66)

Two Degrees of Freedom correspond to every Node, the horizontal u and the vertical v displacement. The cantilever's total Stiffness Matrix is a symmetric square matrix with dimensions 66×66 , as there are 33 Nodes and $33 \cdot 2 = 66$ Degrees of Freedom.

Nodes' External Forces {P}

I calculate the External Load Vector (66x1) and I reorder it.

$$\mathbf{F}_{\text{tot}} = \begin{pmatrix} 0 & \dots & 0 & -1000 & 0 & -1000 & 0 & -1000 \end{pmatrix}^T$$

(66x1)

$$F_{tot,m} = \begin{Bmatrix} F_f \\ (60 \times 1) \\ F_s \\ (6 \times 1) \end{Bmatrix} = \begin{Bmatrix} 0 & \dots & 0 & -1000 & 0 & -1000 & 0 & -1000 \\ (60 \times 1) \\ 0 \\ (6 \times 1) \end{Bmatrix}^T$$

Control Points' Displacements {U}

I reorder the Total Stiffness Matrix and the External Load Vector and then I form the balance equation. I symbolize the unknown displacements with subscript f and the known ones (fixed Nodes) with s.

$$F_{\text{tot,m}} = [K_{\text{tot,m}}] \cdot U_{\text{tot,m}} \Rightarrow \begin{Bmatrix} F_f \\ 60 \times 1 \\ F_s \\ 6 \times 1 \end{Bmatrix} = \begin{bmatrix} K_{ff} & K_{fs} \\ 60 \times 60 & 60 \times 6 \\ K_{sf} & K_{ss} \\ 6 \times 60 & 6 \times 6 \end{bmatrix} \cdot \begin{Bmatrix} U_f \\ 60 \times 1 \\ U_s \\ 6 \times 1 \end{Bmatrix}$$

$$\Rightarrow$$

$$\left\{ \begin{array}{c} 0 \\ \dots \\ 0 \\ -1000 \\ 0 \\ -1000 \\ 0 \\ 0 \\ -1000 \\ 60 \times 1 \\ 0 \\ 6 \times 1 \end{array} \right\} = \left[\begin{array}{cc} K_{ff} & K_{fs} \\ 60 \times 60 & 60 \times 6 \\ K_{sf} & K_{ss} \\ 6 \times 60 & 6 \times 6 \end{array} \right] \cdot \left\{ \begin{array}{c} U_f \\ 60 \times 1 \\ U_s \\ 6 \times 1 \end{array} \right\} \Rightarrow \left\{ \begin{array}{c} U_f \\ 60 \times 1 \\ K_{ff} \\ 60 \times 60 \end{array} \right\} \cdot \left\{ \begin{array}{c} 0 \\ \dots \\ 0 \\ -1000 \\ 0 \\ -1000 \\ 0 \\ -1000 \\ 60 \times 1 \end{array} \right\}$$

Figure 2.102 shows Nodes' horizontal and vertical displacement.

The maximum horizontal displacement is equal to 10,7 cm and corresponds to:

- ❖ Node 31: $u=-10,7$ cm
- ❖ Node 33: $u=+10,7$ cm.

The maximum vertical displacement is equal to 72,7 cm and corresponds to:

- ❖ Node 31: $v=-72,7$ cm
- ❖ Node 33: $v=-72,7$ cm.

Negative value displays that maximum displacement's direction is the negative direction of axis Y, means these Nodes move downstairs as expected.

	horizontal u (cm)	vertical v (cm)
Node 1	0,0	0,0
Node 2	0,0	0,0
Node 3	0,0	0,0
Node 4	-2,0	-1,4
Node 5	0,0	-1,1
Node 6	2,0	-1,4
Node 7	-3,8	-4,4
Node 8	0,0	-4,2
Node 9	3,8	-4,4
Node 10	-5,4	-9,2
Node 11	0,0	-9,0
Node 12	5,4	-9,2
Node 13	-6,8	-15,5
Node 14	0,0	-15,3
Node 15	6,8	-15,5
Node 16	-8,0	-23,0
Node 17	0,0	-22,9
Node 18	8,0	-23,0
Node 19	-8,9	-31,7
Node 20	0,0	-31,5
Node 21	8,9	-31,7
Node 22	-9,7	-41,2
Node 23	0,0	-41,1
Node 24	9,7	-41,2
Node 25	-10,2	-51,3
Node 26	0,0	-51,2
Node 27	10,2	-51,3
Node 28	-10,5	-61,8
Node 29	0,0	-61,8
Node 30	10,5	-61,8
Node 31	-10,7	-72,7
Node 32	0,0	-72,6
Node 33	10,7	-72,7
max	10,7	0,0
min	-10,7	-72,7

Figure 2.102. Nodes' displacements.

Isogeometric Analysis

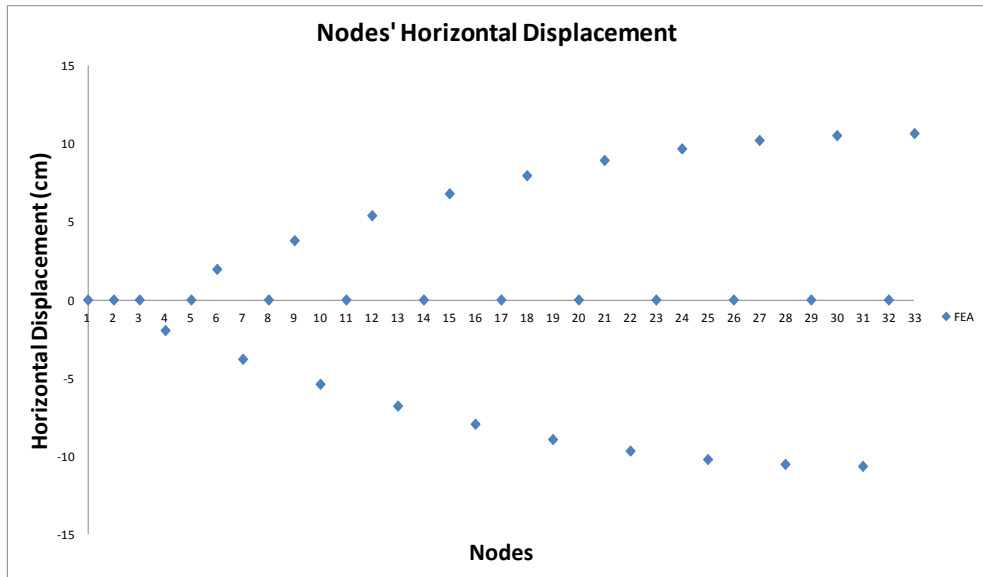


Figure 2.103.a. Nodes' horizontal displacement.

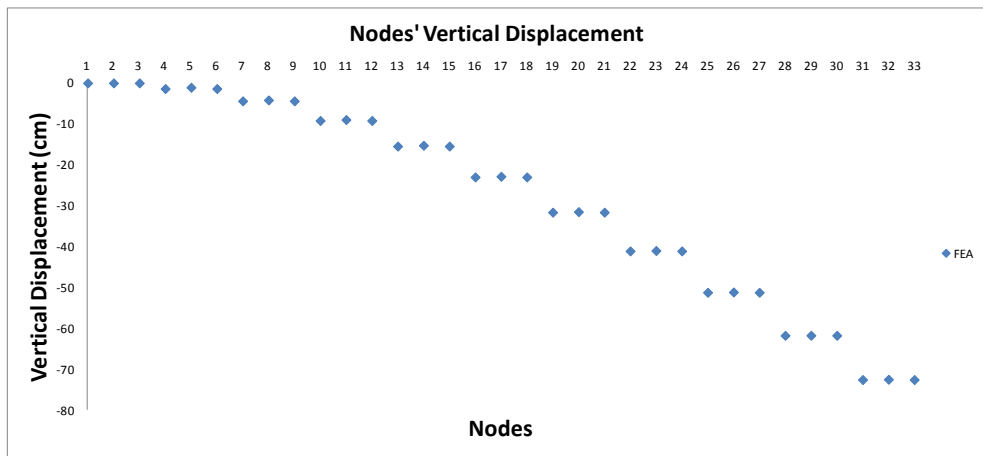


Figure 2.104.b. Nodes' vertical displacement.

Stress Field at Gauss Points

As I know Nodes' displacements, I can calculate the stress field at Finite Elements' Gauss Points.

$$\sigma_{\xi_i, \eta_i} = E \cdot \varepsilon_{\xi_i, \eta_i} = E \cdot [B_{\xi_i, \eta_i}] \cdot d_{18 \times 1}$$

where:

$$\sigma_{\xi_i, \eta_i} = \begin{cases} \sigma_X & \xi_i, \eta_i \\ \sigma_Y & \xi_i, \eta_i \\ \tau_{XY} & \xi_i, \eta_i \end{cases} : \text{stress field at Gauss Point } i \text{ (plane stress problem)}$$

- $$\bullet \quad E_{3x3} = \frac{E}{1-v^2} \cdot \begin{bmatrix} 1 & v & 0 \\ v & 1 & 0 \\ 0 & 0 & \frac{1-v}{2} \end{bmatrix} \quad (\text{plane stress problem})$$
- $$\bullet \quad \varepsilon_{3x1} = \begin{bmatrix} \varepsilon_X & \xi_i, \eta_i \\ \varepsilon_Y & \xi_i, \eta_i \\ \gamma_{XY} & \xi_i, \eta_i \end{bmatrix} : \text{strain field at Gauss Point } i$$
- $$\bullet \quad d_{18x1} : \text{Displacement vector refers to displacements of Finite Element's Nodes (local numbering).}$$

Let's calculate the corresponding stress field to Gauss Point 1 of Finite Element 1.

		$\{d\} (m)$
	Node 1	$u (m) \quad 0$
		$v (m) \quad 0$
	Node 2	$u (m) \quad -0,038$
		$v (m) \quad -0,044$
	Node 3	$u (m) \quad 0,038$
		$v (m) \quad -0,044$
	Node 4	$u (m) \quad 0$
		$v (m) \quad 0$
	Node 5	$u (m) \quad -0,020$
		$v (m) \quad -0,014$
	Node 6	$u (m) \quad 0,000$
		$v (m) \quad -0,042$
	Node 7	$u (m) \quad 0,020$
		$v (m) \quad -0,014$
	Node 8	$u (m) \quad 0$
		$v (m) \quad 0$
	Node 9	$u (m) \quad 0$
		$v (m) \quad -0,011$

**Figure 2.105. Nodes' vertical and horizontal displacement.
Finite Element 1.**

$$\sigma_{\xi_i, \eta_i} = E \cdot [B_{\xi_i, \eta_i}] \cdot d = \begin{Bmatrix} 0 \\ 0 \\ -69.395 \end{Bmatrix} \text{ kPa} \Rightarrow \sigma_{\xi_i, \eta_i} = \begin{Bmatrix} 0 \\ 0 \\ -69,40 \end{Bmatrix} \text{ MPa}$$

Isogeometric Analysis

MPa	element 1			element 2			element 3			element 4			element 5		
	σ_{xx}	σ_{yy}	τ_{xy}												
G.P.1	0,00	0,00	-69,40	0,00	0,00	-85,70	0,00	0,00	-87,51	0,00	0,00	-87,33	0,00	0,00	-83,92
G.P.2	2.388,96	-88,51	-118,18	1.896,44	-10,03	-78,66	1.358,68	-0,90	-74,28	816,86	1,99	-74,72	284,00	18,62	-82,98
G.P.3	1.419,57	-52,59	-86,62	1.126,90	-5,96	-83,22	807,36	-0,54	-82,84	485,39	1,18	-82,88	168,76	11,06	-83,59
G.P.4	-2.388,96	88,51	-118,18	-1.896,44	10,03	-78,66	-1.358,68	0,90	-74,28	-816,86	-1,99	-74,72	-284,00	-18,62	-82,98
G.P.5	-1.419,57	52,59	-86,62	-1.126,90	5,96	-83,22	-807,36	0,54	-82,84	-485,39	-1,18	-82,88	-168,76	-11,06	-83,59
G.P.6	0,00	0,00	-163,35	0,00	0,00	-135,59	0,00	0,00	-132,20	0,00	0,00	-129,65	0,00	0,00	-110,31
G.P.7	2.295,46	61,12	-46,23	1.683,10	11,43	-109,76	1.131,38	4,09	-117,28	584,85	-11,71	-120,76	23,96	-145,22	-144,26
G.P.8	1.364,01	36,32	-122,00	1.000,13	6,79	-126,47	672,29	2,43	-126,93	347,53	-6,96	-126,51	14,24	-86,29	-122,30
G.P.9	-2.295,46	-61,12	-46,23	-1.683,10	-11,43	-109,76	-1.131,38	-4,09	-117,28	-584,85	11,71	-120,76	-23,96	145,22	-144,26
G.P.10	-1.364,01	-36,32	-122,00	-1.000,13	-6,79	-126,47	-672,29	-2,43	-126,93	-347,53	6,96	-126,51	-14,24	86,29	-122,30
G.P.11	0,00	0,00	-118,81	0,00	0,00	-105,16	0,00	0,00	-103,45	0,00	0,00	-101,91	0,00	0,00	-89,82
G.P.12	2.299,11	-113,89	-69,01	1.765,79	-10,22	-86,95	1.223,27	0,90	-89,22	679,76	-3,58	-91,51	136,69	-54,70	-109,62
G.P.13	1.366,18	-67,67	-101,23	1.049,26	-6,07	-98,73	726,89	0,54	-98,43	403,93	-2,13	-98,23	81,22	-32,50	-96,81
G.P.14	-2.299,11	113,89	-69,01	-1.765,79	10,22	-86,95	-1.223,27	-0,90	-89,22	-679,76	3,58	-91,51	-136,69	54,70	-109,62
G.P.15	-1.366,18	67,67	-101,23	-1.049,26	6,07	-98,73	-726,89	-0,54	-98,43	-403,93	2,13	-98,23	-81,22	32,50	-96,81
G.P.16	0,00	0,00	-28,67	0,00	0,00	-120,34	0,00	0,00	130,82	0,00	0,00	-132,67	0,00	0,00	-138,64
G.P.17	2.766,87	709,86	-243,35	2.141,99	75,91	-132,09	1.588,88	3,76	-119,28	1.042,48	-5,60	-116,33	484,21	-16,95	-102,80
G.P.18	1.644,12	421,81	-104,47	1.272,81	45,11	-124,49	944,14	2,24	-126,75	619,46	-3,33	-126,90	287,73	-10,07	-125,99
G.P.19	-2.766,87	-709,86	-243,35	-2.141,99	-75,91	-132,09	-1.588,88	-3,76	-119,28	-1.042,48	5,60	-116,33	-484,21	16,95	-102,80
G.P.20	-1.644,12	-421,81	-104,47	-1.272,81	-45,11	-124,49	-944,14	-2,24	-126,75	-619,46	3,33	-126,90	-287,73	10,07	-125,99
G.P.21	0,00	0,00	-38,78	0,00	0,00	-96,09	0,00	0,00	-102,64	0,00	0,00	-103,70	0,00	0,00	-106,66
G.P.22	2.579,23	271,60	-186,14	2.038,47	28,09	-100,22	1.495,12	0,71	-90,41	951,70	0,04	-88,88	410,18	21,52	-84,98
G.P.23	1.532,63	161,39	-90,81	1.211,30	16,69	-97,55	888,43	0,42	-98,32	565,52	0,03	-98,47	243,74	12,79	-99,00
G.P.24	-2.579,23	-271,60	-186,14	-2.038,47	-28,09	-100,22	-1.495,12	-0,71	-90,41	-951,70	-0,04	-88,88	-410,18	-21,52	-84,98
G.P.25	-1.532,63	-161,39	-90,81	-1.211,30	-16,69	-97,55	-888,43	-0,42	-98,32	-565,52	-0,03	-98,47	-243,74	-12,79	-99,00
max	2.766,87	709,86	-28,67	2.141,99	75,91	-78,66	1.588,88	4,09	-74,28	1.042,48	11,71	-74,72	484,21	145,22	-82,98
min	-2.766,87	-709,86	-243,35	-2.141,99	-75,91	-135,59	-1.588,88	-4,09	-132,20	-1.042,48	-11,71	-132,67	-484,21	-145,22	-144,26

Figure 2.106.a. Stress Field at Gauss Points.

Finite Elements 1-5.

		(Finite Element, G.P.)			
σ_{xx} (MPa)	max	(1,17)	2.766,87	min	(1,19) -2.766,87
σ_{yy} (MPa)	max	(1,17)	709,86	min	(1,19) -709,86
τ_{xy} (MPa)	max	(1,16)	-28,67	min	(1,17), (1,19) -243,35

Figure 2.107. Maximum and Minimum Stress.

Element 2 (G.P.17, nearest to upper horizontal side) experience the largest tension. Tensile stresses are equal to:

$$\max \sigma_{XX}^+ = 2.766,87 \text{ MPa}$$

$$\max \sigma_{YY}^+ = 709,86 \text{ MPa}$$

Element 1 (G.P.19, nearest to lower horizontal side) experience the largest compression. Compressive stresses are equal to:

$$\max \sigma_{XX}^- = -2.766,87 \text{ MPa}$$

$$\max \sigma_{YY}^- = -709,86 \text{ MPa}$$

2.3.3. Comparison

Comparing two methods' results, I will reach interesting conclusions.

- IsoGeometric Analysis (IGA)

Method	IGA
Patches	1
Isogeometric Elements ($\Xi \times H$)	9
Horizontal Spans (Ξ)	9
Vertical Spans (H)	1
Control Points	33
Control Points (Ξ)	11
Control Points (H)	3
p	2
q	2
Gauss Points	5x5

Figure 2.108.a. Analysis Parameters. IGA.

- Finite Element Analysis (FEA)

Method	FEA
Finite Elements (Number)	5
Finite Elements (Type)	isoparametric
	2D
	4-sided
	9-noded
Gauss Points	5x5

Figure 2.108.b. Analysis Parameters. FEA.

Particularly, I will compare:

- B-SPLine Functions (IGA) with Shape Functions (FEA).
- Control Net (IGA) with Node Net (FEA).
- Parameter Space (Mesh).
- Physical Space (Mesh).
- Total Stiffness Matrix.
- Control Points' Displacements (IGA) with Nodes' Displacements (FEA).
- Stress Field at Gauss Points.

Shape Functions

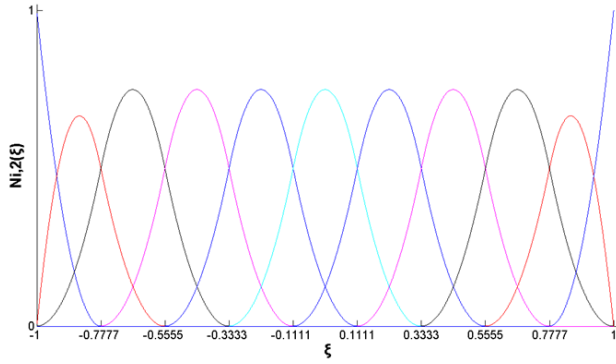


Figure 2.109.a. Quadratic Basis SPLine Functions for open, uniform knot vector
 $\Xi = \{-1, -1, -1, -0.78, -0.56, -0.33, -0.11, 0.11, 0.33, 0.56, 0.78, 1, 1, 1\}$.

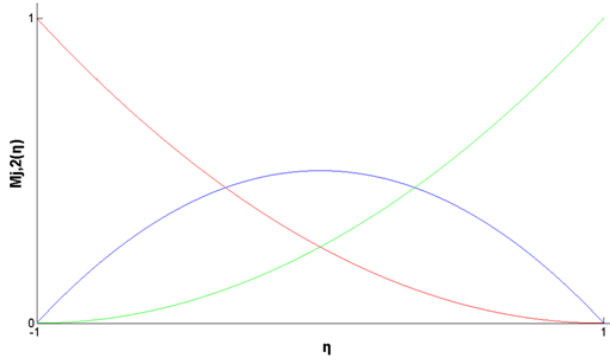


Figure 2.109.b. Quadratic Basis SPLine Functions for open, uniform knot vector
 $H = \{-1, -1, -1, 1, 1, 1, 1\}$.

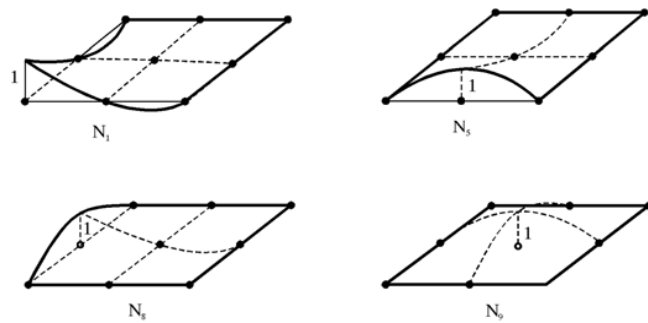


Figure 2.109.c. Shape Functions. Isoparametric 2-Noded Truss Finite Element.

For $p=1$, IGA's B-SPLINE Functions are exactly the same with FEA's Shape Functions. For $p=2$, something like that does not happen. IGA's B-SPLINE functions have larger support than FEA's ones. Unlike in standard finite element analysis, the B-SPLINE parameter space is local to patches rather than elements.

Control/ Node Net

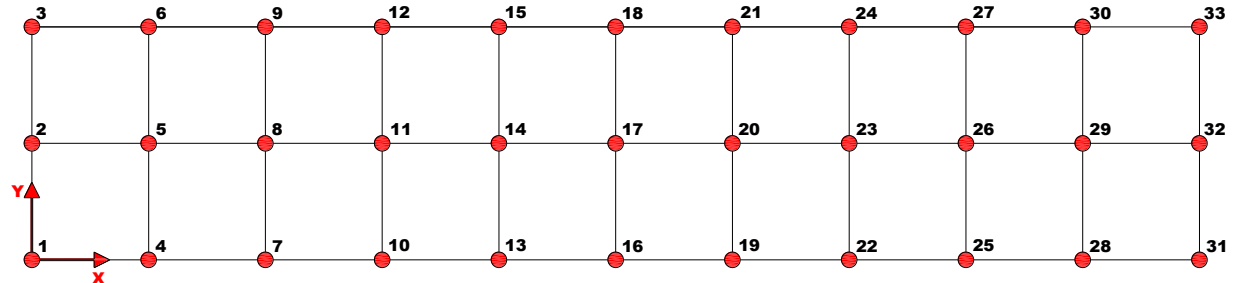


Figure 2.110.a. Control Net. Physical space.

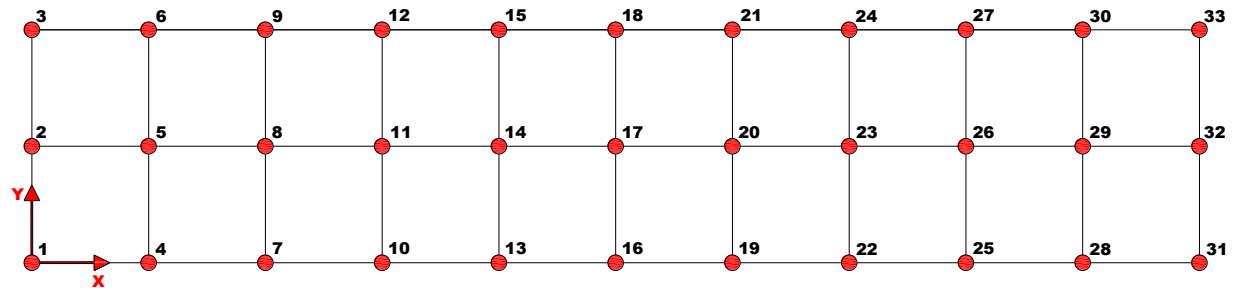


Figure 2.110.b. Node Net. Physical Space.

I choose as many Nodes as Control Points in order to have the same number of Degrees of Freedom. They have the same geometric features.

Parameter Space

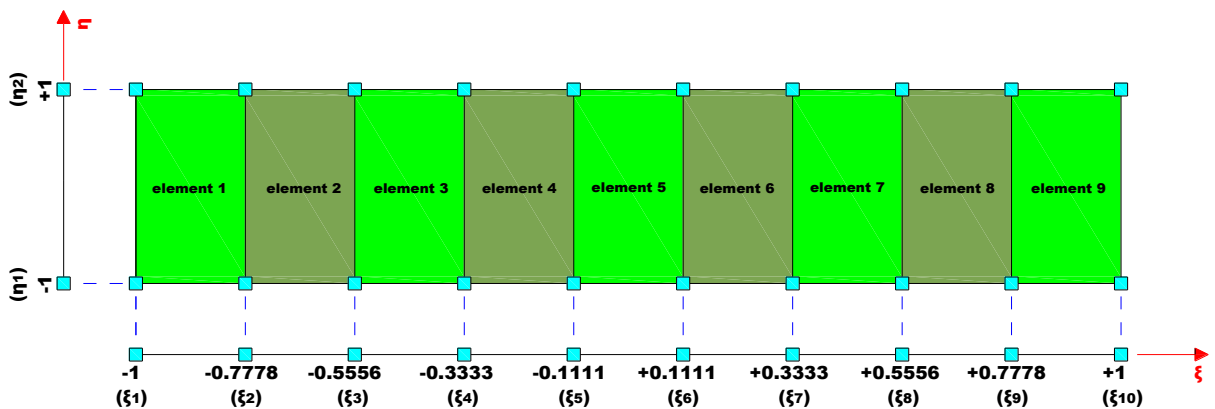
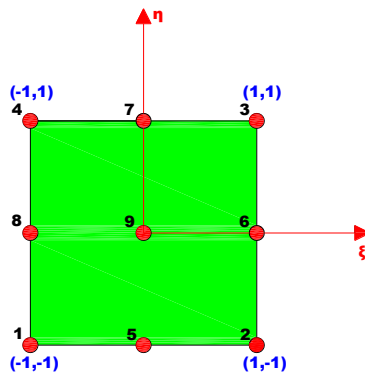


Figure 2.111.a. Isogeometric Elements' Mesh. Parameter Space.



**Figure 2.111.b. Isoparametric 2D 4-sided 9-noded Finite Element.
Parameter Space. Local Numbering.**

In classical Finite Element Analysis (FEA), the parameter space ("reference/ parent element") is local to individual elements and is mapped into a single element in the physical space. Each finite element has its own mapping from the reference element.

In Isogeometric Analysis (IGA), the B-SPLine parameter space is local to the entire patch rather than element. The B-SPLine mapping (a single map) takes a patch of multiple elements in the parameter space into the physical space, but the mapping itself is global to the whole patch, rather than to the elements.

Physical Space

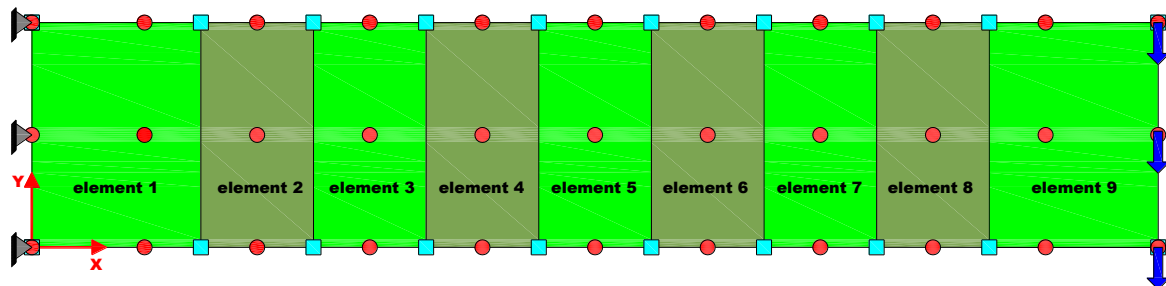


Figure 2.112.a. Physical Space. Mesh. Knots and Control Points.

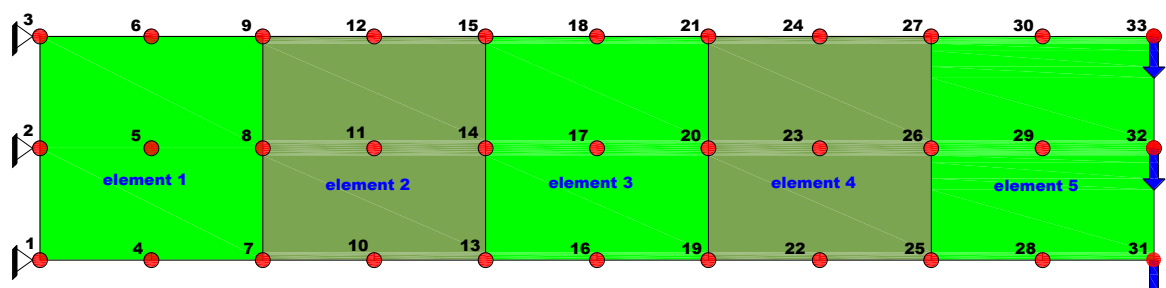


Figure 2.112.b. Physical Space. Mesh. Nodes.

Isogeometric Analysis

Figure 2.112.a. shows both knots (cyan rhombi) and control points (red circles) in the physical space. We observe that knots don't coincide with control points. That's why B-SPLines are not linear, but quadratic. Figure 2.112.b. shows nodes (red circles) in the physical space. We observe that Finite Element Mesh is not exactly the same with Isogeometric Element Mesh, despite the fact that I have chosen Node Net exactly the same with Control Net. That is why Basis SPLine Functions (IGA) and Shape Functions (FEA) are not linear and exactly the same. It is important to mention that Nodes partition structure into Finite Elements and Knots (and not Control Points) partition structure into Isogeometric Elements.

Total Stiffness Matrix [K]

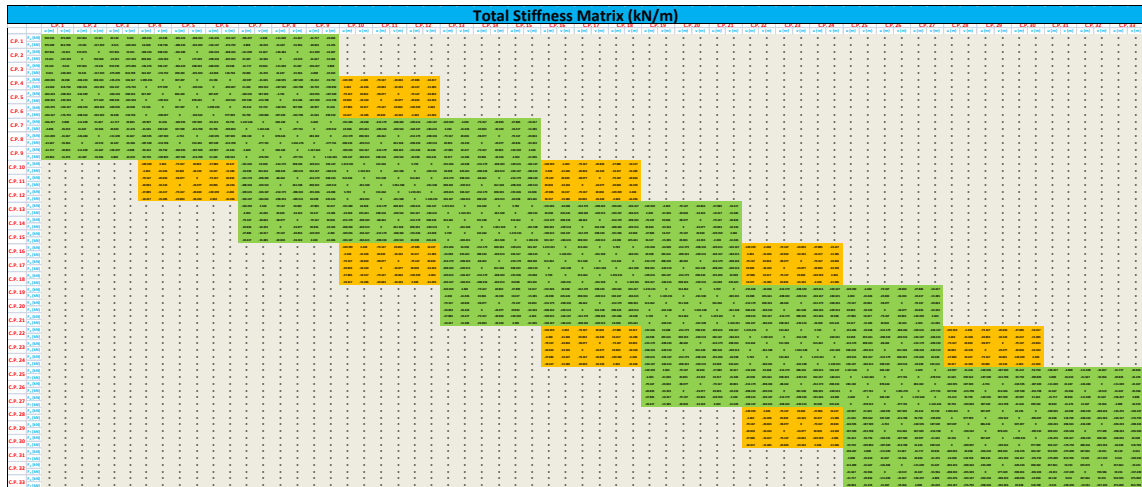


Figure 2.113.a. Total Stiffness Matrix. (66x66). IGA.

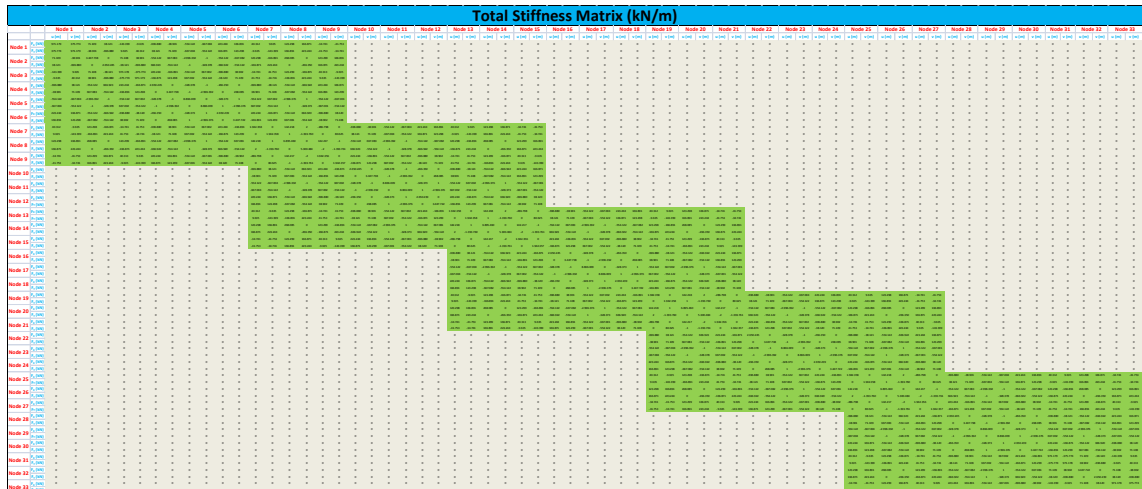


Figure 2.113.b. Total Stiffness Matrix. (66x66). FEA.

The two matrices differ. IGA's Total Stiffness Matrix has more nonzero entries than FEA's one. Figure 2.113.a depicts these additional nonzero elements as orange domains. We know that higher-order functions have support over much larger portions of domain than do classical FEA functions. We can observe this feature in the certain example. IGA's overlapping is more intense than FEA's one. It is important to mention that despite this fact, bandwidth doesn't increase. It is just thicker (additional orange domains).

C.P./ Nodes' Displacements {U}

	(cm)	(cm)		(cm)	(cm)
	horizontal u	vertical v		horizontal u	vertical v
C.P. 1	0,0	0,0	Node 1	0,0	0,0
C.P. 2	0,0	0,0	Node 2	0,0	0,0
C.P. 3	0,0	0,0	Node 3	0,0	0,0
C.P. 4	-1,9	-1,0	Node 4	-2,0	-1,4
C.P. 5	0,0	-0,1	Node 5	0,0	-1,1
C.P. 6	1,9	-1,0	Node 6	2,0	-1,4
C.P. 7	-3,8	-4,1	Node 7	-3,8	-4,4
C.P. 8	0,0	-3,7	Node 8	0,0	-4,2
C.P. 9	3,8	-4,1	Node 9	3,8	-4,4
C.P. 10	-5,4	-8,9	Node 10	-5,4	-9,2
C.P. 11	0,0	-8,4	Node 11	0,0	-9,0
C.P. 12	5,4	-8,9	Node 12	5,4	-9,2
C.P. 13	-6,8	-15,1	Node 13	-6,8	-15,5
C.P. 14	0,0	-14,7	Node 14	0,0	-15,3
C.P. 15	6,8	-15,1	Node 15	6,8	-15,5
C.P. 16	-7,9	-22,7	Node 16	-8,0	-23,0
C.P. 17	0,0	-22,3	Node 17	0,0	-22,9
C.P. 18	7,9	-22,7	Node 18	8,0	-23,0
C.P. 19	-8,9	-31,3	Node 19	-8,9	-31,7
C.P. 20	0,0	-31,0	Node 20	0,0	-31,5
C.P. 21	8,9	-31,3	Node 21	8,9	-31,7
C.P. 22	-9,7	-40,7	Node 22	-9,7	-41,2
C.P. 23	0,0	-40,5	Node 23	0,0	-41,1
C.P. 24	9,7	-40,7	Node 24	9,7	-41,2
C.P. 25	-10,2	-50,8	Node 25	-10,2	-51,3
C.P. 26	0,0	-50,7	Node 26	0,0	-51,2
C.P. 27	10,2	-50,8	Node 27	10,2	-51,3
C.P. 28	-10,5	-61,4	Node 28	-10,5	-61,8
C.P. 29	0,0	-61,3	Node 29	0,0	-61,8
C.P. 30	10,5	-61,4	Node 30	10,5	-61,8
C.P. 31	-10,6	-72,1	Node 31	-10,7	-72,7
C.P. 32	0,0	-72,1	Node 32	0,0	-72,6
C.P. 33	10,6	-72,1	Node 33	10,7	-72,7
max	10,6	0,0	max	10,7	0,0
min	-10,6	-72,1	min	-10,7	-72,7

Figure 2.114. Control Points', Nodes' displacements.

The displacements are not exactly the same. They differ slightly.

max |horizontal displacement|: difference: 0.93%

max |vertical displacement|: difference: 0.83%

Isogeometric Analysis

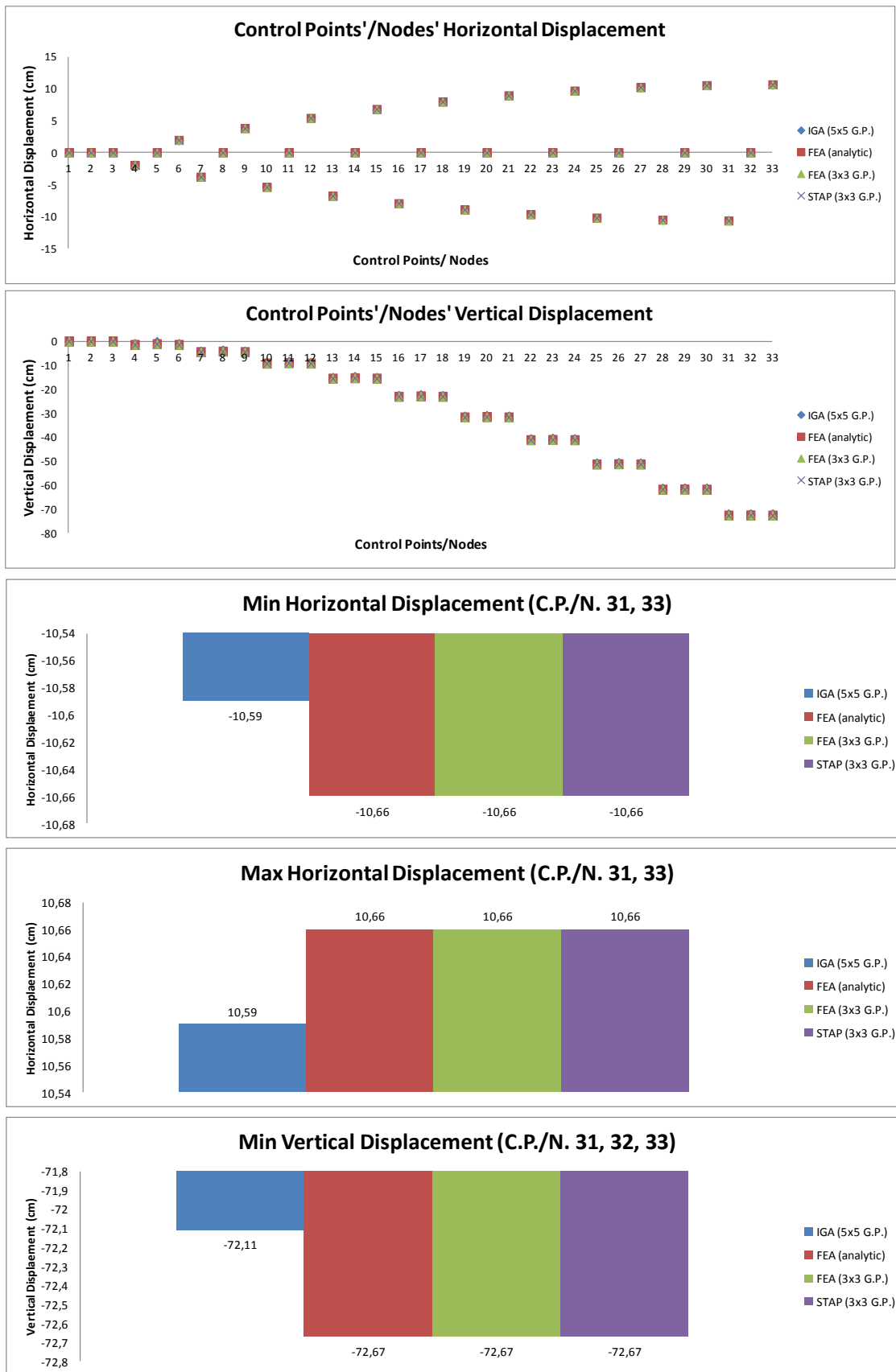


Figure 2.115. Comparison. IGA. FEA (CantiFEA/analytic and quadrature. STAP).

Stress Field at Gauss Points

		(Isogeometric Element, G.P.)	
		max	(1,17)
σ_{xx} (MPa)		min	(1,19)
		max	(1,17)
σ_{yy} (MPa)		min	(1,19)
		max	(1,1)
τ_{xy} (MPa)		min	(1,17), (1,19)
		2.596,46	
		-2.596,46	
		680,31	
		-680,31	
		87,67	
		-424,63	

Figure 2.116.a. Maximum and Minimum Stress. IGA.

		(Finite Element, G.P.)	
		max	(1,17)
σ_{xx} (MPa)		min	(1,19)
		max	(1,17)
σ_{yy} (MPa)		min	(1,19)
		max	(1,16)
τ_{xy} (MPa)		min	(1,17), (1,19)
		2.766,87	
		-2.766,87	
		709,86	
		-709,86	
		-28,67	
		-243,35	

Figure 2.116.b. Maximum and Minimum Stress. FEA.

Literature

1. J. Austin Cottrell, Thomas J.R. Hughes, Yuri Bazilevs (2009), Isogeometric Analysis Toward Integration of CAD and FEA, WILEY
2. Joshua Lee Fisher (2006), An Analysis of the Finite Element Method using B-spline Basis Functions, University of Texas at Austin, Department of Mathematics, 1 University Station C1200 Austin, May 26, 2006
3. Thomas J.R. Hughes, J. Austin Cottrell, Yuri Bazilevs (2004), Isogeometric Analysis: CAD, finite elements, NURBS, exact geometry and mesh refinement, Institute for Computational Engineering and Sciences, The University of Texas at Austin, 1 University Station C0200 Austin, 28 September 2004, 2005 Elsevier
4. A.-V. Vuong, C. Giannelli, B. Juttler, B. Simeon, A hierarchical approach to adaptive local refinement in isogeometric analysis, 2011 Elsevier
5. Παπαδρακάκης Μ. (1996), Ανάλυση Φορέων με τη μέθοδο των πεπερασμένων στοιχείων, Παπασωτηρίου
6. Παπαδρακάκης Μ. (1998), Μη γραμμικά πεπερασμένα στοιχεία, Εκδόσεις ΕΜΠ
7. Yajie Liu, Effect of Knot Vectors on B-SPLINE Curves and Surfaces, Department of Mechanical Engineering, State University of New York at Stony Brook, NY, 11794
8. John Peterson, How to use Knot Vectors, June 1990
9. Yuri Bazilevs, Yongjie Zhang, Victor M. Calo, Samrat Goswami, Chandrajit L. Bajaj, Thomas J.R. Hughes, Isogeometric Analysis of Blood Flow: a NURBS-based approach, Institute for Computational Engineering and Sciences, The University of Texas at Austin, United States
10. Ralph ECHTER, Manfred BISCHOFF, An investigation of the isogeometric approach from the viewpoint of finite element technology, Stuttgart, Germany, 6th International Conference on Computational of Shell and Spatial Structures, 28-31 May 2008
11. Chandrajit L. Bajaj, Samrat Goswami, Zeyun Yu, Yongjie Zhang, Yri Bazilevs, Thomas Hughes, Patient Specific Heart Models from High Resolution CT, Institute for Computational Engineering and Sciences, The University of Texas at Austin, United States